Chiral Alkaloid Derivatives: Synthesis and Medicinal Chemistry Applications

Daniel Canning B.Sc. (Hons)

A thesis presented for the degree of Doctor Philosophy in Organic and Medicinal Chemistry at Dublin City University, School of Chemical Sciences

February 2011

Declarations

I hereby certify that this material, which I now submit for assessment on the programme of study leading to the award of PhD in organic chemistry is entirely my own work, that I have exercised reasonable care to ensure that the work is original, and does not to the best of my knowledge breach any law of copyright, and has not been taken from the work of others save and to the extent that such work has been cited and acknowledged within the text of my work.

Signed:

(Candidate) ID No.:

Date:

Acknowledgments

First I would like to thank my supervisor Dr. Nick Gathergood for his help, encouragement and support throughout this project.

I would also like to thank Dr. David Finn (Dept. of Pharmacology and Therapeutics, NUIG and Centre for Pain Research) for his help and advice on the *mu* opioid receptor binding studies.

I would like to express my gratitude to,

The Irish Research Council for Science, Engineering and Technology (IRCSET) for providing the funding for this research project under the Embark Initiative.

Dr. Simon Lawrence, University College Cork, for X-ray crystallography work and Dr. Florence McCarthy, University College Cork for the HRMS analysis.

The entire technical staff of the School of Chemical Sciences and the National Institute of Cellular Biotechnology, especially Damien, Ambrose, John, Mick, Veronica, Vinny, Brendan, Catherine, Ken and Mary.

A special thanks my colleagues in DCU including Brian D., Brian M., Ewa, Alan, Aine, Shelly, Sonia, Neil, Monika, Thomas, Mags, Debbie, Rohit, Mukund, Ian, Jay, Haibo, Thu, Wioleta, Will and Rachel.

I would particularly like to thank Brian D., Ewa, Shelly, Debbie, Alan and Aine for all their help and encouragement throughout my project and time in DCU.

Finally a special thanks to my family, Mum, Dad, Mark, Brendan and Fiona.

Table of Contents

Abstract

Chiral Alkaloid Derivatives: Synthesis and medicinal chemistry applications

Daniel Canning

The preparation of a selection of novel opioid alkaloids based on alteration at the 1, 3 and 6 positions of codeine and morphine has been achieved. Herein we present the synthetic methodology, structural characterisation and biological evaluation of these novel opioid species.

A range of opioid derivatives with modification at the 6 position to form linked *bis*-opioid species were successfully synthesised. The derived compounds contain both ester and ether linked moieties. A selection of derivatives with modification at the 1 position of codeine were also generated through Heck, Stille and Suzuki palladium catalysed carbon-carbon coupling. A combination of both synthetic approaches has led to a variety of opioid species with modification at both the 1 and 6 positions.

A selection of the opioid species generated were analysed for their binding affinity to the *mu* opioid receptor through radioligand binding techniques. Binding affinities of a variety of the opioid species to a selection of metals were also assessed by metal picrate extraction studies.

List of Abbreviations

$[\alpha]_D$	Specific rotation
DCM	Dichloromethane
DMAP	4-Dimethylaminopyridine
DMF	*N,N*-Dimethylformamide
Eq	Equivalent
GPCR	G-protein-coupled receptors
H	Hour
HRMS	High Resolution Mass Spectrometry
IR	Infrared
J	Coupling constant
m.p.	Melting point
min	Minutes
mol	Mole
NBS	*N*-bromosuccinimide
NCS	*N*-chlorosuccinimide
ND	Not Determined
NIS	*N*-iodosuccinimide
NMR	Nuclear magnetic resonance
NSB	Non-Specific Binding
rpm	Revolutions per minute
RT	Room temperature
SAR	Structure-Activity-Relationship
TBAF	Tetrabutylammonium fluoride
TBDMS	*tert*-butyldimethylsilyl
TFA	Trifluoroacetic acid
THF	Tetrahydrofuran
TLC	Thin layer chromatography
δ	Chemical shift
ν	Frequency

Chapter 1

Literature Survey

1.1 Introduction

The opium alkaloids derived from the seed pods of the opium poppy, *Papaver somniferum* have become some of the most commonly prescribed drugs in medicine. The principle components from the opium poppy, morphine (**1**) and its 3-*O*-methylated form, codeine (**2**) have been employed to treat ailments as diverse as diabetes, asthma, diarrhea, ulcers and alcohol dependence. The vast majority of literature on the opium alkaloids however, understandably focuses on their role as powerful analgesic compounds.[1-4] The activity exhibited by morphine and its derivatives has been shown to be highly dependent on the structural composition of the compound.[5, 6] The potency and efficacy can be controlled efficiently and effectively by alterations of the parent molecular scaffold.

The specific set of structural features common to the opioid family of alkaloids can be defined within a few parameters, namely,

- A tertiary nitrogen with a small alkyl substituent,
- A quaternary carbon,
- A phenyl group or its isosteric equivalent directly attached to the quaternary carbon
- And a two carbon spacer between the quaternary carbon and the tertiary nitrogen.

Any of the derivates of morphine which possess these basic structural components structure can act as either an agonist or antagonist of the opioid receptor.

The opioid receptors belong to the G-protein-coupled receptors (GPCR) and are therefore related structurally to the receptors for many neurotransmitters and other agents acting to modulate the activity of nerve cells. The opioid receptors can be separated into three

main groups divided historically on their binding affinity to certain structural compounds.[7-9]

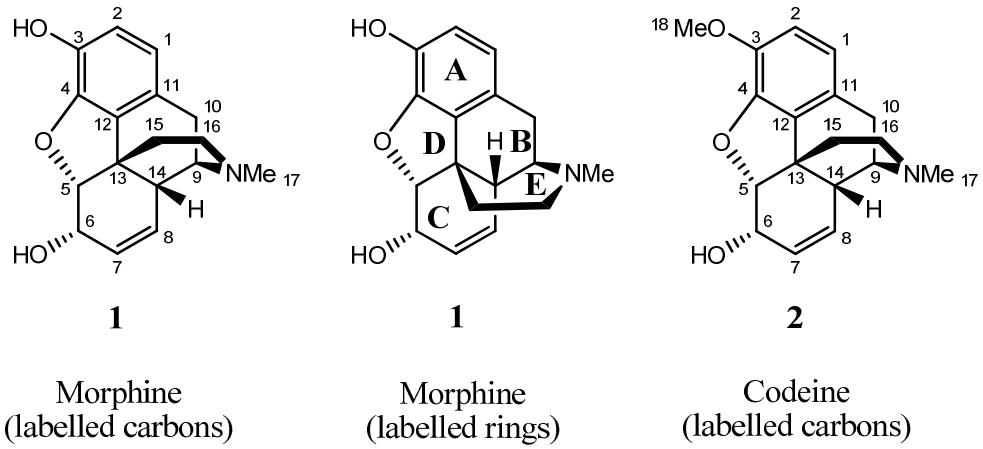

Fig 1.1 Structure of morphine (**1**) and codeine (**2**)

The three main receptor subtypes are, *mu*, μ (referring to binding to the morphine structure), *kappa*, κ (the ketocyclazocine structure) and *delta*, δ (the endorphin/enkephalin structure). It has been demonstrated experimentally that the GPCR opioid receptors can also form homodimer[10-12] (μ-μ, κ-κ, δ-δ) and heterodimer[13-15] (μ-δ, μ-κ) species with different combinations of interacting GPCRs having distinct pharmacological properties. Thus the distinct binding of opioid ligands to the receptor site is dependant on the interaction with receptor subtypes (μ, κ, δ) along with the various combinations of homodimer (μ-μ) and heterodimer species (μ-δ).

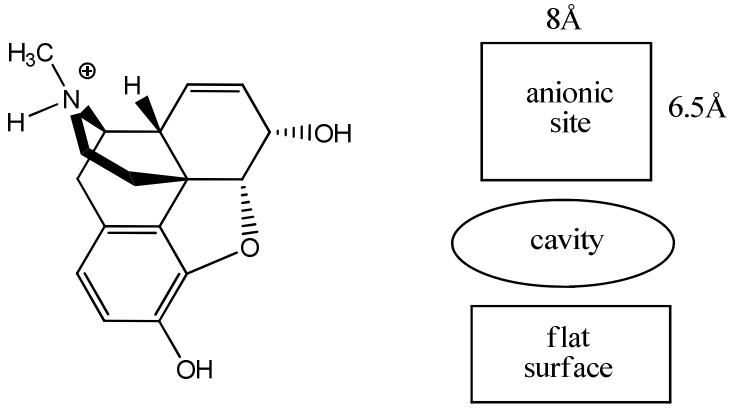

Fig 1.2 Interaction of Morphine with the *Mu* Opioid Receptor Site

Studies into the binding of the opium alkaloids, in particular morphine, show that morphine's interaction is mainly the result of the *mu*, (μ) receptor. [15, 16] An examination of the *mu* receptor (Fig 1.2) shows that there is an anionic site (8 by 6.5 Å) that binds to the charged nitrogen molecule of morphine, a cavity, which accommodates the piperidine ring, and a flat surface for binding the aromatic portion of the molecule. McFadyen *et al*[17] have investigated the pharmacophore of *mu* opioid ligands which provides more information on drug receptor interations (Fig 1.3). All active agonists and antagonists must fit these receptor models to some degree.

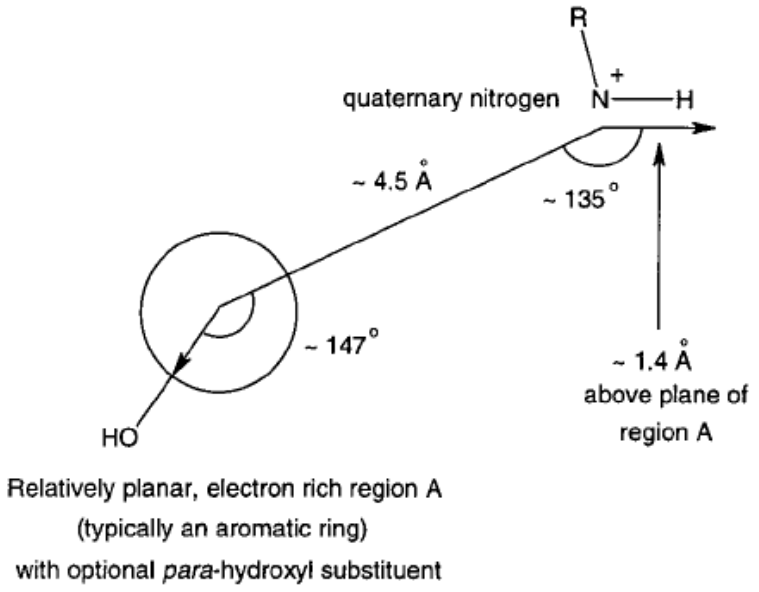

Fig 1.3 Pharmacophore for *mu* opioid ligands[17]

The opium alkaloids, in particular morphine, are a very useful and potent analgesic family of drugs, however, it should be noted that the opium alkaloids have potentially severe side effects.[18, 19] Morphine is a highly addictive compound with the onset of physical and psychological dependence developing very rapidly with administration. Its powerful analgesic effects are accompanied by euphoria, decreased gastrointestinal motility, physical dependence and respiratory depression. Respiratory depression is the main cause of death upon morphine overdose.[20] The numerous damaging side effects of

morphine, in particular its potent addiction, provides much of the impetus for the research of new derivatives.

1.2 Binding Properties of Modified Opioids

Due to the outstanding benefits of morphine aligned with its potent side effects there are continuous efforts to discover and develop new analgesic compounds. Two types of approaches have been used to design and synthesise new opioid drugs. The first approach is modification of previously known morphine analogues. Development of new opioid analgesics based on the morphine, has focused on modifications of the opioid scaffold including addition, replacement and deletion of various ring systems and functional groups. A broad variety of useful classes of analgesic compounds have been developed including the morphinans[21] (**3**), benzomorphans[22] (**4**), phenylpiperidines[23] (**5**) and methadone-type[24] (**6**) compounds (Fig 1.4). As well as providing novel analgesic ligands these compounds also provide a suitable reference for structure activity relationships for further opioid derivatives.

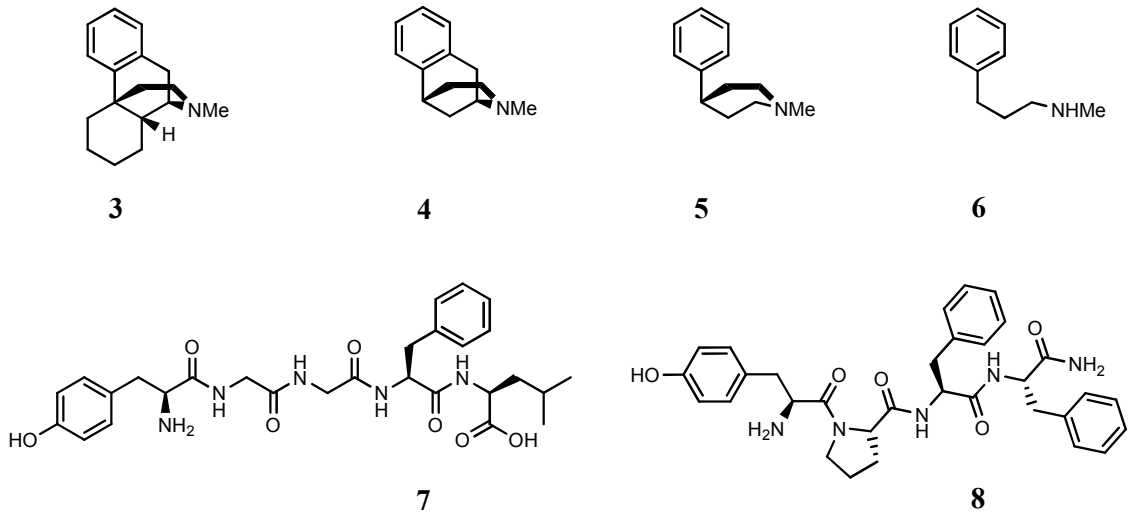

Fig 1.4 Classes of morphine based derivatives (**3**-**6**) and endogenous opioids (**7**-**8**)

The second approach to create novel opioid drugs is the modification of endogenous ligands such as enkephalin[25] (**7**) and endomorphin[26] (**8**) (Fig 1.4). The endogenous

opioid ligands are a series of compounds which are produced naturally within the body by the hypothalamus and pituitary gland. Structurally they consist of a short sequence of amino acids linked by peptide bonds. They are similar to the morphine based opioid ligands in their ability to produce analgesic effects through interaction with the opioid receptors. As with the morphine based ligands a series of peptide based opioid derivatives have been developed with the aim of producing potent and selective agonists at the receptor site without the inherent side effects. Thus there is a huge volume of literature on structural modifications of opioid compounds with the corresponding interactions with the opioid receptor sites. Of particular interest for this project is the morphine derivatives based on modification of the molecule at the phenol, secondary alcohol and nitrogen positions, 3, 6 and 17 respectively (Fig 1.5).

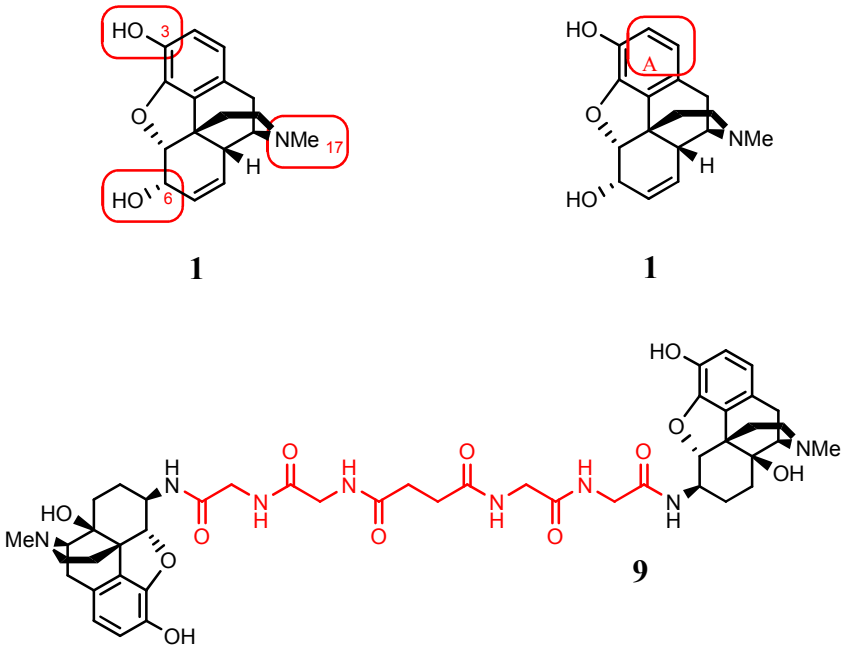

Fig 1.5 Modification of morphine (**1**) at the 3, 6 and 17 positions and formation of "linked" opioids (**9**)

Information in relation to modification of the A-ring of the morphine scaffold along with the formation of "linked" morphine based ligands (**9**, see section 1.2.5) is also highly relevant. For this reason further discussion of opioid ligands-receptor interactions will focus on an in depth analysis of the structural derivatives related to

morphine, modified at these sites in the opiate scaffold. The information provided in this chapter can be utilised to predict the opioid receptor properties of the novel opioid derivatives synthesised as part of this project along with providing methods to selectively control or inhibit the binding affinity.

Where available, data for the affinity of opioid compounds is presented as the equilibrium inhibition constant (K_i) for each sub receptor type (μ, κ, δ). Affinity to the receptor site is also presented as the median effective concentration (EC_{50}) or the median inhibitory concentration (IC_{50}). The lower the K_i, EC_{50} or IC_{50} value the higher affinity to the receptor. The median effective dose (ED_{50}) which relates to the analgesic activity is also included where available. As noted in the literature[15, 16] the interaction of morphine with the opioid receptor is mainly through the *mu* subtype. Thus the data for morphine and its structural derivatives mainly focuses on this subtype. Also important to note is that a high affinity to the opioid receptor site does not imply that the compound will be a potent analgesic. Some compounds which bind strongly to the opioid receptors may be antagonists and thus exhibit no analgesic effect.

1.2.1 Nitrogen Modification

The tertiary nitrogen in the morphine skeleton has proven to be a very important feature required for analgesic activity. In fact it should be noted that a tertiary nitrogen will be found in every potent analgesic compound. Modification of the tertiary nitrogen portion of the morphine skeleton has been shown to drastically effect the analgesic action (Fig 1.6).[5] Formation of the quaternary nitrogen has a significant effect on the analgesic properties.[27] Both *N*-methylmorphine chloride (**11**) and *N*-methylcodeine chloride (**12**) exhibit much lower analgesic activity than the corresponding tertiary nitrogen opioids, morphine and codeine.

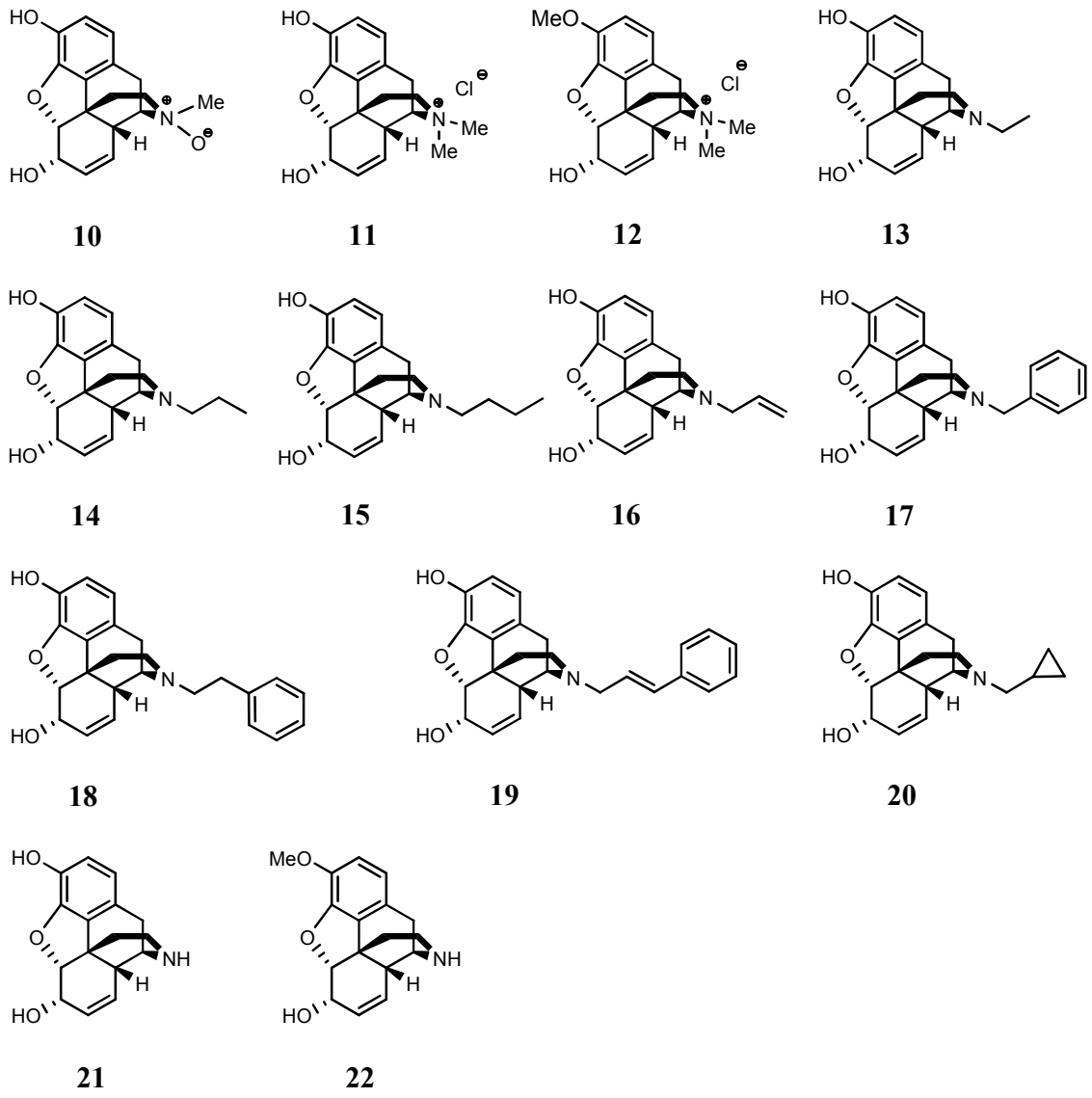

Fig 1.6 Structures of N-modified opioids

An examination of modified morphine derivatives shows that N-substitution and analgesic activity are dependent strongly on the functional group attached. In general substitution of the nitrogen atom lowers the analgesic activity. Conversion of the methyl group on the nitrogen atom to other alkyl groups has been shown to dramatically reduce or completely inhibit analgesia. Portoghese[28] has investigated some of the derivatives of morphine with the N-substituent of the molecule altered from the methyl functionality (Fig 1.6). Results from the studies show that substitution of the nitrogen atom (ie

replacing the CH_3 group) with *n*-propyl (**14**), *n*-butyl (**15**) or allyl (**16**) functionalities results in compounds which have significantly lower analgesia (Table 1.1).

The analgesic activity of compounds **17** and **19** is also lowered by substitution with an aromatic ring. However the presence of the aromatic ring with a two carbon spacer between the nitrogen atom and the aromatic ring in compound **18** results in increased analgesic activity. Compound **18** has a six fold increase in analgesic activity relative to morphine.[28, 29] The combination of the two carbon spacer and the aromatic ring aids the analgesic effect. If the carbon spacer is only one carbon (**17**) or three carbons (**19**) the same increase in analgesia is not observed.

Compound	**Analgesic Activity***
Morphine, **1**	1
13	< 0.1
14	0
15	< 0.1
16	< 0.1
17	< 0.1
18	6
19	< 0.1

Table 1.1 Relative analgesic activity of N-substituted morphine derivatives (*Analgesic activity is relative to morphine (**1**), a value of 10 signifies the compound is 10 times more potent than morphine (**1**))

Substitution of a cyclopropylmethyl functional group on the nitrogen is shown to increase the affinity.[30] Compound **20** exhibits an IC_{50} value of 2.16 ± 0.14 nM which is over thirty times higher than the calculated value for morphine (**1**) at 68.2 ± 15.0 nM (Table 1.2).

Compound	**IC_{50} (nM)**
Morphine, **1**	68.2 ± 15.0
20	2.16 ± 0.14

Table 1.2 IC_{50} values for morphine and **20**

Compound	EC_{50} (nM) (μ)
Morphine, **1**	4.4
21	37
Codeine, **2**	2,500
22	1,500

Table 1.3 EC_{50} values for morphine (**1**), codeine (**2**) and their corresponding N-demethylated derivatives, **21** and **22**

Removal of the methyl substitution on the nitrogen also exhibits an effect on the affinity of opioid derivatives at the opioid receptor site (Table 1.3).[31, 32] For morphine (**1**) there is a considerable reduction in the affinity with N-dealkylation to compound **21**. The calculated EC_{50} value for the normorphine derivative (**21**) is over eight times higher than morphine. However there is a much smaller effect for codeine (**2**) and its N-dealkylated derivative (**22**). Removal of the methyl group on the nitrogen results in a small increase in the EC_{50} value for the codeine derivative **22**. A widely used N-substituted compound is *N*-allylnormorphine (**16**). *N*-allylnormorphine acts as an antagonist at the *mu* opioid receptor site and is used to counter act the respiratory depressant properties of morphine.[33]

1.2.2 Hydroxyl Modification

Modification of the phenolic hydroxyl at position 3 or the secondary hydroxyl at the position 6 has an important effect on the affinity and analgesic activity of morphine derivatives (Fig 1.7). In general alteration of the phenolic hydroxyl has been shown to greatly affect the activity while adjustment at the secondary hydroxyl has a much lower effect.

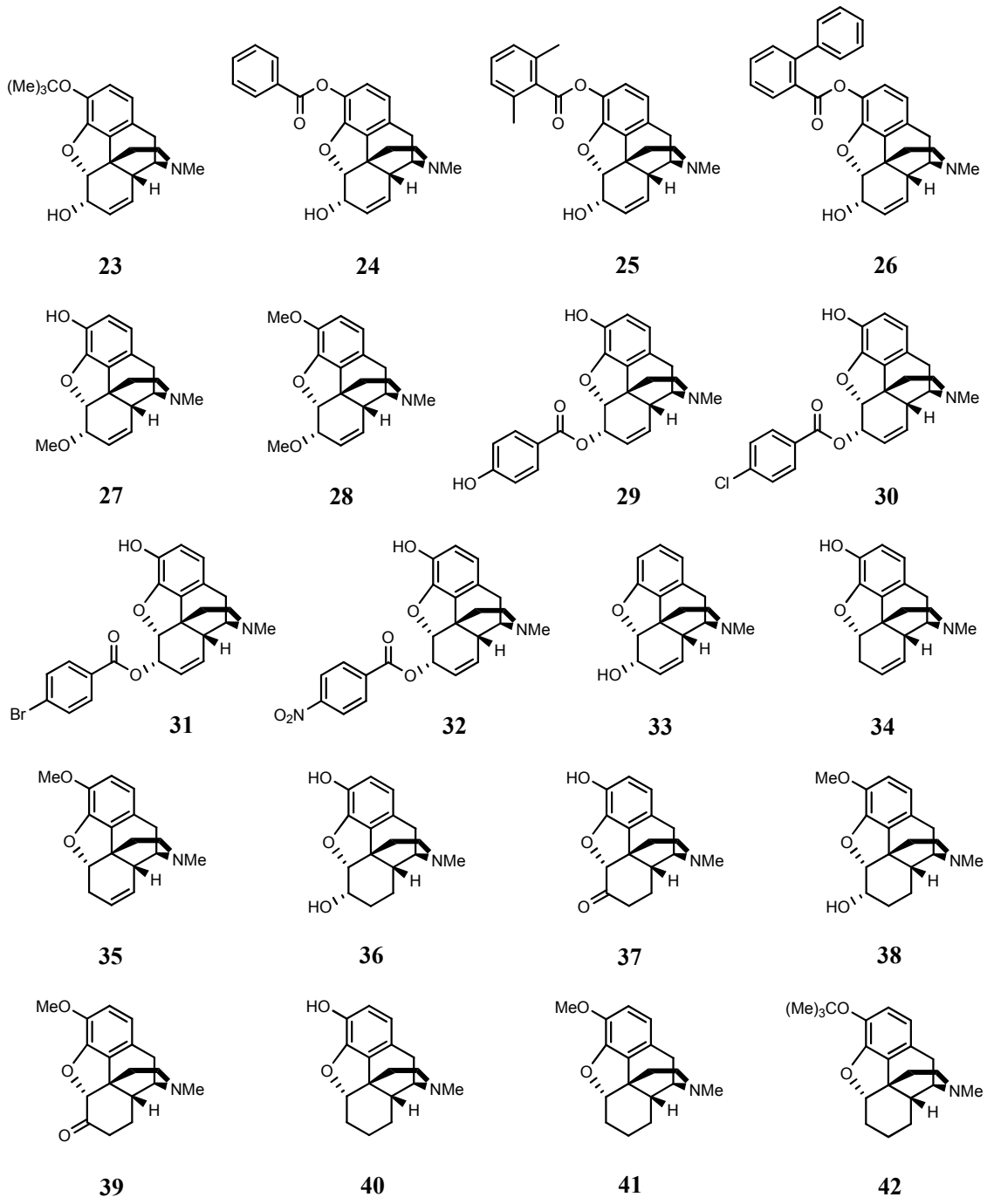

Fig 1.7 Structures of hydroxyl modified opioids

Modification of the phenolic hydroxyl has been shown to significantly lower the analgesic activity of morphine derivatives (Table 1.4).[34] Alteration of the phenolic hydroxyl at the 3 position in morphine (**1**) to the methoxy derivative (codeine, **2**) lowers

the analgesic activity by 5 times with ED_{50} values of 0.26-0.83 and 1.21-3.91 mg/kg respectively. If the bulkier *t*-butyl group is substituted at this position as in **23** then the activity is reduced by almost 60 times with an ED_{50} value of 13.40-53.60 mg/kg. Binding affinities (IC_{50}) to the opioid receptor for codeine (**2**) and **23** are also reduced by 370 and 740 times respectively.

Mignat and co-workers[35] have investigated the binding affinity of a selection of morphine-3-esters to the opioid receptor site (Table 1.5). As expected it was found that modification of the phenolic hydroxyl lowered the affinity for the *mu* opioid site. As the steric "bulk" of the substituent is increased from compounds **24**, **25** and **26** the affinity to the *mu* opioid receptor is decreased by 16, 178 and 1444 times respectively.

Compound	**IC_{50} (nM)**	**ED_{50} (mg/kg)**
Morphine, **1**	27	0.26 – 0.83
Codeine, **2**	10,000	1.21 – 3.91
23	20,000	13.40 - 53.60

Table 1.4 IC_{50} and ED_{50} values for morphine (**1**), codeine (**2**) and **23**

As expected morphine exhibits the highest affinity to the *mu* opioid receptor site with a K_i value of 1.8 ± 0.2 nM. Affinity to the other two opioid subtype receptors, *kappa* and *delta* is reduced by over 32 and 88 times respectively. Compound **24** exhibits much higher binding to the *mu* receptor site than codeine (**2**). The affinity of codeine (**2**) is over 370 times lower than morphine (**1**) but the affinity of compound **24** is only 16 times lower. It would be expected that the greater steric "bulk" of the aromatic ring present in **24** would lower the affinity more than the methyl substitution in codeine (**2**). The higher affinity displayed by **24** can be explained by analysis of the pharmacophore of the *mu* opioid site. Affinity to the *mu* opioid receptor site is increased by providing a relatively planar electron rich region at this position of the drug scaffold. Therefore, while the aromatic ring in **17** provides undesired steric bulk, the extra electron rich aromatic ring aids binding to the *mu* opioid receptor site.

Compound	**K_i (nM)**		
	μ	***κ***	***δ***
Morphine, **1**	1.8 ± 0.2	58 ± 8	160 ± 50
24	29 ± 7	1,000 ± 100	2,500 ± 300
25	320 ± 30	20,000 ± 1,100	530 ± 40
26	2,600 ± 300	70,000 ± 3,500	39,000 ± 7,500

Table 1.5 K_i values for morphine (**1**) and morphine-3-esters, **24**-**26**.

Modification at the secondary hydroxyl 6 position has a much lower effect on binding to the opioid receptor site relative to modification at the phenolic hydroxyl.[36, 37] Substitution at the 6 position with a methyl group for morphine and codeine has a very small effect on affinity to the *mu* receptor (Table 1.6).[36] Compound **27** which has a methoxy functional group at the 6 position exhibits slightly higher affinity to the *mu* opioid receptor site than morphine (**1**) with K_i values of 1.1 ± 0.5 and 1.7 ± 0.5 nM respectively. In comparison the same modification of morphine at the phenolic hydroxyl results in codeine (**2**) which has a binding affinity to the *mu* opioid receptor of approximately 370 times lower. The same trend is noted for the codeine derivative (**28**), substitution with a methoxy group at the 6 hydroxy position only has a minor effect on *mu* receptor affinity.

Compound	**K_i (nM)**		
	μ	***κ***	***δ***
Morphine, **1**	1.7 ± 0.5	65.5 ± 22.6	104.57 ± 27.18
27	1.1 ± 0.5	22.8 ± 11.0	65.8 ± 17.2
Codeine, **2**	727 ± 128	25,411 ± 10,015	52,207 ± 25,421
28	1,910 ± 930	5,430 ± 2,290	4,410 ± 1,500

Table 1.6 K_i values for morphine (**1**), codeine (**2**), **27** and **28**

Compound	K_i (nM)		
	μ	***κ***	***δ***
Morphine, **1**	6.22 ± 0.86	84.7 ± 4.01	218.0 ± 41.2
29	1.73 ± 0.26	157.0 ± 12.6	22.2 ± 3.4
30	17.7 ± 2.8	149.9 ± 12.2	84.9 ± 8.4
31	28.4 ± 5.2	832.9 ± 24.1	205.0 ± 10.2
32	30.1 ± 1.4	>10,000	68 ± 4.6

Table 1.7 K_i values for morphine (**1**) and morphine-6-esters, **29**-**32**

Marples and co-workers have synthesized a variety of morphine-6-esters along with examining their binding affinities to the opioid receptor (Table 1.7).[37] As expected modification at the 6 position has a much lower effect on the affinity relative to the phenolic hydroxyl. Compound **32** displayed the lowest affinity at 30.1 ± 1.4 nM which is almost 5 times lower than morphine at 6.22 ± 0.86 nM. It is interesting to note that a hydroxyl functional group on the aromatic ring at the *para* position (**29**) results in a compound with an affinity to the *mu* opioid receptor site of 1.73 ± 0.26 nM, over 3 times higher than the calculated value for morphine (**1**). Removal of the hydroxyl functional groups at the 3 and 6 positions of the morphine scaffold also has an effect on binding to the opioid receptor.[36, 38] There is a much greater effect upon removal of the phenolic hydroxyl relative to the secondary hydroxyl group. Removal of the phenolic hydroxyl at the 3 position for **33** lowers the ED_{50} over 2.5 times and the binding affinity by over 30 (Table 1.8).[38]

Compound	EC_{50} (nmol)	ED_{50} (μmol/kg)
Morphine, **1**	3.0	2.4 – 4.4
33	100	6.7 – 11.2

Table 1.8 EC_{50} and ED_{50} values for morphine (**1**) and **33**

In contrast removal of the secondary hydroxyl group at the 6 position has a much lower effect on the efficacy of the opioid derivatives.[36] Removal of the hydroxyl group at the 6 position for the morphine derivative **34** only has a minor effect on its affinity to the

mu opioid receptor with K_i values for morphine (**1**) and **34** of 1.7 ± 0.5 and 2.9 ± 1.1 nM respectively. In contrast there is a slight increase in affinity for the *mu* receptor for the codeine derivative, **35** with a K_i value of 305 ± 79 nM in comparison to codeine (**2**) at 727 ± 128 nM (Table 1.9).

Compound	**K_i (nM)**		
	μ	***κ***	***δ***
Morphine, **1**	1.7 ± 0.5	65.5 ± 22.6	104.57 ± 27.18
34	2.9 ± 1.1	45.5 ± 3.1	11.8 ± 3.1
Codeine, **2**	727 ± 128	25,411 ± 10,015	52,207 ± 25,421
35	305 ± 79	3090 ± 150	4,520 ± 710

Table 1.9 K_i values for morphine (**1**), codeine (**2**), **34** and **35**.

Removal of the the allylic double bond has only a small effect on binding to the *mu* receptor site (Table 1.10).[32] If the allylic double bond is removed from morphine for the dihydromorphine derivative (**36**) there is almost no change on the binding affinity to the *mu* opioid receptor site, with EC_{50} values of 194 ± 34 and 190 ± 35 nM respectively. For codeine (**2**) and its corresponding derivative, dihydrocodeine (**38**), the affinity is lowered by approximately half with EC_{50} values of 10,640 ± 840 and 20,350 ± 2,990 nM respectively.

Compound	**EC_{50} (nM)**
	(*μ*)
Morphine, **1**	194 ± 34
36	190 ± 35
37	51 ± 3
Codeine, **2**	10,640 ± 840
38	20,350 ± 2,990
39	2,230 ± 280

Table 1.10 EC_{50} values for morphine (**1**), codeine (**2**), **36**-**39**

Removal of the allylic double bond combined with formation of the ketone functional group results in a significant increase in the binding affinity to the *mu* receptor (Table 1.10).[32] Formation of the ketone functionality along with removal of the allylic double bond increases the affinity of the hydromorphone derivative (**37**) by almost four times. The EC_{50} value for morphine (**1**) is calculated at 194 ± 34 nM with the corresponding ketone derivative (**37**) at 51 ± 3 nM. A similar result is observed with the hydrocodone derivative (**39**), the affinity increases four fold.

Removal of the hydroxyl group at the 6 position combined with the removal of the allylic double bond has a significant effect on the analgesic activity and affinity of the opioid derivatives (Table 1.11).[34] Removal of these two functionalities from the opioid scaffold significantly increases the analgesic effects and affinity of the opioid derivatives. For the morphine derivative **40**, the ED_{50} is increased by almost 5 times while the IC_{50} increases by almost 7. A similar trend is noted for the codeine derivative **41**, with the ED_{50} increasing by almost 4 times and affinity by 5 times. Compounds **40**, **41** and **42** also display the expected trend *vide supra*, increasing steric "bulk" at the phenolic hydroxyl 3 postion leads to lower affinity to the receptor site.

Compound	**IC_{50} (nM)**	**ED_{50} (mg/kg)**
Morphine, **1**	27	0.26 – 0.83
Codeine, **2**	10,000	1.21 – 3.91
23	20,000	13.40 - 53.60
40	4	0.06 – 0.18
41	2,000	0.34 – 1.22
42	3,000	3.13 – 8.00

Table 1.11 IC_{50} and ED_{50} values for morphine (**1**), codeine (**2**), **23** and **40**-**42**

1.2.3 Amine Derivatives at the Hydroxyl Positions

Replacement of the oxygen atom by a nitrogen leads to a variety of novel opioid derivatives. Modifications of the opioid skeleton have been achieved at both the 3 phenolic and 6 hydroxyl positions (Fig 1.8). An examination of some modified morphine derivatives by Wentland and co-workers[39] have investigated if the NH_2 group is a suitable bioisoteric replacement of the phenolic functional group (Table 1.12).

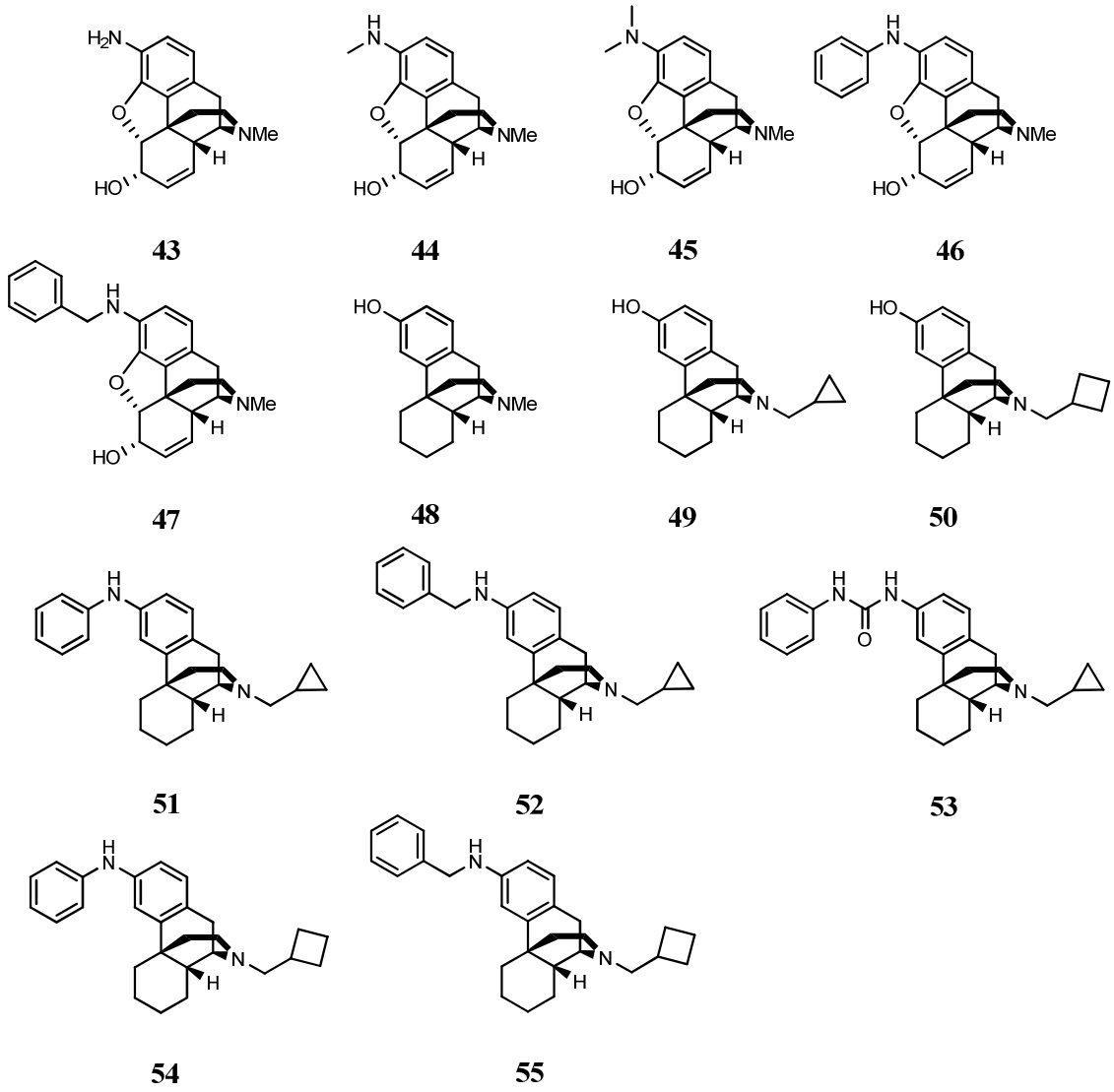

Fig 1.8 Structures of amine modified opioids at the phenolic 3 position

Replacement of the phenolic hydroxyl group by the NH_2 moiety lowered the affinity for the *mu* receptor from 0.88 ± 0.14 nM (morphine, **1**) to 53 ± 3 nM (**43**) corresponding to a lower affinity of approximately 60 times. If an aromatic ring is connected to the nitrogen this increases the affinity. The *mu* affinity of **44** at 63 ± 15 nM is almost doubled if the methyl group is replaced by an aromatic ring as in compound **47** at 33 ± 5.1 nM. This would be expected as a similar pattern is noted for codeine (**1**) and the closely related aromatic derivative (**24**).

Compound	**K_i (nM)**		
	μ	***κ***	***δ***
Morphine, **1**	0.88 ± 0.14	24 ± 2.3	140 ± 18
43	53 ± 3	740 ± 75	2,400 ± 190
44	63 ± 15	2,800 ± 420	5,700 ± 1,100
45	240 ± 16	290 ± 8.1	1,600 ± 110
46	59 ± 3.7	240 ± 23	1,500 ± 100
47	33 ± 5.1	3,400 ± 540	5,500 ± 190

Table 1.12 K_i values for morphine (**1**) and **43**-**47**

A selection of further amine modified opioid derivatives at the 3 phenolic position were synthesised and analysed by Decker and co-workers.[40] Decker studied amine modified opioids based on levorphanol (**48**), cyclorphan (**49**) and butorphan (**50**). Levorphanol (**48**) is a structural derivative of morphine in which the oxygen bridge from the D ring is removed along with the hydroxyl at the 6 position. Levorphanol (**48**) cylorphan (**49**) and butorphan (**50**) have potent affinities to the *mu* opioid receptor site with K_i values of 0.21 ± 0.2 nM, 0.062 ± 0.003 nM and 0.23 ± 0.01 nM respectively (Table 1.13).[41]

Compound	**K_i (nM)**		
	μ	***κ***	***δ***
Morphine, **1**	0.88 ± 0.14	24 ± 2.3	140 ± 18
Levorphanol, **48**	0.21 ± 0.2	2.3 ± 0.3	4.2 ± 2.3
49	0.062 ± 0.003	0.034 ± 0.002	1.9 ± 0.1
50	0.23 ± 0.01	0.079 ± 0.003	5.9 ± 0.6

Table 1.13 K_i values for, morphine (**1**) and **48**-**50**

Compound	**K_i (nM)**		
	μ	***κ***	***δ***
Cyclorphan, **49**	0.062 ± 0.003	0.034 ± 0.002	1.9 ± 0.1
51	0.26 ± 0.012	0.34 ± 0.031	29 ± 4.4
52	0.080 ± 0.005	0.047 ± 0.0035	5.4 ± 0.11
53	3.9 ± 0.28	1.6 ± 0.15	16 ± 1.5
Butorphan, **50**	0.23 ± 0.01	0.079 ± 0.003	5.9 ± 0.6
54	1.7 ± 0.24	1.5 ± 0.17	39 ± 3.5
55	1.7 ± 0.053	2.8 ± 0.33	130 ± 11

Table 1.14 K_i values for compounds **49**-**55**

Cyclorphan (**49**) exhibits a much higher affinity to the *mu* receptor due to the cyclopropylmethyl functional group on the nitrogen. This correlates with the results observed for compound **20**. Decker and co-workers observed a similar result to Wentland, that replacement of the phenolic hydroxyl at the 3 position by a selection of amine functional groups resulted in lower affinity to the *mu* receptor site (Table 1.14). The calculated K_i values for the *mu* receptor for cyclorphan (**49**) and its related amine derivatives **51**, **52** and **53** are 0.062 ± 0.003, 0.26 ± 0.012, 0.080 ± 0.005 and 3.9 ± 0.28 nM respectively.

Amine modification at the hydroxyl 6 position of the opioid skeleton has focused primarily on the β-naltrexamine opioid derivatives (Fig 1.9). Along with modification of the hydroxyl at the 6 position the naltrexamine derivatives also have the allylic

double bond reduced and a new hydroxyl group substituted at the 14 position. Reduction of the allylic double bond has shown to have little effect on the binding affinity of opioids to the receptor site (Table 1.10).[32]

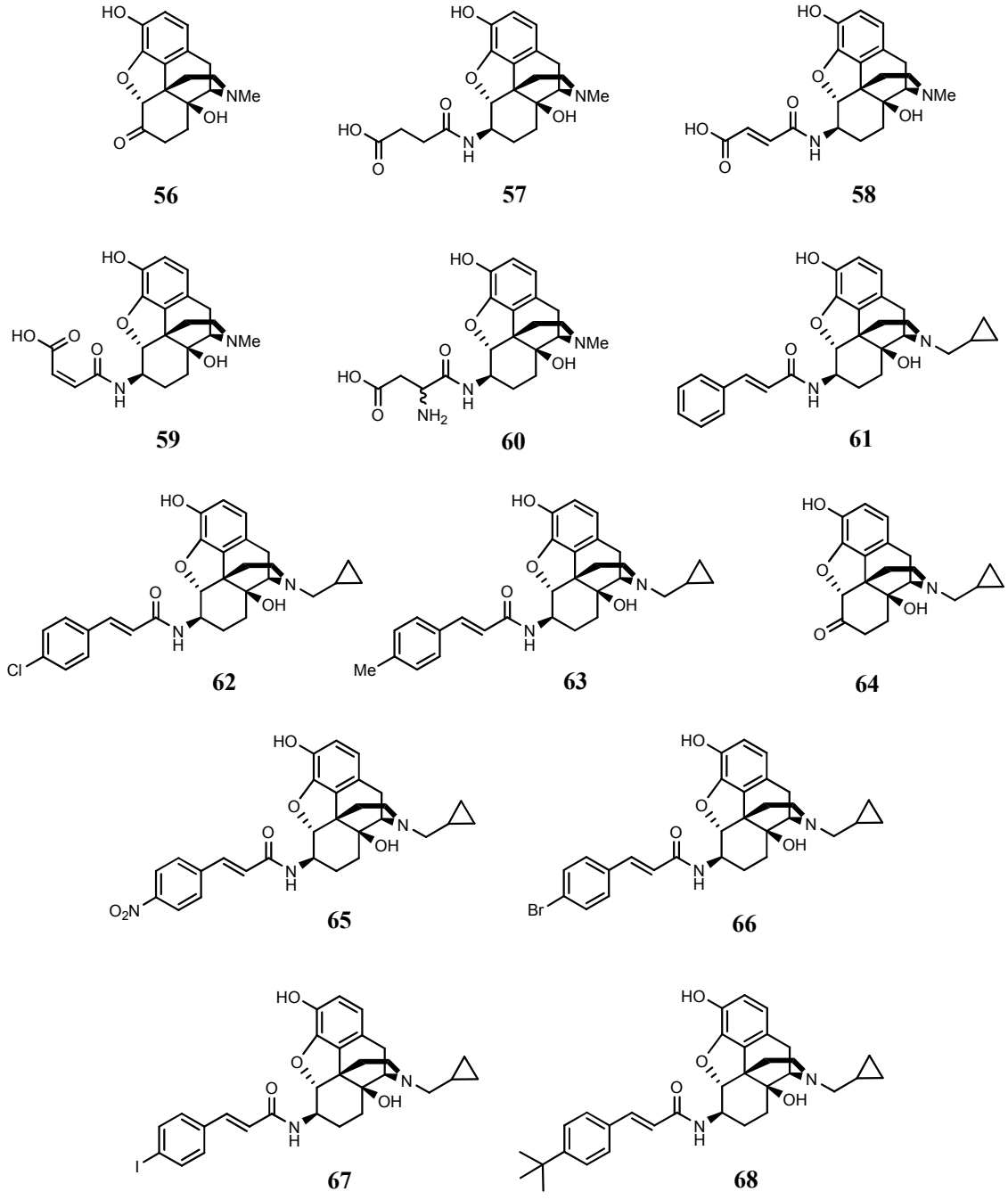

Fig 1.9 Structures of amide opioids

Substitution of a hydroxyl at the 14 position also has a small effect on the analgesic activity (Table 1.15).[6, 42] Substitution of a hydroxyl group at the 14 position almost doubles the analgesic activity with respect to compounds **37** and oxymorphone (**56)** with ED_{50} values of 0.3 and 0.17 mg/kg respectively.

Compound	**ED_{50} (mg/kg)**
Morphine, **1**	2.1
37	0.3
Oxymorphone, **56**	0.17

Table 1.15 ED_{50} value for morphine (**1**), **37** and **56**

Bostros and co-workers synthesised and analysed a variety of amide derivatives based on β-naltrexamine (Table 1.16).[43] Formation of the amide bond at the 6 position results in opioid derivatives with significant binding to the receptor site. It is also significant to note that the *cis* derivative (**59**) results in a lower IC_{50} value than the corresponding *trans* derivatives (**58**) at values of 39 ± 22 and 130 ± 60 nM respectively.

Compound	**IC_{50} (nM)**	**ED_{50} (µmol/kg)**
57	144 ± 94	9.6 - 10.0
58	130 ± 60	ND
59	39 ± 22	3.0 – 31.8
60	31 ± 10	< 20

Table 1.16 IC_{50} and ED_{50} values for **57**-**60**, (ND, not determined)

Further amide derivatives also exhibit relatively high binding to the *mu* opioid receptor site (Table 1.17).[44] Relatively high affinity to the receptor site is noted for compounds with the aromatic ring present on the amide functional group. However it should be noted that further substitution on the aromatic ring has a detrimental effect on potency of the opioid compound. For the unmodified aromatic ring derivative (**61**) the K_i value is calculated at 0.07 nM. If a chlorine atom is substituted into the aromatic ring (**62**) the

affinity is lowered to 0.1 nM, while inserting a methyl group (**63**) lowers the affinity to 0.23 nM.

Compound	**K_i (nM)**		
	μ	***κ***	***δ***
61	0.07	0.2	3.1
62	0.1	0.2	5.0
63	0.23	0.6	9.6
65	0.2	0.8	5.1

Table 1.17 K_i values for **61**-**63** and **65**.

Ghirmai and co-workers have investigated further amide derivatives (Table 1.18).[45] As expected formation of the amide functional group at the 6 hydroxyl position only results in a slight effect on the binding affinity to the *mu* opioid receptor. Relative to naltrexone (**64**) at a K_i value of 0.30 ± 0 nM the amide functionalized opioids **62**, **66**, **67** and **68** exhibit K_i values of 0.61 ± 0.09, 0.88 ± 0.10, 0.82 ± 0.10 and 1.09 ± 0.20 nM respectively. As noted by Derrick and co-workers[44] increasing modification of the aromatic ring results in lower affinity. The *t*-butyl derivative (**68**) exhibits the lowest affinity at 1.09 ± 0.20 nM.

Compound	**K_i (nM)**		
	μ	***κ***	***δ***
Naltrexone, **64**	0.30 ± 0	0.81 ± 0.02	16.31 ± 1.10
62	0.61 ± 0.09	0.23 ± 0.03	2.6 ± 0.3
66	0.88 ± 0.10	0.29 ± 0.04	2.2 ± 0.3
67	0.82 ± 0.10	0.37 ± 0.05	1.4 ± 0.2
68	1.09 ± 0.20	0.37 ± 0.06	1.4 ± 0.1

Table 1.18 K_i values for, **62**, **64** and **66**-**68**

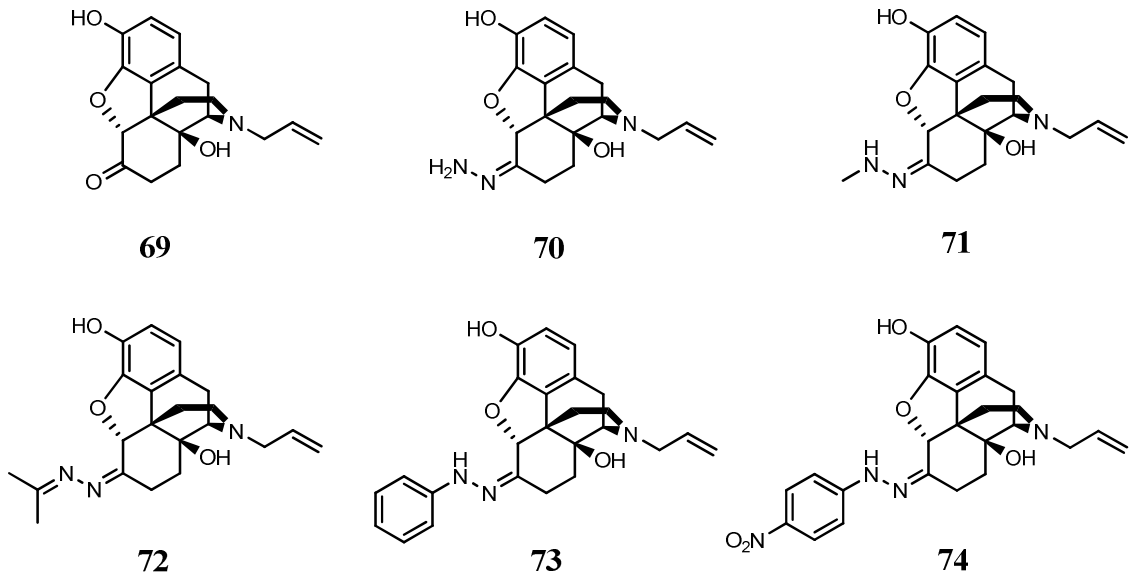

Fig 1.10 Structures of hydrazone based opioids

Another approach for modification of the secondary hydroxyl at the 6 position is the formation of hydrazone derivatives (Fig 1.10).[46, 47] Hahn and co-workers have synthesised a selection of hydrazone derivatives based on modification of naloxone (**69**) and oxymorphone (**56**).[47] Formation of the hydrazone functional group at the 6 hydroxy position does not have a significant effect on binding to the receptor site for the naloxone based compounds (Table 1.19). For naloxone (**69**) and **70** the IC_{50} values are almost identical at 3.1 ± 1.5 and 3.0 ± 1.1 nM respectively. The highest affinity is observed for **71** at 1.1 ± 0.5 nM while the lowest is observed **74** at 8.0 ± 1.7 nM.

Compound	**IC_{50} (nM) (μ)**
Naloxone, **69**	3.1 ± 1.5
70	3.0 ± 1.1
71	1.1 ± 0.5
72	1.8 ± 0.2
73	7.5 ± 2.5
74	8.0 ± 1.7

Table 1.19 IC_{50} values for naloxone (**69**) and **70-74**

1.2.4 A-Ring Modification

Research has shown that substitution of the aromatic A-ring on the opioid scaffold at the 1 and 2 positions results in a marked decrease affinity to the opioid receptor (Fig 1.11).[5, 6] The bromocodeine (**75**) and chlorocodeine (**76**) derivatives exhibit only about half the analgesic activity of the parent codeine (**2**) molecule. The presence of an acetyl group at the 1 position for acetocodeine (**77**) also results in a significant decrease in analgesic action. Lousberg and co-workers[48] also investigated the effect of a fluorine atom at the 1 position of the codeine scaffold (**78**). The resulting ED_{50} values for fluorocodeine (**78**) at 7.9 mg/kg and codeine (**2**) at 7.5 mg/kg suggest that the decrease in analgesic potency from substitution of the aromatic A-ring is strongly influenced by the steric bulk of the functional group attached (Table 1.20).

Compound	**ED_{50} (mg/kg)**
Codeine, **2**	7.5
78	7.9

Table 1.20 ED_{50} values for codeine (**2**) and **78**

Substitution at the 2 position for the levorphanol type derivatives (**79**, **80**) also show a significant decrease in analgesic activity. The placement of a methyl group at the 2 position of levorphanol (**48**) results in an increase in the ED_{50} value of over 18 times with values of 0.5 mg/kg and 9.1 mg/kg for levorphanol (**48**) and **80** respectively (Table 1.21).[6] The calculated ED_{50} value for **80** is over 20 times higher than levorphanol (**48**) at 2.9 - 5.0 mg/kg and 0.06 - 0.22 mg/kg respectively (Table 1.22).[49]

Compound	**ED_{50} (mg/kg)**
Morphine, **1**	2.1
Codeine, **2**	14.2
Levorphanol, **48**	0.5
79	9.1

Table 1.21 ED_{50} values for morphine (**1**), codeine (**2**), **48** and **79**

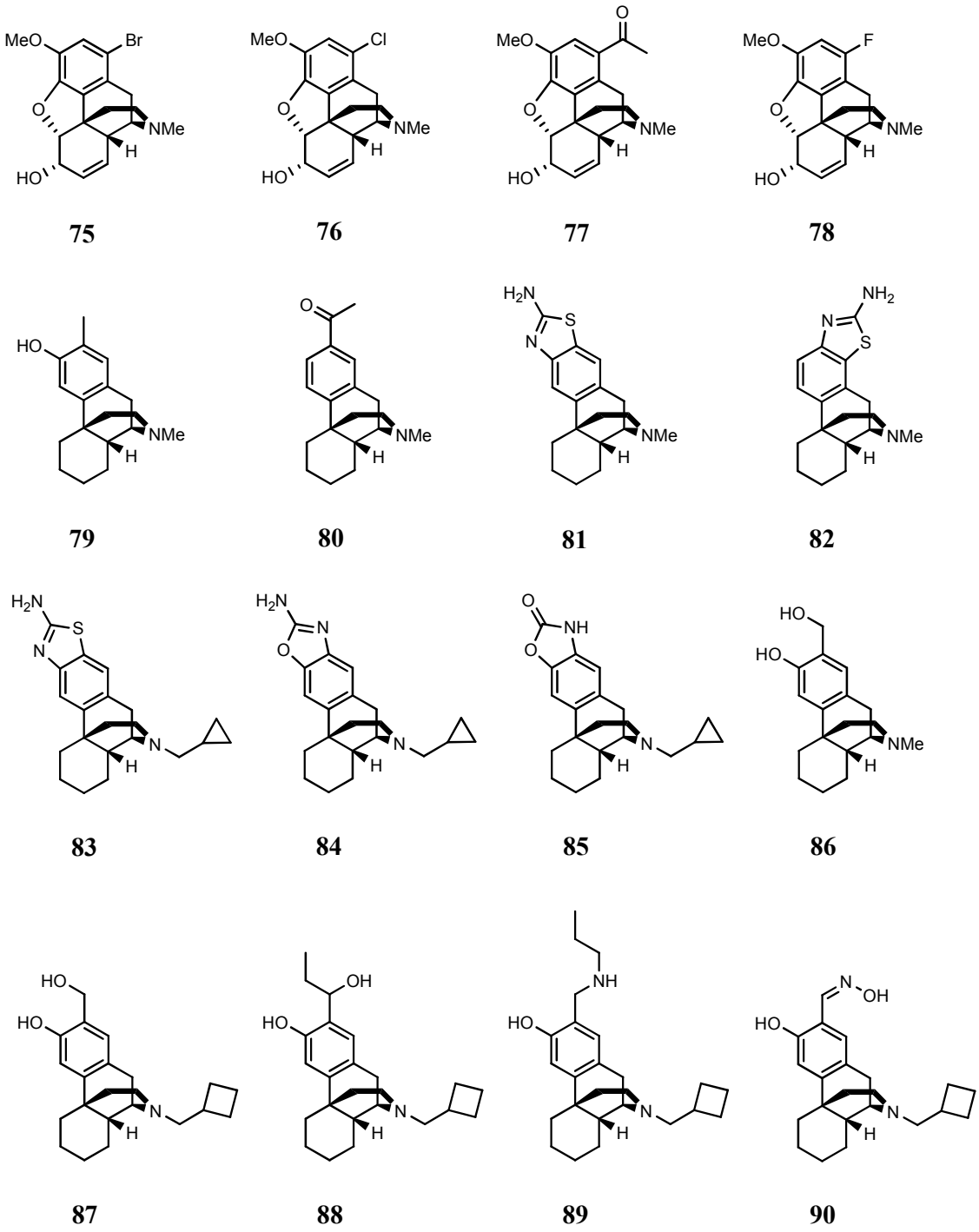

Fig 1.11 Structures of A-ring modified opioids

The binding affinity to the *mu* opioid receptor is also much lower for **80** with respect to levorphanol (**48**) at IC_{50} values of 13,000 nM and 4 nM respectively. However it should

be noted that compound **80** also lacks the phenolic hydroxyl at the 3 position which has been shown previously (Table 1.8, **33**) to be important in binding to the receptor site.

Compound	**IC_{50} (nM) (μ)**	**ED_{50} (mg/kg)**
Morphine, **1**	27	0.26 – 0.83
Codeine, **2**	10,000	1.40 – 4.45
Levorphanol, **48**	4	0.06 – 0.22
80	13,000	2.9 – 5.0

Table 1.22 IC_{50} and ED_{50} values for morphine (**1**), codeine (**2**), **48** and **80**

The aminothiazole type morphinans (**81-83**) also provide additional information on the effect A-ring substitution has on drug receptor interactions.[41, 50] The formation of an aminothiazole at 2/3 position of the aromatic A-ring (**81**) results in the affinity for the *mu* receptor decreasing by over 5 times with respect to levorphanol (**48**). The calculated K_i values for **81** and levorphanol (**48**) are 1.1 ± 0.1 and 0.21 ± 0.02 nM respectively (Table 1.23).[41]

Compound	**K_i (nM)**		
	μ	κ	δ
Morphine, (**1**)	0.88 ± 0.14	24 ± 2	140 ± 18
Levorphanol, (**48**)	0.21 ± 0.02	2.3 ± 0.3	4.2 ± 2.3
81	1.1 ± 0.1	6.4 ± 0.5	190 ± 10
82	130 ± 6	29 ± 1	1100 ± 30

Table 1.23 K_i values for morphine (**1**), **48**, **81** and **82**

However, if the aminothiazole ring is in the 1/2 position on the aromatic ring (**82**) the affinity for the *mu* receptor is decreased by over 600 times with respect to levorphanol (**48**). Modification of the fused aminothiazole ring system to compounds **84** and **85** results in lower affinity to the receptor site with respect to **83** (Table 1.24).[50] The affinities to the *mu* opioid recptor site for **83**, **84** and **85** were calculated at 1.5 ± 0.1,

150 ± 5.1 and 160 ± 21 nM respectively. The affinities for the *kappa* receptor for **83**, **84** and **85** were calculated at 0.049 ± 0.005, 52 ± 1.0 and 47 ± 1.6 nM respectively.

Compound	**K_i (nM)**		
	μ	***κ***	***δ***
Cyclorphan, **49**	0.062 ± 0.003	0.034 ± 0.002	1.9 ± 0.072
83	1.5 ± 0.2	0.049 ± 0.005	29 ± 2
84	150 ± 5.1	52 ± 1.0	ND
85	160 ± 21	47 ± 1.6	ND

Table 1.24 K_i values **49** and **83**-**85** (ND, not determined)

Decker and co-workers have synthesized and analysed a variety of butorphan (**50**) based opioids with modifications at the 2 position of the aromatic A-ring (Table 1.25). Depending on the functional group attached to the A-ring the affinity to the *mu* opioid receptor site is reduced by between 1,500 times (**87**) and over 16 times (**90**) with respect to butorphan (**50**). The affinity to the *kappa* receptor is also reduced with calculated K_i values for butorphan (**50**), **87** and **88** of 0.079 ± 0.003, 86 ± 2.2 and 72 ± 3.1 nM respectively.

Compound	**K_i (nM)**		
	μ	***κ***	***δ***
Butorphan, **50**	0.23 ± 0.01	0.079 ± 0.003	5.9 ± 0.55
86	15 ± 1.5	40 ± 4.2	1,400 ± 121
87	360 ± 27	86 ± 2.2	>10, 000
88	180 ± 21	72 ± 3.1	>10,000
89	330 ± 55	350 ± 20	>10,000
90	3.8 ± 0.46	0.62 ± 0.058	180 ± 11

Table 1.25 K_i values **50** and **86**-**90**

1.2.5 Bivalent Opioid Derivatives

The formation of bivalent opioid ligands is an important aspect of modern opioid drug research.[51-53] The presence of two pharmacophores within an opioid ligand, which can interact with more than one receptor site, dramatically enhances the therapeutic range of opioid drugs. As the opioid receptor contains three distinct subtypes (μ, κ, δ)[7-9] along with homodimer[10-12] (μ-μ, κ-κ, δ-δ) and heterodimer[13-15] (μ-δ, μ-κ) sites, the interaction of bivalent opioids leads to unique benefits over the corresponding monovalent equivalents. The presence of a second opioid pharmacophore with a distinct binding profile can lead to opioid drugs with improved analgesia, reduced side effects and a decrease in opioid analgesic tolerance.[54] The variety of bivalent opioid drugs includes peptide derivatives (**91**)[55], morphine type derivatives (**9**)[52] and mixed type ligands (**92**) (Fig 1.12).[53, 56]

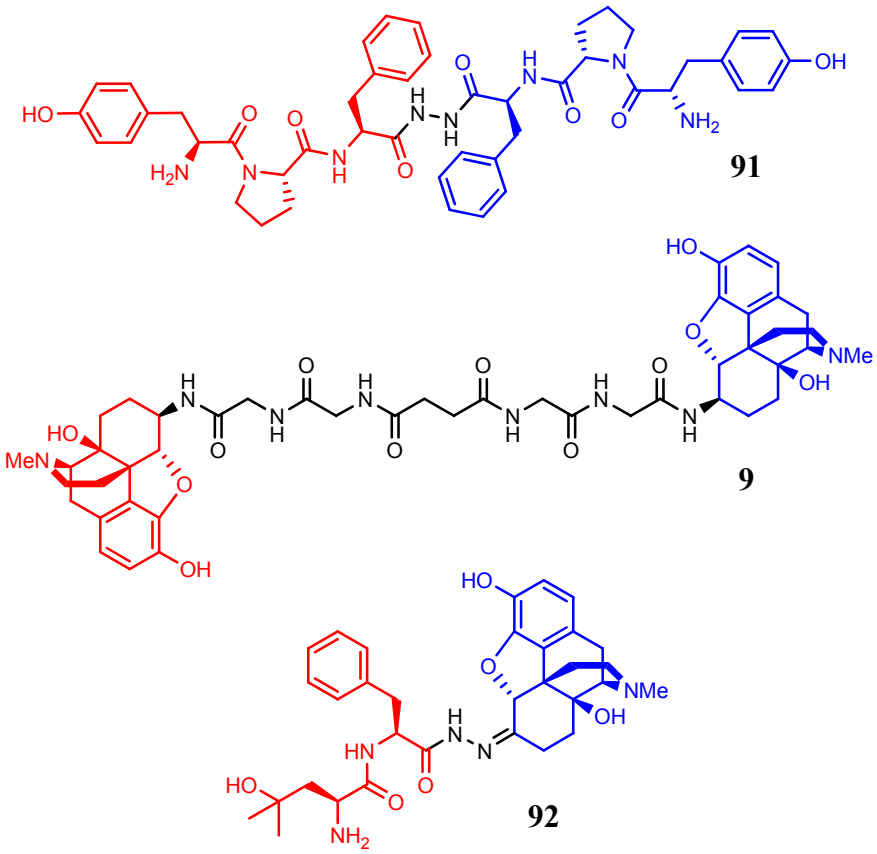

Fig 1.12 Structures of bivalent opioids **9**, **91** and **92** with two pharmacophores

An in depth discussion of the biological interaction of bivalent ligands with the opioid receptor is beyond the scope of this review. However it is relevant to examine the binding affinities and analgesic effects from a structure activity relationship aspect. Of particular interest for this research project is the bivalent opioid compounds based on the morphine scaffold which are linked through the 3 and 6 positions.

A series of bivalent opioid compounds, based on modification at the 3 position of cyclorphan (**49**) and butorphan (**50**) have been synthesized and evaluated for their binding affinity to the μ, κ and δ opioid receptors.[57] Neumeyer and co-workers have investigated a variety of bivalent opioid compounds (Fig 1.13) based on butorphan (**50**) and linked *via* ester and ether spacers (Table 1.26).[58] The length of the spacer group has an effect on binding to the receptor site. The affinity for the *mu* opioid receptor of **93** is over two times higher than **95** at K_i values of 29 ± 1.2 and 66 ± 4.3 nM respectively. The affinity for the *kappa* receptor is over six times higher when the carbon chain spacer is shortened from ten carbons (**95**) to four carbons (**93**). The same result is observed with the ester linked compounds **94** and **96** with K_i values at the *mu* opioid receptor site of 0.16 ± 0.01 and 0.090 ± 0.004 nM respectively. The ester linked compounds **94** and **96** also exhibit much higher affinities to the opioid receptor than the corresponding ether linked ligands **93** and **95**.

Compound	**K_i (nM)**		
	μ	***κ***	***δ***
Butorphan, **50**	0.23 ± 0.01	0.079 ± 0.003	5.9 ± 0.55
93	29 ± 1.2	18 ± 1.3	730 ± 29
94	0.16 ± 0.01	0.076 ± 0.002	9.4 ± 0.44
95	66 ± 4.3	120 ± 8.2	2,500 ± 91
96	0.090 ± 0.004	0.049 ± 0.001	4.2 ± 0.44
97	0.23 ± 0.22	0.070 ± 0.03	44 ± 6.8
98	4.7 ± 0.64	4.2 ± 0.81	400 ± 46
99	3.3 ± 0.26	3.4 ± 0.08	920 ± 95

Table 1.26 K_i values for **50** and **93-99**

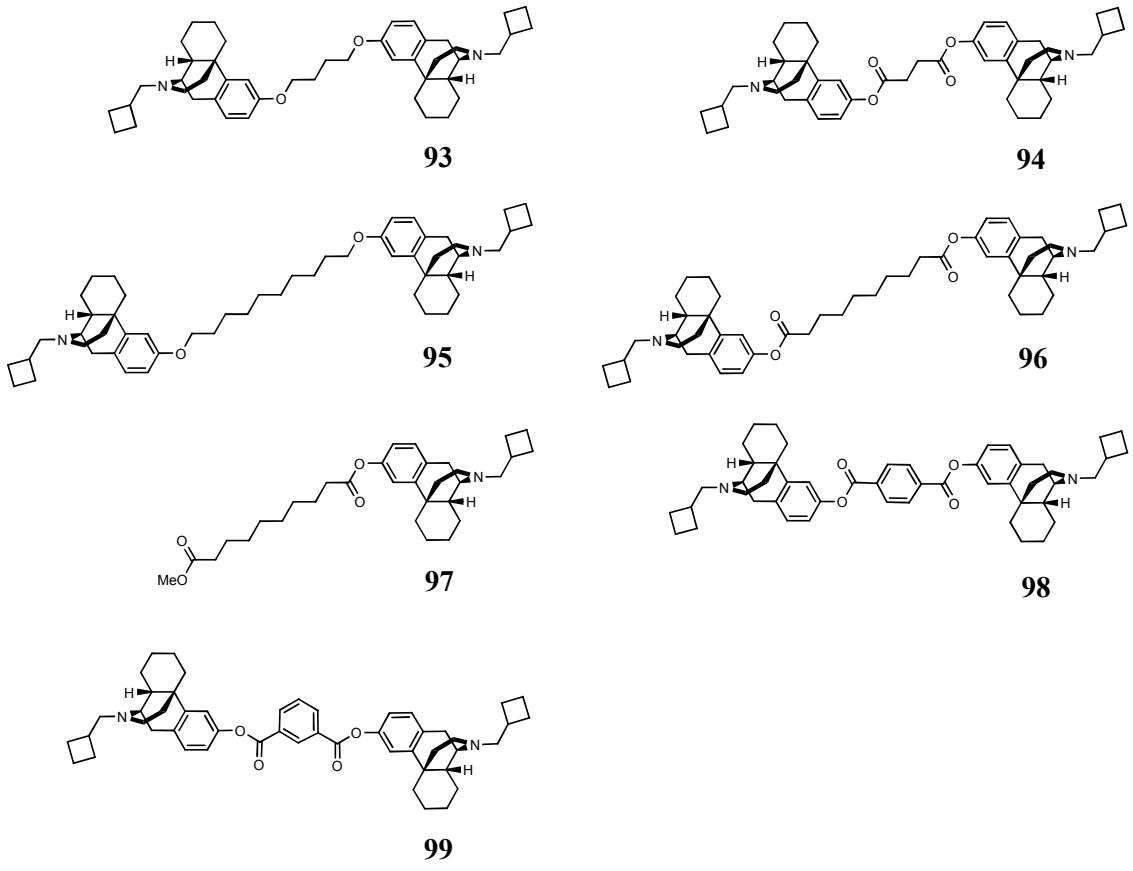

Fig 1.13 Structures of bivalent opioids based on butorphan linked through the 3 positions

The K_i value at the *mu* receptor for the ether linked compound **93** is over 180 times lower than the corresponding ester derivative **94**. Compound **94** also exhibits a higher affinity to the *mu* opioid receptor than the non-linked butorphan (**50**). The non-linked derivative **97** displays a binding affinity to the *mu* receptor of 0.23 ± 0.22 nM which is identical to butorphan (**50**) at 0.23 ± 0.01 nM. Therefore the presence of a second pharmacophore introduced by the bivalent ligand **94** has an effect on the affinity to the *mu* opioid receptor. Introduction of an aromatic ring in the spacer moiety lowers that affinity for the *mu* opioid receptor with respect to **94**. The calculated K_i values for the *mu* receptor for **94**, **98** and **99** are 0.16 ± 0.01, 4.7 ± 0.64 and 3.3 ± 0.26 nM.

Fulton and co-workers have investigated further varieties of bivalent opioids (Fig 1.14) linked through the 3 position of the aromatic ring (Table 1.27).[59] If the length of the carbon spacer is reduced, as in **100**, the affinity to the *mu* opioid receptor is increased

with respect to the butyl linked compound (**93**). Introduction of a hydroxyl functional group within the spacer unit also increases the affinity to the *mu* receptor.

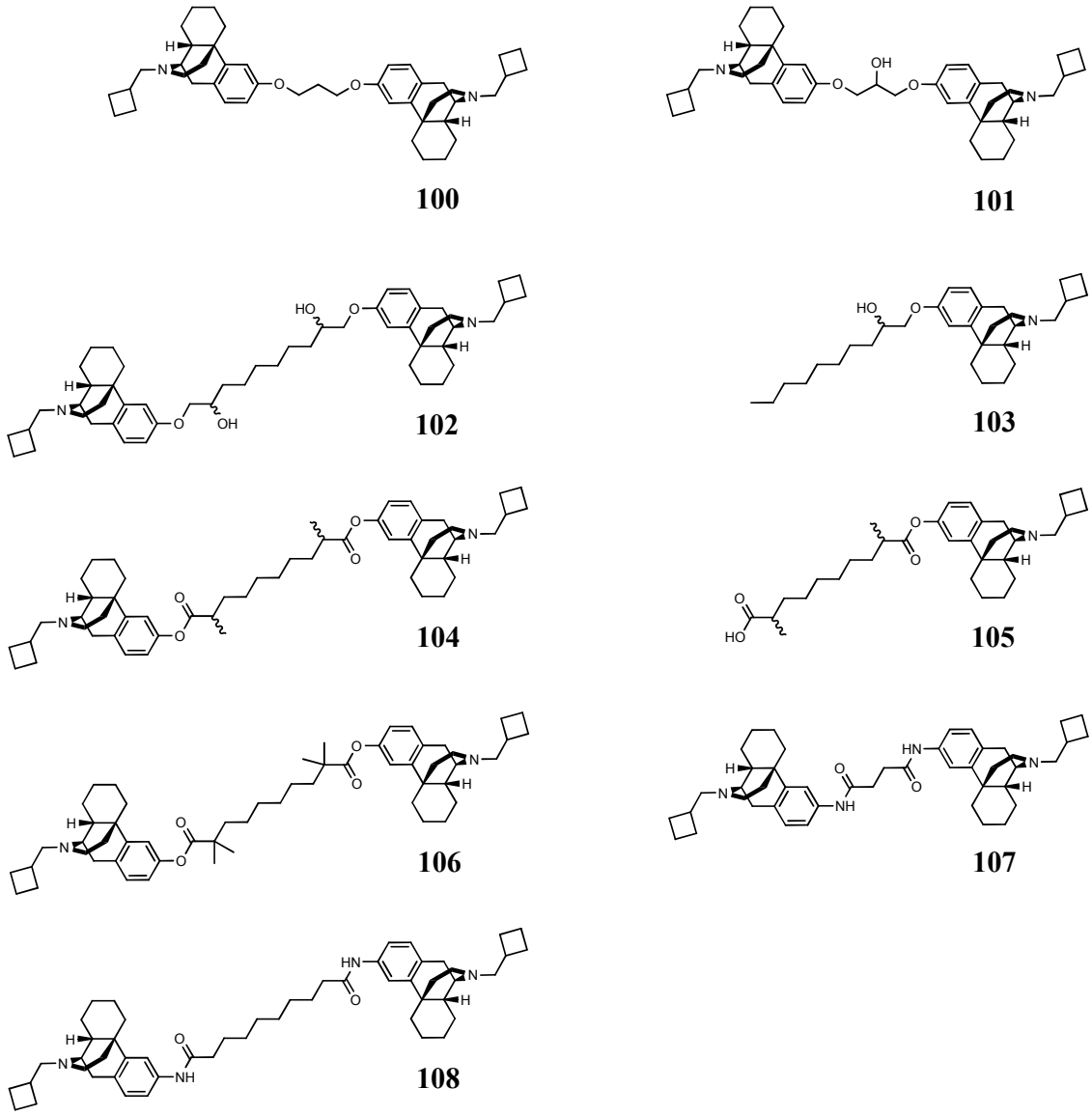

Fig 1.14 Structures of bivalent opioids linked through the 3 position

Compound **100** exhibits a K_i value of 7.1 ± 0.19 nM, however when a hydroxyl group is introduced into the spacer unit the affinity is increased over seven times, as in **101** at 0.95 ± 0.16 nM. The bivalent opioid (**102**) has a greater affinity to the *mu* opioid receptor than the equivalent monovalent ligand (**103**) at K_i values of 2.4 ± 0.43 and 7.4 ± 0.26 nM respectively.

Compound	K_i (nM)		
	μ	***κ***	***δ***
Butorphan, **50**	0.23 ± 0.01	0.079 ± 0.003	5.9 ± 0.55
100	7.1 ± 0.19	6.2 ± 0.53	180 ± 3.3
101	0.95 ± 0.16	0.99 ± 0.022	37 ± 3.3
102	2.4 ± 0.43	120 ± 8.2	27 ± 1.9
103	7.4 ± 0.26	8.3 ± 0.68	52 ± 2.8

Table 1.27 K_i values for **50** and **100**-**103**

Substitution of methyl groups into the carbon spacer moiety for the ester linked bivalent opioids (Fig 1.14) lowers the affinity to the *mu* opioid receptor (Table 1.28).[60] The calculated K_i values for the *mu* receptor for **96** and **104** are 0.090 ± 0.004 and 0.95 ± 0.057 nM respectively corresponding to over 10 times lower affinity with substitution of a methyl group in the spacer region.

Compound	K_i (nM)		
	μ	***κ***	***Δ***
Butorphan, **50**	0.23 ± 0.01	0.079 ± 0.003	5.9 ± 0.55
96	0.090 ± 0.004	0.049 ± 0.001	4.2 ± 0.44
104	0.95 ± 0.057	0.62 ± 0.071	37 ± 1.8
105	0.46 ± 0.024	0.42 ± 0.0081	20 ± 0.074
106	0.47 ± 0.027	0.47 ± 0.046	15 ± 0.86

Table 1.28 K_i values for **50**, **96** and **104**-**106**

Peng and co-workers have examined some bivalent opioid ligands (Fig 1.14) linked by amide bonds (Table 1.29).[61] Affinity to the *mu* opioid receptor site is lowered if the ester bonds linker are replaced with amides. **107** has a K_i value of 3.3 ± 0.3 nM which is over 20 times higher than the ester analogue **94** at 0.16 ± 0.01 nM. The same trend is noted when the spacer length is increased as in compounds **96** and **108**.

Compound	K_i (nM)		
	μ	***κ***	***Δ***
Butorphan, **50**	0.23 ± 0.01	0.079 ± 0.003	5.9 ± 0.55
94	0.16 ± 0.01	0.076 ± 0.002	9.4 ± 0.44
96	0.090 ± 0.004	0.049 ± 0.001	4.2 ± 0.44
107	3.3 ± 0.3	3.8 ± 0.4	ND
108	5.7 ± 0.1	7.5 ± 1.0	38 ± 3.7

Table 1.29 K_i values **50**, **94**, **96**, **107** and **108** (ND, not determined)

Formation of bivalent opioids at the 6 position of the morphine scaffold has focused on naltrexamine and oxymorphamine derivatives.[62, 63] Portoghese and co-workers have synthesised a selection of bivalent opioid ligands (Fig 1.15) and investigated the binding affinity to the μ, κ and δ opioid receptors (Table 1.30).[64]

Compound	K_i (nM)		
	μ	***κ***	***Δ***
9	14 ± 3	460 ± 78	50 ± 2
109	50 ± 10	500 ± 45	100 ± 45
110	44 ± 7	590 ± 118	110 ± 10
111	180 ± 41	6,400 ± 262	480 ± 32
113	34 ± 3	1,000 ± 128	26 ± 4

Table 1.30 K_i values for **9**, **109**-**111** and **113**

Compound **9** exhibits the highest affinity for the *mu* receptor at 14 ± 3 nM. If the spacer length is increased (**113**) or decreased (**110**) the affinity for the *mu* receptor is lower, with values for **113** and **110** of 34 ± 3 and 44 ± 7 nM respectively. The affinity for the *mu* receptor for the bivalent opioid, **9** is 12 times higher than the related monomer derivative (**111**).

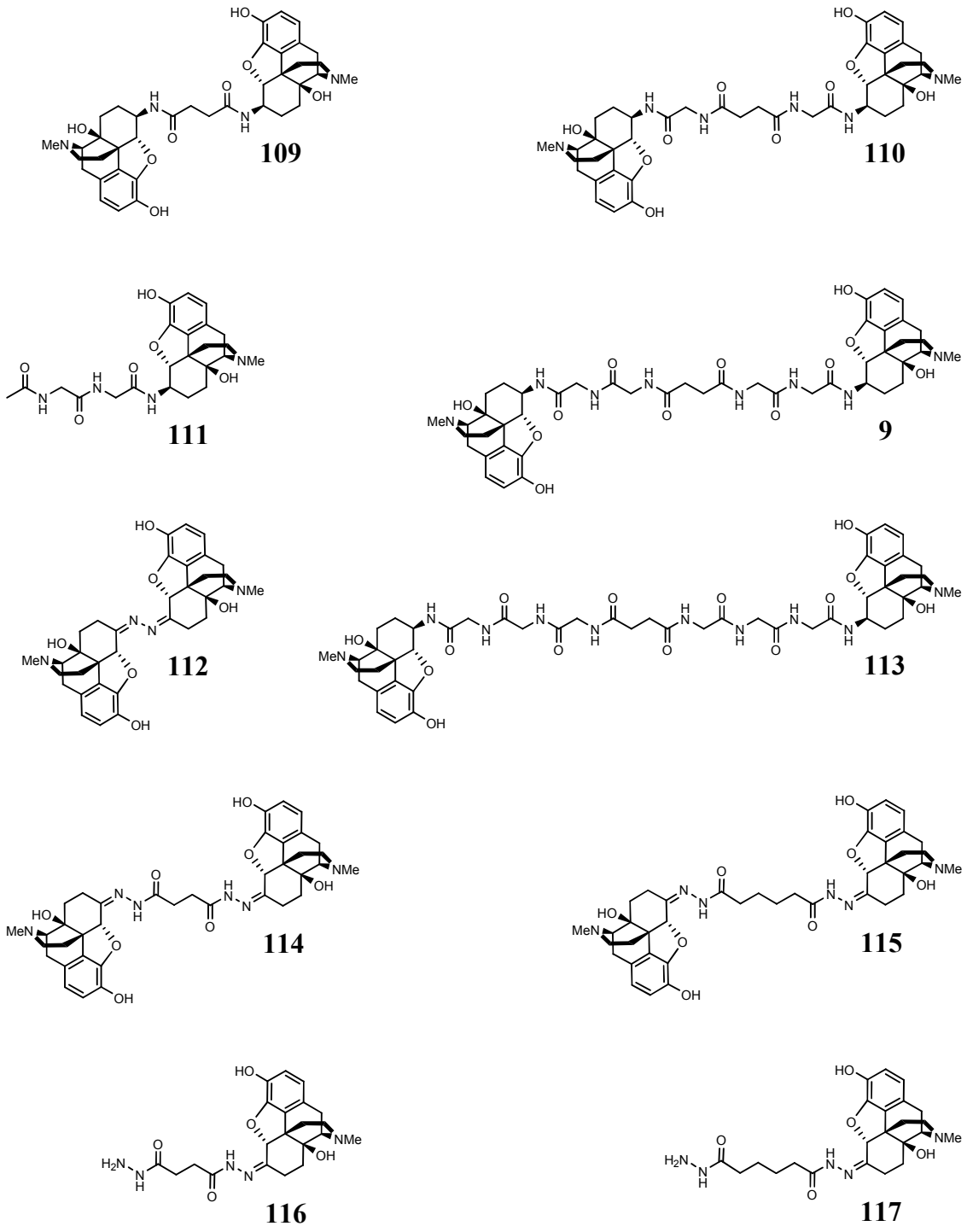

Fig 1.15 Structures of bivalent opioids linked through the 6 position

Another selection of bivalent opioids have been generated based on opioid azine linked derivatives (Fig 1.15).[65, 66] Hahn and co-workers have synthesised a variety of oxymorphone based bivalent opioid ligands and analysed the binding affinity to the μ, κ

and δ opioid receptors (Table 1.31).[66] The binding affinity to the opioid receptors for the azine linked bivalent ligands are identical to the parent opioid compounds. The highest affinity to the *mu* receptor was noted for **115** at 1.4 ± 0.2 nM while the lowest was **112** at 1.8 ± 0.6 nM. No difference was observed in the binding affinities for the bivalent ligands (**114**, **115**) and the related monomers (**116**, **117**)

Compound	**IC_{50} (nM)**		
	μ	***κ***	***Δ***
Oxymorphone, **56**	1.8 ± 0.6	1.0 ± 0.4	4.9 ± 2.7
112	1.8 ± 0.6	1.2 ± 0.6	2.9 ± 1.2
114	1.6 ± 0.4	2.4 ± 0.6	21.6 ± 17
115	1.4 ± 0.2	2.0 ± 0.4	3.9 ± 0.2
116	1.6 ± 0.6	0.7 ± 0.6	7.4 ± 3.0
117	1.4 ± 0.2	1.8 ± 0.1	9.7 ± 1.2

Table 1.31 K_i values for **56**, **112** and **114-117**

1.3 Conclusion

The morphine based opioid alkaloids are hugely important to modern medicine due to their potent analgesic effects. However the powerful analgesic effects are coupled with possible severe side effects including decreased gastrointestinal motility, physical dependence and respiratory depression. Therefore a major research initiative has been undertaken to develop a variety of opioid analogues which will retain the potent analgesic properties without the detrimental side effects. As such there is a substantial volume of literature in relation to SAR (structure activity relationship) analysis of the opioid scaffold. Of particular interest for this project is the morphine derivatives based on modification at the phenol, secondary alcohol and nitrogen positions (3, 6 and 17 respectively). Information in relation to modification of the A-ring of the morphine scaffold along with the formation of "linked" morphine based bivalent ligands is also highly relevant.

The tertiary nitrogen present within morphine is vital for analgesic activity. In general modification at the 17 position of the morphine scaffold has been shown to lower the potency of the parent compound however substitution with a cyclopropylmethyl group (**20**) has been shown to enhance the activity. Modification at the phenol hydroxyl group has a major effect on the receptor affinity while the secondary alcohol has only a minor influence. Substitution at the aromatic ring lowers the affinity to the receptor site especially substitution at the 1 position of the opioid scaffold. Formation of "linked" opioid compounds can lead to bivalent opioid ligands which contain two pharmacophores linked by a spacer unit. The affinity of the bivalent opioids is dependant on the distance between the two pharmacophores as well as the functional groups present along the spacer unit.

The following chapters outline the synthesis of a series of novel opioid derivatives along with analysis of their *mu* opioid receptor and metal binding affinities. The information provided by this chapter can be utilised to assist the prediction of the opioid receptor properties of these novel opioid derivatives along with methods to selectively control the binding affinity.

Chapter 2

Synthesis and Structural Characterisation of Ester and Ether Linked Codeine Derivatives

2.1 Introduction

This chapter details the synthesis of a series of novel opioid derivatives based on structural modification of codeine (**2**) to form linked di-codeine derivatives. Both ester and ether linked derivatives are included along with their structural characterisation. Previous studies on opioid derivatives[37, 67, 68] have shown that it is possible to convert the secondary alcohol bond at the 6 position (Fig 2.1) to an ester or ether moiety.

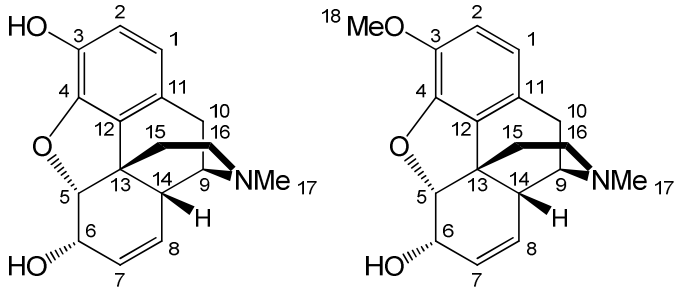

1 **2**

Fig 2.1 Structure of morphine (**1**) and codeine (**2**)

If we take this process further it should be possible to use a diacid chloride (**118**) which will react with two codeine molecules. Therefore, the diacid chloride species will act as a bridge linking the two codeine molecules through ester bonds (Scheme 2.1). In addition the formation and structural characterisation of ether linked opioid derivatives is included (Scheme 2.2). Modification at this position of the molecule has been shown to affect the binding affinity to the opioid receptors (Chapter 1, 1.2.2) thus formation of these bivalent opioid derivatives could have uses as potential novel analgesic therapeutics (Chapter 4).

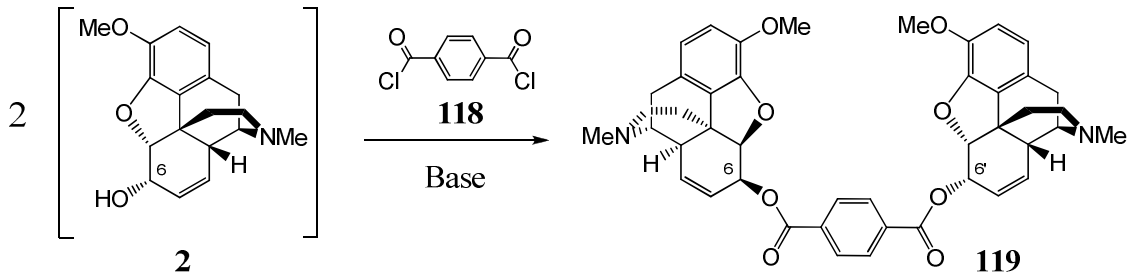

Scheme 2.1 General reaction scheme for the formation of di-codeine derivative **119**

Due to the presence of the numerous oxygen donor atoms in the "cavity site" formed within the molecule there is potential for interactions between metal cationic species (Chapter 5). Thus it could be envisioned that metal complexes may form with the linked opioid derivatives which may lead to sensor applications.

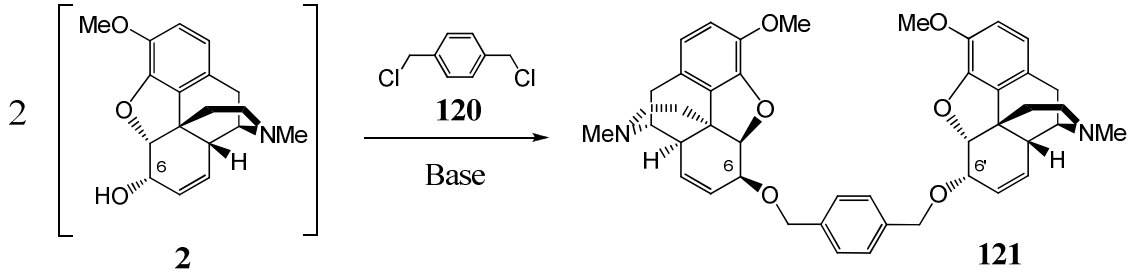

Scheme 2.2 General reaction scheme for the formation of di-codeine derivative **121**

2.2 Synthesis of Ester Linked Codeine Derivatives

Preliminary work on the generation of the ester linked compounds was investigated using NEt_3 as the base and DCM as the solvent, as previous work within the research group had shown this to be a suitable method for esterification of similar systems. However, the conversions to the desired linked compound (**119**) were poor when using terephthaloyl dichloride (**118**), with only trace amounts of product formed (Scheme 2.3). By replacing NEt_3 with K_2CO_3 the conversion was increased to 62%.

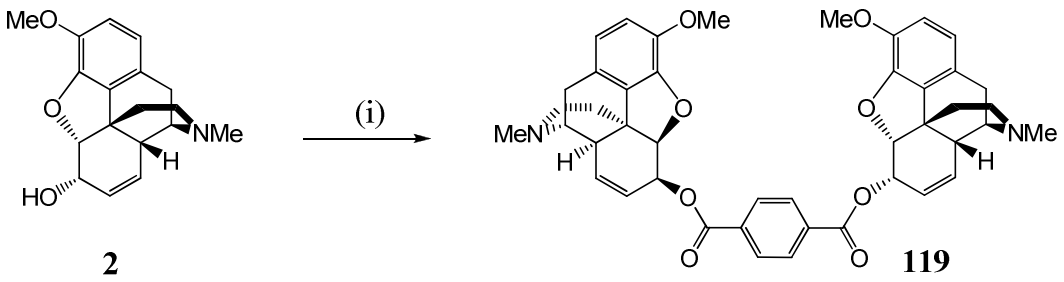

2 **119**

Reaction Conditions; (i) Terephthaloyl dichloride (0.5 Eq), NEt_3 (2 Eq), DCM, N_2, RT

Scheme 2.3 Reaction scheme for the formation of **119** using NEt_3

Compound	Diacid Chloride	Conversion (from ^{1}H NMR)
119	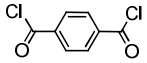 **118**	62%
126	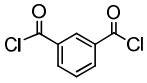 **122**	50%
127	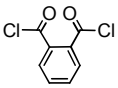 **123**	69%
128	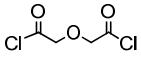 **124**	Trace

Table 2.1 Conversions to desired linked compounds using K_2CO_3

However, when K_2CO_3 was employed for other diacid chlorides, the conversions to the desired linked compounds in general were still lower than desired (Table 2.1). Some of the reaction parameters were explored further with the aim of developing a suitable method that would result in good conversions to the desired linked compounds regardless of the diacid chloride. The main parameters investigated were base, solvent and temperature. An examination of some of the reaction conditions investigated for the formation of **119** are outlined in (Table 2.2). The mono addition product was not observed by ^{1}H NMR of the crude or isolated from column chromatography.

Solvent	Temp	Base (2 Eq)	Conversion (from ^{1}H NMR)
DCM	RT	NEt_3	Trace
DCM	RT	K_2CO_3	62%
DCM	40 °C	K_2CO_3	59%
DCM	RT	Na_2CO_3	17%
DCM	RT	KOH	26%
DCM	RT	NaOH	19%
DCM	RT	NaH	50%
DCM	RT	DMAP	82%
DCM	40 °C	DMAP	83%
THF	RT	K_2CO_3	Trace
THF	66 °C	K_2CO_3	Trace
THF	RT	Na_2CO_3	Trace
THF	RT	NaH	41%
Pyridine	RT	Solvent (pyridine)	21%
Pyridine	115 °C	Solvent (pyridine)	22%

Table 2.2 Analysis of reaction parameters on formation of **119**

The preferred base was either K_2CO_3 or DMAP with conversions of 62% and 82% respectively. Conversions were also satisfactory (50%) when using NaH however numerous by products were seen in the crude ^{1}H NMR. When the solvent was changed from DCM to THF the % conversions lowered significantly, employing THF with either K_2CO_3 or Na_2CO_3 resulted in almost no product. When pyridine was used as the solvent the % conversion was very low at 21%. Increasing the temperature for DCM, THF or pyridine with a range of bases (Table 2.2) showed no affect on product formation. As DMAP was found to be the most suitable base for generation of **119** it was investigated using other diacid chloride compounds (Table 2.3). When potassium carbonate is replaced with DMAP the percentage conversion went from 50% to 92 %, 69% to 95% and trace amounts to 67% for compounds **126**, **127** and **128** respectively. Therefore, employing DMAP resulted in increased conversions for all the tested diacid

chlorides. DMAP is a well known activating agent for acid chlorides and it has been reported previously in the formation of ester bonds at the 6 hydroxyl position.[37] Reducing the equivalents of DMAP used in the reaction to 1.1 Eq resulted in no discernible reduction in formation of the product.

Compound	Base	Conversion (from ^{1}H NMR)
126	K_2CO_3	50%
126	DMAP	92%
127	K_2CO_3	69%
127	DMAP	95%
128	K_2CO_3	Trace
128	DMAP	67%

Table 2.3 Comparison of product formation from K_2CO_3 and DMAP

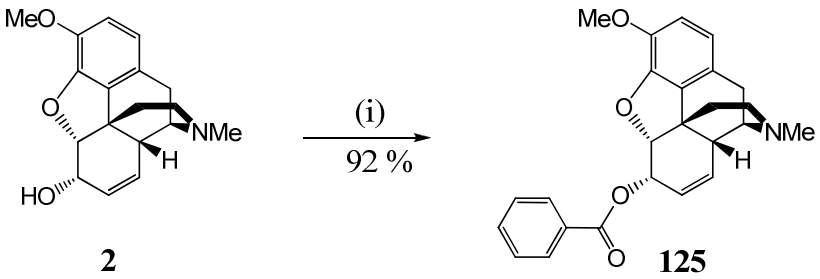

2 **125**

Reaction Conditions; (i) Benzoyl chloride (1 Eq), DMAP (1.1 Eq), DCM, N_2, RT

Scheme 2.4 Reaction scheme for the formation of **125**

When this reaction condition was utilised for the benzoyl product (**125)** (Scheme 2.4), it resulted in almost 100% conversion to the desired product, isolated yield of 92%. The variance in formation of the linked compounds was most likely due to the relative reactivity's of the acid dichlorides employed and steric effects. Using the reaction conditions outlined (Scheme 2.5) a selection of eight ester linked opioid products were synthesised in isolated yields of 39% - 82% (Fig 2.2). These isolated yields could be improved by further development of the reaction conditions and improved purification

of the resulting crude mixtures. However the aim was not to develop a high isolated yield process but to synthesise the compounds for further analysis.

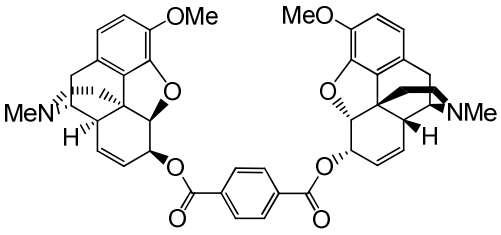

119, 73%

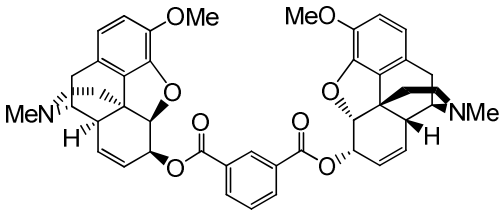

126, 82%

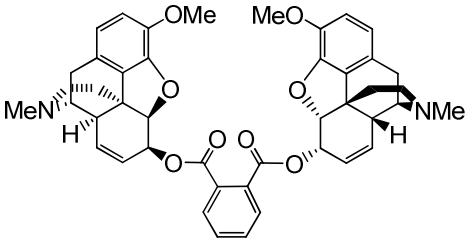

127, 72%

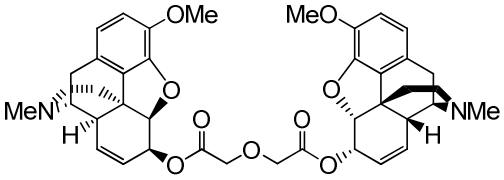

128, 40%

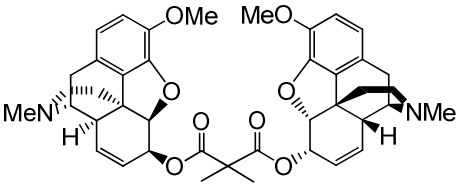

129, 39%

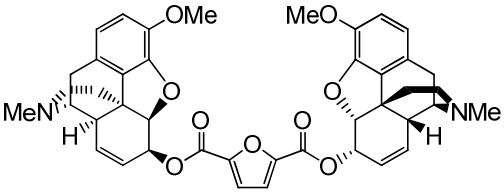

130, 51%

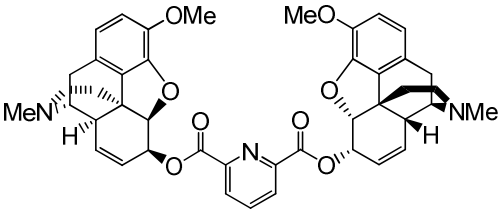

131, 49%

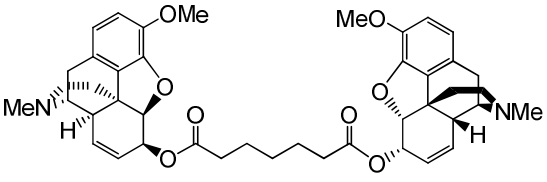

132, 63%

Fig 2.2 Ester linked codeine derivatives with isolated yields

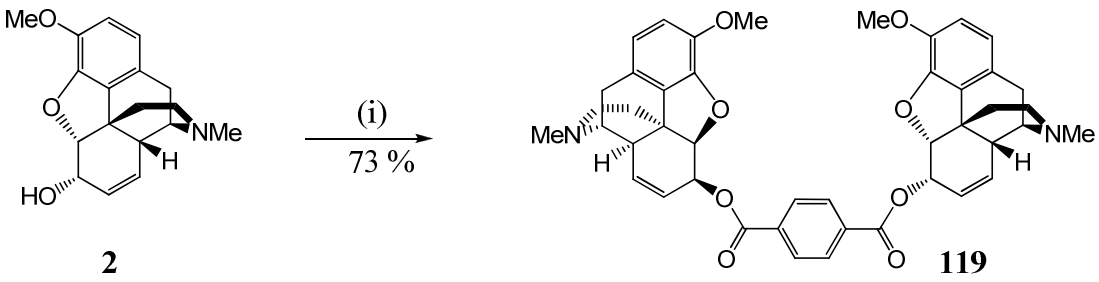

2 **119**

Reaction Conditions; (i) Terephthaloyl dichloride (0.5 Eq), DMAP (1.1 Eq), DCM, N_2, RT

Scheme 2.5 Reaction scheme for the formation of **119** using DMAP

Purification of the ester compounds was achieved through column chromatography followed by recrystallisation. The mobile phase employed for these compounds was a DCM methanol mixture with small amounts of ammonia solution added to the mobile phase to prevent tailing (SiO_2 10% MeOH/DCM, 1% NH_4OH). The acidic nature of the silica column results in some sites to which the basic nitrogen moieties present in the structures can interact. This causes the target compound to drag giving a broad *Rf* value. When column chromatography is performed on the linked products using silica it was noted that there was some degradation of the ester bonds, resulting in the linked products degrading to the codeine starting material. While no significant percentage of the ester bonds degraded the amount of time spent on the silica column is an important factor to consider. Recrystallisations were performed *via* slow cooling technique for single solvent recrystallisations (acetone) and solvent diffusion for two solvent recrystallisations ($CHCl_3$:Hexane).

2.3 Synthesis of Ether Linked Codeine Derivatives

2.3.1 Method Development

Formation of ether linked opioid derivatives has previously been presented by Frensch and Voegtle (1979) (Fig 2.3).[69] The method involves refluxing 1,2-*bis*(2-chloroethoxy)ethane or 1-chloro-2-(2-(2-(2-chloroethoxy)ethoxy)ethoxy)ethane with

morphine in butanol in the presence of sodium hydroxide. Compound **133** was isolated in 8% yield while **134** was only isolated in 10% yield. However attempts to join the two morphine units with 2,6-*bis*(bromomethyl)pyridine to form the ether linked derivative proved unsuccessful with only **135** isolated as the major product in 10% yield. While this work illustrates that it is possible to form ether linked opioid compounds the low yield is undesirable. Frensch and co-workers have not published further studies in this area since 1979.

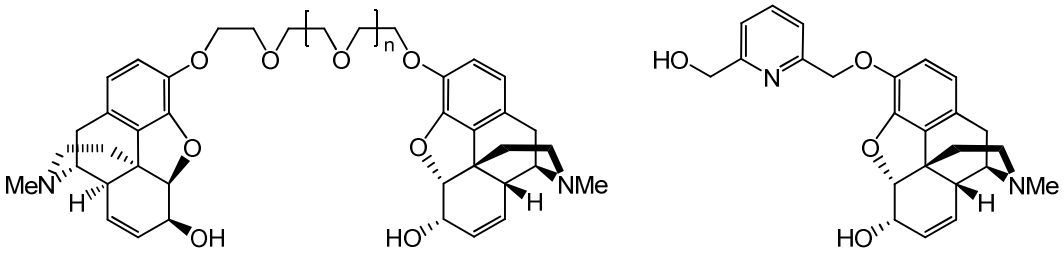

133, n = 1
134, n = 2

135

Fig 2.3 Ether linked morphine derivatives, **133**, **134** and **135**

Previous studies within the research group investigating the formation of ether linked opiate compounds based on modification of morphine have previously been undertaken.[70] After extensive investigation suitable methods were developed to form a variety of ether linked morphine opioids in 64% - 94% yield.

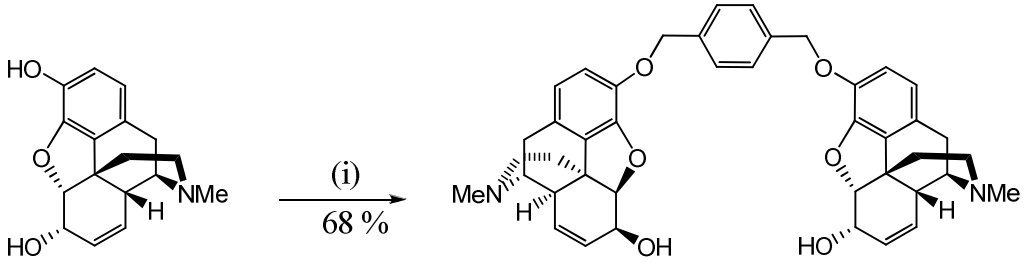

1 **136**

Reaction Conditions; (i) 1,4-*bis*(bromomethyl)benzene, NaOMe, MeOH, 66°C

Scheme 2.6 Reaction scheme for the formation of **136**

If the reaction is carried out in methanol under reflux with the addition of sodium methoxide the *para* linked morphine ether, **136** can be formed in 68% yield (Scheme 2.6). Of curent interest for this research project is the reaction conditions required for the formation of ether linked compounds at the 6 position. Formation of ether linkers at the 6 position has previously been undertaken in the research group as part of an investigation to form macrocyclic opiate derivatives (Scheme 2.7). The optimum conditions for the formation of the linked ether compound **138** involve refluxing **137** in THF with the addition of the dichloride, KOH and KI.

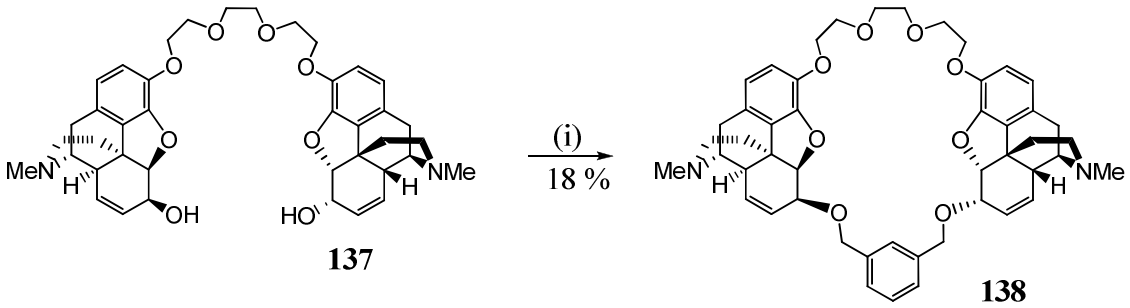

137 **138**

Reaction Conditions; (i) 1,3-*bis*(bromomethyl)benzene, KOH, KI, THF, 66°C

Scheme 2.7 Reaction scheme for the formation of **138**

2.3.2 Synthesis of Novel Ether Linked Codeine Compounds

The previously developed reaction conditions were utilised to form the ether linked codeine compounds. Both the *para* (**121**) and *meta* (**139**) linked ether derivatives were synthesised using the same method (Scheme 2.8) in modest yields of 55% and 59% respectively (Fig 2.4). The reaction was performed using both the 1,4-*bis*(bromomethyl)benzene (Scheme 2.8) and 1,4-*bis*(chloromethyl)benzene (Scheme 2.9) with the bromo-derivative resulting in better yields.

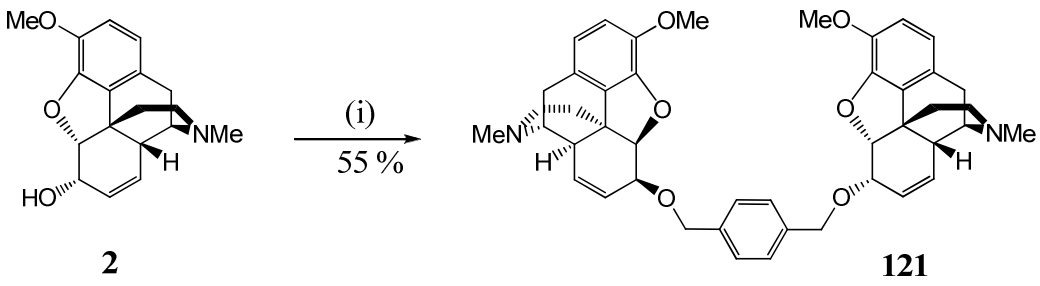

2 **121**

Reaction Conditions; (i) 1,4-*bis*(bromomethyl)benzene (0.5 Eq), KOH (12 Eq), KI (0.2 Eq), THF, 66°C

Scheme 2.8 Reaction scheme for the formation of **121** using 1,4-*bis*(bromomethyl)benzene

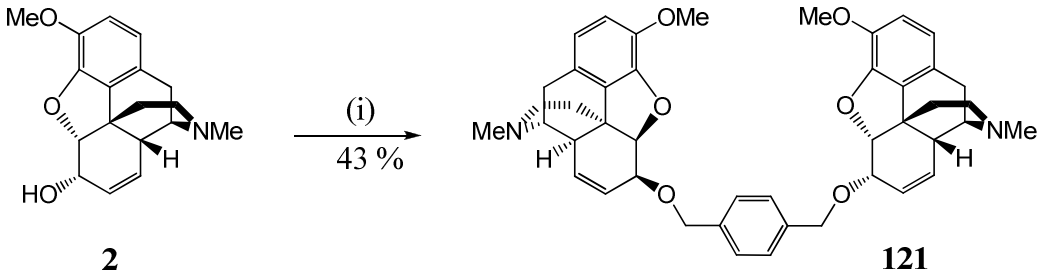

2 **121**

Reaction Conditions; (i) 1,4-*bis*(chloromethyl)benzene (0.5 Eq), KOH (12 Eq), KI (0.2 Eq), THF, 66°C

Scheme 2.9 Reaction scheme for the formation of **121** using 1,4-*bis*(chloromethyl)benzene

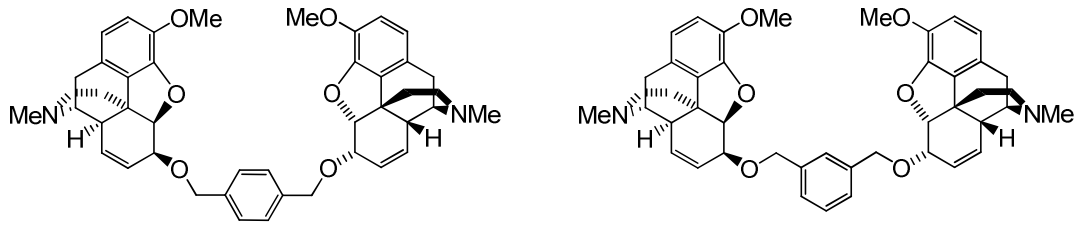

121, 55% **139**, 59%

Fig 2.4 Codeine derivatives **121** (from Scheme 2.8) and **139** (using 1,3-*bis*(bromomethyl)benzene under same reaction conditions) with isolated yields

Purification of the ether compounds was achieved through column chromatography followed by recrystallisation. The mobile phase employed was a DCM methanol mixture with small amounts of ammonia solution added to the mobile phase to prevent

tailing (SiO_2 10% MeOH/DCM, 1% NH_4OH). Recrystallisations for both compounds were performed *via* solvent diffusion using a $CHCl_3$:Hexane mixture.

2.4 NMR Study of Ester and Ether Linked Compounds

2.4.1 NMR Study of Compound 119

A study of **119** was performed by analysis of ^{1}H, ^{13}C, ^{13}C DEPT, COSY, HMQC and HMBC NMR spectra. The structure of compound **119** is outlined below in Fig 2.5. In total **119** contains $C_{44}H_{44}N_2O_8$ corresponding to a molecular mass of 728.8288. The molecule contains two codeine structural units resulting in a symmetrical compound, ie H14 and H14' are identical under NMR analysis. Compound **119** has been fully labeled in Fig 2.5, however for clarity in further discussions H14 will refer to both H14 and H14', C1 will refer to both C1 and C1' etc. The majority of the peaks in the ^{1}H proton spectrum for **119** can be assigned based on their relative δ values and splitting patterns. Most peaks in the ^{1}H proton NMR for **119** are broadly similar to the codeine starting material (Figs 2.6–2.7).

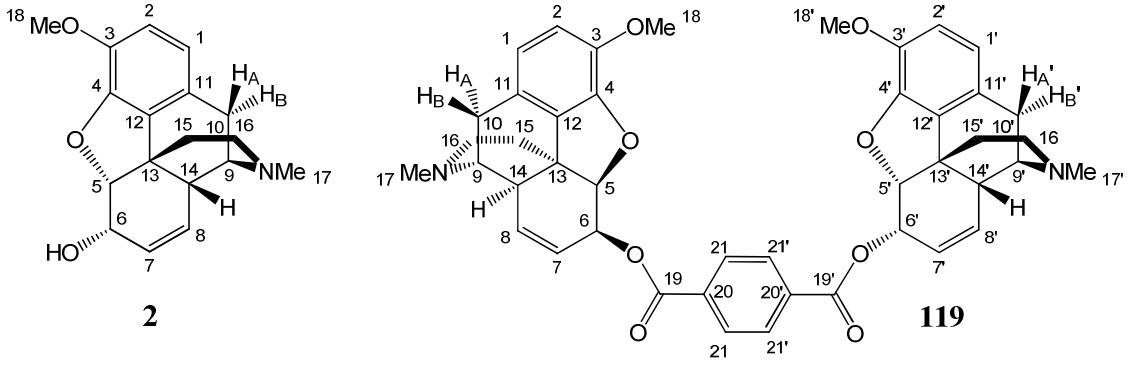

Fig 2.5 Structure of codeine (**2**) and **119** with labelled atoms

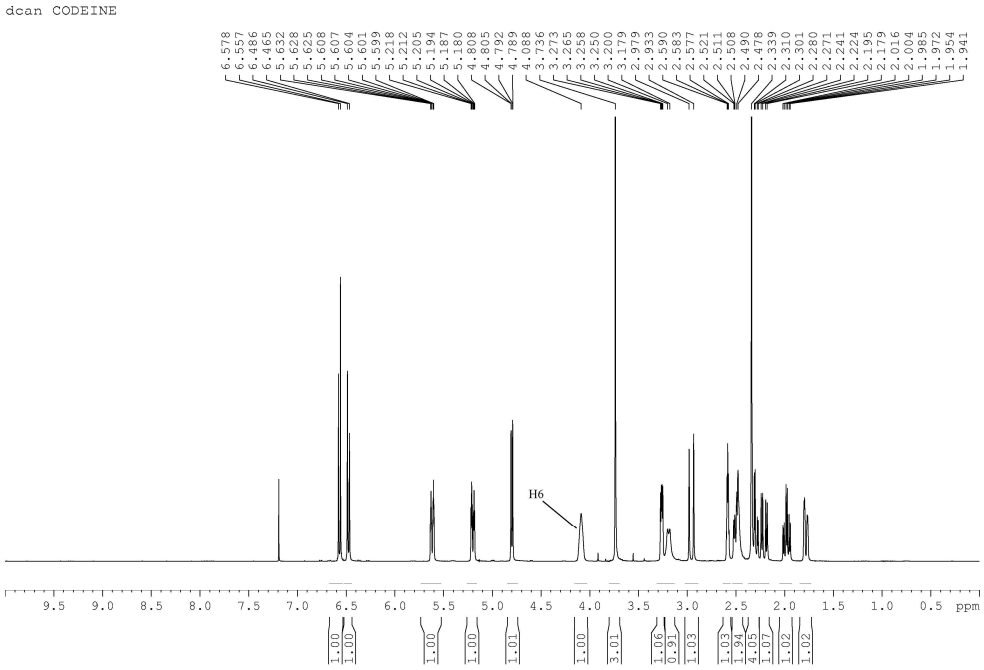

Fig 2.6 ^{1}H Proton NMR of Codeine (**2**)

Analysis of the ^{1}H NMR spectrum of **119** (Fig 2.7) shows protons H21 in the aromatic linker moiety appear as the expected singlet at δ 8.07. The aromatic peaks corresponding to H2 and H1 appear as doublets with *J* values of 8.0 Hz (consistent with vincinal coupling constants for protons in an aromatic ring system) and chemical shifts of δ 6.59 and δ 6.50 respectively. Proton H7 at δ 5.74-5.70 couples with H8, H6, and H14, however accurate *J* coupling can not be calculated due to peak overlap. The strongest coupling for H7 can be calculated roughly at 10.0 Hz which would correspond to coupling with H8 (consistent with vicinal coupling constants on alkenes). Weak coupling is also observed with H6 and H14 however *J* values cannot be accurately determined due to peak overlap. Proton H8 (δ 5.48-5.44) has a similar pattern to H7, strong coupling with H7 (*J* value 10.0 Hz) and weak coupling to H6 and H14. Proton H5 appears as a doublet with a *J* value of 6.8 Hz at δ 5.14 while the methyl protons corresponding to H18 and H17 appear as singlets at δ 3.64 and δ 2.39

respectively. The multiplets at δ 3.33-3.31 and δ 2.77-2.74 relate to protons H9 and H14 respectively.

The methylene protons H10, H16 and H15 all have two different δ values for each proton as they are diastereotopic hydrogens. Proton $H10_A$, at δ 2.99 appears as a doublet with a *J* value of 18.4 Hz due to geminal coupling. Proton $H10_B$ at δ 2.35-2.23 appears as a doublet of doublets due to geminal and H9 coupling. However due to peak overlap *J* values can not be accurately determined. Proton H16 at δ 2.54 appears as a doublet of doublets due to geminal and weak H15 coupling with *J* values of 12.0 and 4.0 Hz. Proton H16 at δ 2.35-2.23 appears as a multiplet due to peak overlap. Proton H15 at δ 2.02 appears as a doublet of doublet of doublets due to geminal and strong H16 coupling with *J* values of 12.4, 12.4 and 4.8 Hz. Proton H15 at δ 1.83 appears as a doublet of doublets due to geminal and weak H16 coupling with *J* values of 12.8 and 2.0 Hz.

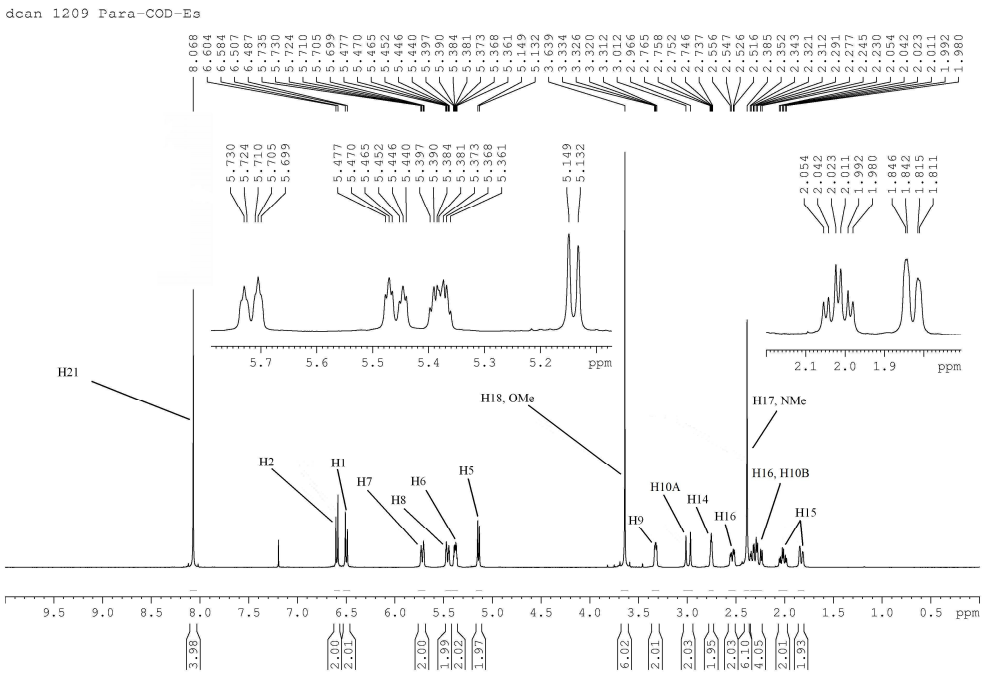

Fig 2.7 ^{1}H Proton NMR of **119**

The most significant peak in the spectrum corresponds to H6. It is expected that conversion from the secondary alcohol (codeine, **2**) to the ester (**119**) at the 6 position of the molecule should have a large effect on the chemical shift. As expected the proton at this position is downfield shifted from δ 4.09 to δ 5.40-5.36 (Fig 2.6 and Fig 2.7). As a result this peak can be used to calculate to a good estimation the percentage formation of product from the crude reaction mixture.

While most peaks can be assigned based on the ^{1}H proton spectrum the COSY spectrum provides additional and complementary information (Figs 2.8-2.10).

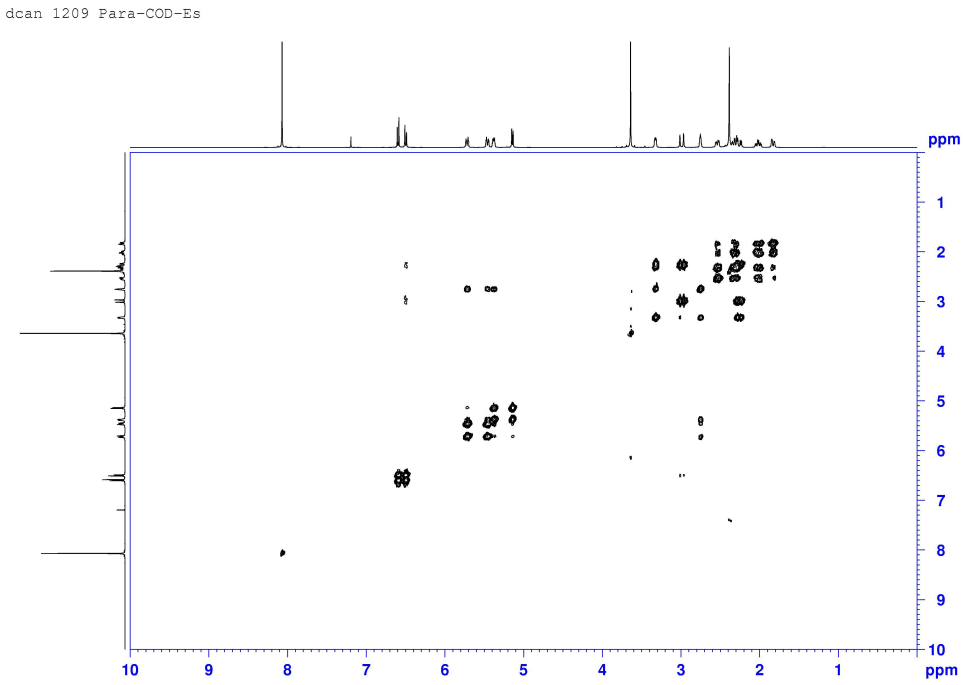

Fig 2.8 COSY spectrum of **119**

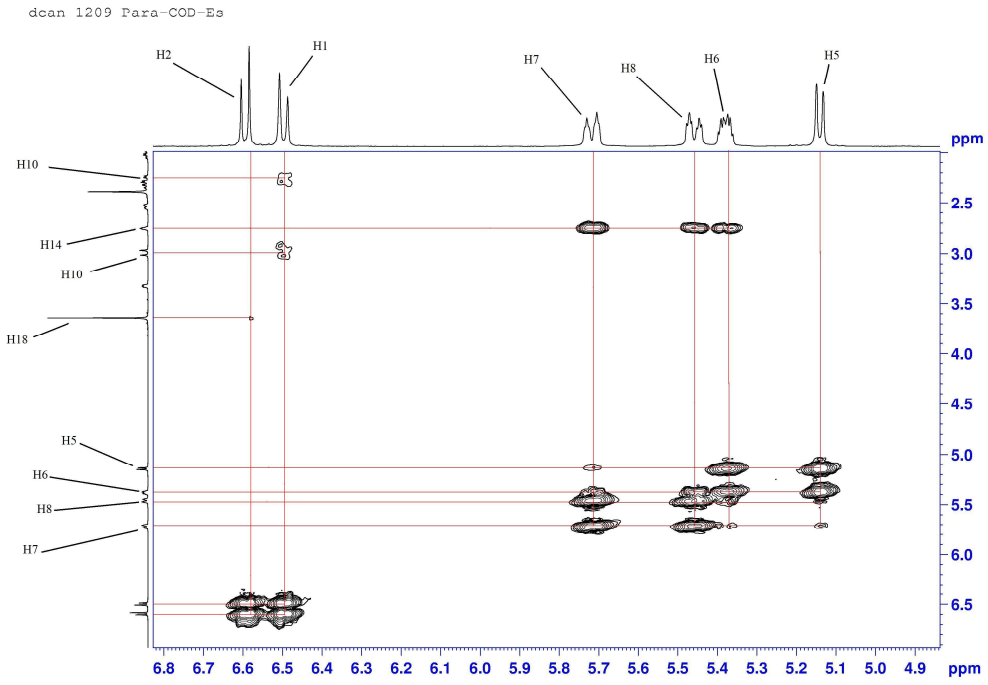

Fig 2.9 COSY spectrum of **119** showing cross peak correlations between δ 5.0-7.0

Examining the δ region of 5.0-7.0 (Fig 2.9) displays the strong coupling between H2 and H1 (10.0 Hz). H1 also shows weak coupling to H10 while H2 exhibits very weak coupling with H18. As expected there is strong coupling observed between protons H5 and H6 *via* three bond coupling. Proton H5 also couples very weakly with H7 and H8. Protons H7 and H8 display strong coupling with each other (10.0 Hz), while, weaker coupling to protons H14 and H6 is observed.

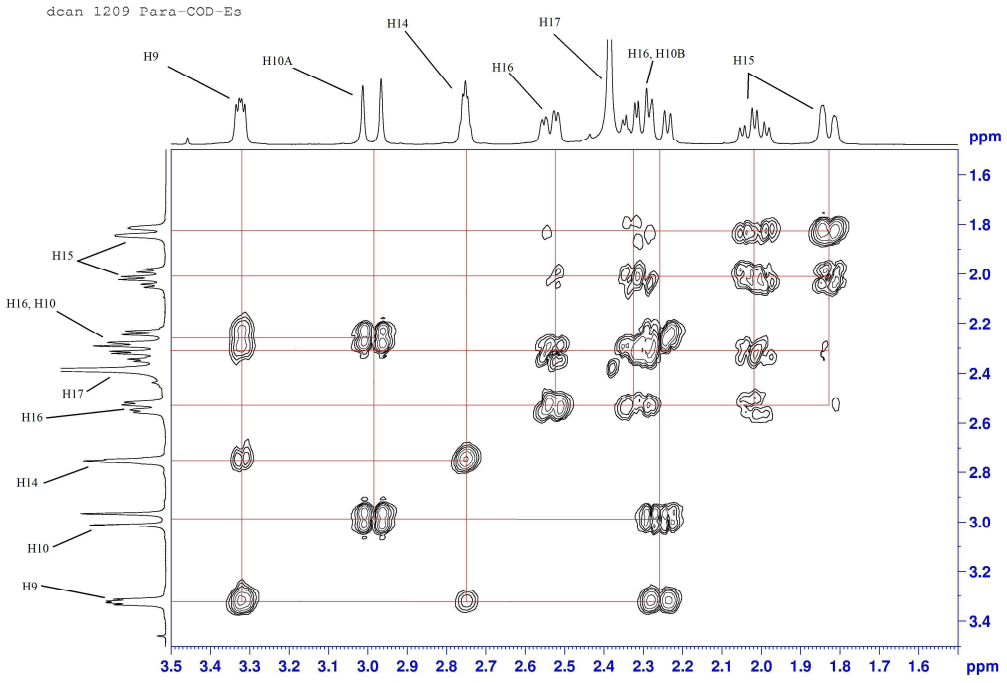

Fig 2.10 COSY spectrum of **119** showing peak correlations between δ 1.5-3.5

Analysis of the δ region of 1.5-3.5 (Fig 2.10) displays the remaining correlations in **119**. Proton H9 couples to H14 and $H10_B$, while proton $H10_B$ also couples with $H10_A$ through geminal coupling. Protons H16 and H15 couple with each other as well as displaying the expected geminal coupling for diastereotopic hydrogens. Overall analysis of **119** by COSY NMR illustrates that the coupling patterns assigned based on the ^{1}H NMR analysis are correct. A summary of the proton proton coupling for **119** is provided in Table 2.4.

Proton No.	Couples with
21	21
2	2, 1, 18*
1	1, 2, 10*
7	7, 8, 14, 6*, 5*
8	8, 7, 14, 6*, 5*
6	6, 5, 14, 7*, 8*
5	5, 6, 7*, 8*
18	18, 2*
9	9, 14, 10
10	10, 9
14	14, 7, 8, 6, 9
16	16, 15
17	17
15	15, 16

Table 2.4 Proton proton correlations from COSY spectrum of **119**, *denotes weak coupling.

An examination of the ^{13}C, ^{13}C DEPT, HMQC and HMBC allows the carbon atoms of **119** to be accurately assigned. The majority of the peaks for **119** can be assigned based on their relative δ values in the ^{13}C spectrum (Fig 2.11) with most peaks again similar to the codeine starting material. Further analysis by ^{13}C DEPT, HMQC and HMBC provides additional information.

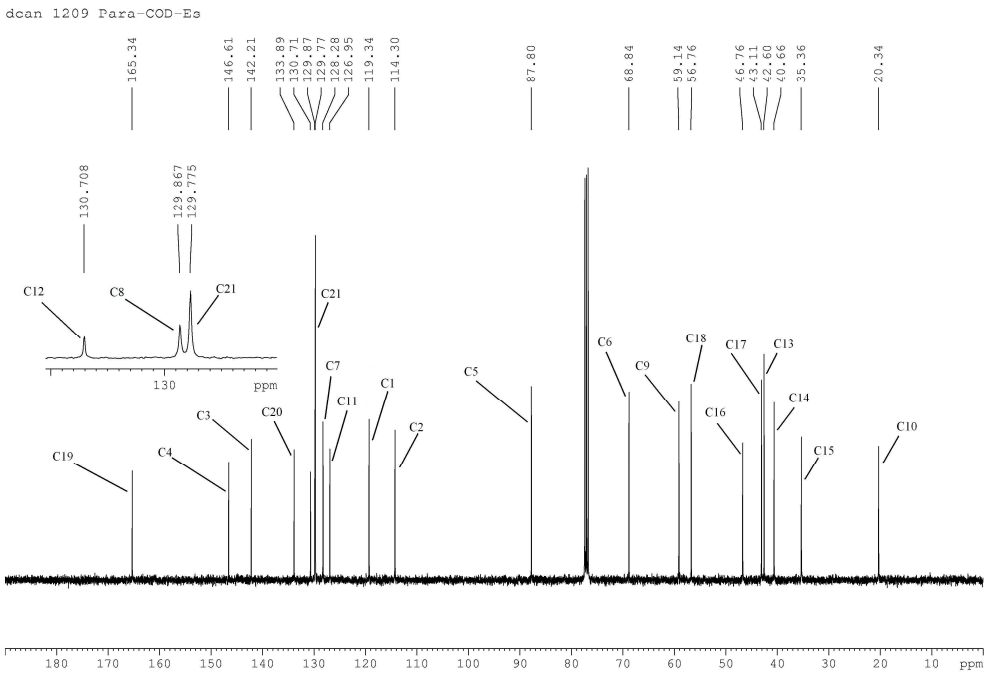

Fig 2.11 ^{13}C spectrum of **119**

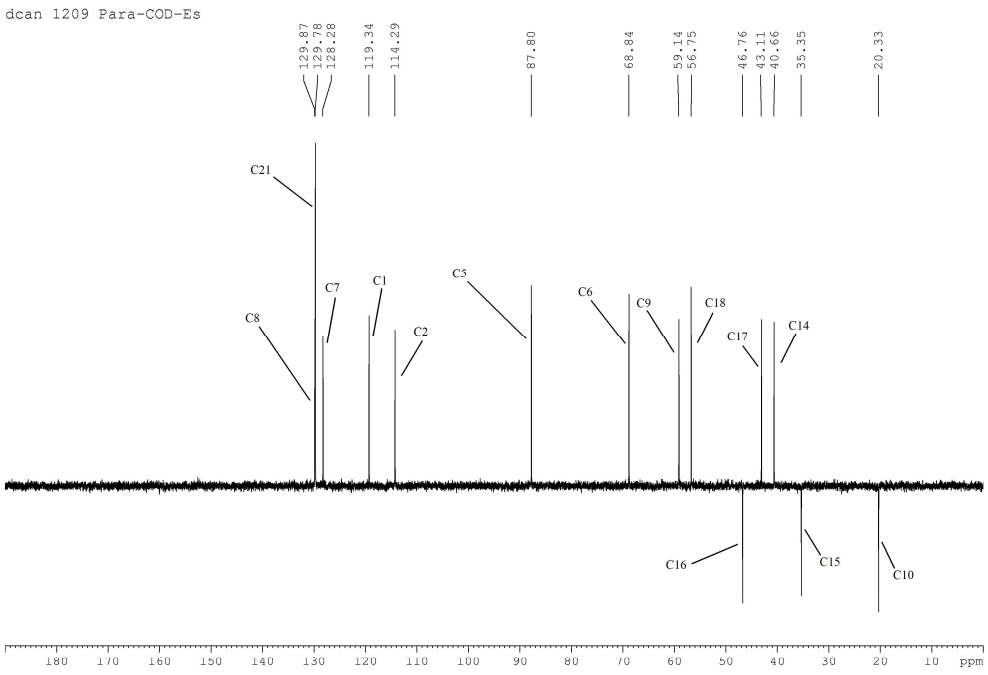

Fig 2.12 ^{13}C DEPT spectrum of **119**

As expected the carbonyl carbon C19 has the highest δ value at 165.34 with C20 and C21 appearing at the expected δ values for aromatic carbons at 133.89 and 129.77 respectively. From ^{13}C DEPT analysis it is clear which carbons correspond to the quaternary and methylene carbons (Fig 2.12). In total **119** contains 7 quaternary carbons corresponding to C19, C4, C3, C20, C12, C11 and C13 at δ values of 165.34, 146.61, 142.21, 133.89, 130.71, 126.95 and 42.60 respectively. The three methylene carbons for C16, C15 and C10 have δ values of 46.76, 35.36 and 20.34 respectively. Some of the carbon peaks appear at very similar δ values and accurate peak assignment is not possible from ^{13}C and ^{13}C DEPT alone. Accurate confirmation about assigning the carbon peaks is aided by HMQC (Fig 2.13-2.16) and HMBC (Fig 2.17, 2.18) NMR analysis. A summary of the carbon proton coupling is provided in Table 2.5.

Assigned Peak No.	**δ Value (ppm)**	
	Carbon	**Proton**
8	129.87	5.48-5.44
21	129.77	8.07
7	128.28	5.74-5.70
1	119.34	6.50
2	114.30	6.59
5	87.80	5.14
6	68.84	5.40-5.36
9	59.14	3.33-3.31
18	56.76	3.64
16	46.76	2.54, 2.35-2.23
17	43.11	2.39
14	40.66	2.77-2.74
15	35.36	2.02, 1.83
10	20.34	2.99, 2.35-2.23

Table 2.5 Carbon proton correlations from HMQC of **119**

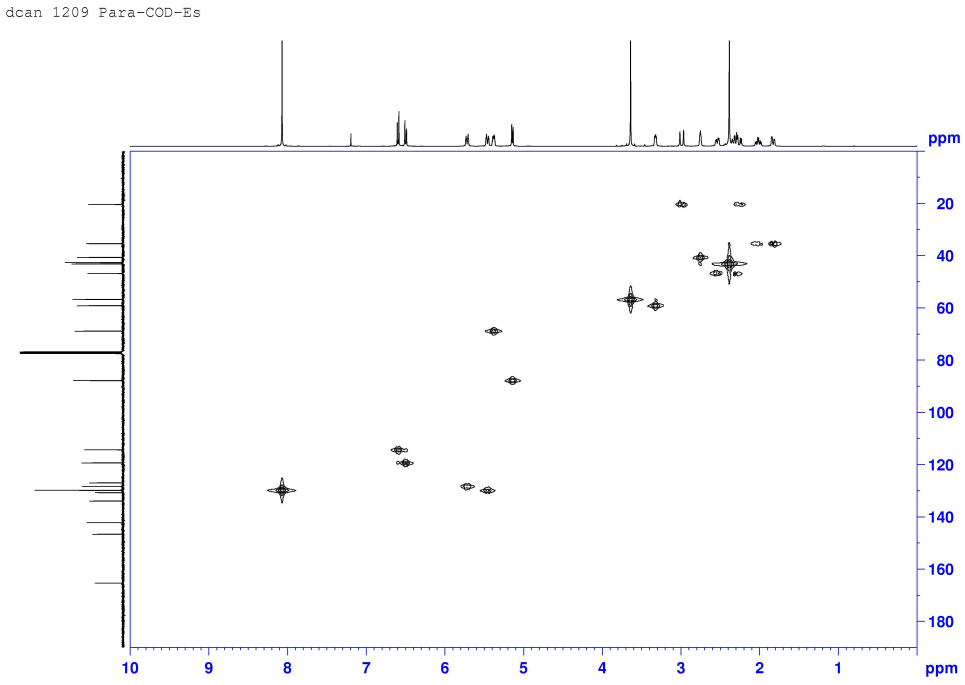

Fig 2.13 HMQC spectrum of **119**

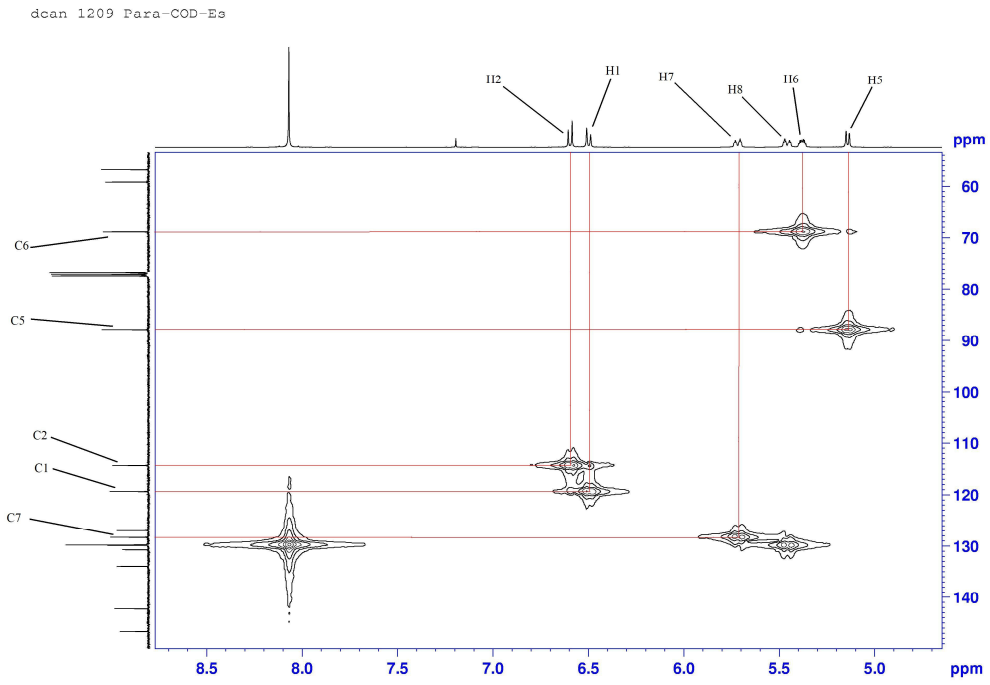

Fig 2.14 HMQC spectrum of **119** showing peak correlations between δ 5.0-8.5

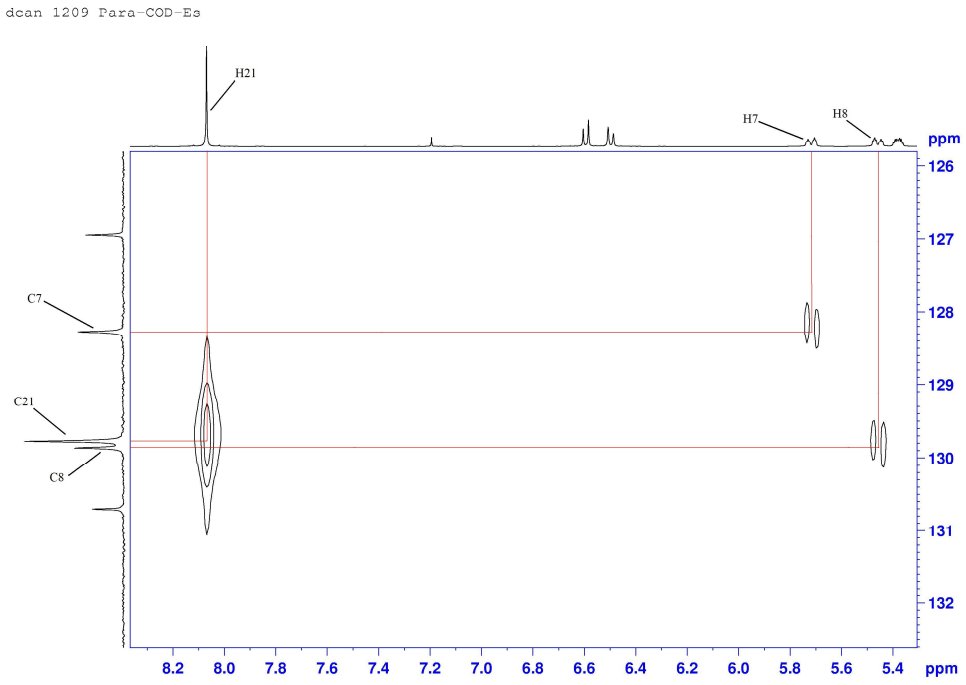

Fig 2.15 HMQC spectrum of **119** showing peak correlations between δ 5.5-8.2 for C8, C21 and C7

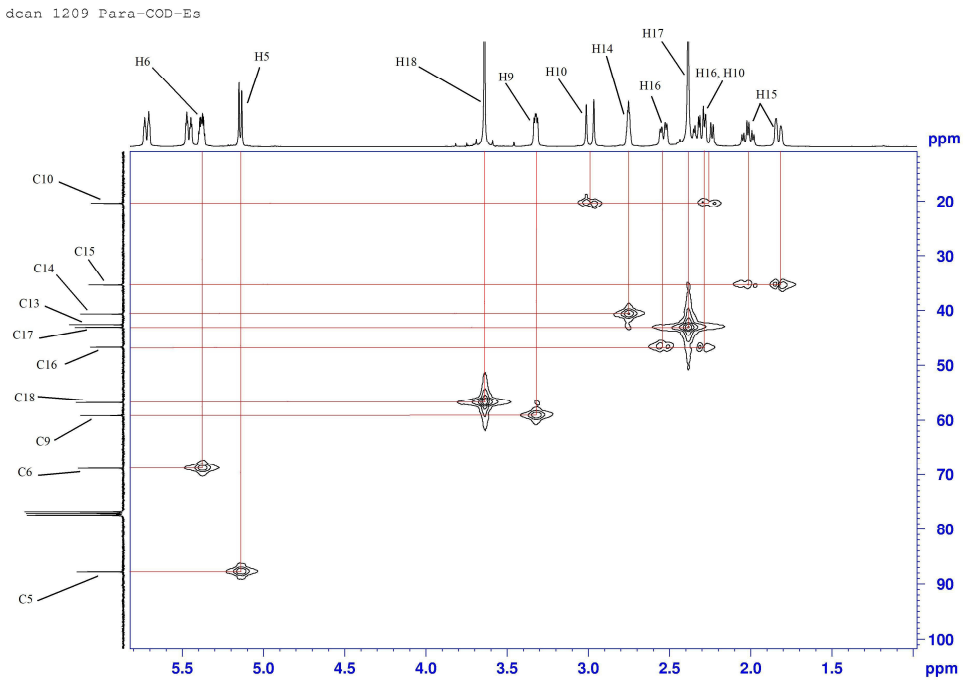

Fig 2.16 HMQC spectrum of **119** showing peak correlations between δ 1.5-5.5

For full peak assignment of the carbon spectrum it is also helpful to examine the HMBC of **119** which provides important structural information about the correlation between protons and the quaternary carbons (Figs 2.17-2.18). As expected proton H21 shows coupling with carbons C19, C20 and C21. Proton H2 displays coupling with carbons C4, C3 and C11, while proton H1 exhibits coupling with C3 and C12. Proton H5 displays coupling with carbons C4, C12 and C7.

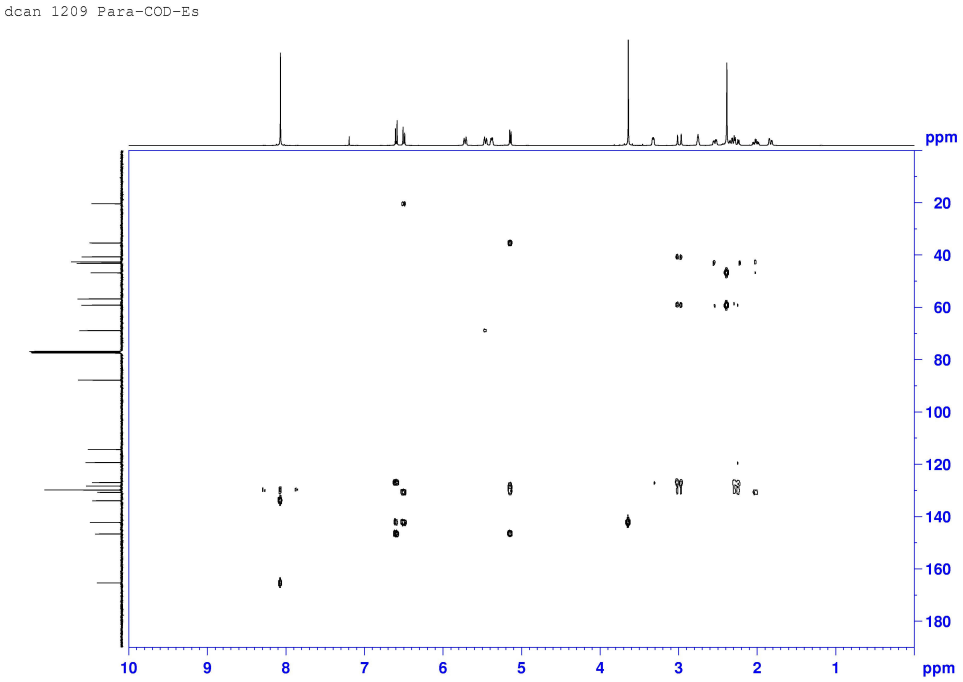

Fig 2.17 HMBC spectrum of **119**

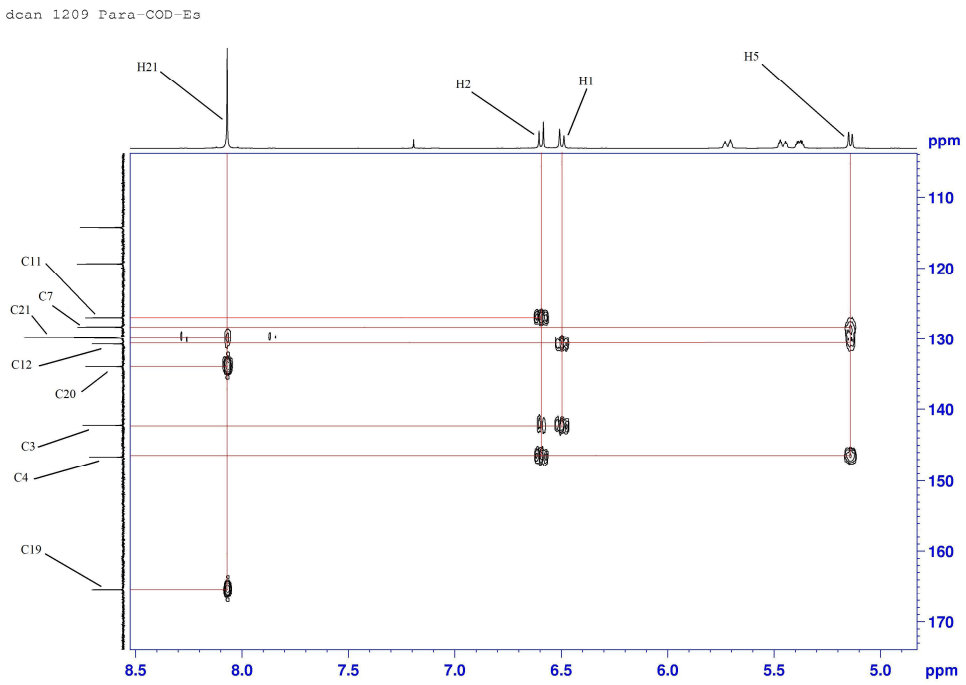

Fig 2.18 HMBC spectrum of **119** showing peak correlations between δ 5.0-8.5

2.4.2 NMR Study of Compound 121

The same approach was employed to fully assign the proton and carbon spectra for the ether linked *para* derivative **121** (Fig 2.19). In total **121** contains $C_{44}H_{48}N_2O_6$ corresponding to a molecular mass of 700.8617. Compound **121** contains much of the same skeleton as **119** and as such the ^{1}H, ^{13}C, ^{13}C DEPT, COSY, HMQC and HMBC spectra will appear very similar. As per **119**, compound **121** the molecule contains two codeine structural units resulting in a symmetrical compound, ie H14 and H14' are identical under NMR analysis. Compound **121** has been fully labeled in Fig 2.19, however for clarity in further discussions H19 will refer to both H19 and H19', C21 will refer to both C21 and C21' etc.

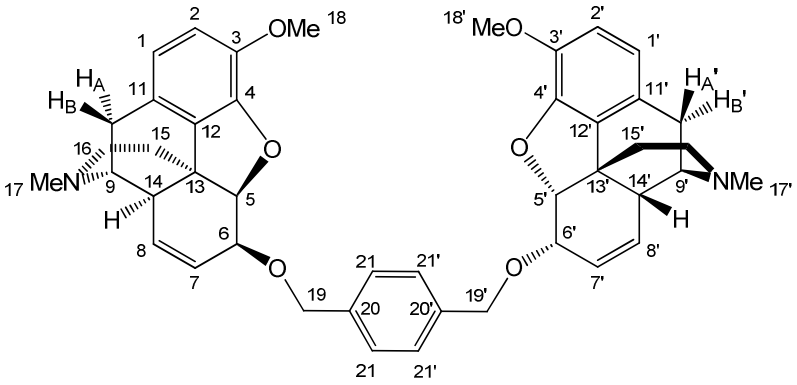

Fig 2.19 Structure of **121** with labeled atoms

Analysis of the ^{1}H NMR spectrum of **121** (Fig 2.20) shows that the protons corresponding to the opiate scaffold are similar to **119**. As expected the main differences are due to the modification of the linker species from the ester to the ether.

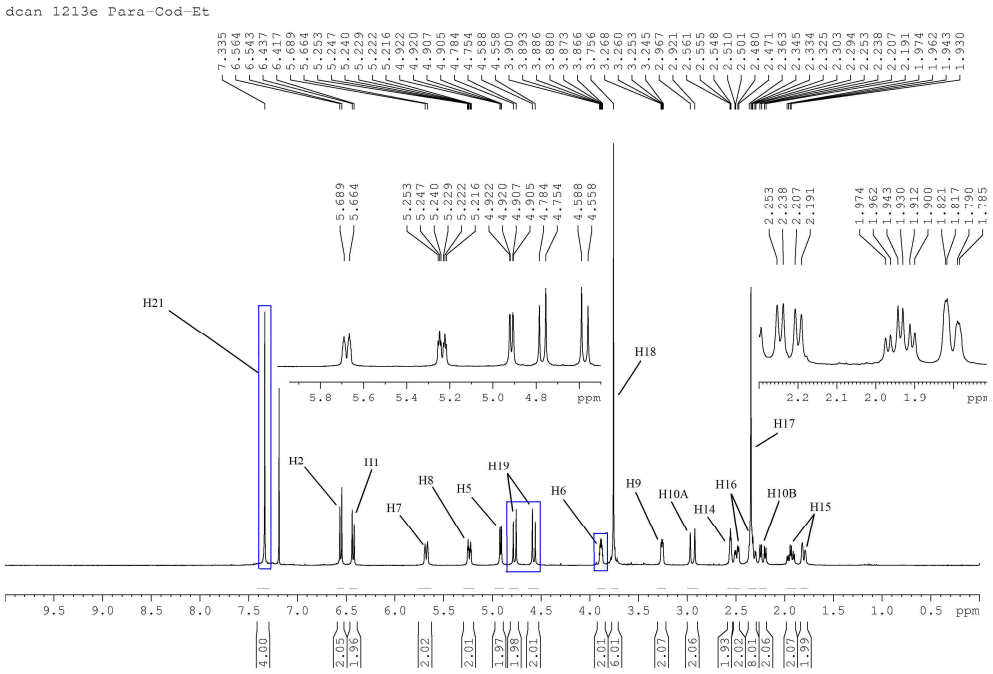

Fig 2.20 ^{1}H spectrum of **121**

In comparison with **119** the most significant peaks in the spectrum correspond to H21, H6 and H19 (Table 2.6). Proton H21 for **119** is at a δ value of 8.07 while proton H21 for **121** is shifted upfield at δ 7.34. Proton H6 for **121** is at the expected δ value of 3.90-3.87 while it is downfield shifted to δ 5.40-5.36 when attached to the carbonyl in **119**. Protons H19 at δ 4.77 and 4.57 correspond to the expected AB splitting pattern with *J* values of 12.0 Hz.

Proton	**δ Value (ppm)**	
	119	**121**
1	6.50	6.43
2	6.59	6.55
5	5.14	4.91
6	5.40-5.36	3.90-3.87
7	5.74-5.70	5.69-5.66
8	5.46	5.23
21	8.07	7.34

Table 2.6 Comparison of selected δ values for **119** and **121** from ^{1}H NMR

The COSY spectrum for **121** provides additional information in relation to peak assigments (Figs 2.21-2.23). Again the coupling pattern for **121** as expected, is similar to **119** with the main difference corresponding to H19 at δ 4.77 and 4.57. A summary of the proton proton coupling for **121** is provided in Table 2.7.

Proton No.	Couples with
21	21
2	2, 1
1	1, 2, 10*
7	7, 8, 14, 6*, 5*
8	8, 7, 14, 6*, 5*
5	5, 6, 7*, 8*
19	19,
6	6, 5, 14, 7*, 8*
18	18
9	9, 14, 10
10	10, 9
14	14, 7, 8, 6, 9
16	16, 15
17	17
15	15, 16

Table 2.7 Proton proton correlations from COSY spectrum of **121**, *denotes weak coupling.

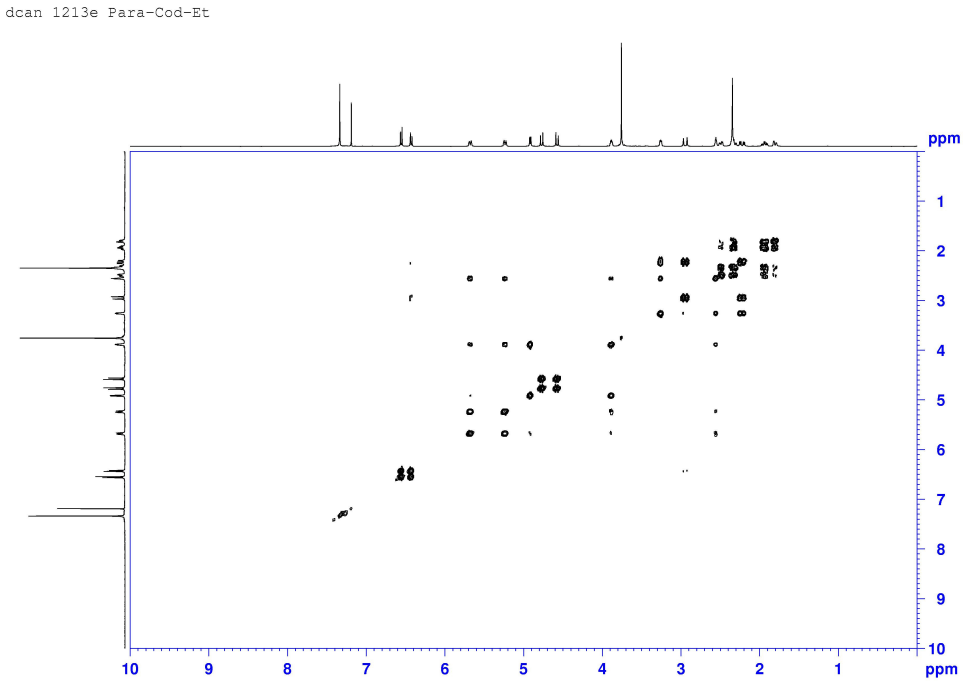

Fig 2.21 COSY spectrum of **121**

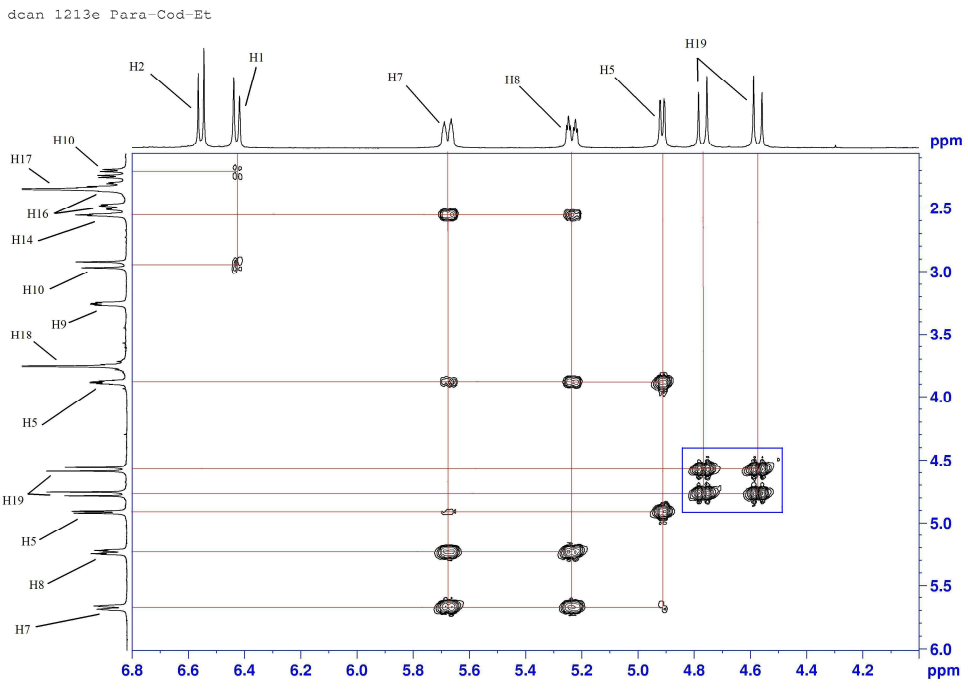

Fig 2.22 COSY spectrum of **121** showing cross peak correlations between δ 4.0-6.8

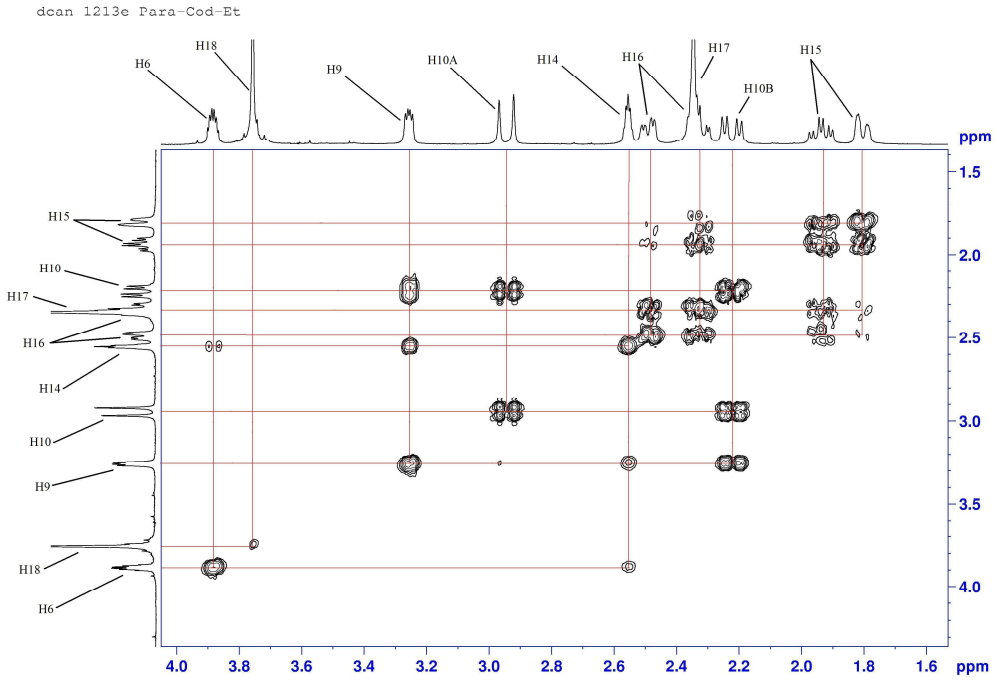

Fig 2.23 COSY spectrum of **121** showing cross peak correlations between δ 1.6-4.0

An examination of the ^{13}C, ^{13}C DEPT, HMQC and HMBC allows the carbon atoms of **121** to be accurately assigned. The majority of the peaks for **121** can be assigned based on their relative δ values in the ^{13}C spectrum (Fig 2.24) with most peaks again similar to **119** (Table 2.8). Further analysis by ^{13}C DEPT, HMQC and HMBC provides additional information. The most significant difference between **119** and **121** from ^{13}C analysis corresponds to C19. As expected the absence of the carbonyl group at the C19 position results in C19 at a δ value of 70.44 for **121**, compared to a δ value of 165.34 for **119**.

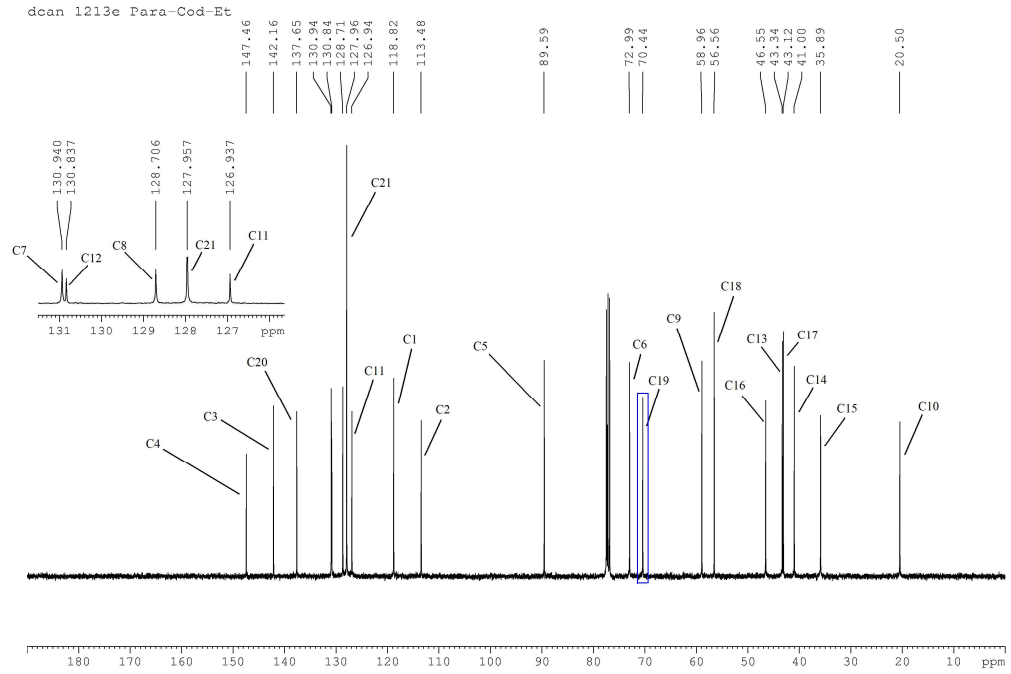

Fig 2.24 ^{13}C spectrum of **121**

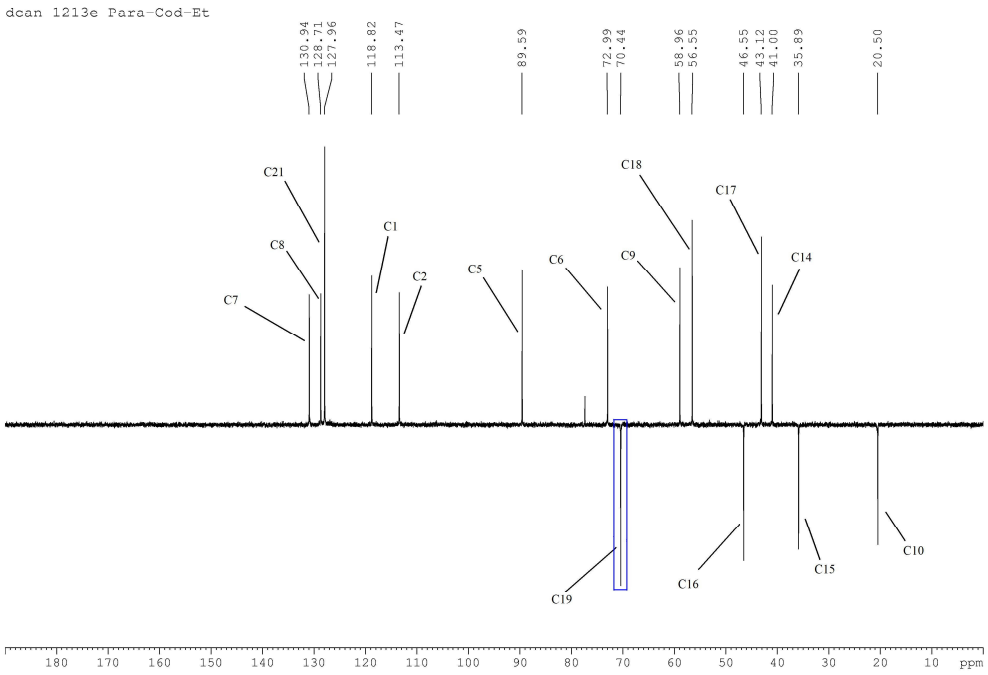

Fig 2.25 ^{13}C DEPT spectrum of **121**

Carbon	δ Value (ppm)	
	119	**121**
1	119.34	118.82
2	114.30	113.48
5	87.80	89.59
6	68.84	72.99
7	128.28	130.94
8	129.87	128.71
19	165.34	70.44
20	133.89	137.65
21	129.77	127.96

Table 2.8 Comparison of selected δ values for **119** and **121** from ^{13}C NMR

From ^{13}C DEPT it is clear which carbons correspond to the quaternary and methylene carbons (Fig 2.25). In total **121** contains 6 quaternary carbons corresponding to C4, C3, C20, C12, C11 and C13 at δ values of 147.46, 142.16, 137.65, 130.84, 126.94 and 43.34 respectively. The four methylene carbons for C19, C16, C15 and C10 have δ values of 70.44, 46.55, 35.89 and 20.50 respectively.

Analysis by HMQC NMR provides proton carbon coupling for **121** (Figs 2.26-2.28). The main difference between **119** and **121** is the proton H19 and carbon C19 coupling (Fig 2.28). A summary of the carbon proton coupling for **121** is provided in Table 2.9.

Assigned Peak No.	δ Value (ppm)	
	Carbon	**Proton**
7	130.94	5.69-5.66
8	128.71	5.23
21	127.96	7.34
1	118.82	6.44
2	113.48	6.56
5	89.59	4.91
6	72.99	3.90-3.87
19	70.44	4.77, 4.57
9	58.96	3.27-3.25
18	56.55	3.76
16	46.55	2.49, 2.36-2.29
17	43.12	2.36
14	41.00	2.56-2.55
15	35.89	1.94, 1.80
10	20.50	2.94, 2.22

Table 2.9 Carbon proton correlations from HMQC of **121**

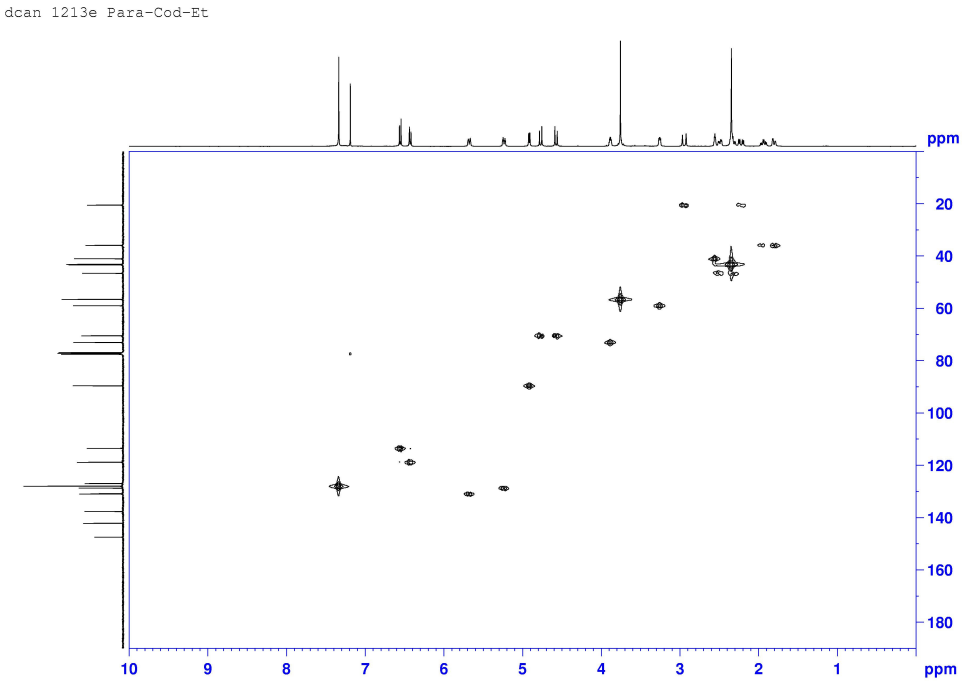

Fig 2.26 HMQC spectrum of **121**

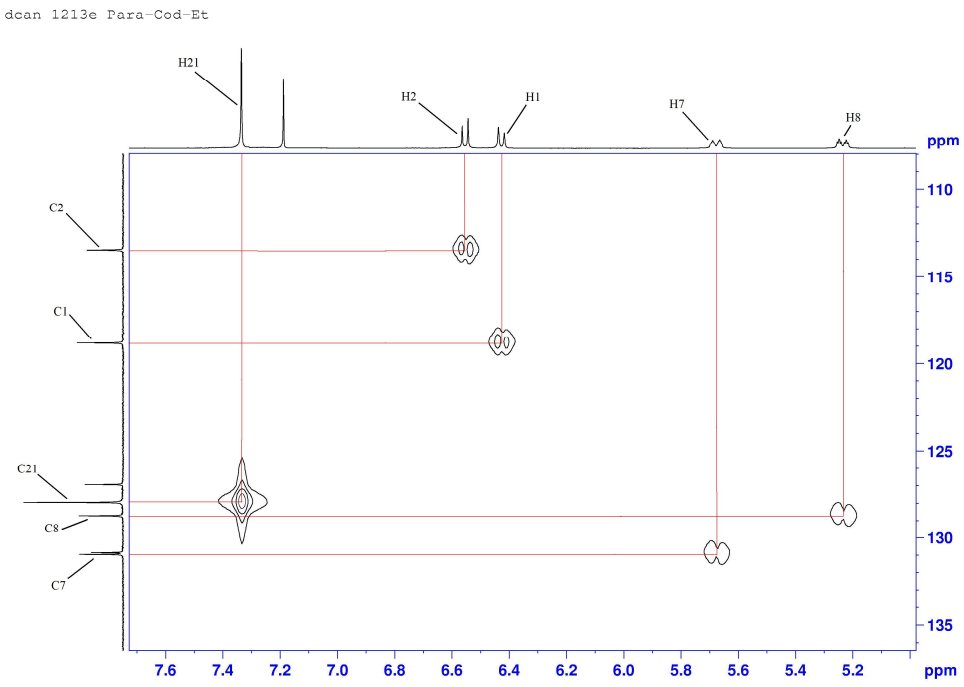

Fig 2.27 HMQC spectrum of **121** showing peak correlations between δ 5.1-7.6

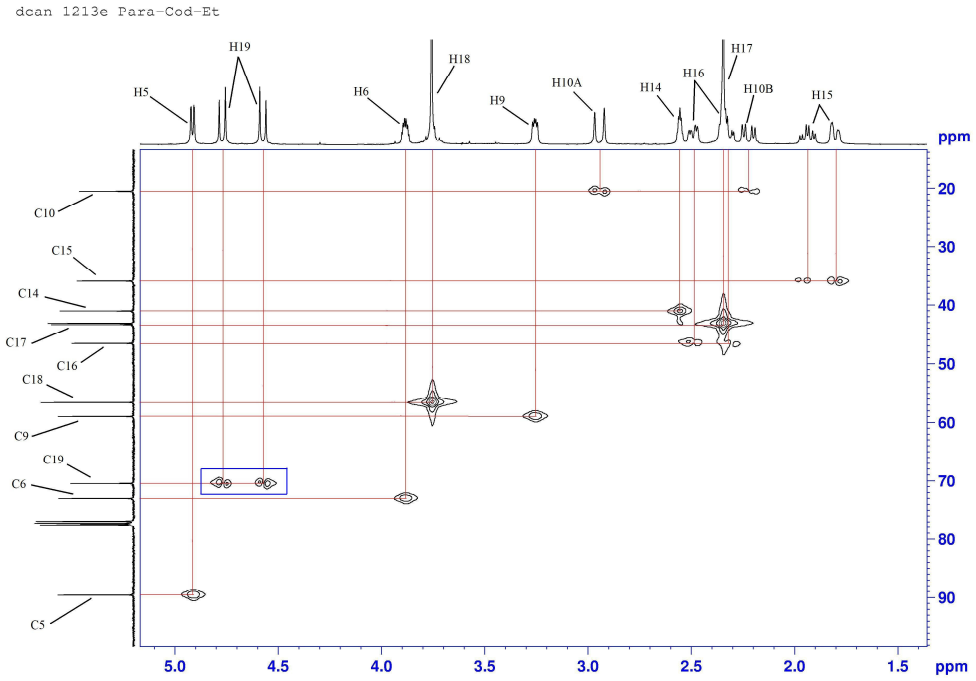

Fig 2.28 HMQC spectrum of **121** showing peak correlations between δ 1.5-5.0

For full peak assignment of the carbon spectrum it is also helpful to examine the HMBC of **121** (Figs 2.29-2.30). As expected proton H21 shows coupling with carbons C19, C20, and C21. Proton H2 exhibits coupling with carbons C4, C3 and C11, while proton H1 exhibits coupling with C3 and C12. Proton H5 displays coupling with carbons C4, and C12, while proton H19, shows coupling with C20, and C21'.

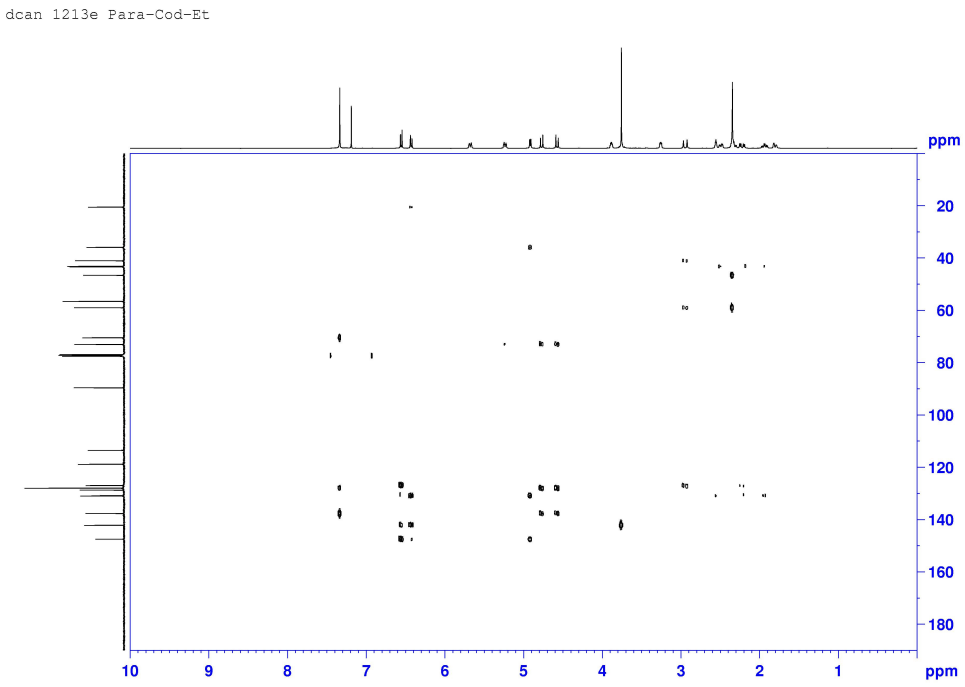

Fig 2.29 HMBC spectrum of **121**

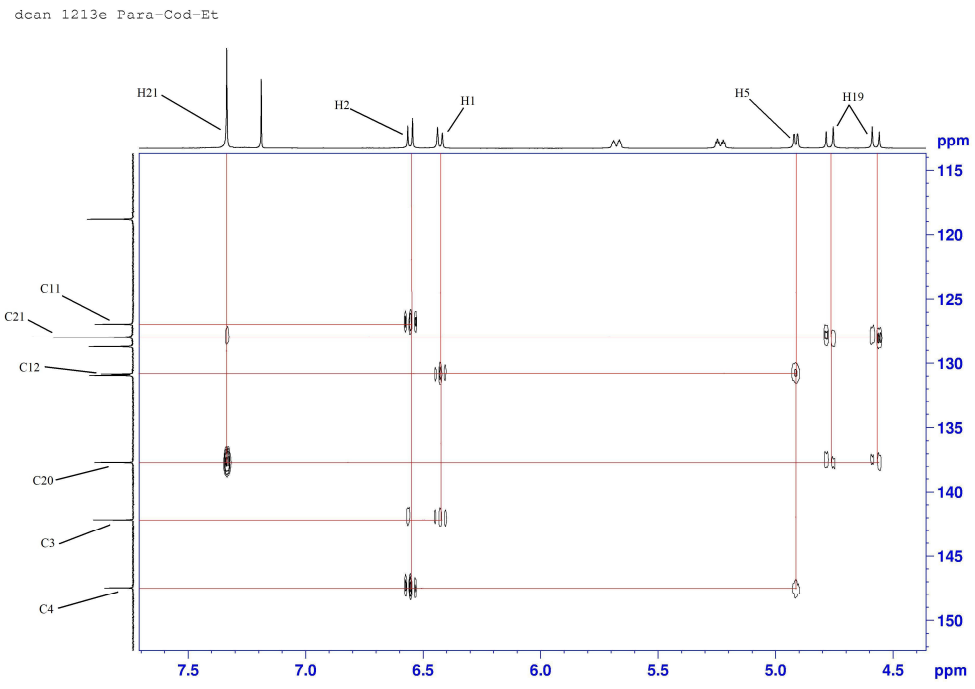

Fig 2.30 HMBC spectrum of **121** showing peak correlations at δ 4.5-7.5

2.5 X-ray Crystallography Studies of Ester Linked Codeine Derivatives

An understanding of the crystal structure of the linked opioid derivatives can provide valuable information in relation to the drug-receptor interaction at the receptor binding sites (Chapter 4). This may aid in the understanding of the mode of action of these therapeutic agents. Also analysis of the crystal structure can provide important information on the potential of these compounds to interact with metal cationic species (Chapter 5). From the x-ray crystallographic analysis the structural data of the linked opioid compounds **126** and **127** was estimated using *Mercury 2.3* software. This data is based on solid state and it must be emphasised that the opioid compounds may undergo significant conformational changes when interacting with the opioid receptor site (Chapter 4) or metal cation species (Chapter 5).

2.5.1 X-ray Crystallography Study of 126

Crystals suitable for single crystal X-ray determination of **126** were grown by slow evaporation from $CHCl_3$:hexane (1:4), yielding colourless block shaped crystals. Compound **126** crystallises in the space group $P2_1$ with selected bond distances, bond angles and torsion angles given in Table 2.10. As expected ring conformations for each codeine structural unit are similar to previously reported opioid derivatives which each codeine unit adopting the classic T-shaped configuration.[71, 72]

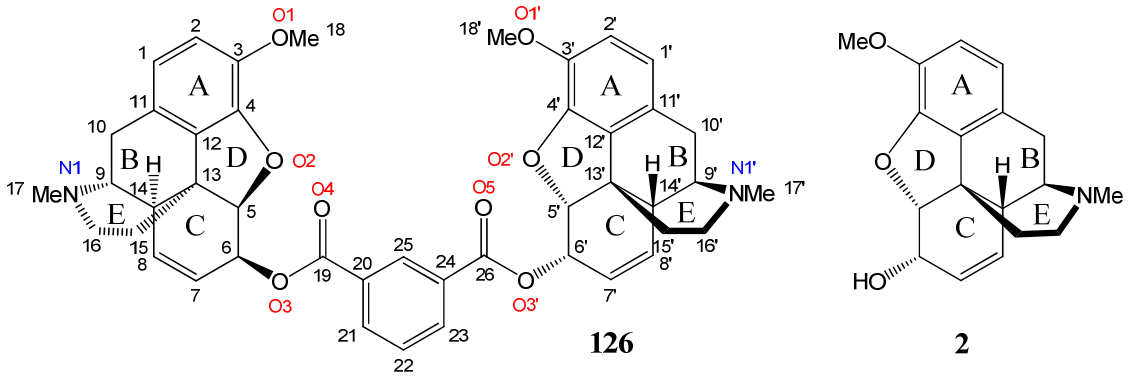

Fig 2.31 Structure of **126** and codeine (**2**) with ring labels and atom labels

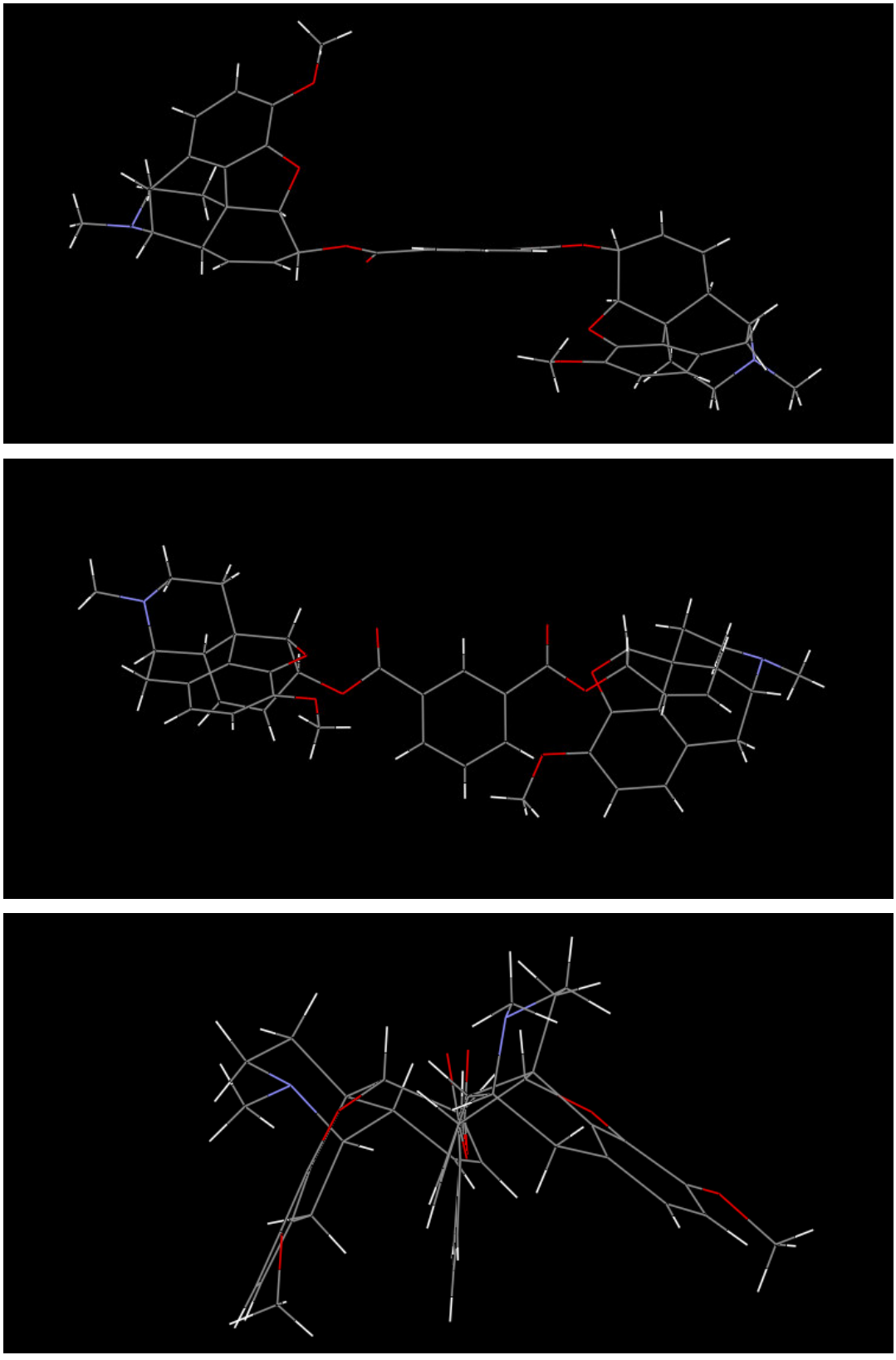

Fig 2.32 X-ray crystal structure of **126**

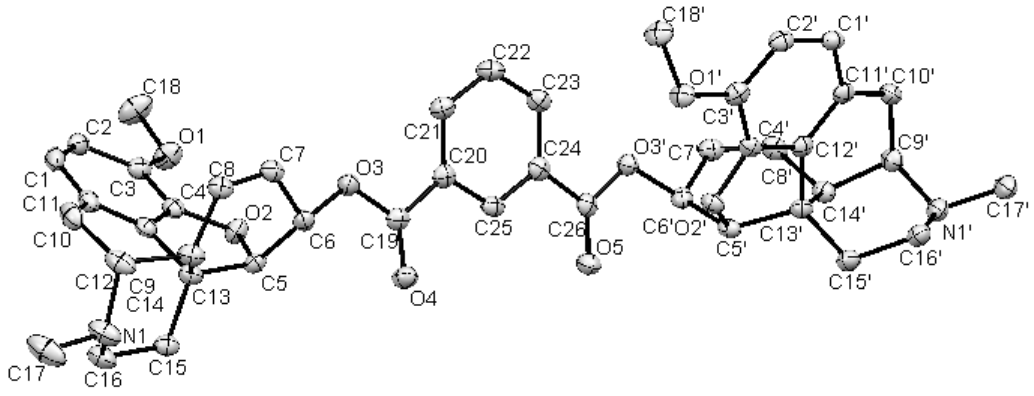

Fig 2.33 ORTEP diagram of **126** with atom labels

The bond length for C6-O3 is 1.445(2) Å while C6'-O3' is slightly longer at 1.455(2) Å. The bond length for C5-C6 is 1.544(2) Å with the corresponding bond C5'-C6', in the other codeine moiety again slightly longer at 1.564(2) Å. The bond lengths for O3-C19 and O3'-C26 are identical at 1.346(2) Å and 1.347(2) Å respectively. The bond angle for C5-C6-O3 is 112.3(1)° while C5'-C6'-O3' is calculated at 110.1(1)°. The bond angles for C7-C6-O3 and C7'-C6'-O3' are comparable at 106.6(1)° and 106.8(1)° respectively. The most noticeable differences in **126** are the variations in relative torsion angles for each codeine moiety. There are minimal differences in the torsion angles between each codeine unit for the A and B rings. The torsion angle for C1-C2-C3-C4 is 0.7(2) while the value for C1'-C2'-C3'-C4' is 3.5(2). The torsion angle for C10-C11-C12-C13 is 7.0(2) while the value for C10'-C11'-C12'-C13'is 3.8(2). As expected the major differences between each codeine scaffold correspond to the C-ring and the linker section of the molecule. The torsion angle for C5-C6-C7-C8 is 42.7(2) while the related torsion angle for C5'-C6'-C7'-C8' on the other codeine unit is 24.8(2). Likewise the calculated torsion angles for C7-C8-C14-C13 and C7'-C8'-C14'-C13' are -40.9(2) and -27.7(2) respectively. For O2-C5-C6-O3 the torsion angle was calculated at -34.3(2)° however the corresponding torsion angle of O2'-C5'-C6'-O3'

was calculated at -11.5(2)°. A similar result is displayed with C19-O3-C6-C5 and C26-O3'-C6'-C5' with torsion angles of -76.8(2)° and -66.8(2)° respectively. For more details on the X-ray crystal data for **126** see Appendix A, A.1.

Bond Lengths (Å)			
C6-O3	1.445(2)	C6'-O3'	1.455(2)
C5-C6	1.544(2)	C5'-C6'	1.564(2)
O3-C19	1.346(2)	O3'-C26	1.347(2)
Bond Angles (°)			
C5-C6-O3	112.3(1)	C5'-C6'-O3'	110.1(1)
C7-C6-O3	106.6(1)	C7'-C6'-O3'	106.8(1)
C6-O3-C19	116.5(1)	C6'-O3'-C26	114.1(1)
Torsion Angles (°)			
A Ring			
C11-C1-C2-C3	-3.9(3)	C11'-C1'-C2'-C3'	-0.8(3)
C1-C2-C3-C4	0.7(2)	C1'-C2'-C3'-C4'	3.5(2)
B Ring			
C14-C9-C10-C11	31.9(2)	C14'-C9'-C10'-C11'	37.6(2)
C10-C11-C12-C13	7.0(2)	C10'-C11'-C12'-C13'	3.8(2)
C Ring			
C5-C6-C7-C8	42.7(2)	C5'-C6'-C7'-C8'	24.8(2)
C6-C7-C8-C14	-3.2 (2)	C6'-C7'-C8'-C14'	-6.5 (3)
C13-C5-C6-C7	-31.8 (2)	C13'-C5'-C6'-C7'	-6.3 (2)
C7-C8-C14-C13	-40.9 (2)	C7'-C8'-C14'-C13'	-27.7 (2)
Linker Section			
O2-C5 –C6-O3	-34.3 (2)	O2'-C5'-C6'-O3'	-11.5 (2)
C19-O3-C6-C5	-76.8 (2)	C26-O3'-C6'-C5'	-66.8 (2)

Table 2.10 Selected bond distances and bond angles and torsion angles for **126** with estimated standard deviations in parenthesis

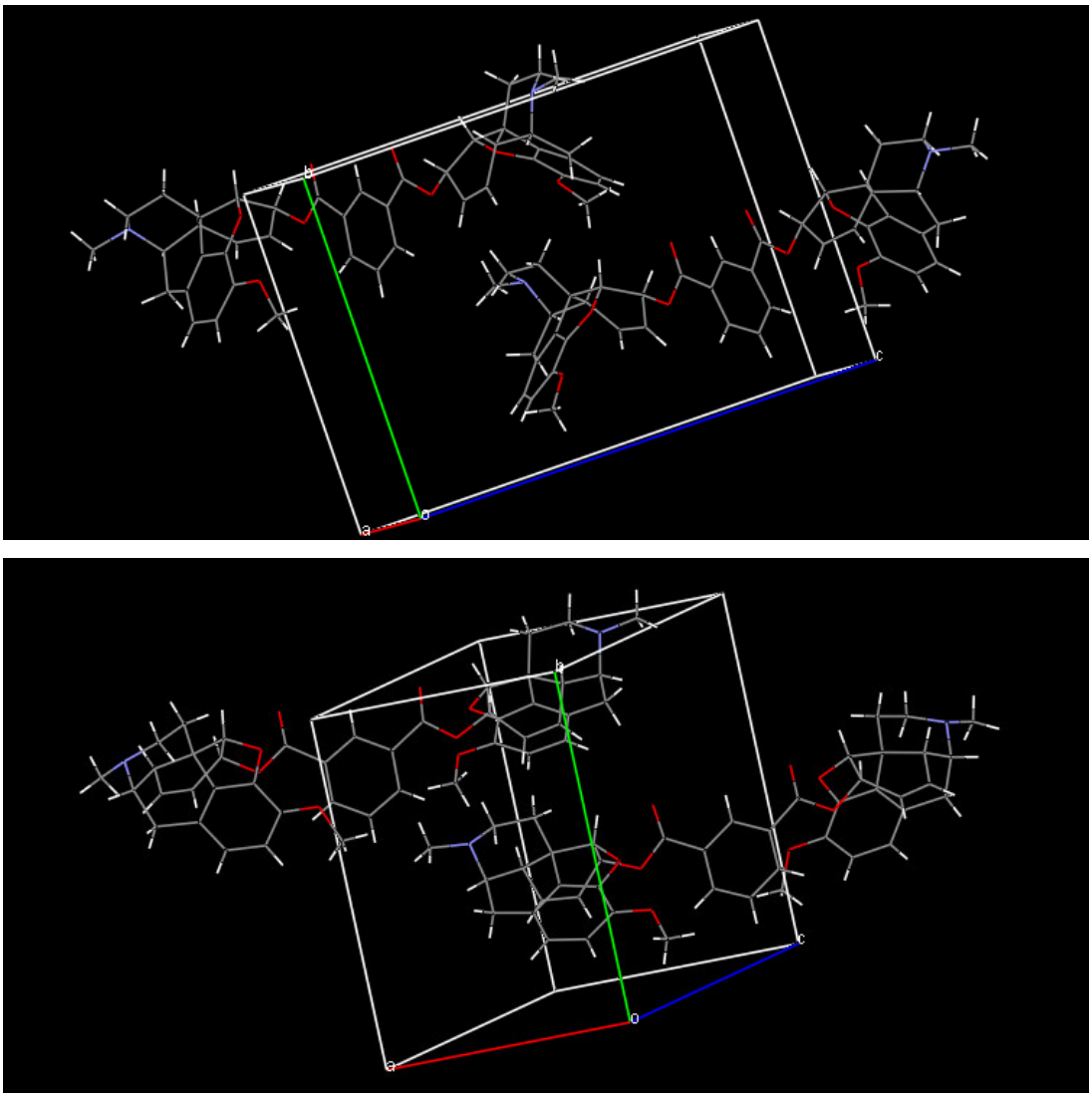

Fig 2.34 X-ray crystal packing of **126**

2.5.2 X-ray Crystallography Study of 127

Crystals suitable for single crystal X-ray determination of **127** (Fig 2.35) were grown by slow evaporation from chloroform:hexane (1:4), yielding colourless block shaped crystals. Compound **127** crystallises in the space group $P2_12_12_1$ with selected bond distances, bond angles and torsion angles given in Table 2.11. As noted with **126** each codeine unit adopts the T-shaped configuration of classic opioid compounds.

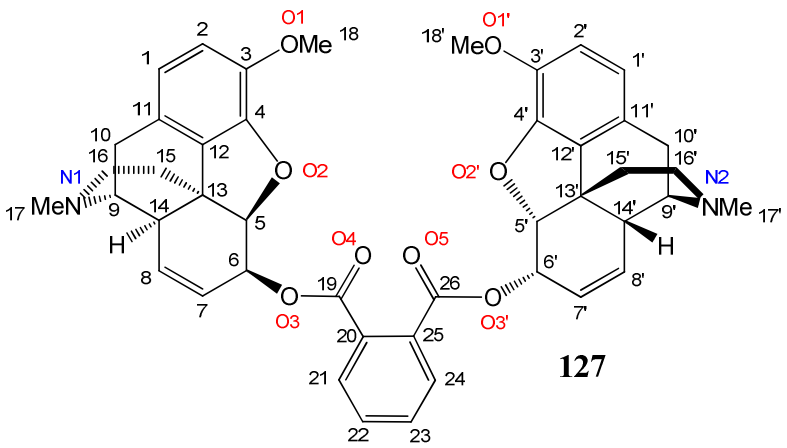

Fig 2.35 Structure of **127** with atom labels

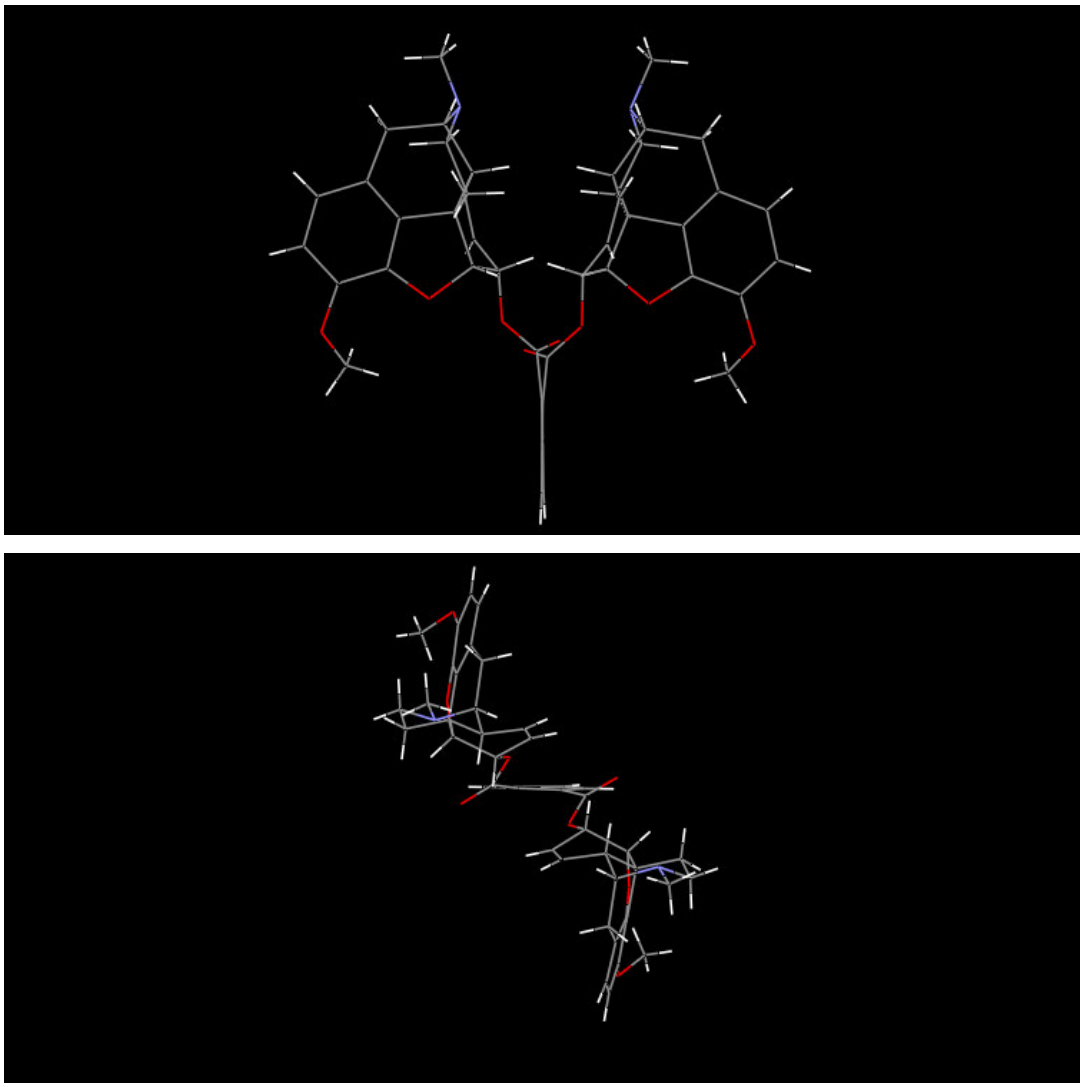

Fig 2.36 X-ray crystal structure of **127**

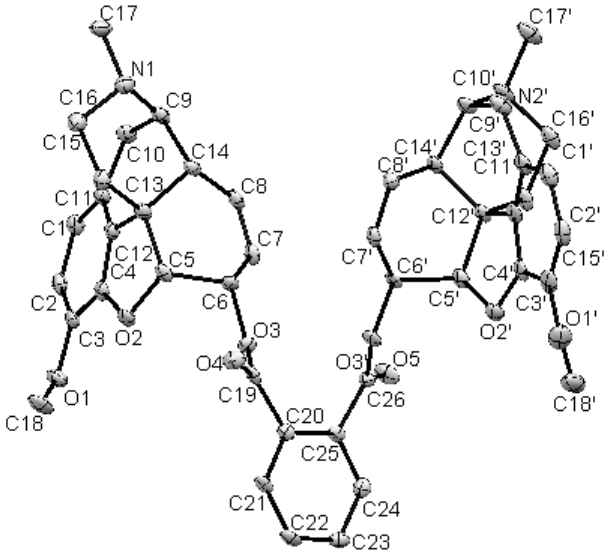

Fig 2.37 ORTEP diagram of **127** with atom labels

The bond length for C6-O3 is 1.450(2) Å while C6'-O3' is almost identical at 1.455(2) Å. The bond length for C5-C6 is 1.537(2) Å with the corresponding bond C5'-C6', in the other codeine moiety identical at 1.536(2) Å. The bond lengths for O3-C19 and O3'-C26 are also identical at 1.340(2) Å and 1.344(2) Å respectively. The bond angle for C5-C6-O3 is 114.1(1)° which is identical to C5'-C6'-O3' at 114.0(1)°. The bond angles for C7-C6-O3 and C7'-C6'-O3' are similar at 106.1(1)° and 106.9(1)° respectively. The most noticeable differences in **127** are the variations in relative torsion angles for each codeine structural unit however there is much less variation than was noted for **126**. As expected there is only minimal difference between the torsion angles for the A and B rings. The most noticeable differences are in the C ring and the linker section. The torsion angle for C5-C6-C7-C8 is 44.0(2) while the related torsion angle for C5'-C6'-C7'-C8' on the other codeine unit is 49.5(2). Likewise the calculated torsion angles for C7-C8-C14-C13 and C7'-C8'-C14'-C13' are -40.0(2) and -41.4(2) respectively. For O2-C5-C6-O3 the torsion angle was calculated at -35.5(2)° with the corresponding torsion angle of O2'-C5'-C6'-O3' calculated at -42.1(2)°. The torsion angles for C19-O3-C6-C5 and C26-O3'-C6'-C5' were calculated at -77.4(2)° and -

75.1(2)° respectively. Compound **127** is not symmetrical in the solid state. For more details on the X-ray crystal data for **127** see Appendix A, A.2.

Bond Lengths (Å)			
C6-O3	1.450(2)	C6'-O3'	1.455(2)
C5-C6	1.537(2)	C5'-C6'	1.536(2)
O3-C19	1.340(2)	O3'-C26	1.344(2)
Bond Angles (°)			
C5-C6-O3	114.1(1)	C5'-C6'-O3'	114.0(1)
C7-C6-O3	106.1(1)	C7'-C6'-O3'	106.9(1)
C6-O3-C19	117.8(1)	C6'-O3'-C26	116.7(2)
Torsion Angles (°)			
A Ring			
C11-C1-C2-C3	-4.1(3)	C11'-C1'-C2'-C3'	-4.1(3)
C1-C2-C3-C4	0.6(3)	C1'-C2'-C3'-C4'	0.9(3)
B Ring			
C14-C9-C10-C11	31.9(2)	C14'-C9'-C10'-C11'	31.2(2)
C10-C11-C12-C13	3.0(3)	C10'-C11'-C12'-C13'	1.9(3)
C Ring			
C5-C6-C7-C8	44.0(2)	C5'-C6'-C7'-C8'	49.5(2)
C6-C7-C8-C14	-4.6(3)	C6'-C7'-C8'-C14'	-6.3(3)
C13-C5-C6-C7	-32.2(2)	C13'-C5'-C6'-C7'	-37.6(2)
C7-C8-C14-C13	-40.0(2)	C7'-C8'-C14'-C13'	-41.4(2)
Linker Section			
O2-C5 -C6-O3	-35.5(2)	O2'-C5'-C6'-O3'	-42.1(2)
C19-O3-C6-C5	-77.4(2)	C26-O3'-C6'-C5'	-75.1(2)

Table 2.11 Selected bond distances and bond angles and torsion angles for **127** with estimated standard deviations in parenthesis

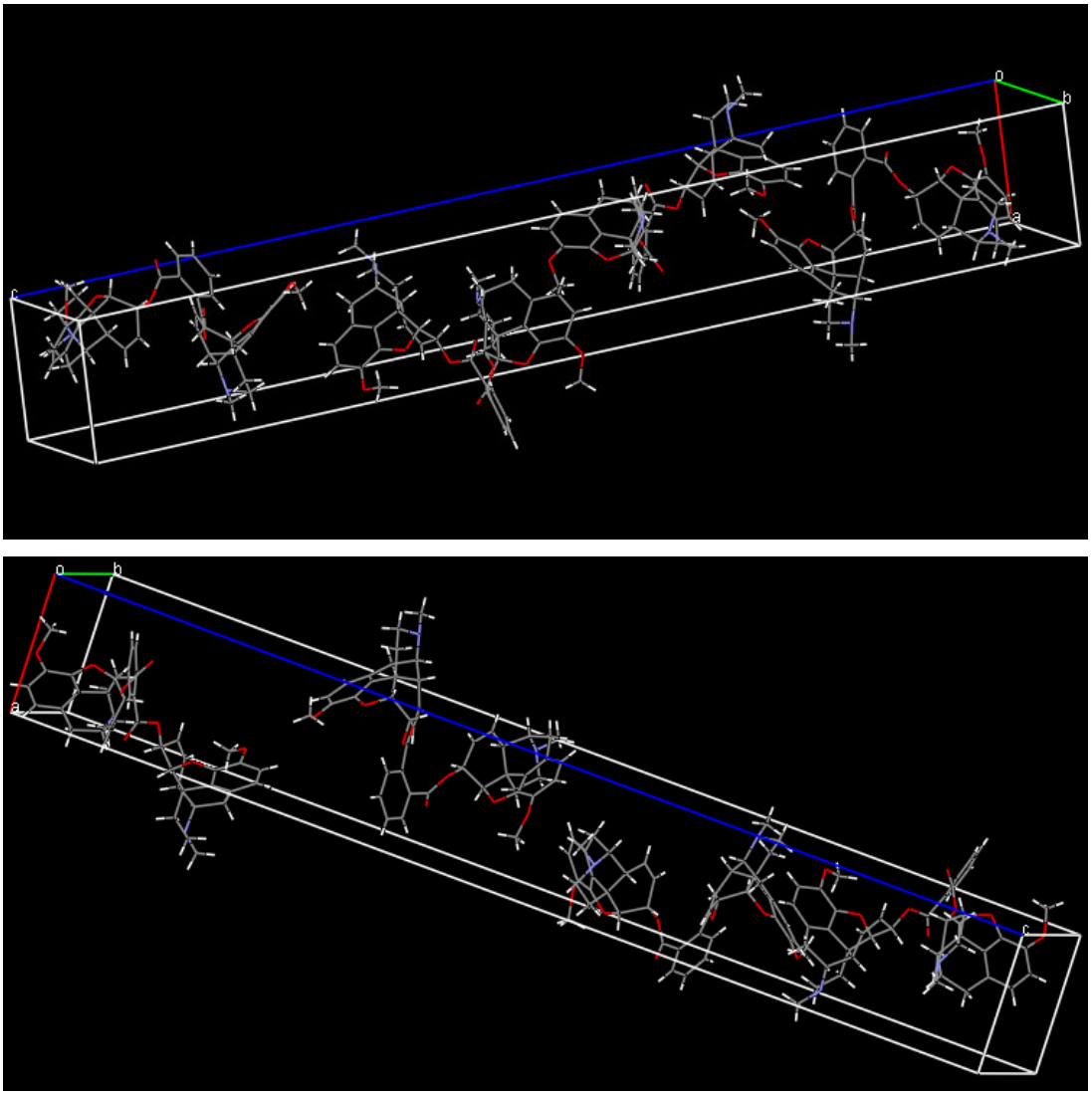

Fig 2.38 X-ray crystal packing of **127**

2.6 Conclusion

The synthesis and structural characterisation of ester and ether "linked" codeine derivatives has been achieved. A selection of eight novel ester linked codeine derivatives (**119**, **126-132**) were successfully synthesised in modest to good isolated yields of 39% - 82%. Initial synthesis of the ester linked codeine derivatives *via* NEt_3 in DCM under N_2 resulted in minimal conversion to the desired compounds. An investigation into improved reaction conditions was performed with the choice of base

(NEt_3, K_2CO_3, Na_2CO_3, NaH, KOH, NaOH, DMAP), solvent (DCM, THF, pyridine) and temperature analysed. After analysis it was found that the ester linked codeine compounds can be generated in modest to good yields *via* the reaction of codeine with the appropriate acid chloride species in the presence of DMAP in DCM under N_2. Increasing the temperature of the reaction had no discernable affects on product formation. Purification was achieved by a combination of column chromatography and recrystallisation. Full characterisation was performed by m.p., IR, $[\alpha]_D$, HRMS, ^{1}H NMR, ^{13}C NMR, DEPT, COSY, HMQC and HMBC. An in depth NMR analysis of one of the ester linked compounds (**119**) was also performed with full peak assignments. An examination of the X-ray crystal structures of two of the ester linked codeine derivatives was also performed (**126**, **127**).

Successful generation of two ether linked compounds (**121**, **139**) was also achieved in isolated yields of 55% and 59%. Based on previous experiments within the research group the compounds were synthesised *via* the reaction of codeine with the appropriate ether linker in the presence of KOH, KI in THF at 66 °C. Purification was similar to the ester derivatives *via* combination of column chromatography and recrystallisation. The 1,4-*bis*(bromomethyl)benzene species resulted in a higher yield than the 1,4-*bis*(chloromethyl)benzene species. Full characterisation was performed by m.p., IR, $[\alpha]_D$, HRMS, ^{1}H NMR, ^{13}C NMR, DEPT, COSY, HMQC and HMBC. An in depth NMR analysis of an ether linked compound (**121**) was also performed with full peak assignments.

Chapter 3

Synthesis and Structural Characterisation of A-Ring Modified Codeine Derivatives

3.1 Introduction

This chapter details the synthesis of a series on novel opioid compounds based on structural modification at the 1 and 6 positions of the codeine (**2**) scaffold. Previous studies on opioid derivatives have shown that modification at the 1 position of the aromatic ring is possible through halogenation[73] (**75**) and palladium coupling[74] (**140**) (Fig 3.1). By combining the palladium coupling techniques with the formation of linked codeine derivatives (Chapter 2) a series of novel opioid derivatives can be generated (Scheme 3.1).

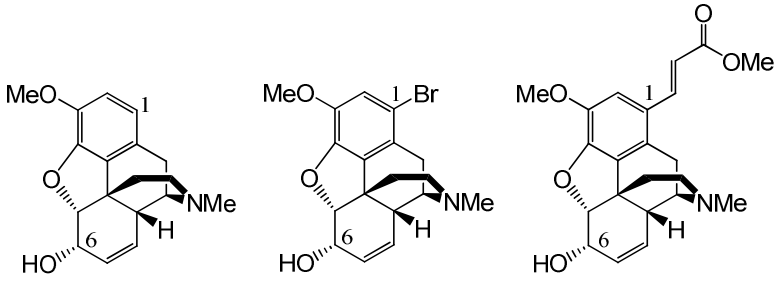

2 **75** **140**

Fig 3.1 Codeine (**2**) and A-ring modified codeine derivatives, **75** (halogenated derivative) and **140** (palladium catalysed carbon-carbon coupled derivative).

Palladium coupling chemistry has received a lot of interest over recent years with much of the work involving Heck[75], Stille[76], and Suzuki[77] coupling. Heck coupling involves the reaction of an unsaturated halide with an alkene in the presence of a base such as triethylamine and a palladium catalyst, most commonly palladium acetate. The halide species is usually an aryl, benzyl or vinyl compound with the alkene often electron-deficient, such as an acrylate ester. Normally a phosphine ligand is also used for the

reaction, usually triphenylphosphine. For the purposes of this research the opioid derivatives are acting as the halide species.

Stille coupling is a versatile method for the formation of carbon-carbon bonds which employs the reactions between halides and stannanes. The main benefit of this method is that there are very few limitations on the halide group which is an important factor that has to be considered when the opioids are acting as the halide species. However, it must also be noted that many of the tin compounds have high toxicity[78] and trace amounts of tin impurities can often be difficult to remove successfully during purification. The other important general coupling method employed is Suzuki coupling. The reaction proceeds *via* the reaction of an aryl or vinyl boronic acid species with an aryl or vinyl halide compound again catalysed by palladium.

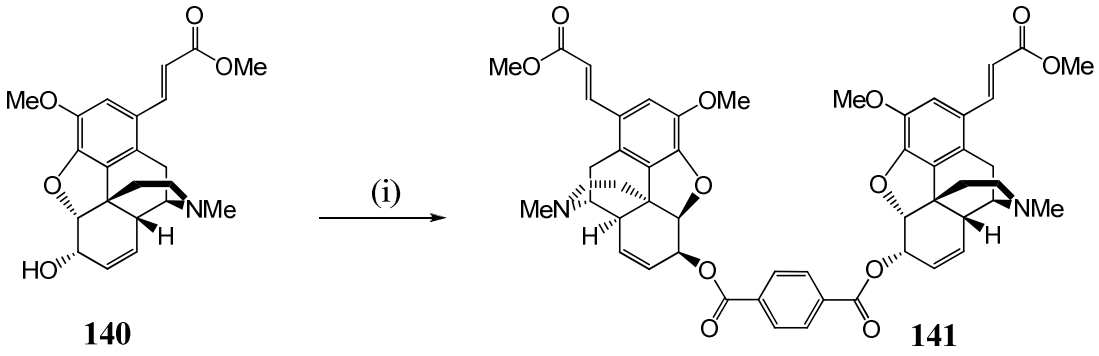

140 **141**

Reaction Conditions; (i) Terephthaloyl dichloride (0.5 Eq), DMAP (1.1 Eq), DCM, N_2, RT

Scheme 3.1 Formation of *para* ester linked codeine compound (**141**) with A-ring modification

Modification of the A-ring of opioids has been shown to lower the binding affinity to the *mu* opioid receptor (Chapter 1, 1.2.4) thus formation of these compounds could have important applications in relation to analgesic therapeutics (Chapter 4). A-ring modification on the linked codeine species (Scheme 3.1) could also affect metal binding thus expanding the scope for sensor applications.

3.2 Synthesis of A-ring Modified Codeine Derivatives

3.2.1 Halogenated Codeine Derivatives

The first step in the formation of A-ring modified opioids is the generation of the halogenated codeine structures, bromocodeine (**75**), iodocodeine (**142**) and chlorocodeine (**76**). Wilson *et al* have previously shown that halogenation at the 1 position is possible using the appropriate halogenated *N*-succinimide in an acidic environment.[73] Halogenation was only observed at the aromatic 1 position of the ring (Fig 3.2).

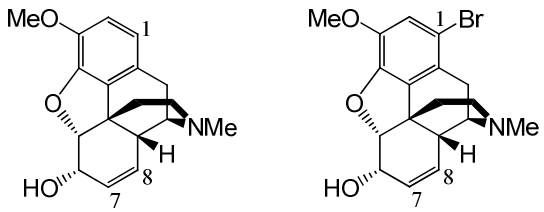

2 **75**

Fig 3.2 Structure of codeine (**2**) and bromocodeine (**75**) showing halogenation at the 1 position

No halogenation of the carbon-carbon double bond (positions 7 and 8) was observed or at the 2 position of the aromatic ring. Halogenation of the aromatic ring preferentially favours the 1 position due to the strong *para*-directing moiety of the ring fusion ether at the 4 position. Synthesis of these compounds was performed using the appropriate halogenated *N*-succinimide in TFA (Scheme 3.2). Isolated yields for the halogenated compounds (**75**, **76**, **142**) were between 62-89% (Fig 3.3). The highest isolated yield was achieved for the iodine derivative (**142**) at 89% while the chlorine derivative (**76**) resulted in the lowest isolated yield at 62%. To achieve chlorination at the 1 position of the aromatic ring it was necessary to increase the reaction temperature to 90°C. When the reaction with *N*-chlorosuccinimide was performed at RT no product was observed, with only codeine starting material recovered. The reactivity of the *N*-halosuccinimide compounds are in agreement with the literature.[73,79]

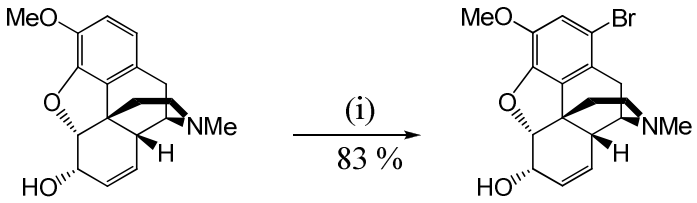

2 **75**

Reaction Conditions; (i) *N*-Bromosuccinimide (1.1 Eq), 0.1M TFA, RT

Scheme 3.2 Reaction scheme for the formation of bromocodeine (**75**)

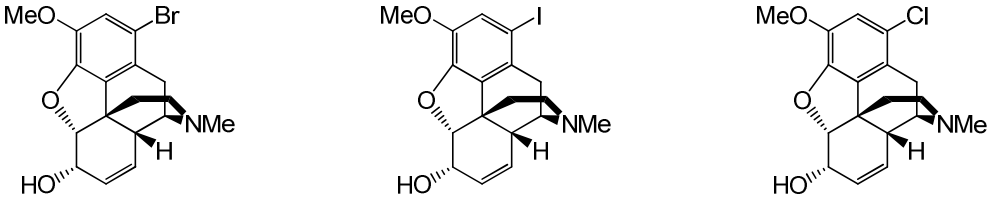

75, 83% **142**, 89% **76**, 62%

Fig 3.3 Halogenated derivatives of codeine with isolated yields using *N*-halosuccinimides

3.2.2 Halogenated Ester Linked Codeine Derivatives

As esterification has previously been demonstrated at the secondary alcohol sites (Chapter 2, 2.2.1) to form the linked opioid derivatives we decided to generate the halogenated analogues of the linked species. There are two routes to synthesise the desired esterified halogenation species (Scheme 3.3). Generation of the ester linked compound (**7**) followed by halogenation (route A) or halogenation of the aromatic ring followed by esterification (route B). Of note is the possible susceptibility of the ester bonds to hydrolysis especially in the presence of an acid or base.

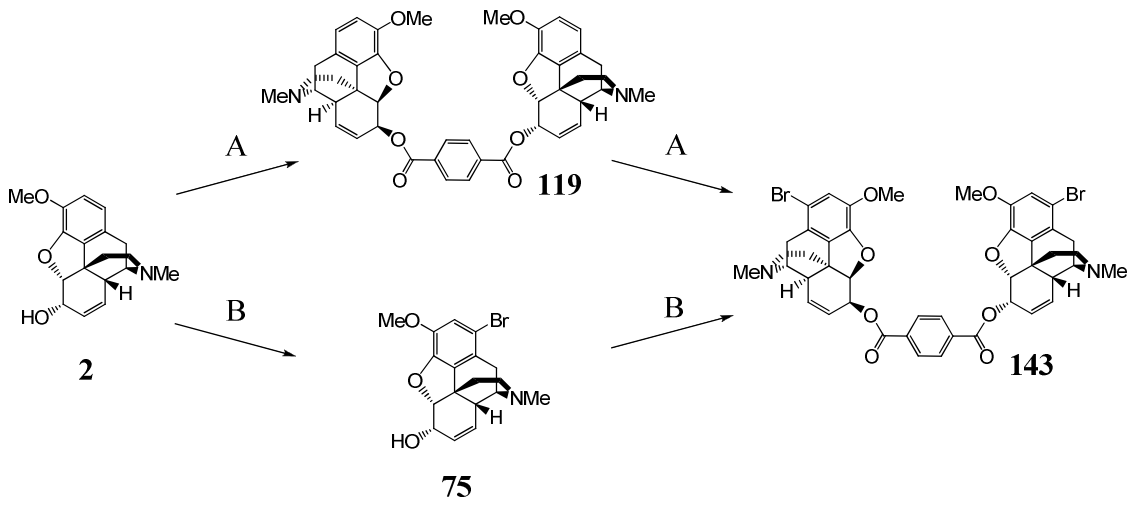

Scheme 3.3 Two possible routes to the formation of ester linked halogenated codeine derivative (**143**)

Synthesis of the halogenated species is *via* the acid catalysed reaction of the appropriate opioid with *N*-halogenated succinimide.[73] The ester bonds would be highly prone to hydrolysis under these conditions and would degrade to the corresponding alcohol. Thus route A (Scheme 3.3) would not be a suitable path to approach the generation of the desired halogenated ester compounds. For this reason route B, initial halogenation of the aromatic A-ring followed by esterification was chosen.

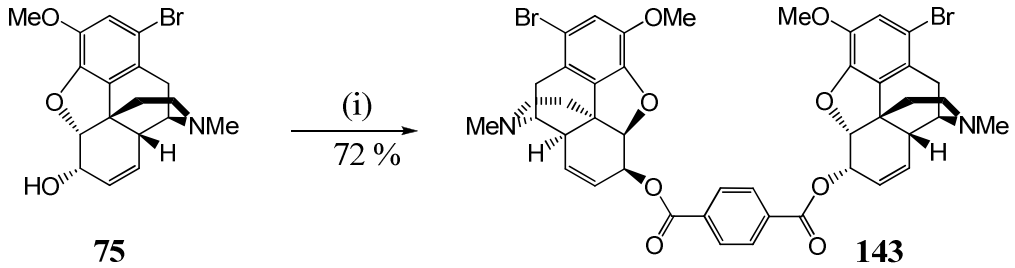

Reaction Conditions; (i) Terephthaloyl dichloride (0.5 Eq), DMAP (1.1 Eq), DCM, N_2, RT

Scheme 3.4 Reaction scheme for the formation of **143**

A selection of linked bromocodeine (**143**-**148**) and iodocodeine (**149**, **150**) derivatives were synthesised with alteration dependent on the diacid chloride employed in the reaction. The halogenated codeine derivatives were synthesised according to Wilson *et*

al.[73] The same method, catalytic DMAP as the base, was employed for the generation of all the brominated ester linked compounds (Scheme 3.4). The isolated yields for the six brominated ester compounds (**143**-**148**) were between 39% and 89%, (Fig 3.4).

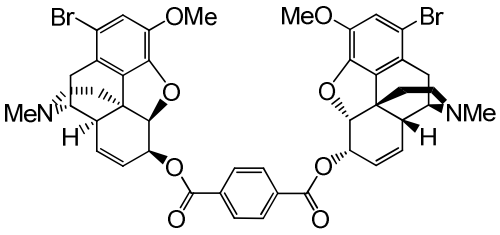

143, 72%

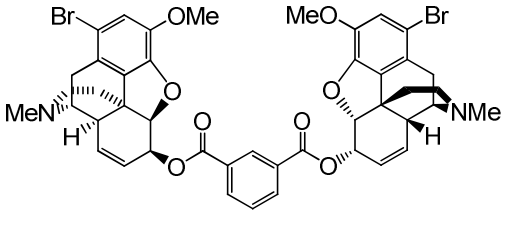

144, 75%

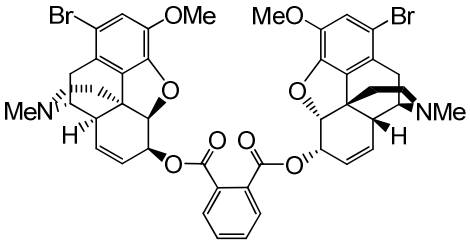

145, 71%

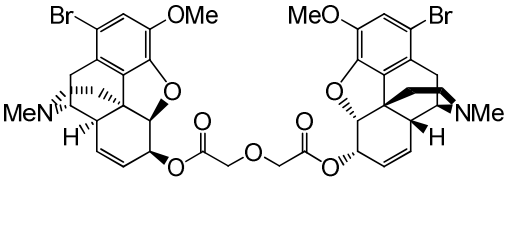

146, 39%

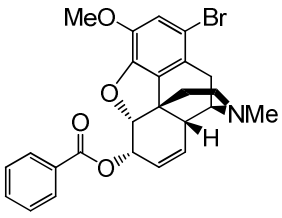

147, 89%

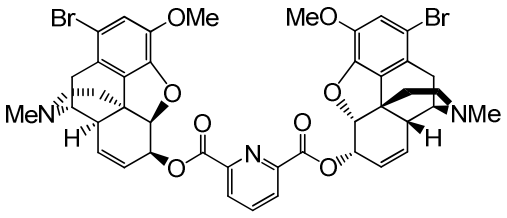

148, 51%

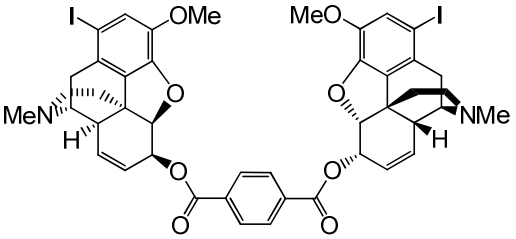

149, 76%

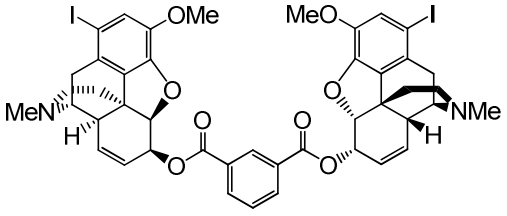

150, 79%

Fig 3.4 Ester linked bromocodeine (**143**-**148**) and iodocodeine (**149**, **150**) derivatives with isolated yields

As noted for the codeine linked esters the isolated yields could be improved through futher development of reaction conditions and purification if necessary. Purification on the brominated species was performed as per the codeine linked esters, *via* column chromatography and recrystallisation. As observed in the reactions of the acid chlorides with codeine the conversions from bromocodeine to the ester linked structures varied depending on the diacid chloride (Chapter 2, 2.2.1). As expected the conversions for bromocodeine to the desired linked species are similar to that of codeine. Again lower conversions were seen when using diglycolyl dichloride or 2,6-pyridinedicarbonyl dichloride. Esterification was also attempted using iodocodeine as the halogenated derivative (**149**, **150**) (Fig 3.4). As expected these reactions exhibited similar results to the bromocodeine derivatives.

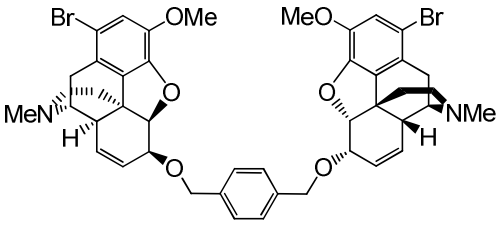

151, 53%

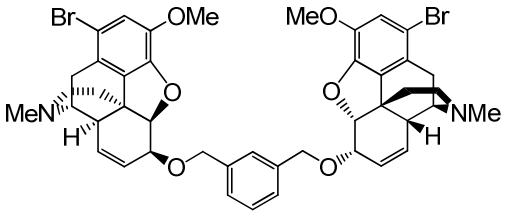

152, 59%

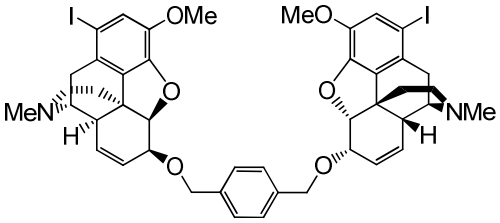

153, 60%

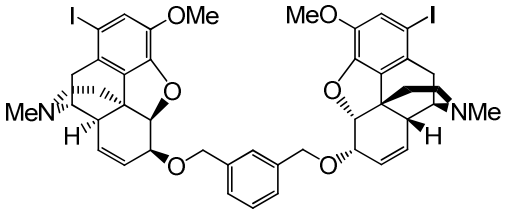

154, 45%

Fig 3.5 Ether linked bromocodeine (**151, 152**) and iodocodeine (**153, 154**) derivatives with isolated yields

Synthesis of the halogenated versions of the ether linked compounds was also undertaken (**151**-**154**). The same route as the ester linked products was employed, initial formation of the halogenated codeine species followed by completion of the ether linked compound. In total four halogenated compounds were synthesized using

both the bromocodeine (**75**) and iodocodeine (**142**) derivatives with the α,α'-dibromo-*p*-xylene and α,α'-dibromo-*m*-xylene linker units. Isolated yields for the halogenated derivatives (**151**-**154**) were comparable to the non halogenated compounds (**121**, **139**) in the range of 45% - 59% (Fig 3.5). Purification of the ether derivatives was achieved through a combination of recrystallisation and column chromatography. The mobile phase employed for these compounds was similar to the ester derivatives, a DCM methanol mixture with small amounts of ammonia solution added to the mobile phase to prevent tailing.

3.2.3 Palladium Coupling of the Halogenated Codeine

With the formation of a variety of halogenated opioid derivatives proving successful (**143**-**154**) further modification of the aromatic A-ring *via* palladium coupling techniques was undertaken. Previous studies into carbon-carbon coupling have shown that the chlorine atom is less reactive than bromine and iodine. As the chlorine derivative (**76**) was also isolated in significantly lower yields the bromocodeine (**75**) and iodocodeine (**142**) compounds were used for palladium coupling.

Davies *et al*[74] had previously shown that palladium coupling was possible on bromocodeine resulting in a variety of A-ring modified opiates in high yields (Fig 3.6). Four opioid derivatives (**140**, **155**-**157**) previously reported by Davies and co-workers[74] were synthesised as these would be important intermediates in the future synthesis of A-ring modified linked opioids (**141**, Scheme 3.1). An examination of the halogenated opiate structure reveals that there may be some side reactions possible due to the presence of the allylic ether moiety which has been shown to react under palladium catalysis to the corresponding vinyl ether.[74, 80] In addition there could be some competition from intermolecular Heck reactions.

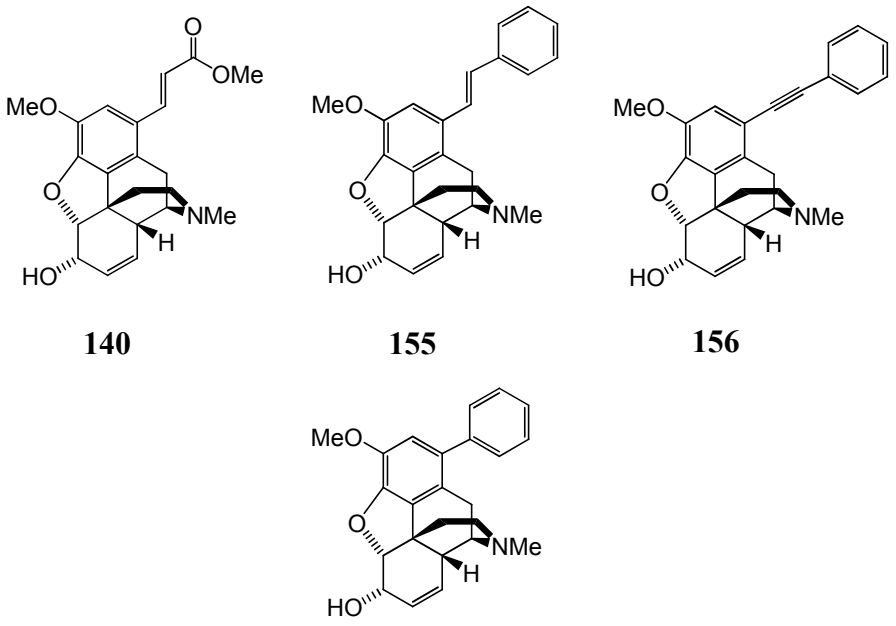

140 **155** **156**

157

Fig 3.6 A-ring modified codeine derivatives previously reported

The allylic alcohol at the 6 position was protected as a *t*-butyldimethylsilyl ether (Scheme 3.5). The bromocodeine (**158**) and iodocodeine (**159**) derivative were protected in yields of 89% and 86% respectively. This is comparable to the isolated yield observed for the protection of codeine to form **160** (Fig 3.7). Following the palladium coupling step, facile deprotection by TBAF in THF resulting in high conversions to the desired compounds is expected.

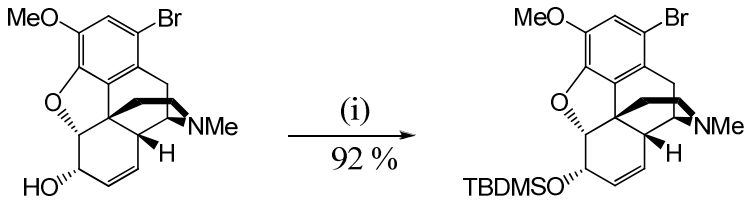

75 **158**

Reaction Conditions; (i) Imidazole (1.2 Eq), TBDMSCl (1.2 Eq), DMF, RT

Scheme 3.5 Reaction conditions for protection of the secondary alcohol

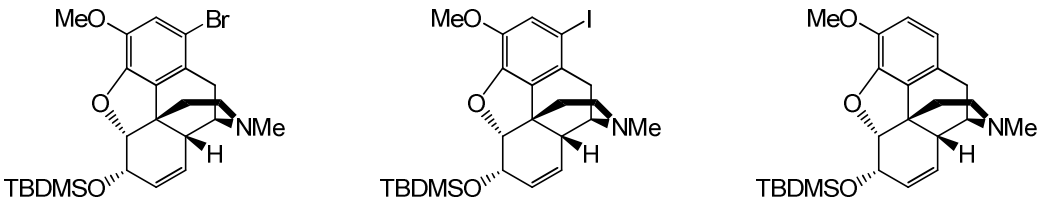

158, 89% **159**, 86% **160**, 87%

Fig 3.7 TBDMS protected opioid derivatives, **158**-**160** with isolated yields

Generation of compounds **140** and **155** (Scheme 3.6) was initially undertaken with the bromocodeine derivative (**158**) using 2 mol% of palladium acetate, leading to moderate yields of 53% and 43 % for **140** and **155** respectively. The mol% of palladium acetate was increased to 5 mol% resulting in increased yields of 54% and 50% for **140** and **155** respectively. However when the percentage of palladium acetate was increased to 10 mol% and 20 mol% no further improvement on the isolated yields was observed. Employing the iodocodeine derivative (**159**) instead of the bromocodeine (**158**) resulted in increased yields for **140** and **155** of 63% and 62% respectively (Scheme 3.6).

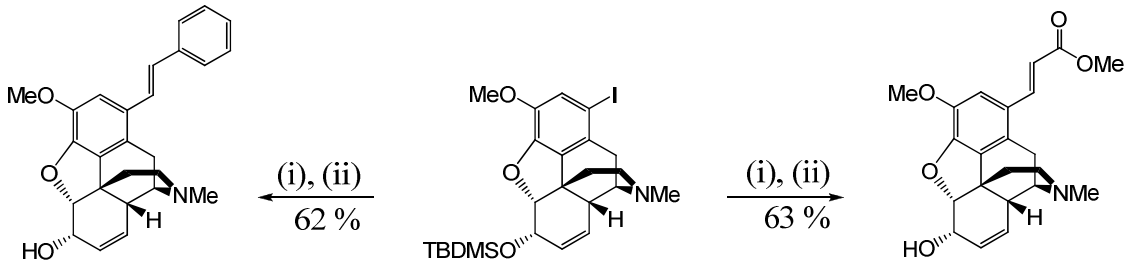

155 **159** **140**

Reaction Conditions; (i) $Pd(OAc)_2$ (5 mol %), PPh_3 (20 mol %), DMF, NEt_3 (3.5 Eq), [Methyl acrylate or Styrene] (4 Eq), N_2, 100°C, (ii) TBAF (2 Eq), THF, RT

Scheme 3.6 Reaction scheme for the formation of **140** and **155**

Analysis of the crude ^{1}H NMR spectra for both compounds did not reveal the presence of any side reactions taking place. The carbon-carbon double bond for both derivatives was assigned as the *trans* conformer due to the *J* coupling value of 16.0 Hz, corresponding to an (*E*)-geometry. Examination of the crude ^{1}H NMR spectra also

showed that the protecting group was stable to the palladium coupling reaction conditions. Confirmation of the stability of the protecting group was provided by isolation of **161** (Scheme 3.7) The isolated yield for **161** was 85%, comparable to the reported value.[74] Thus a significant portion of the product is being lost through the deprotection step *via* the reaction workup and purification.

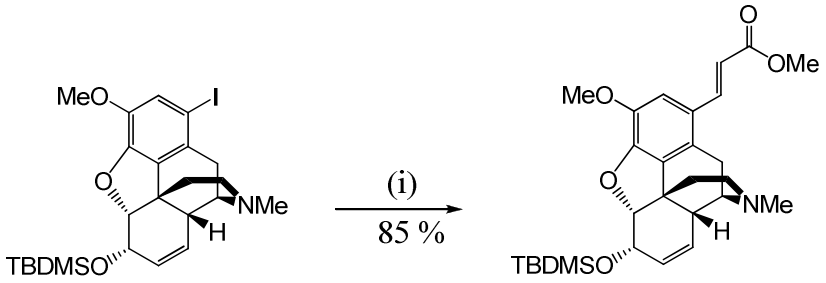

159 **161**

Reaction Conditions; (i) $Pd(OAc)_2$ (5 mol %), PPh_3 (20 mol %), DMF, NEt_3 (3.5 Eq), Methyl Acrylate (4 Eq), N_2, 100°C

Scheme 3.7 Reaction scheme for the formation of **161**

The two further opioid derivatives (**156**, **157**) were synthesized *via* Stille and Suzuki palladium coupling methodologies. The iodocodeine derivative (**159**) was utilised in the synthesis as this had previously resulted in improved yields relative to the bromocodeine derivative (**158**). Compound **156** was generated using tributyl(phenylethynyl)tin in an isolated yield of 48% after TBDMS deprotection (Scheme 3.8). Evidence from the crude ^1H NMR spectra showed that the secondary alcohol was still protected after the palladium coupling step which is in agreement with the protected methyl acrylate (**161**) isolated previously.

Davies *et al*[74] also reported the formation of **157** using phenyltributyltin however it was decided to explore an alternative method for the formation of this derivative. One of the main drawbacks of Stille coupling is the potential toxicity of the tin complexes employed in the reaction.[78] Compound **157** could also be formed through Suzuki coupling by utilizing phenylboronic acid (Scheme 3.9). Suzuki coupling proved

successful for the formation of **157** with the isolated yield of 80% after deprotection comparable to the other palladium coupled derivatives.

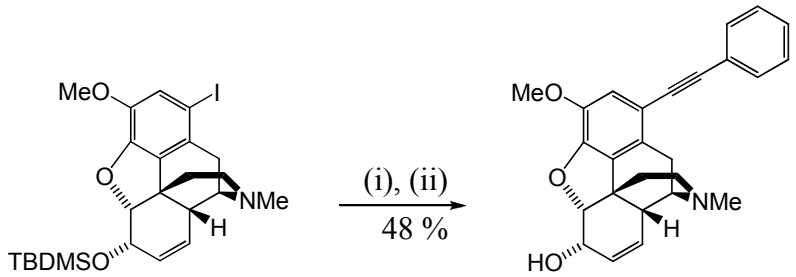

159 **156**

Reaction Conditions; (i) $Pd(OAc)_2$ (5 mol%), tributyl-(phenylethynyl)-tin (1.2 Eq), PPh_3 (20 mol%), NEt_3, DMF, 100°C (ii) TBAF (2 Eq), THF, RT

Scheme 3.8 Reaction conditions for the formation of **156**

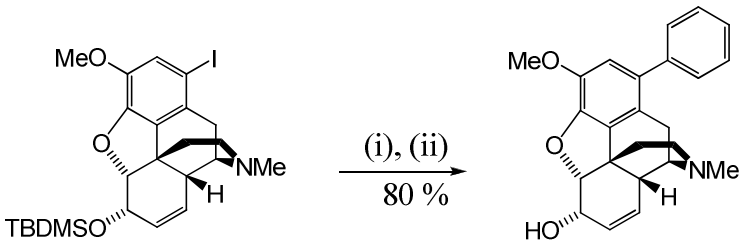

159 **157**

Reaction Conditions; (i) $Pd(OAc)_2$ (5 mol%), phenylboronic acid (2 Eq), PPh_3 (20 mol%), Na_2CO_3 (3.5 Eq), DMF, 100°C (ii) TBAF (2 Eq), THF, RT

Scheme 3.9 Reaction conditions for the formation of **157**

Two novel pyridine derivatives, **162** and **163** were also successfully synthesised using the same Heck coupling methodology in isolated yields of 79% and 64% respectively, after deprotection (Scheme 3.10). The TBDMS protected derivatives **164** and **165** were also isolated for these compounds in yields of 92% and 81% (Fig 3.9) again illustrating that Heck palladium catalysed coupling proceeds successfully for these opioid derivatives. Isolated yields for the formation of A-ring modified opioid compounds are

presented in Fig 3.8 and Fig 3.9. Isolated yields based on the work of Davies *et al*[74] are presented in Fig 3.8 while novel A-ring modified codeine derivatives are presented in Fig 3.9.

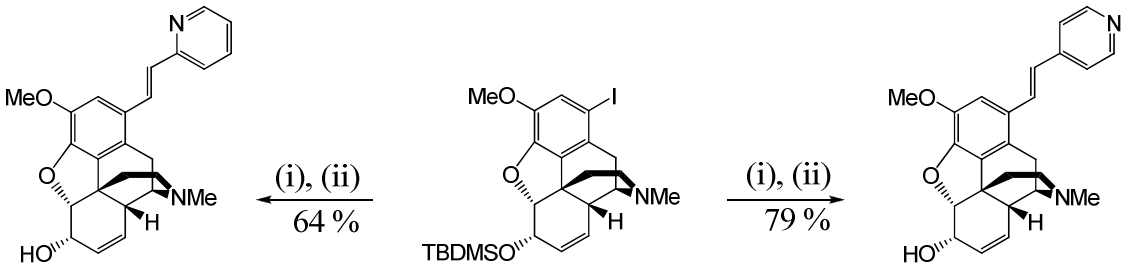

163 **159** **162**

Reaction Conditions; (i) $Pd(OAc)_2$ (5 mol %), PPh_3 (20 mol %), DMF, NEt_3 (3.5 Eq), [2-Vinylpyridine or 4-Vinylpyridine] (4 Eq), N_2, 100°C, (ii) TBAF (2 Eq), THF, RT

Scheme 3.10 Reaction scheme for the formation of **162** and **163**

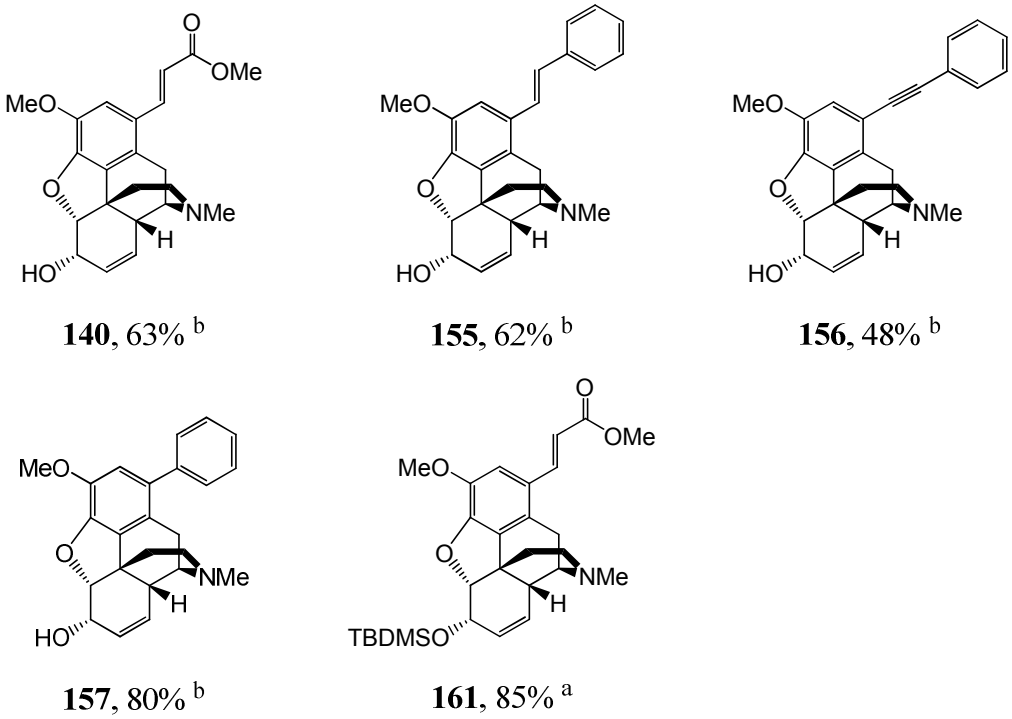

140, 63% [b] **155**, 62% [b] **156**, 48% [b]

157, 80% [b] **161**, 85% [a]

Fig 3.8 Isolated yields for compounds, **140**, **155**-**157** and **161** based on the work of Davies *et al*[74], [a](isolated yields after palladium coupling step), [b](isolated yields after both coupling and deprotection step)

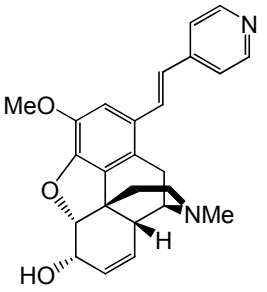

162, 79% [b]

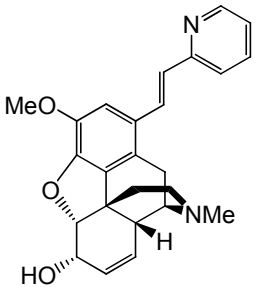

163, 64% [b]

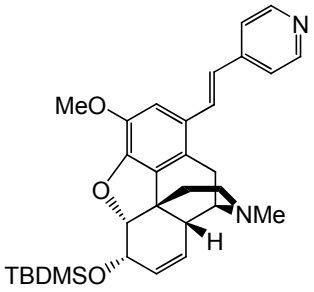

164, 92% [a]

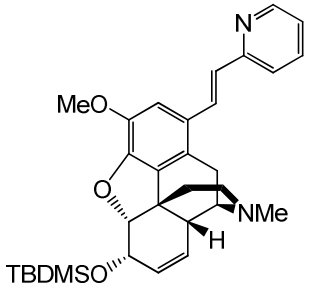

165, 81% [a]

Fig 3.9 Novel palladium coupled opioid derivatives (**162**-**165**) with isolated yields, [a](isolated yields after palladium coupling step), [b](isolated yields after both coupling and deprotection step)

3.2.4 Palladium Coupling of the Linked Codeine Compounds

With the successful generation of a series of palladium catalysed carbon-carbon coupled codeine derivatives (Fig 3.8 and Fig 3.9) the next process was to combine the palladium coupling methods developed with the methods for formation of the linked derivatives (Chapter 2, 2.2). Thus, it should be possible to synthesise linked codeine derivatives at the 6 position with A-ring modification. Analysis of the desired compounds illustrated that there was two synthetic avenues of approach (Scheme 3.11). Either we first perform the palladium coupling of the aromatic ring and then esterification (route A) or first generate the ester linked compounds and then perform the palladium coupling (route B). Again it is important to take into consideration the susceptibility of the ester bonds to hydrolysis especially in the presence of an acid or base.

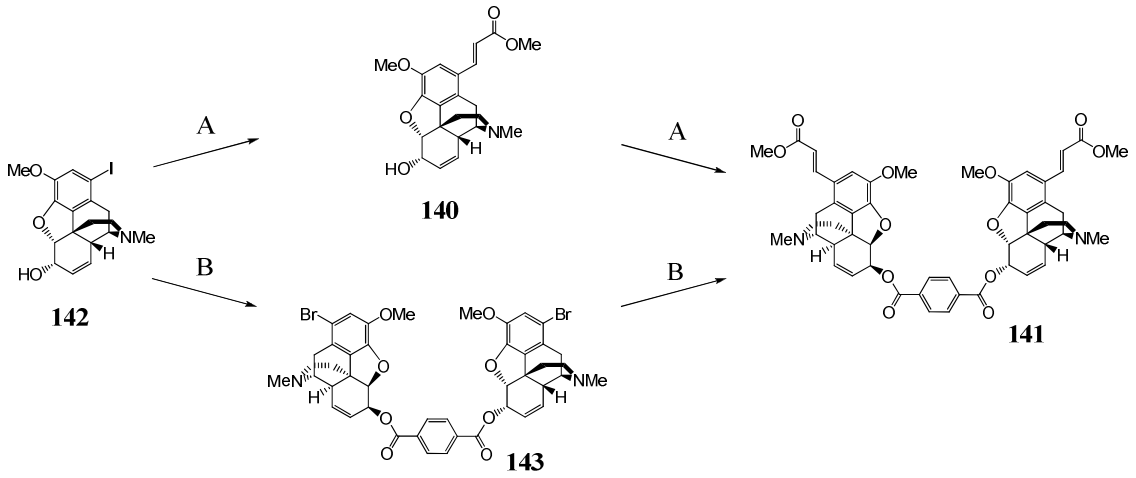

Scheme 3.11 Possible routes to the formation of ester linked A-ring modified codeine derivative (**141**)

It was decided to examine both routes to generate the desired compounds. While the ester bond may be susceptible to degradation under the palladium coupling conditions this route could potentially be more beneficial because it would involve less synthetic steps. As the secondary alcohol for the ester linked derivatives is already "blocked" there is no need for the protection and deprotection steps. Overall from the starting material of iodocodeine (**142**), route B (Scheme 3.13) would take only two synthetic steps in comparison to four steps for route A (Scheme 3.12).

Initially synthesis of the A-ring modified linked codeine compounds was investigated using route A to avoid any potential complications from the ester bond degradation. Once the compounds had successfully been generated then investigation of route B would be undertaken and compared. The compounds were generated based on terephthaloyl dichloride as previous analysis (Chapter 2 and Chapter 3) had illustrated that the *para* linked ester derivatives (**119**, **143**, **149**) can be isolated in good yields.

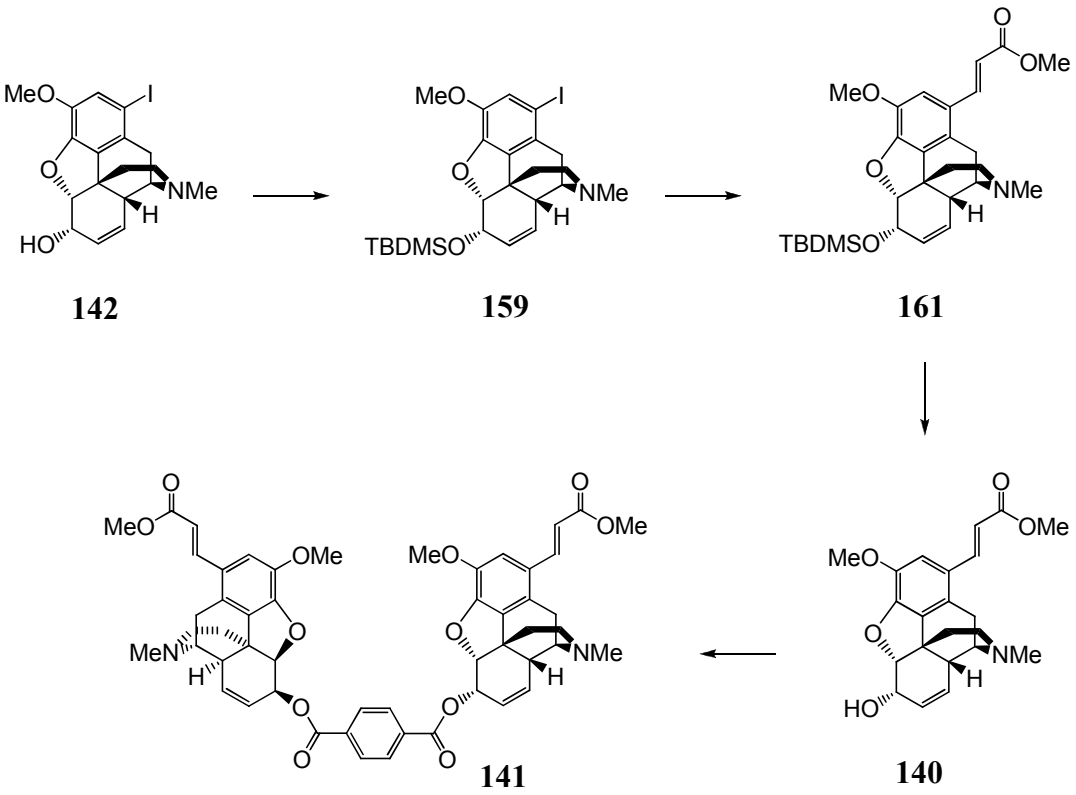

Scheme 3.12 Possible synthetic route for the formation of **141**, *via* route A

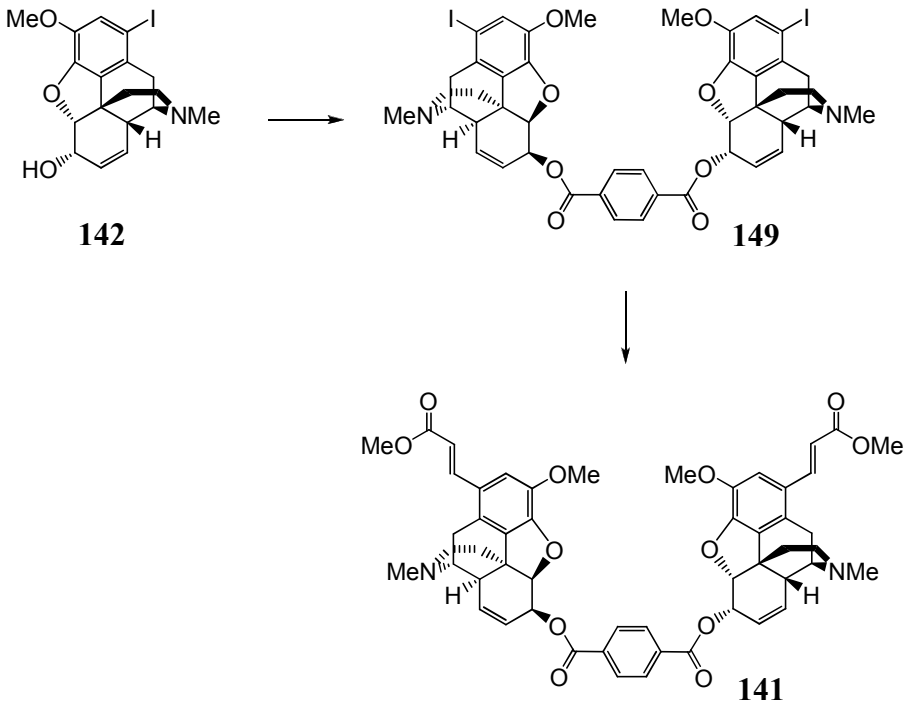

Scheme 3.13 Possible synthetic route for the formation of **141**, *via* route B

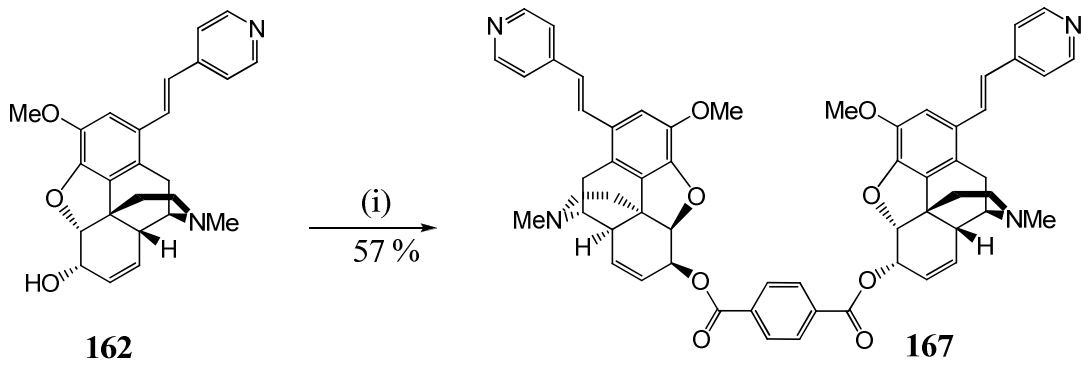

162 **167**

Reaction Conditions; (i) Terephthaloyl dichloride (0.5 Eq), DMAP (1.1 Eq), DCM, N_2, RT

Scheme 3.14 Reaction conditions for the formation of **167** *via* synthetic route A

Using the synthetic methods developed in Chapter 2 it was possible to generate six A-ring modified opioid derivatives (**141**, **166**-**170**) with the *para* ester linker (Scheme 3.14) in isolated yields of 49% - 65% (Fig 3.10) following route A. The *meta* ester linked derivative (**171**) was also synthesised *via* route A. Purification of these compounds was achieved through a combination of recrystallisations and column chromatography. Route B as an alternative synthetic method for the generation of three A-ring modified opioid derivatives (**166**-**168**) also proved successful (Scheme 3.15). Isolated yields for the *para* ester linked derivatives (**166**-**168**) of 42% - 63% were achieved for route B.

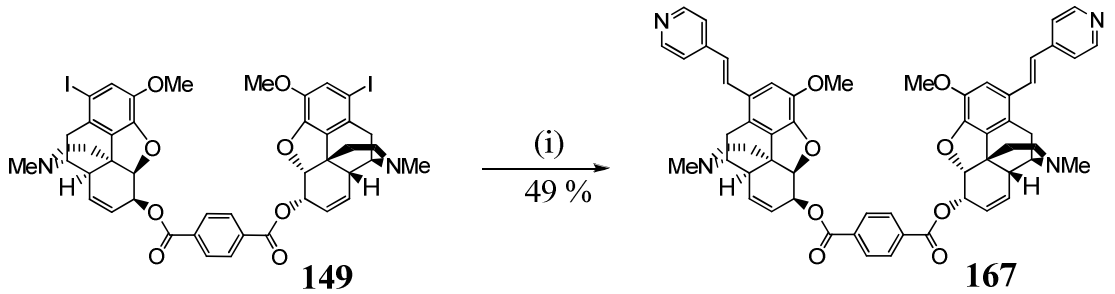

149 **167**

Reaction Conditions; (i) $Pd(OAc)_2$ (10 mol %), PPh_3 (40 mol %), DMF, NEt_3 (7 Eq), 4-Vinylpyridine (8 Eq), N_2, 100°C

Scheme 3.15 Reaction conditions for the formation of **167** *via* synthetic route B

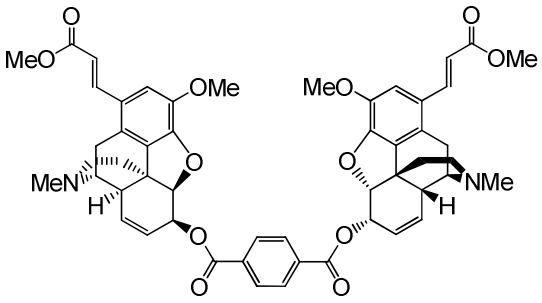

141, 65% [a]

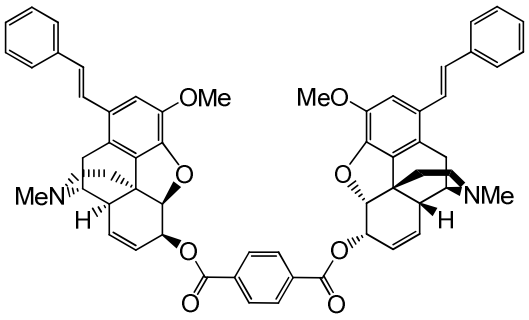

166, 56% [a], 42% [b]

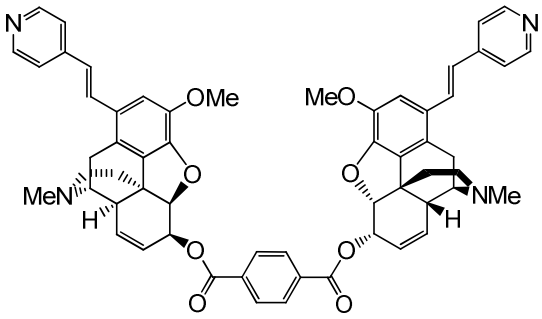

167, 57% [a], 49% [b]

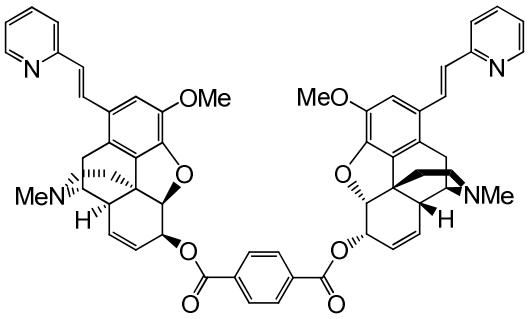

168, 49% [a], 44% [b]

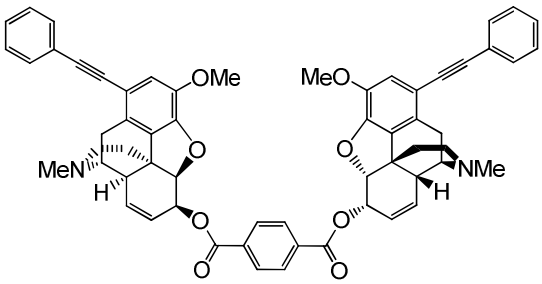

169, 53% [a]

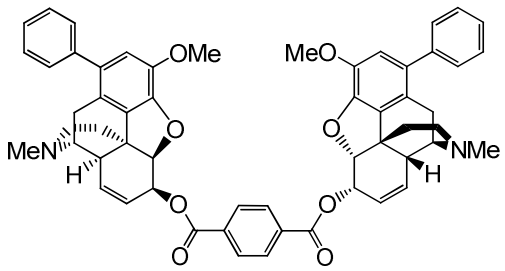

170, 61% [a]

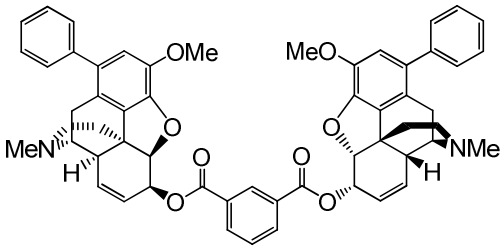

171, 39% [a]

Fig 3.10 Isolated yields for **141**, **166**-**171** for the final synthetic step, [a](route A) or [b](route B)

As the linked iodinated derivative (**149**) contains two active sites for palladium coupling the relative mol% for palladium acetate was doubled along with the equivalents of the other reactants. The most significant aspect of these reactions was the stability of the ester bonds. From analysis of the crude ^{1}H NMR spectra no product degradation at the 6 position was observed, thus, the ester bonds are stable to the palladium coupling reaction conditions.

Route A results in higher yields for the final synthetic step of the reaction (Fig 3.10), however, route A contains four synthetic steps in comparison to only two for route B. If we examine the overall yield for the final product taking the isolated yields from each step then route B is comparable to route A for compounds **166**-**168** (Table 3.1). A schematic representation for the synthesis of **167** from iodocodeine (**142**) for route A and route B is provided in Schemes 3.16 and 3.17. The overall yield of **167** from the starting material (iodocodeine, **142**) for route A is 39% while from route B the overall yield is 37%. As the final isolated yields for each route are comparable route B is more practical as it contains less synthetic steps.

Compound	**Overall % yield from iodocodeine (142)**	
	Route A	**Route B**
166	30%	32%
167	39%	37%
168	27%	33%

Table 3.1 Comparison of overall % yields for **166**-**168** from iodocodeine (**142**) for synthetic route A and route B

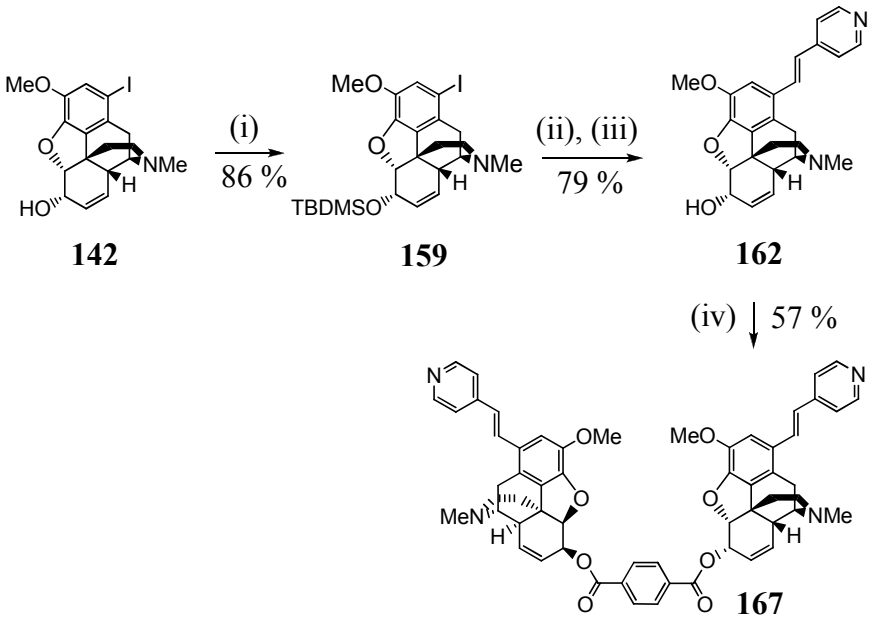

142 159 162 167

Reaction Conditions; (i) Imidazole (1.2 Eq), TBDMSCl (1.2 Eq), DMF, RT, (ii) $Pd(OAc)_2$ (5 mol %), PPh_3 (20 mol %), DMF, NEt_3 (3.5 Eq), 4-Vinylpyridine (4 Eq), N_2, 100°C, (iii) TBAF (2 Eq), THF, RT, (iv) Terephthaloyl dichloride (0.5 Eq), DMAP (1.1 Eq), DCM, N_2, RT

Scheme 3.16 Synthetic route A for the formation of **167** with isolated yields

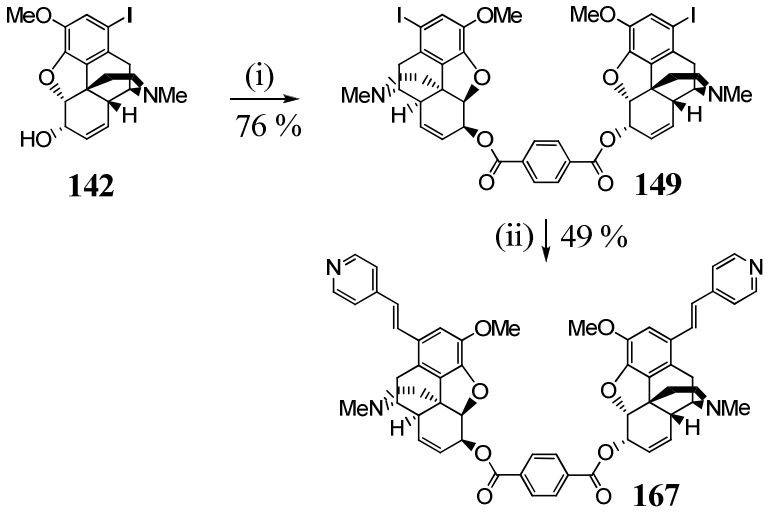

142 149 167

Reaction Conditions; (i) Imidazole (1.2 Eq), TBDMSCl (1.2 Eq), DMF, RT, (ii) $Pd(OAc)_2$ (5 mol %), PPh_3 (20 mol %), DMF, NEt_3 (3.5 Eq), 4-Vinylpyridine (4 Eq), N_2, 100°C, (iii) TBAF (2 Eq), THF, RT, (iv) Terephthaloyl dichloride (0.5 Eq), DMAP (1.1 Eq), DCM, N_2, RT

Scheme 3.17 Synthetic route B for the formation of **167** with isolated yields

3.3 NMR Study of Compound 141

An NMR study of **141** was performed *via* analysis of ^{1}H, ^{13}C, ^{13}C DEPT, COSY, HMQC and HMBC NMR experiments. The structure of compound **141** is outlined below in Fig 3.11. In total **141** contains $C_{52}H_{52}N_2O_{12}$ corresponding to a molecular mass of 896.3520. Compound **141** contains much of the same skeleton as **119** (Chapter 2) and as such the NMR spectra will appear very similar. The molecule contains two codeine structural units with the protons and carbons from each structural unit being the same. Thus the molecule contains H14 and H14' both of which are identical under NMR analysis. Compound **141** has been fully labelled in Fig 3.11, however for clarity in further discussions H19 will refer to both H19 and H19', C21 will refer to both C21 and C21' etc.

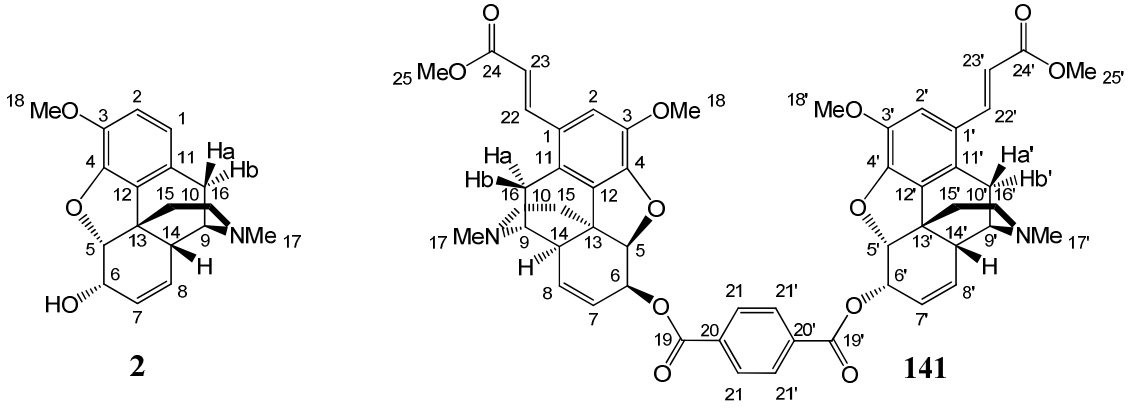

Fig 3.11 Structure of codeine (**2**) and compound **141**

Analysis of the ^{1}H NMR spectrum of **141** (Fig 3.12) shows that the protons corresponding to the opiate scaffold are similar. As expected the main differences between **141** and **119** are due to the modification of the A-ring from the methyl acrylate functional group. In comparison with **119** the most significant peaks in the ^{1}H NMR spectrum correspond to H2, H22, H23 and H25 (Table 3.2). Proton H2 for **119** appears as a doublet at δ 6.59 while it appears as a singlet (due to the absence of coupling with H1) for **141** at δ 6.91. Protons H22 and H23 appear as doublets at δ 7.76 and δ 6.18 respectively with *J* values of 16.0 Hz. A coupling constant of 16.0 Hz corresponds to

the *trans* isomer, therefore **141** adopts an (*E*)-geometry. The methyl proton corresponding to H25 appears as singlet at δ 3.73.

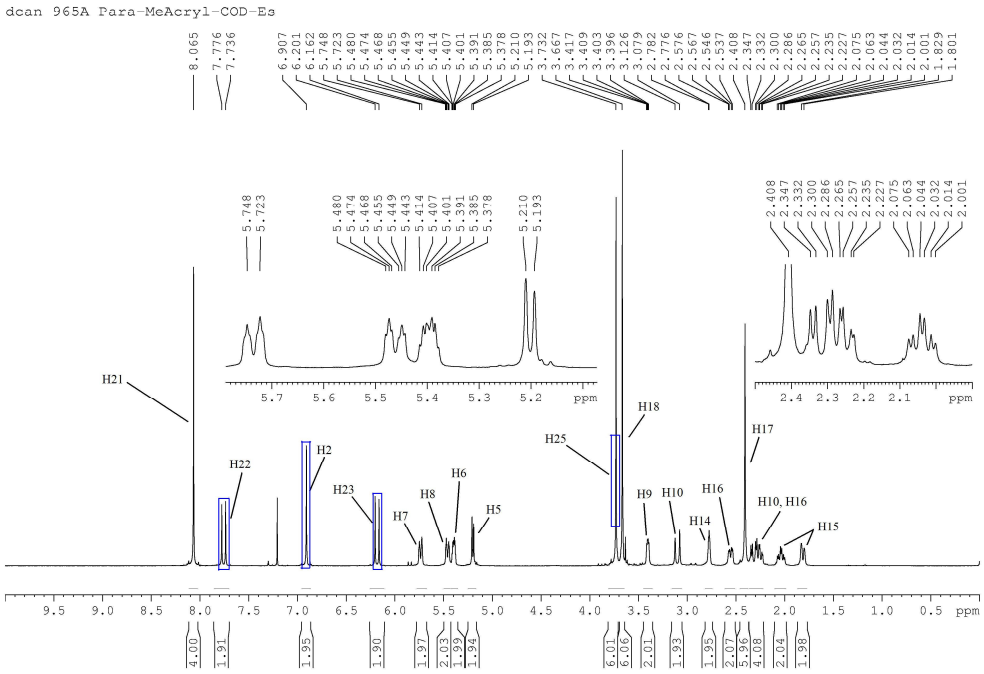

Fig 3.12 ^{1}H Proton NMR of **141**

Proton	δ Value (ppm)	
	119	**141**
1	6.50	N/A
2	6.59	6.91
5	5.14	5.20
6	5.40-5.36	5.41-5.38
7	5.74-5.70	5.75-5.72
8	5.48-5.44	5.48-5.44
18	3.64	3.67
25	N/A	3.73

Table 3.2 Comparison of selected δ values for **119** and **141** from ^{1}H NMR

Analysis of the COSY spectrum for **141** provides additional and complementary information in relation to peak assigments (Figs 3.13-3.15). The coupling pattern for **141** is similar to **119** with the main difference corresponding to H2, H22, H23 and H25. As expected protons H22 and H23 exhibit strong coupling with each other. A summary of the proton proton coupling for **141** is provided in Table 3.3

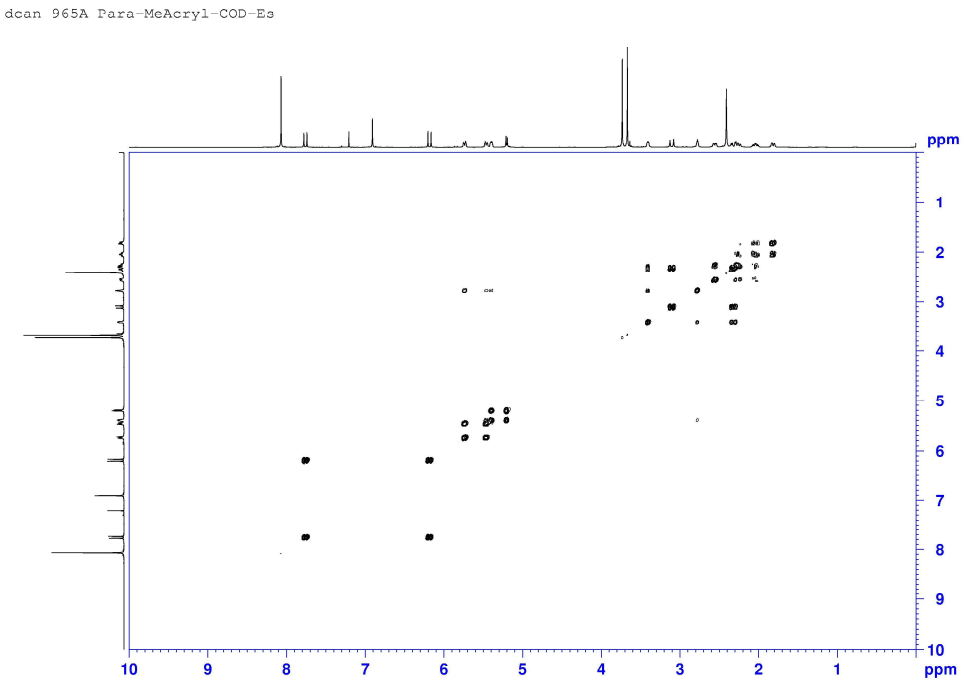

Fig 3.13 COSY spectrum of **141**

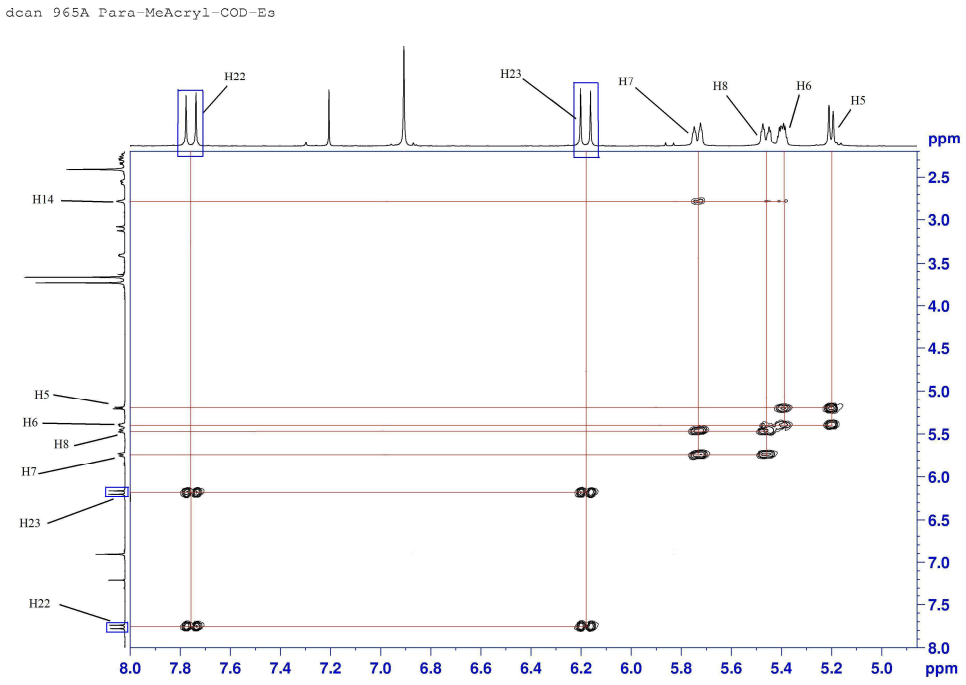

Fig 3.14 COSY spectrum of **141** showing cross peak correlations between δ 5.0-8.0

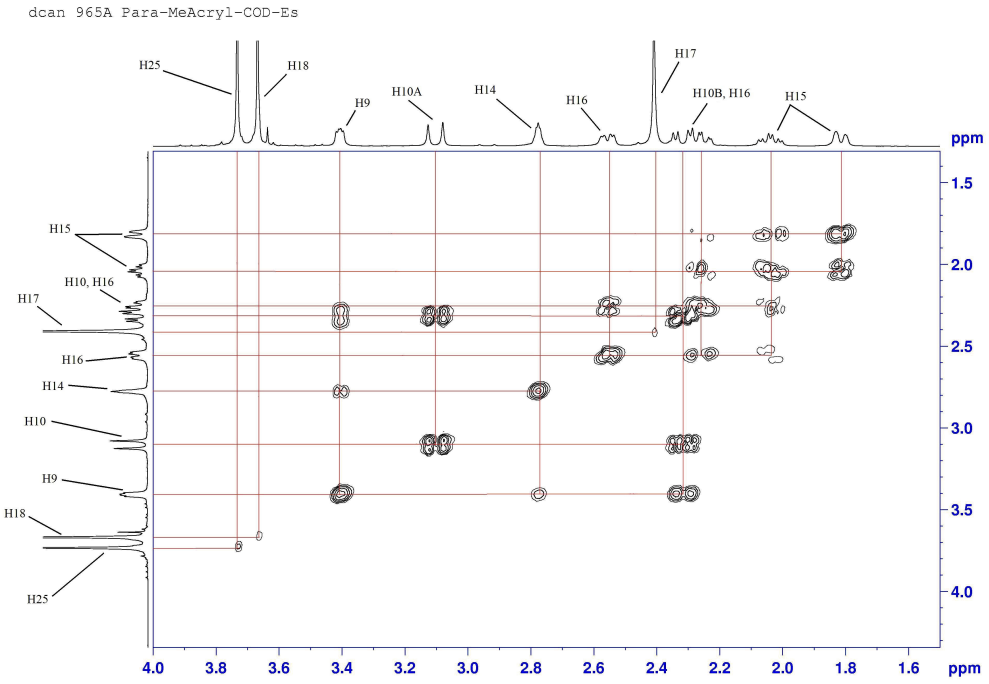

Fig 3.15 COSY spectrum of **141** showing peak correlations between δ 1.6-4.0

Proton No.	Couples with
21	21
22	22,23
2	2,
23	23, 22
7	7, 8, 14, 6*, 5*
8	8, 14, 6*, 5*
6	6, 5, 14, 7*, 8*
5	5, 6, 7*, 8*
25	25
18	18
9	9, 14, 10,
10	10, 9,
14	14, 7, 8, 6, 9
16	16, 15
17	17
15	15, 16

Table 3.3 Proton proton correlations from COSY spectrum of **141**, *denotes weak coupling.

Analysis of the ^{13}C, ^{13}C DEPT, HMQC and HMBC allows the carbon atoms of **141** to be accurately assigned. The majority of the peaks for **141** can be assigned based on their relative δ values in the ^{13}C spectrum (Fig 3.16) with most peaks again broadly similar to **119** (Table 3.4). Further analysis by ^{13}C DEPT, HMQC and HMBC provides additional information. The most significant difference between **119** and **141** from ^{13}C analysis corresponds to C1 and C2. C1 for **119** appears at δ value of 119.34 but it is downfield shifted for **141** at a δ value of 125.01. From ^{13}C DEPT analysis it is clear which carbons correspond to the quaternary and methylene carbons (Fig 3.17). In total **141** contains 9 quaternary carbons corresponding to C24, C19, C4, C3, C20, C12, C11, C1 and C13 at δ values of 167.84, 165.21, 149.14, 142.77, 133.80, 131.29, 127.69, 125.04 and 42.67 respectively.

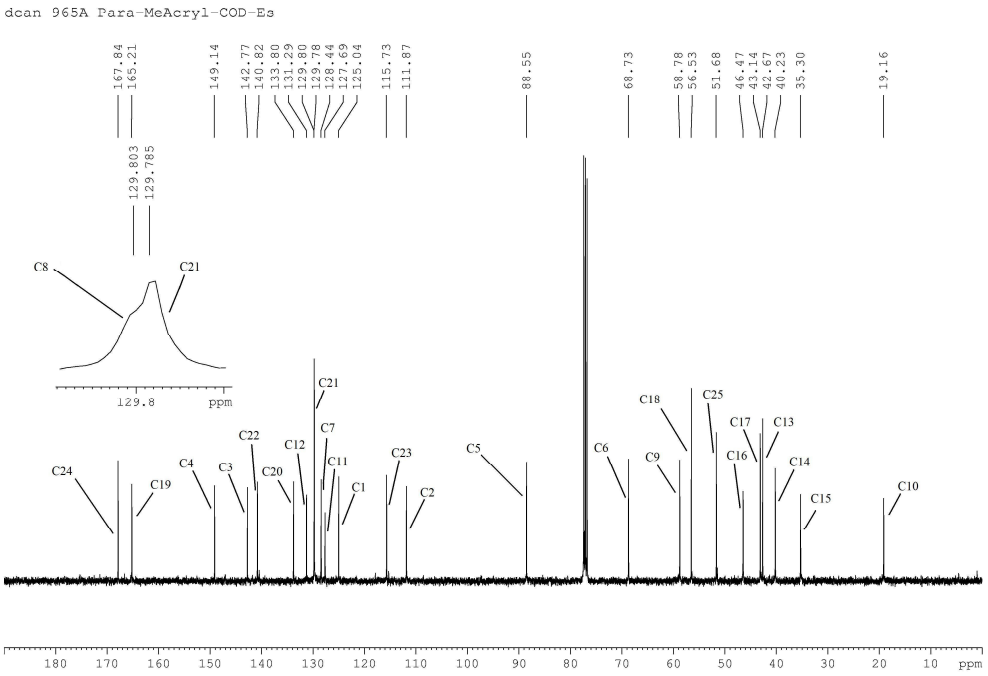

Fig 3.16 ^{13}C spectrum of **141**

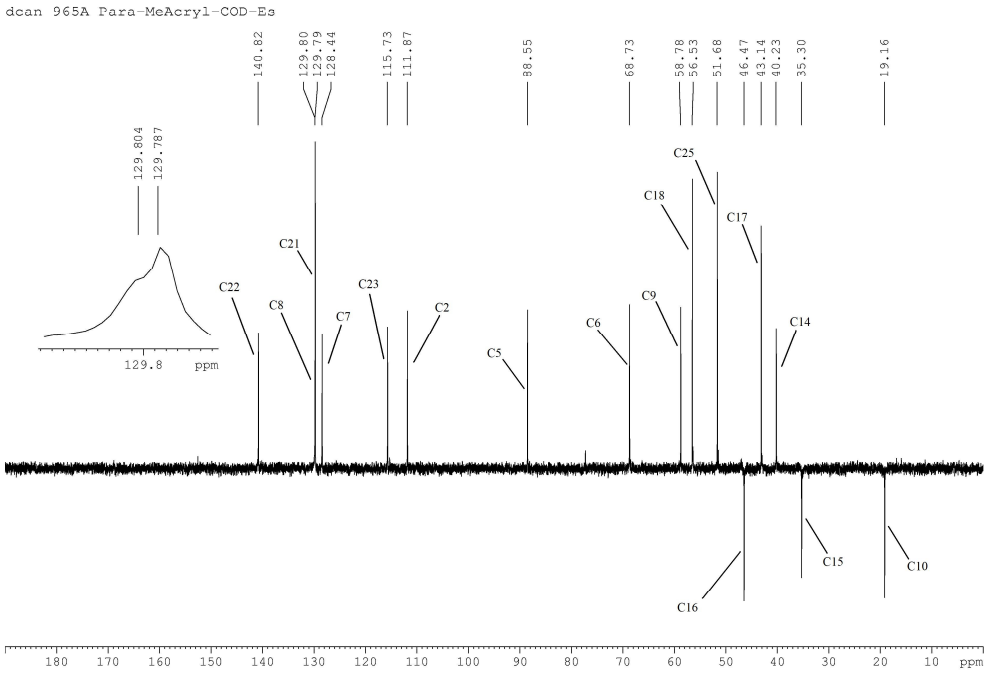

Fig 3.17 ^{13}C DEPT spectrum of **141**

Carbon	δ Value (ppm)	
	119	**141**
1	119.34	125.04
2	114.30	111.87
5	87.80	88.55
6	68.84	68.73
7	128.28	128.44
8	129.87	129.80
18	56.76	56.53
25	N/A	51.68

Table 3.4 Comparison of selected δ values for **119** and **141** from ^{13}C NMR

As expected C1 now corresponds to a quaternary carbon due to A-ring modification. The three methylene carbons for C16, C15 and C10 have δ values of 46.47, 35.30 and 19.16 respectively. Analysis by HMQC NMR provides proton carbon coupling for **141** (Figs 3.18-3.20).

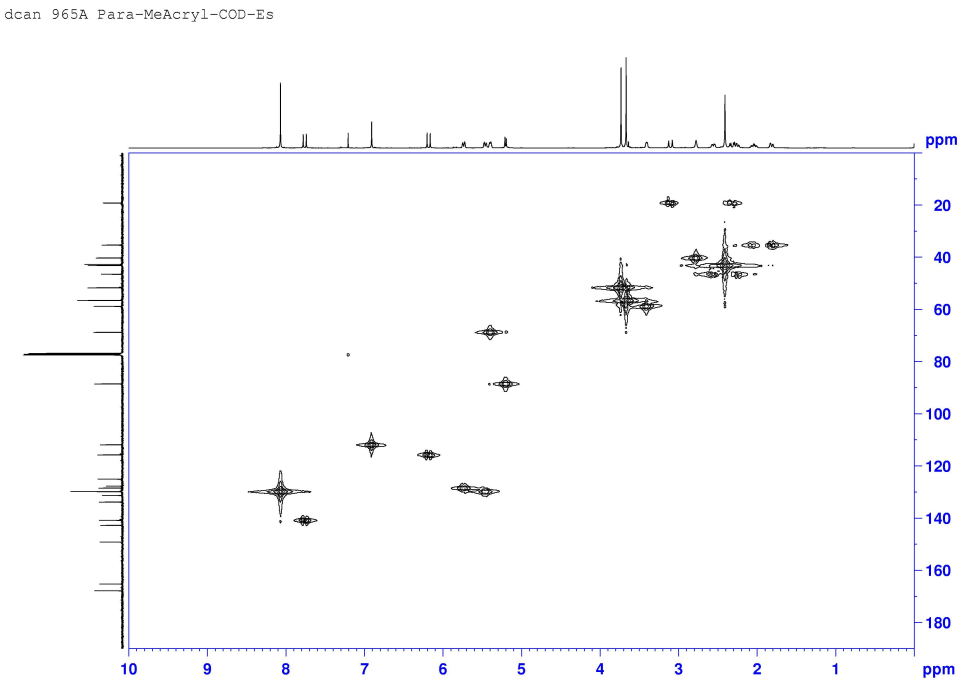

Fig 3.18 HMQC spectrum of **141**

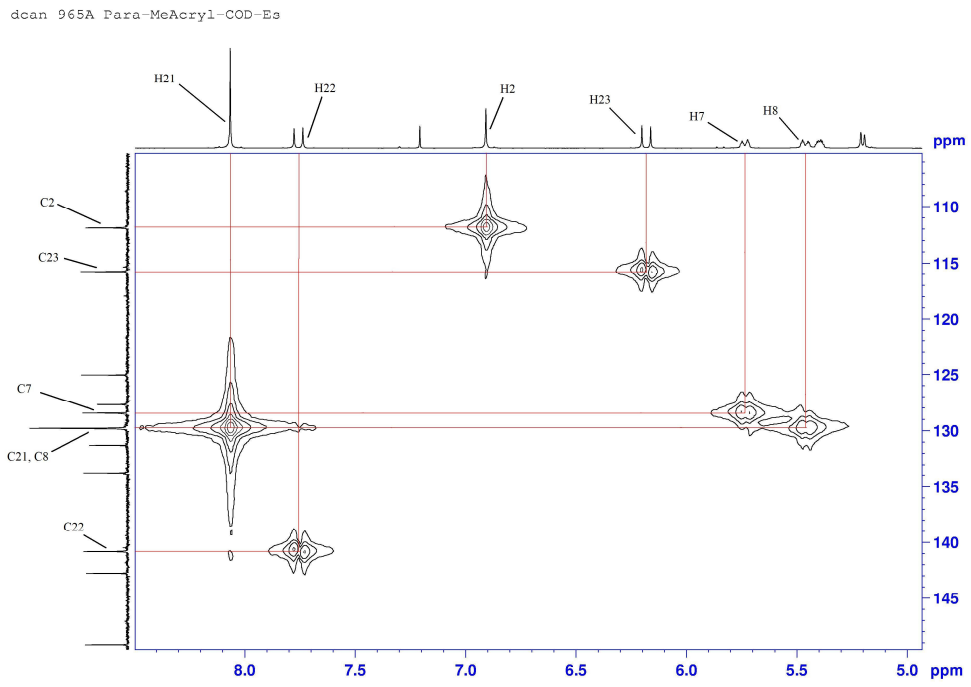

Fig 3.19 HMQC spectrum of **141** showing peak correlations between δ 5.0-8.5

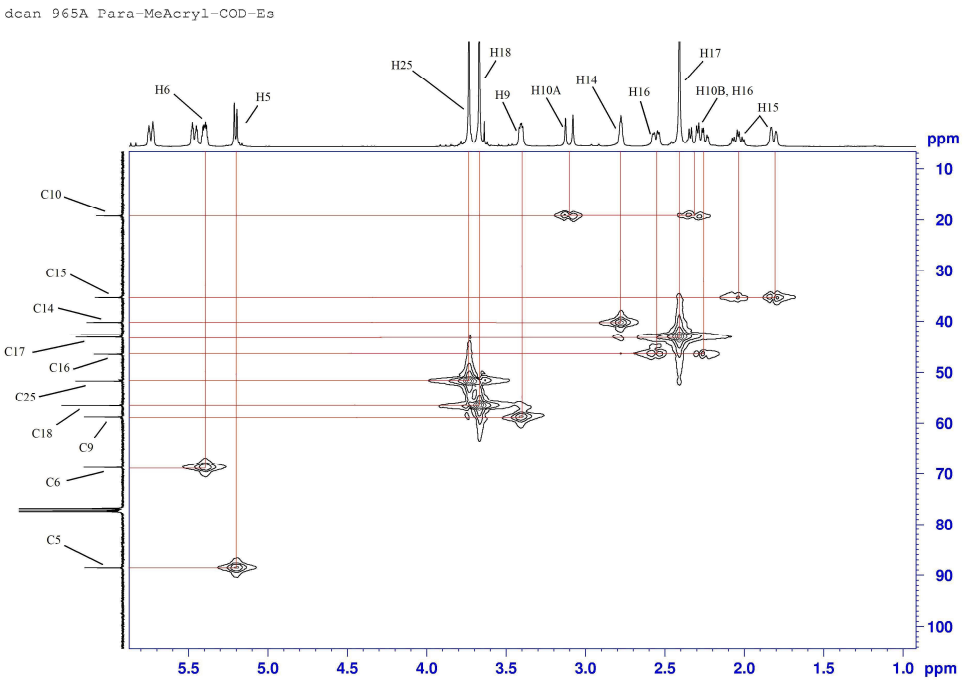

Fig 3.20 HMQC spectrum of **141** showing peak correlations between δ 1.0-5.8

The main difference between **119** and **141** is the proton carbon coupling observed for protons H22, H23 and H25 and their corresponding carbons. A summary of the carbon proton coupling for **141** is provided in Table 3.5. For full peak assignment of the carbon spectrum it is also helpful to examine the HMBC of **141** (Figs 3.21-3.22). As expected proton H22 shows coupling with carbons C2, C23 (weak coupling), C11 and C24. Proton H23 exhibits coupling with carbons C1 and C24. Definitive assignment of H18 and H25 is provided by HMBC with H25 coupling with the expected C24 and H18 coupling with C3.

Assigned Peak No.	**δ Value (ppm)**	
	Carbon	**Proton**
22	140.82	7.76
8	129.80	5.48-5.44
21	129.78	8.07
7	128.44	5.75-5.72
23	115.73	6.18
2	111.87	6.91
5	88.55	5.20
6	68.73	5.41-5.38
9	58.78	3.42-3.40
18	56.53	3.67
25	51.68	3.73
16	46.47	2.56, 2.35-2.23
17	43.14	2.41
14	40.23	2.78
15	35.30	2.04, 1.82
10	19.16	3.10, 2.35-2.23

Table 3.5 Carbon proton correlations from HMQC of **141**

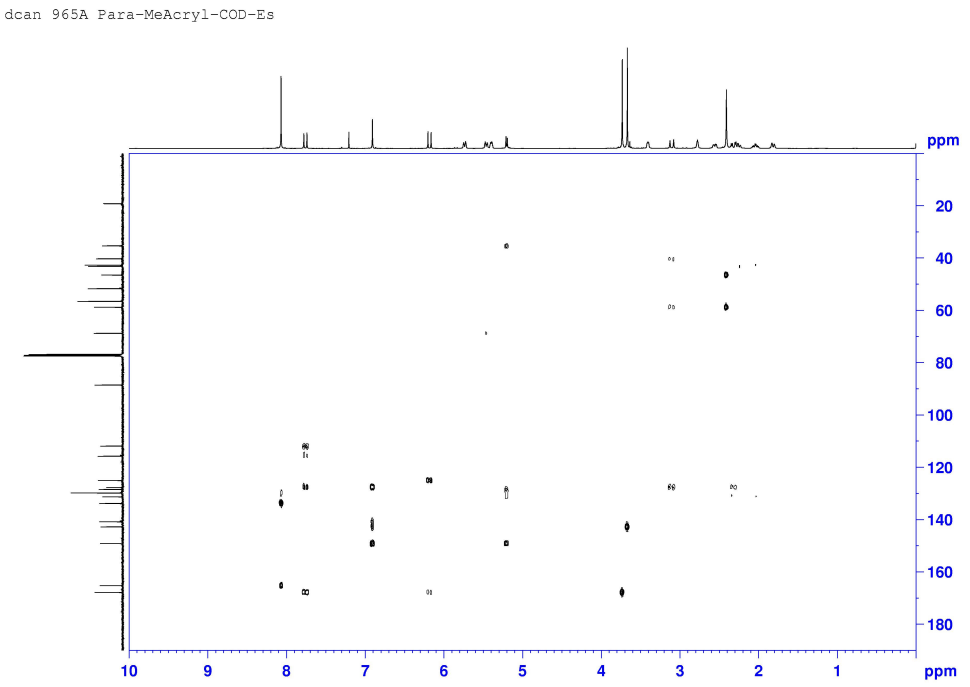

Fig 3.21 HMBC spectrum of **141**

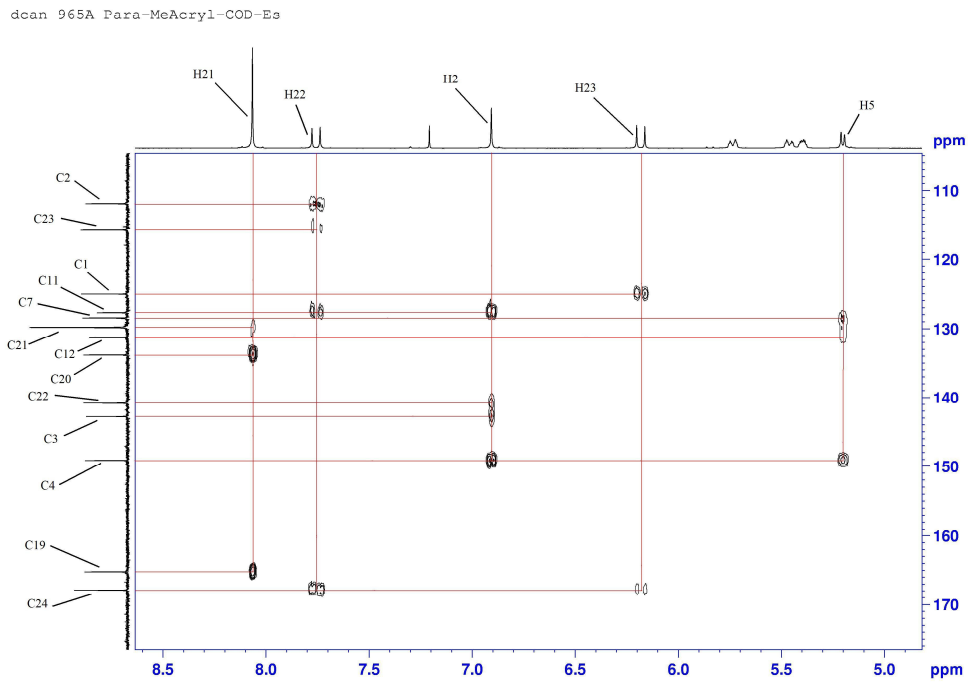

Fig 3.22 HMBC spectrum of **141** showing peak correlations between δ 5.0-8.5

3.4 X-ray Crystallography Study of 162

Crystals suitable for single crystal X-ray determination of **162** were grown by slow evaporation from chloroform:hexane (1:4), yielding colourless block shaped crystals. Compound **162** crystallises in the space group P 2_1 with selected bond distances, bond angles and torsion angles given in Table 3.6. As expected the ring conformations for the codeine scaffold are similar to previously reported opioid derivatives with the compound adopting the classic T-shaped configuration.[71, 72]

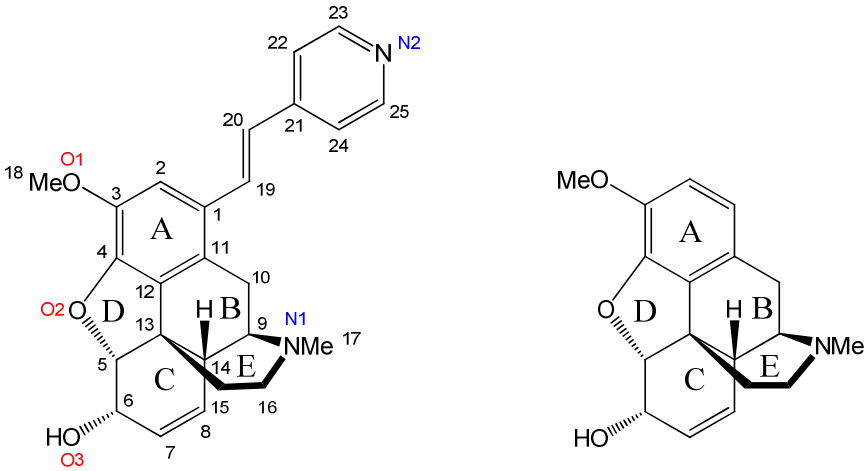

162 **2**

Fig 3.23 Structure of compound **162** and codeine (**2**) with ring labels and atom labels

The aromatic A-ring and the pyridine ring adopt a planar confirmation while the E ring adopts the chair confirmation. As expected the A-ring exhibits some deviation from planarity with torsion angles for C11-C1-C2-C3 and C1-C2-C3-C4 of -1.4(2) and 2.3(2) respectively. From the x-ray crystal structure it is clear that the molecule adopts the (*E*) geometry for the alkene double bond at carbons C19-C20. Formation of the (*E*) geometry is in agreement with ^{1}H NMR analysis with the *J* coupling constant for protons H19 and H20 calculated at 16.0 Hz. For more details on the X-ray crystal data for **162** see Appendix A, A.3.

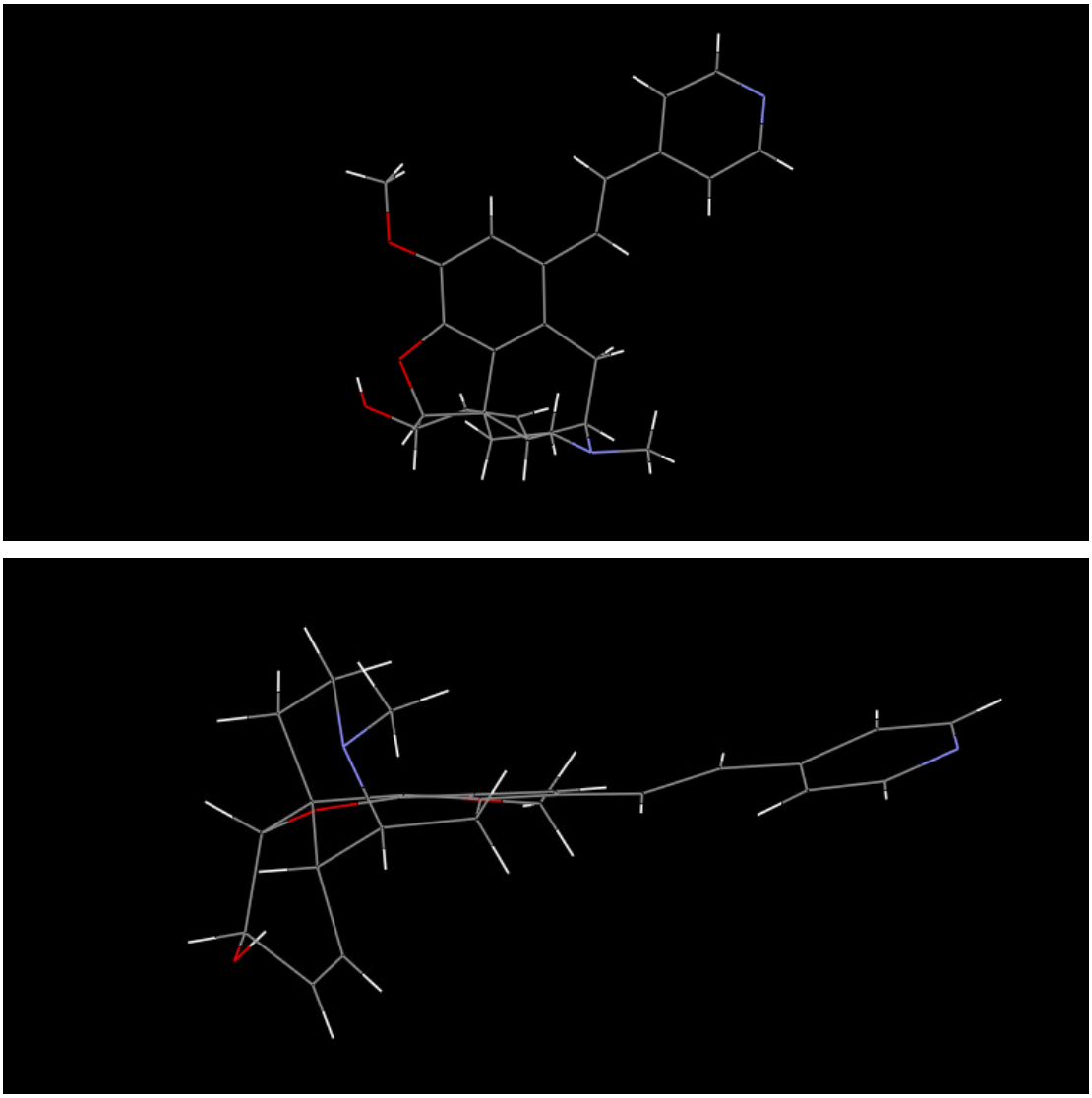

Fig 3.24 X-ray crystal structure of **162**

Bond Lengths (Å)			
C1-C19	1.465(2)	C20-C21	1.463(2)
C1-C2	1.412(2)	C11-C1	1.415(2)
C5-C6	1.538(2)	C6-O3	1.419(2)
Bond Angles (°)			
C1-C19-C20	127.9(1)	C21-C20-C19	125.6(1)
C11-C1-C2	119.5(1)	C22-C21-C24	115. 6(1)
C5-C6-O3	110.4(1)	C7-C6-O3	113.0(1)
Torsion Angles (°)			
A-ring			
C11-C1-C2-C3	-1.4(2)	C1-C2-C3-C4	2.3(2)
B Ring			
C14-C9-C10-C11	32.8(2)	C10-C11-C12-C13	4.6(2)
C Ring			
C5-C6-C7-C8	40.1(2)	C6-C7-C8-C14	-5.4(2)
Pyridine Ring			
C20-C21-C22-C23	178.5(2)	C20-C21-C24-C25	-178.2(2)
C21-C22-C23-N2	0.4(3)	C1-C19-C20-C21	175.8(1)

Table 3.6 Selected bond distances and bond angles and torsion angles for **162** with estimated standard deviations in parenthesis

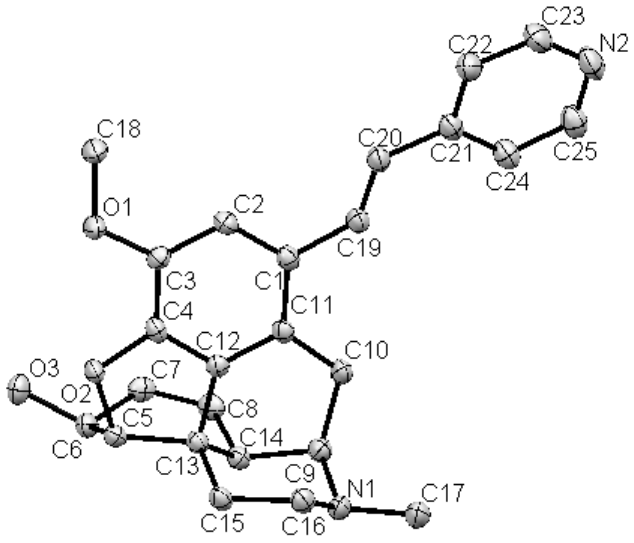

Fig 3.25 ORTEP diagram of **162** with atom labels

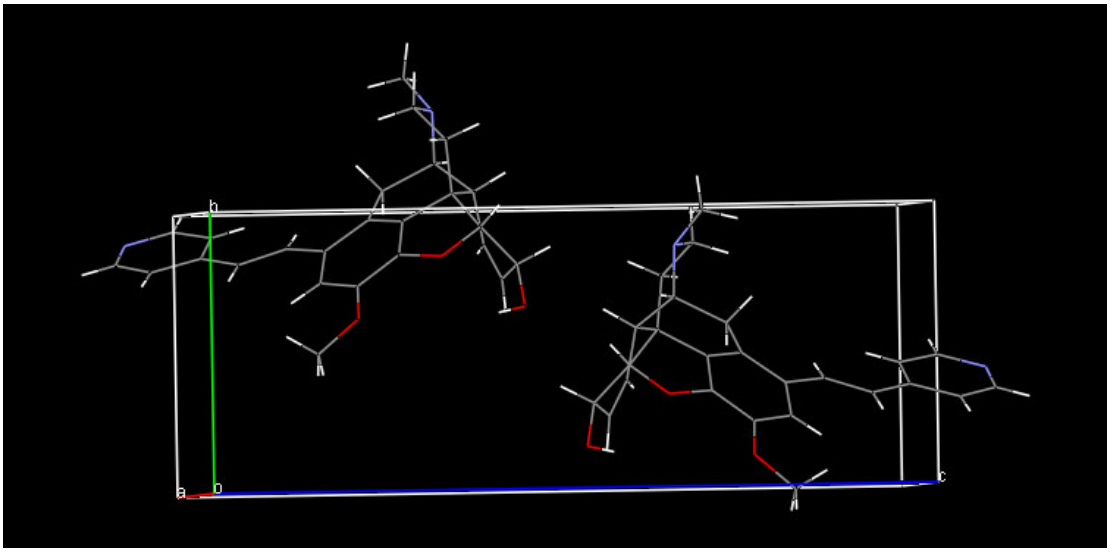

Fig 3.26 X-ray crystal packing of **162**

3.5 Conclusion

The synthesis and structural characterisation of a variety of ester and ether "linked" codeine derivatives with modification at the 1 position of the aromatic ring has been achieved.

A selection of twelve novel ester (**143**-**150**) and ether (**151**-**154**) linked codeine derivatives with halogenation at the 1 position of the aromatic ring were successfully synthesised in modest to good isolated yields of 39% - 89%. Synthesis of the ester and ether linked codeine derivatives was achieved by initially forming the appropriate halo-codeine derivatives (**75**, **142**) followed by formation of the "linked" compounds (methodology from chapter 2). Halogenation at the 1 position of codeine was achieved by using the appropriate halogenated *N*-succinimide in an acidic environment. Purification was achieved by a combination of column chromatography and recrystallisation. Full characterisation was performed by m.p., IR, $[\alpha]_D$, HRMS, ^{1}H NMR, ^{13}C NMR, DEPT, COSY, HMQC and HMBC.

A selection of five previously reported[74] palladium coupled codeine derivatives (**140**, **155**-**157**, **161**) and four novel palladium coupled codeine derivatives (**162**-**165**) were successfully synthesised in modest to good isolated yields of 39% - 89%. Synthesis of the palladium coupled codeine derivatives involved the use of Heck, Stille and Suzuki coupling methods. The palladium coupled codeine derivatives were further utilised in the synthesis of a selection of seven (**141**, **166**-**171**) novel linked codeine derivatives with modification at the 1 position of the aromatic ring. Purification of the opioid derivatives was achieved by a combination of column chromatography and recrystallisation. Full characterisation was performed by m.p., IR, $[\alpha]_D$, HRMS, ^{1}H NMR, ^{13}C NMR, DEPT, COSY, HMQC and HMBC. An in depth NMR analysis of one of the palladium modified ester linked compounds (**141**) was performed with full peak assignments. An examination of the X-ray crystal structure of one of the palladium modified codeine derivatives (**162**) was also performed.

Chapter 4

Mu Opioid Receptor Binding Studies

4.1 Introduction

This chapter outlines the binding affinity of a selection of opioid derivatives for the *mu* opioid receptor. Experimental analysis was performed *via* radioligand competitive binding techniques resulting in calculation of the K_i and IC_{50} values of a series of novel opioid derivatives.

Radioligand receptor binding studies are a widely used technique to determine the affinity of drugs for specific receptor sites. Thus they can be used to determine if a drug is likely to have therapeutic or adverse affects at different receptors. They can often provide vital information in relation to receptor subtypes and be used to chart the distribution of receptors throughout the body or tissue sample. The basis of receptor binding techniques is the formation of a receptor-ligand (drug) complex which contains a radiolabelled ligand. Once the receptor-ligand complex is formed then its radioactivity can be measured. Based on the radioactivity (Ci/mmol) of the sample the relative percentage of ligand bound can be deduced and thus the binding affinity ($1/K_d$) for the receptor site can be calculated. The two basic types of receptor binding experiments are saturation and competition binding experiments.

4.1.1 Saturation Binding Experiment

Saturation binding experiments are used to directly determine the affinity ($1/K_d$) of a radiolabelled ligand for a receptor site. In this case the ligand (drug) being analysed is a radiolabelled species (often with ^{3}H or ^{125}I) which is incubated at increasing concentrations with the receptor (Fig 4.1).[81] As the concentration of radioligand increases, more of the receptor-ligand complex will form. The dissociation constant (K_d, concentration at which 50% of the receptor sites are occupied) can then be directly

calculated from the resulting graph (Fig 4.2). As the concentration of radioactive ligand increases, a point is reached where no more receptor-ligand complex is formed. This value is known as B_{max} and it refers to the amount of radioactive ligand required to saturate the receptor sites. B_{max} can also be used as a measure of the number of receptor sites present in a tissue sample. The main drawback of saturation binding experiments is the requirement that the ligand (drug) being analysed must be radiolabelled. This is often an impractical and costly procedure to undertake especially if numerous ligand species need to be analysed.

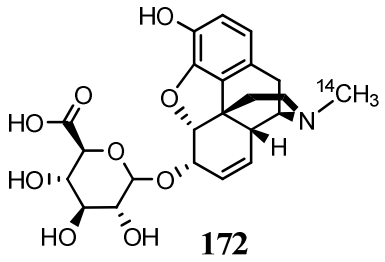

172

Fig 4.1 Radiolabelled opioid, morphine-[*N*-methyl-^{14}C]-6-glucuronide (**172**)

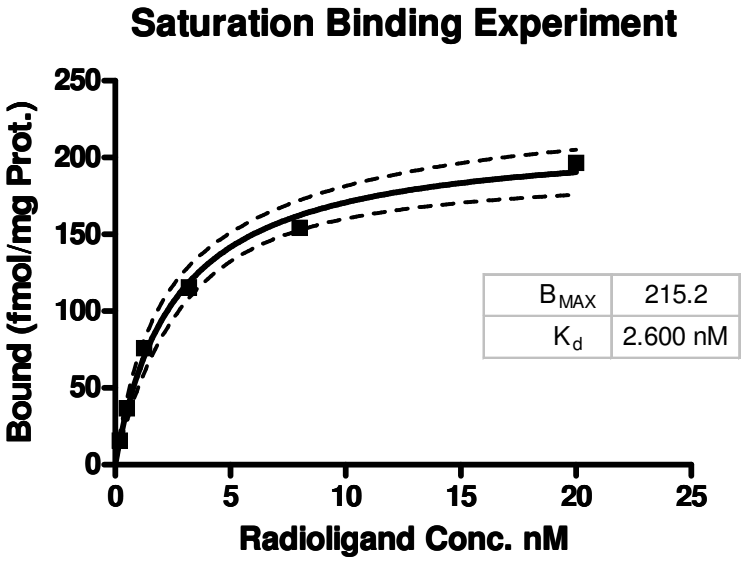

Fig 4.2 Saturation Binding Experiment with calculated B_{max} and K_d values

4.1.2 Competition Binding Experiment

Competition binding experiments on the other hand can be used to determine the affinity of unlabelled ligand species. The affinity of an unlabelled ligand for a receptor can be measured indirectly by analysing its ability to compete with and inhibit the binding of a known radioactive ligand to the same receptor site. In competition binding experiments, the unlabelled ligand is incubated at various concentrations with the receptor in the presence of a fixed concentration of radiolabeled ligand species. As the concentration of the unlabelled ligand increases, the amount of radioligand bound to the receptor site decreases. As the formation of the receptor-radioligand complex decreases then so too does the measured radioactivity in the tissue sample (Fig 4.3). The affinity of the unlabelled ligand for the receptor site can thus be calculated based on the inhibition of the formation of the radioligand-receptor complex. The dissociation constants for the unlabelled ligands from competitive binding experiments are often referred to as K_i (instead of K_d) due to the fact that they are calculated based on the inhibition of a radioligand and not the direct ligand-receptor complex formation (as in saturation binding experiments). The K_i value for an unlabelled drug should be the same as the K_d obtained for the same drug in radiolabelled form.

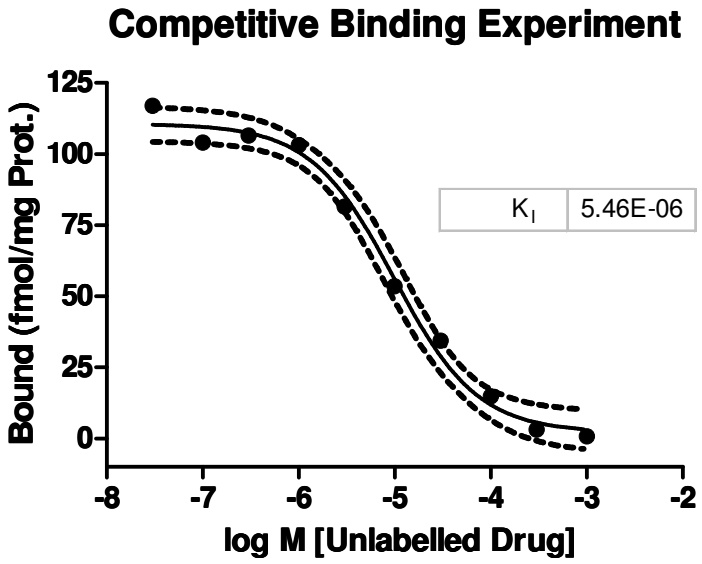

Fig 4.3 Competition Binding Experiment with calculated K_i value

4.2 Results and Discussion

4.2.1 Method Development

The opioid receptors belong to the G-protein-coupled family of receptors with three main subtypes, *mu* (μ), *kappa* (κ) and *delta* (δ), (for further information on opioid receptors please see chapter 1). Studies into the binding of the opium alkaloids, in particular morphine, show that morphine's binding to brain tissue is mainly the result of a single receptor, called the *mu* (μ) receptor.[16] Therefore as the novel compounds synthesised in this project are analogues of morphine analysis is based on the affinity to the *mu* opioid receptor site. As the opioid derivatives contain no radioactive labelled atoms it was necessary to analyse them *via* competition binding experiments. It was decided to use ^{3}H DAMGO (**173**) as the radioligand species because it displays high affinity and specificity for the *mu* opioid receptor site (Fig 4.4).[82-84] Although our collaborator Dr. David Finn (Dept. of Pharmacology and Therapeutics, NUIG and Centre for Pain Research) is an expert in cannabinoid analgesia, no previous investigation of competitive binding experiments had been performed on opioid derivatives in their research labs. As the affinities ($1/K_i$) of the unlabelled opioid compounds are based on their ability to compete with the radiolabeled ligand, it was necessary to investigate the experimental parameters of ^{3}H DAMGO binding to the receptor site. Thus prior to the analysis of the affinity ($1/K_i$) of the novel opioid compounds, a robust and reliable method had to be developed

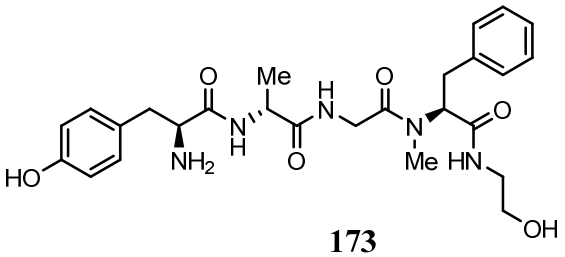

173

Fig 4.4 Structure of DAMGO (**173**)

Prior to development of an experimental method for a competitive binding experiment the tissue samples expressing the *mu* opioid receptor were prepared according to standard methods[85, 86] as outlined in the experimental (4.4.1). The samples were prepared from the brain tissue of male Lister-hooded rats as the highest expression of *mu* opioid receptors is found in the brain tissue. An important part of the receptor tissue preparation is the removal of endogenous opioids from the receptor sites. The rat brain tissue will contain endogenous opioid species and it is important to remove these ligands from the tissue samples to avoid interference with the radioligand binding assay. The samples were homogenised and stored at -80°C in 1 mL aliquots until required for experimental analysis.

For each experimental analysis, tissue samples were removed from the -80°C freezer and allowed to thaw. Once the samples had thawed they were combined and vortexed / sonicated to ensure a homogenous sample. For each thawed homogenous sample it was necessary to analyse the protein concentration *via* the Bradford-dye binding procedure.[87] This was to ensure that for each experiment, the exact same amount of protein was being added. Each brain tissue membrane homogenate would contain slight differences in protein concentrations and thus different concentrations of receptor sites. Therefore by analysing the protein concentration of each thawed tissue sample the same amount of receptor-expressing tissue (400 µg) could be employed in every experiment.

Before any analysis is performed, it is important to discuss the role of specific and non-specific binding (NSB) for radioligand binding techniques. Specific binding refers to the binding of the radioactive ligand to the particular receptor site being analysed. However, it is usually possible for radioligands to bind to more than one site. These extra binding sites are referred to as the non-specific binding sites. Non-specific binding sites can be receptors in the same family or other receptor families which recognise the radiolabelled ligand. There may also be non-specific binding to non-receptor portions of the tissue sample or sites on the test-tubes or glass filter paper. In order to distinguish binding to specific sites from non-specific binding a set of

incubations can be run alongside the tested sample in which an unlabelled ligand is added in an excess concentration which blocks the radioligand binding to the specific receptor site, but not the non-specific sites. It is important to choose a non-labelled inhibitor which displays high binding to the receptor site in question but low affinity for the non-specific sites. Thus the specific sites will be essentially "blocked" and only the non-specific sites will interact with the radioactive ligand species. Therefore, from analysis of the radioactivity of the resulting samples, the non-specific binding of the radiolabelled compound can be estimated. When the experiment is performed in the absence of the unlabelled ligand, the binding can be referred to as the total binding. Thus the specific binding of the radioactive ligand can be calculated by the difference between the total and non-specific binding.

- Total Binding – Non-Specific Binding = Specific Binding

A suitable unlabelled ligand for the *mu* opioid receptor is naloxone (**69**) (Fig 4.5).[83] Naloxone has a very high affinity for the *mu* opioid receptor and acts as a competitive antagonist. Thus it can be used to block the specific binding site of ^{3}H DAMGO to the *mu* opioid receptor.

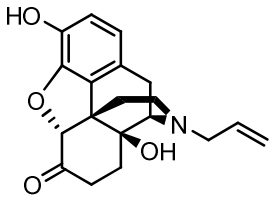

69

Fig 4.5 Structure of Naloxone (**69**)

The experimental design first focused on the association kinetics of ^{3}H DAMGO to the tissue receptor site. The kinetics study was performed to calculate the time at which equilibrium conditions are met for ^{3}H DAMGO binding to the *mu* receptor in the tissue homogenate. A fixed concentration of ^{3}H DAMGO was incubated with the tissue

membrane sample and analysed at different time intervals (Fig 4.6). Once the radioactive ligand (^{3}H DAMGO) is added to the tissue membrane it will begin to bind to or associate with the receptor site. As more ^{3}H DAMGO binds to the receptor site, the radioactivity of the analysed sample will increase. After a certain period of time the receptor and ligand will have reached equilibrium also known as steady state conditions. For each experiment duplicate samples were assayed for each time point with the mean taken for the total binding value. Non-specific binding was calculated using naloxone. After approximately sixty minutes, ^{3}H DAMGO had reached steady state conditions with the receptor site. Therefore the required incubation time for the competitive binding experiments was sixty minutes.

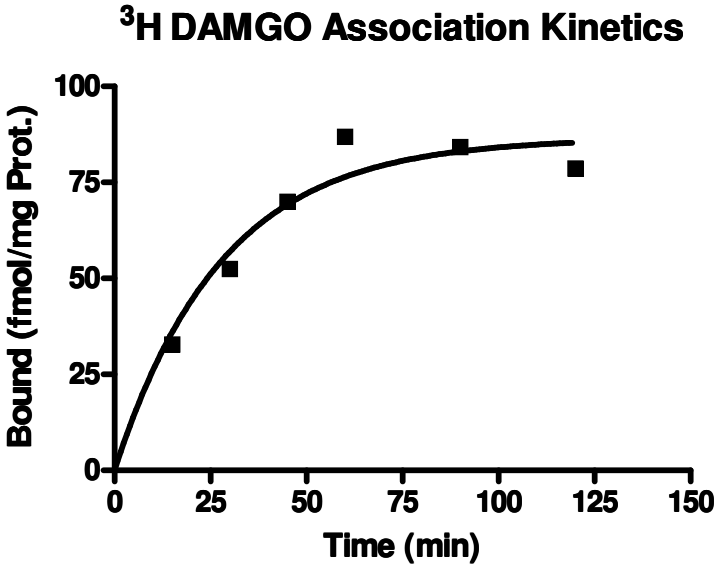

Fig 4.6 Association kinetics for ^{3}H DAMGO to receptor site

Once the incubation time for ^{3}H DAMGO to the tissue membrane sample had been calculated, it was necessary to accurately calculate the equilibrium dissociation constant (K_d) for same. Knowledge of the exact dissociation constant for ^{3}H DAMGO to the tissue samples was necessary in order to develop an accurate and reliable experiment for the determination of the novel opioid compounds. Generally for competition binding experiments the concentration of radioligand is 80% of the K_d value. If the

radioactive ligand is used in too high a concentration then excessively high concentrations of the unlabelled drug will be necessary to inhibit binding to the receptor site. However, if the concentration of radioactive ligand used is too low then the resulting radioactive counts of the tissue samples may be too low for accurate results. Therefore a saturation binding experiment was performed for ^{3}H DAMGO binding to the tissue membrane samples to calculate its K_d value (Fig 4.7).

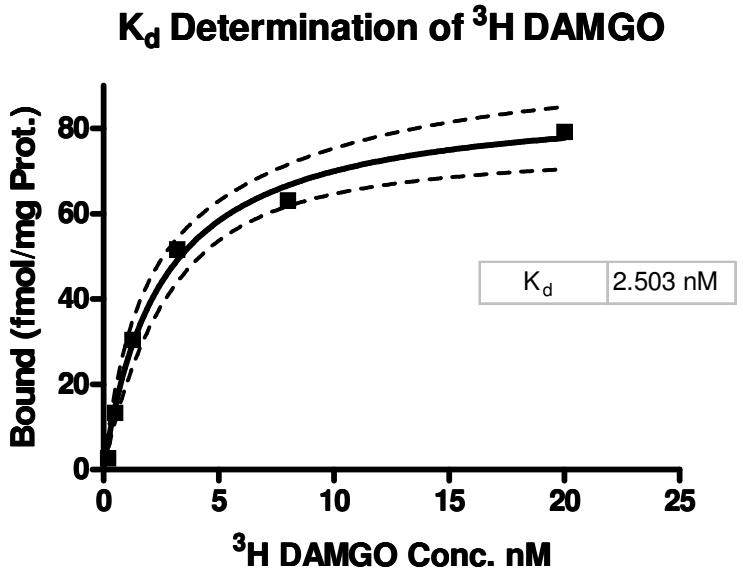

Fig 4.7 K_d determination for ^{3}H DAMGO

^{3}H DAMGO was analysed over a range of six concentrations from 2 – 20 nM. For each experiment duplicate samples were made for each concentration with the mean taken for the total binding value. Non-specific binding was calculated using naloxone. The experiment was performed in triplicate with the average of the three values used to calculate the K_d value for ^{3}H DAMGO to the tissue membrane. The average value for the K_d of ^{3}H DAMGO was calculated at 2.484 nM. Therefore the concentration used for the competitive binding experiments was 2.000 nM (approximately 80%).

Once the incubation time and K_d value for the radiolabelled ligand, (^{3}H DAMGO) in the rat tissue membrane homogenate had been calculated, the experimental analysis of

the novel compounds could be investigated. The experimental procedure involves addition of a fixed amount of radioligand (^{3}H DAMGO) 2.000 nM, to each sample vial, followed by the addition of the unlabelled drugs at a range of 10 different concentrations. A fixed amount of tissue membrane (corresponding to 400 µg protein) sample was then added to each vial followed by incubation at 20°C for 60 minutes.

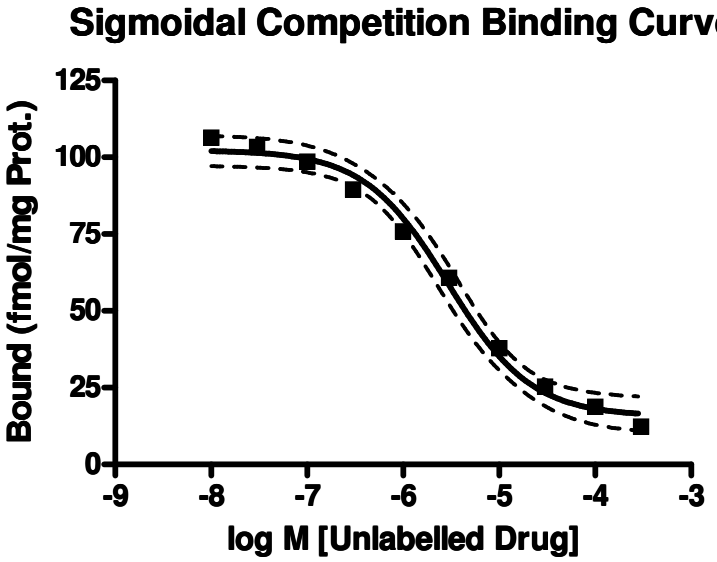

Fig 4.8 Sigmoidal competition binding curve

It should be noted that different drug compounds will have higher or lower affinity for the receptor site therefore the concentration range used for each unlabelled drug (ligand) could be different. An initial stock solution of opioid compound in the aqueous buffer solution is made up and then diluted to the desired concentration range. If a drug has low affinity for the receptor site then the concentration range will need to be increased to allow it to compete with the radioactive ligand (^{3}H DAMGO). Conversely if the drug compound has a very high affinity for the receptor site then the concentration range will need to be lowered, otherwise very little of the radioactive ligand may bind to the receptor site, resulting in low radioactive readings from the tissue sample. Ideally, the resulting sigmoidal competition binding curve should appear as outlined in Fig 4.8.

4.2.2 Results and Analysis

Once a method had been successfully developed, the *mu* opioid receptor affinity of a selection of opioid derivatives with modification at the 1, 3 and 6 positions were analysed. In total 24 compounds were analysed (**1**, **2**, **75**, **76**, **119**, **126**-**128 142**, **144**, **145**, **160**, **161, {174-176, 181}**[88], {**137**, **138**, **177**-**180**, **182}**[70]) with the results presented in Tables 4.1–4.7. For each experiment duplicate samples were run for each concentration with the mean taken for the total binding value. Non-specific binding was calculated using naloxone. Each compound was analysed in triplicate with the results presented as the mean and errors reported as SEM (Standard Error of the Mean). Each compound was analysed as the free base except for morphine (**1**) which was analysed as the hydrochloride trihydrate derivative.

Opioid	IC_{50} (nM)	K_i (nM)
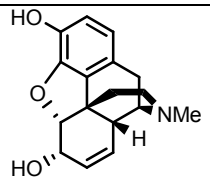 **1**	19.7 ± 0.3	10.9 ± 0.2
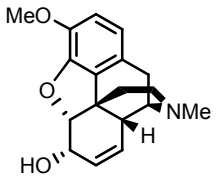 **2**	4,500 ± 1,010	2,500 ± 559

Table 4.1 IC_{50} and K_i values for opioid standards, morphine (**1**) and codeine (**2**)

Opioid	IC_{50} (nM)	K_i (nM)
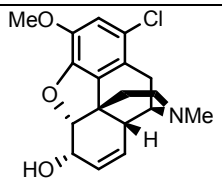 **76**	6,180 ± 266*	3,420 ± 181*
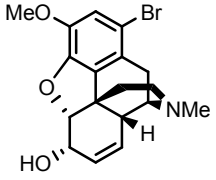 **75**	18,000 ± 2,290*	9,990 ± 1,550*
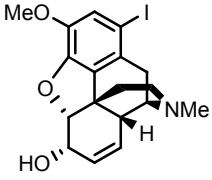 **142**	16,800 ± 1,480*	9,290 ± 1,000*
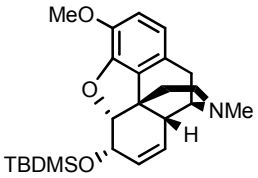 **160**	17,900 ± 2,540	9,920 ± 1,410
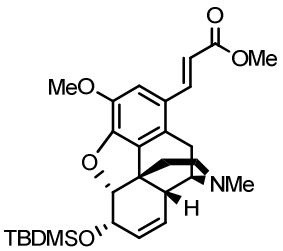 **161**	107,000 ± 21,600	59,100 ± 12,000

Table 4.2 IC_{50} and K_i values for A-ring modified codeine compounds, *samples analysed in duplicate

Opioid	IC_{50} (nM)	K_i (nM)
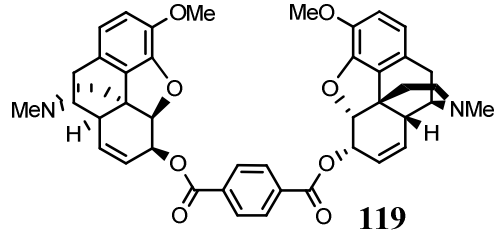 **119**	17,800 ± 4,810	9,750 ± 2,680
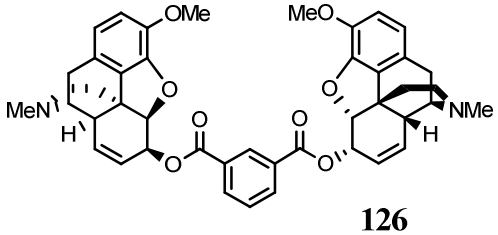 **126**	39,400 ± 7,380	21,800 ± 4,090
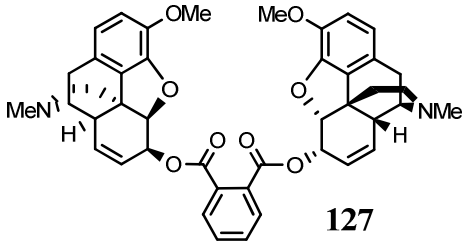 **127**	10,500 ± 1,140	5,860 ± 654
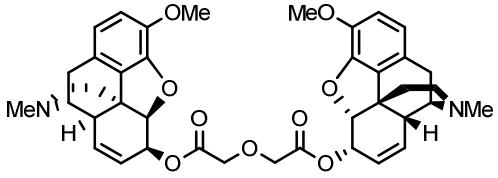 **128**	876 ± 110	486 ± 61
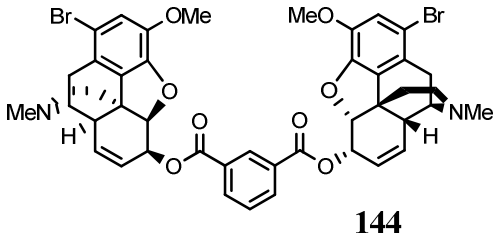 **144**	25,700 ± 3,410	14,300 ± 1890
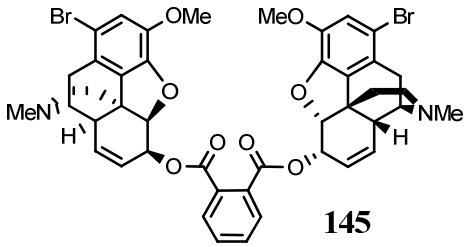 **145**	15,600 ± 1,960	8,650 ± 1,080

Table 4.3 IC_{50} and K_i values for linked codeine ester compounds

Opioid	IC_{50} (nM)	K_i (nM)
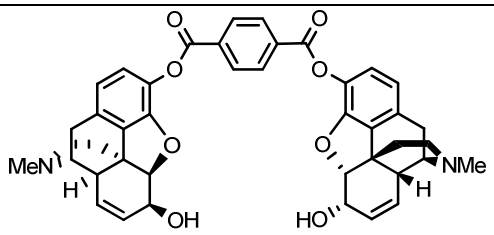 **174**	159 ± 32	87.9 ± 18
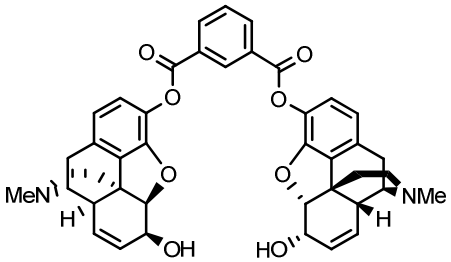 **175**	74.3 ± 4	41.2 ± 2
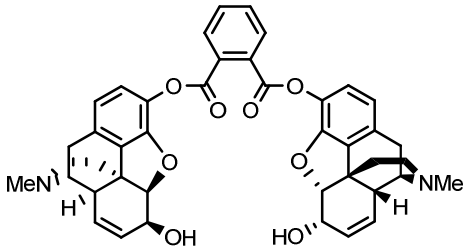 **176**	133 ± 34	73.9 ± 19

Table 4.4 IC_{50} and K_i values for linked morphine ester compounds

Opioid	IC_{50} (nM)	K_i (nM)
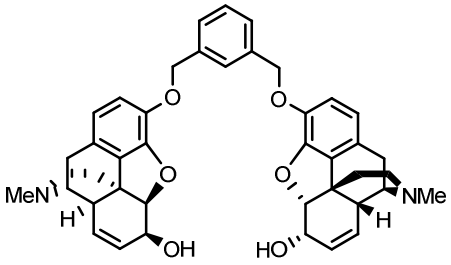 **177**	226 ± 27	125 ± 15
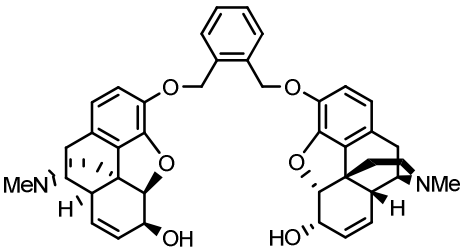 **178**	230 ± 28	128 ± 15
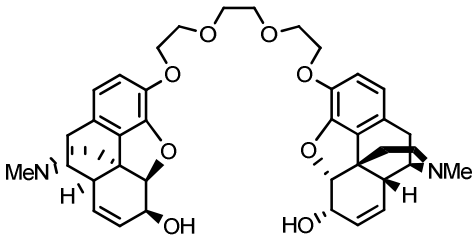 **137**	1,090 ± 158	603 ± 87
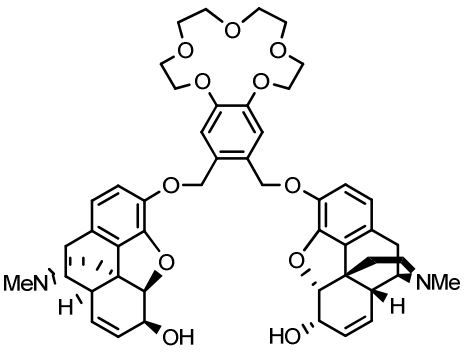 **179**	1,930 ± 424	1070 ± 235

Table 4.5 IC_{50} and K_i values for linked morphine ether compounds

Opioid	IC_{50} (nM)	K_i (nM)
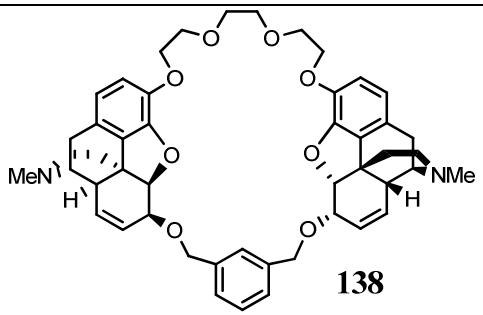 **138**	316 ± 28	175 ± 15
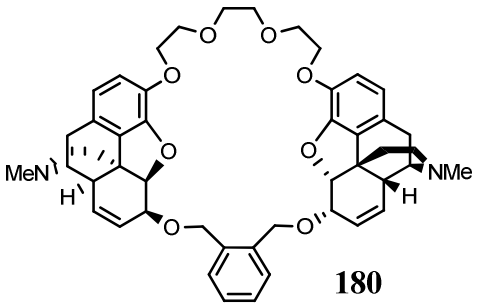 **180**	557 ± 73	309 ± 41

Table 4.6 IC_{50} and K_i values for morphine macrocyclic compounds

Model System	IC_{50} (nM)	K_i (nM)
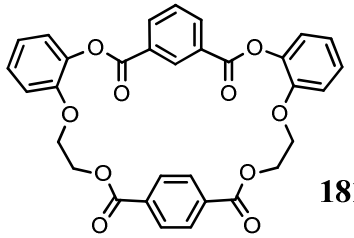 **181**	164,000 ± 69,900	90,800 ± 38,700
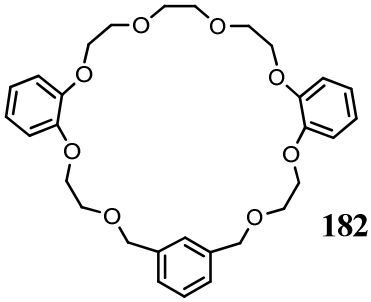 **182**	56,100 ± 9,470	31,100 ± 5,240

Table 4.7 IC_{50} and K_i values for macrocyclic diol model systems

Initial experimental analysis was performed on morphine and codeine as they could be used as standards for the experiment. These results could be used to validate the method and also for comparisons to the novel opioid compounds. The calculated K_i of both the morphine (**1**) and codeine (**2**) standards (10.9 ± 0.2 nM and 2,500 ± 559 respectively) compare favourably with other similar investigations found in the literature.[31, 34, 35, 37, 89] Depending on the tissue sample analysed the K_i values of codeine are usually found to be between 200-600 times greater than that of morphine (Table 4.8).

Tissue Sample	**Morphine (nM)**	**Codeine (nM)**
Rat Brain Tissue (K_i)[89]	1.2 ± 0.32	248 ± 101.1
Rat Brain Tissue (IC_{50})[34]	27	10,000
Mouse Brain Tissue (K_i)[37]	6.22 ± 0.86	ND
Guinea Pig Brain Tissue (K_i)[35]	1.8 ± 0.6	350 ± 110
Monkey Brain Tissue (EC_{50})[31]	4.4	2,500

Table 4.8 Comparison of literature values for *mu* opioid receptor affinities for morphine (**1**) and codeine (**2**) in brain tissue (ND, not determined)

Morphine (**1**) and codeine (**2**) with K_i values of 10.9 ± 0.2 nM and 2,500 ± 559 nM respectively corresponds to codeine having a K_i value approximately 230 times higher (i.e. lower affinity) than morphine. Accurate analysis of the opioid standards validates the method used to test the compounds as well as providing a reference point for the analysis of the unknown opioids. Sigmoidal competition binding curves for codeine and morphine opioid standards with reported K_i and IC_{50} values are shown in Fig 4.9

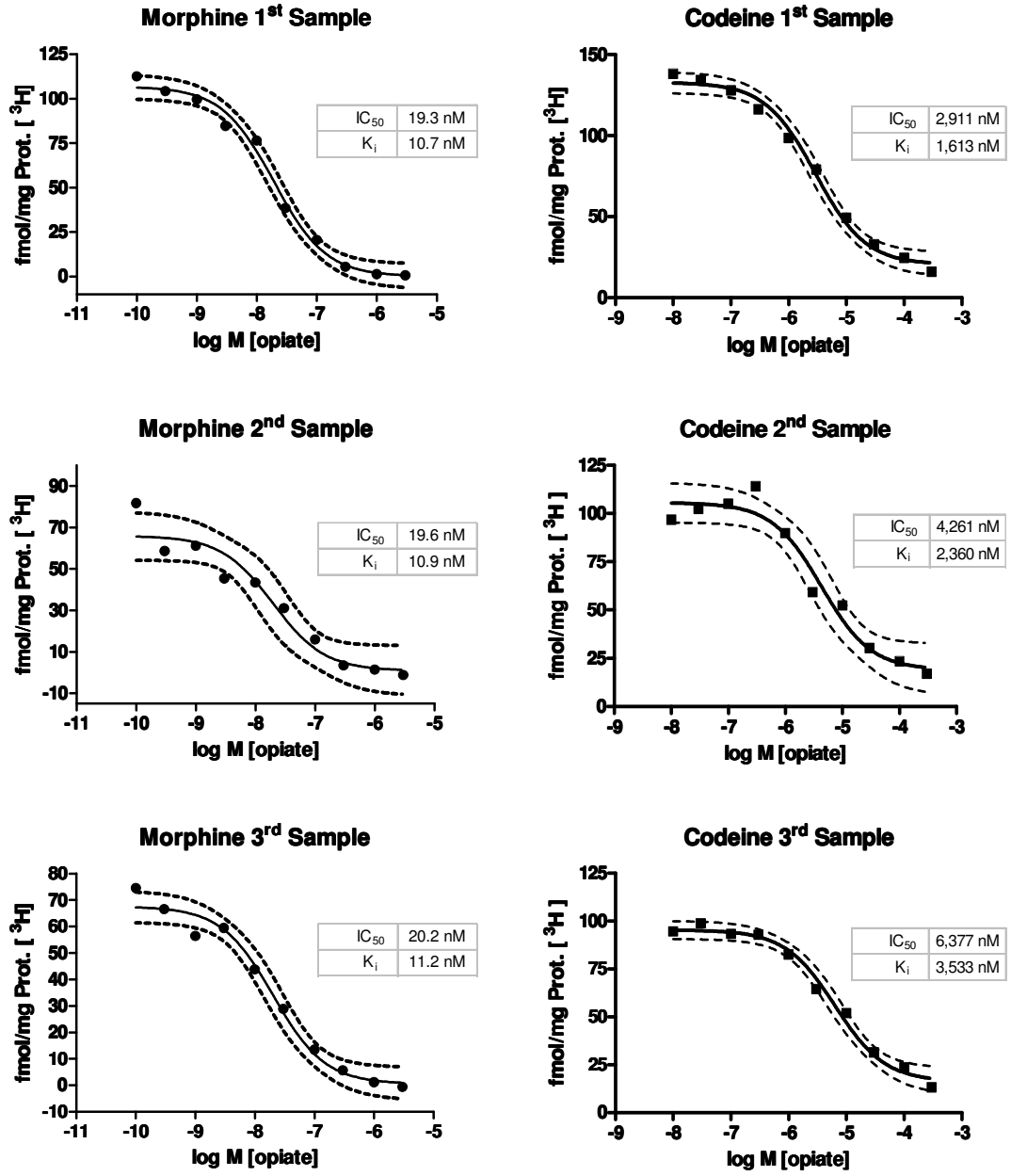

Fig 4.9 Sigmoidal competition binding curves for morphine (**1**) and codeine (**2**) with calculated IC_{50} and K_i values (performed in triplicate)

It should be noted that the concentration ranges used for the competitive binding experiments for morphine are much lower than for codeine, as can be seen in the sigmoidal dose response curves (Fig 4.9). As morphine has a much higher affinity for the *mu* opioid receptor site it inhibits ^{3}H DAMGO at much lower concentrations. An

examination of the pharmacophore of *mu* opioid ligands[17] (Fig 4.10) illustrates the structural components which have a significant impact on the affinity of the drug for the opioid receptor site.

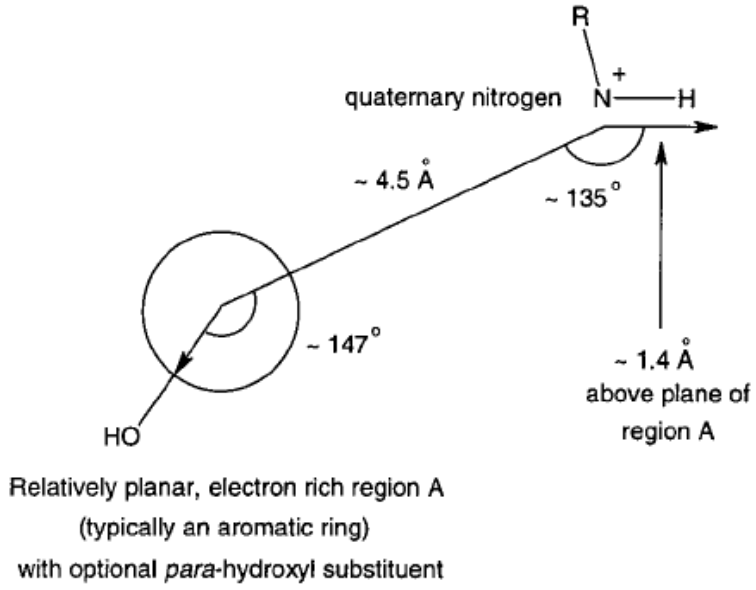

Fig 4.10 Pharmacophore for *mu* opioid ligands

Previous studies have shown that halogen substitution of the aromatic ring lowers the binding affinity for the receptor site.[5] For all the tested A-ring modified codeine derivatives (**76**, **75**, **142**, **161**) there was a higher K_i value, corresponding to lower affinity for the receptor site (Table 4.2). The most notable increase was the K_i value for **161**, at 59,100 ± 12,000 nM (Graph 4.1). The K_i value for **161** is almost 24 times greater than codeine (**2**) at 2,500 ± 559 nM. This is most likely due to the increased steric bulk of the methyl acrylate moiety. Therefore modification at this position of the aromatic ring of codeine has a significant affect on the binding affinities for the *mu* opioid receptor site. Modification of the secondary alcohol at the six position of **160** increased the K_i value to 9,920 ± 1,410 nM.

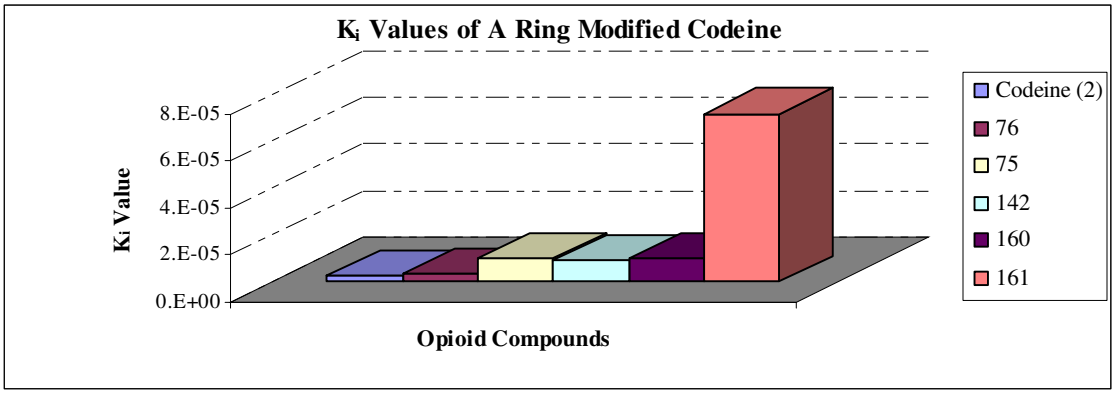

Graph 4.1 Comparison of K_i values for codeine (**2**) and A-ring modified derivatives (**76**, **75**, **142**, **160**, **161**)

For the experimental analysis of the linked opioid species (Tables 4.3 - 4.6) 0.1% TWEEN 80 was added to the stock solutions of the opioid compounds to aid solubility in the aqueous solution. Many of the linked opioid derivatives are only sparingly soluble in water and the addition of TWEEN 80 allowed the opioid compounds to solubilise into the aqueous incubation media at the desired concentrations. Before analysis of the linked opioid compounds was undertaken it was decided to investigate if TWEEN 80 would affect the resulting radioligand binding assay which had previously been developed. To analyse the affect of TWEEN 80 on the radioligand binding assay an experiment was performed on codeine (**2**) as the results could be directly compared with the previous data. The experiment was performed in duplicate and it was observed that the addition of 0.1% TWEEN 80 to the stock solution of codeine for the experiment had a minimal effect on the binding data. The resulting K_i from the TWEEN 80 experiments was calculated at 3,940 ± 637 nM (Fig 4.11) which is comparable to the results obtained when no TWEEN 80 is employed in formation of the opioid stock solutions for codeine (**2**) at 2,500 ± 559 nM (Fig 4.9).

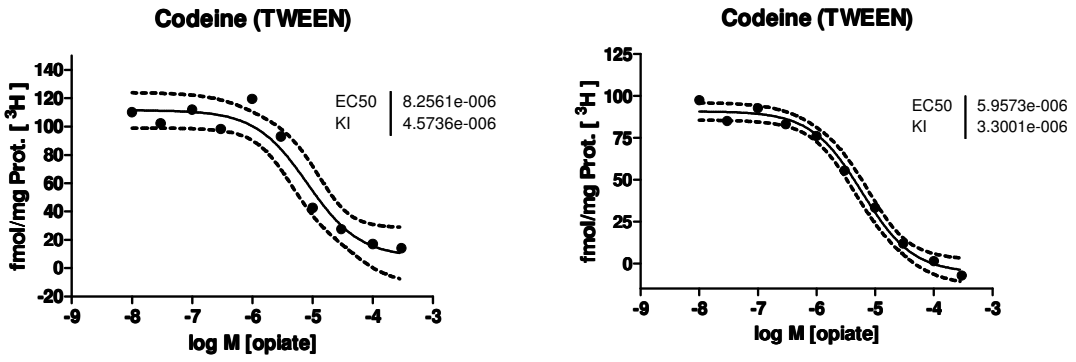

Fig 4.11 Sigmoidal competition binding curves for codeine with the addition of 0.1% TWEEN 80 to the stock solution

The calculated K_i values for the codeine ester compounds (Table 4.3) were between 2 (**127**, 5,860 ± 654 nM) and almost 9 (**126**, 21,800 ± 4090 nM) times greater than codeine (**4**, 2,500 ± 559 nM) (Graph 4.2). It is interesting to examine the different binding affinities for the brominated (**144**, **145**) and non-brominated (**126**, **127**) ester linked compounds (Graph 4.3). For **127** the calculated K_i value of 5,860 ± 654 nM is lower than bromocodeine (**75**), at 9,990 ± 1,550 nM. Therefore when the A-ring of **127** is brominated as in **145** the K_i value increases to 8,650 ± 1,080 nM. This would be expected as bromination of the A ring has been shown to lower the binding affinity of opioids for the *mu* receptor site.[5]

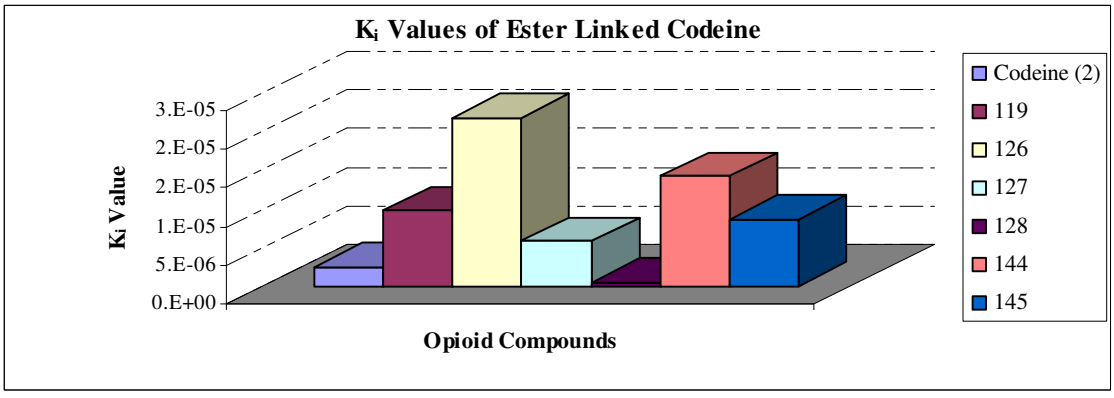

Graph 4.2 Comparison of K_i values for codeine (**2**) and ester linked derivatives (**119**, **126**-**128**, **144**, **145**)

Thus it could be concluded that for compound **145** it is the bromination of the A-ring which is the limiting factor in relation to binding to the *mu* receptor site, as opposed to the *ortho* linked ester modification. For compound **126** the calculated K_i value of 21,800 ± 4,090 nM is already much higher than bromocodeine (**7**) at 9,990 ± 1,550 nM. For the brominated derivative, **144**, the calculated K_i value is 14,300 ± 1890 nM. Therefore it could be concluded that for compound **144** it is the *meta* linked ester modification which exerts a bigger influence on binding to the *mu* receptor. The most interesting result from the ester linked codeine derivatives was noted for the compound **128**. Its K_i value at 486 ± 61 nM was calculated at 5 times lower than codeine (**2**, 2,500 ± 559 nM), therefore **128** has a higher affinity for the *mu* opioid receptor than codeine.

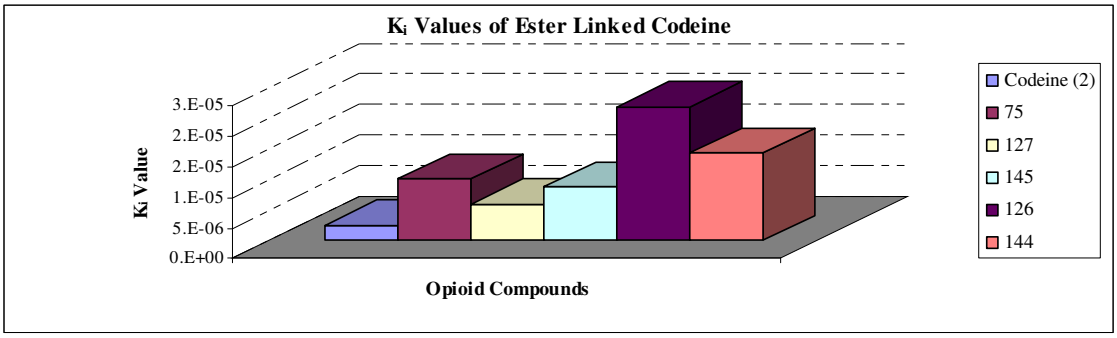

Graph 4.3 Comparison of K_i values for codeine (**2**) and bromocodeine (**75**) with brominated (**144**, **145**) and non-brominated (**126**, **127**) ester linked codeine derivatives.

A selection of nine morphine derivatives (**137**, **138**, **174**-**180**) were also investigated for their affinities for the *mu* opioid receptor (Tables 4.4-4.6). The morphine derivatives tested included both ester (**174**-**176**) and ether (**137**, **177**-**179**) linked morphine compounds as well as ether linked opiate macrocycles (**138**, **180**). The three ester linked morphine structures (Table 4.4) investigated resulted in K_i values between 4 (**175**, 41.2 ± 2 nM) and 8 (**174**, 87.9 ± 18 nM) times greater than morphine (**5**, 10.9 ± 0.2 nM) (Graph 4.4). The ester linked morphine derivatives (**174**-**176**) exhibited the highest affinity to the *mu* opioid receptor site for the tested "linked" compounds. Compound **175** displayed the highest affinity of the linked opioid derivatives at 41.2 ± 2 nM.

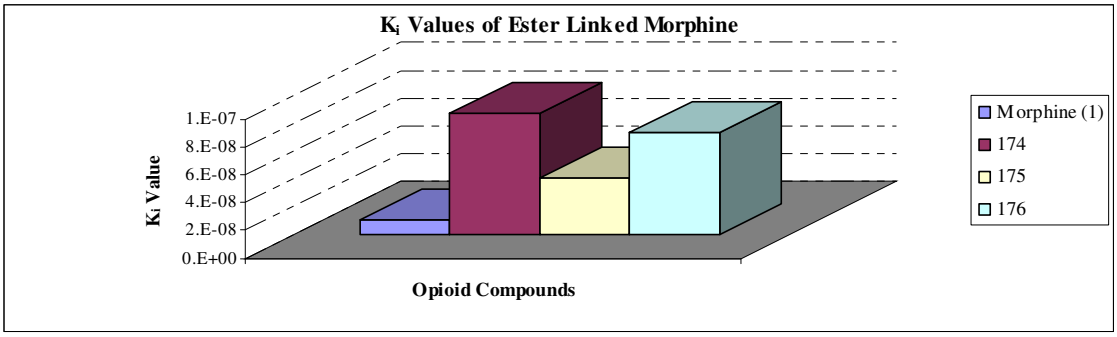

Graph 4.4 Comparison of K_i values for morphine (**1**) and ester linked morphine derivatives (**174**-**176**)

The calculated K_i values for the morphine ether derivatives were between 11 (**177**, 125 ± 15 nM) and almost 100 (**179**, 1070 ± 235 nM) times greater than that of morphine (**1**, 10.9 ± 0.2 nM) (Graph 4.5). The most noticeable increase in the K_i value was noted for the "open" linked morphine compound with the macrocyclic moiety in the linker species, **179**, at 1070 ± 235 nM. This is probably due to steric effects with the bulky crown ether moiety in the linker species lowering the formation of the receptor ligand complex at the *mu* opioid receptor site

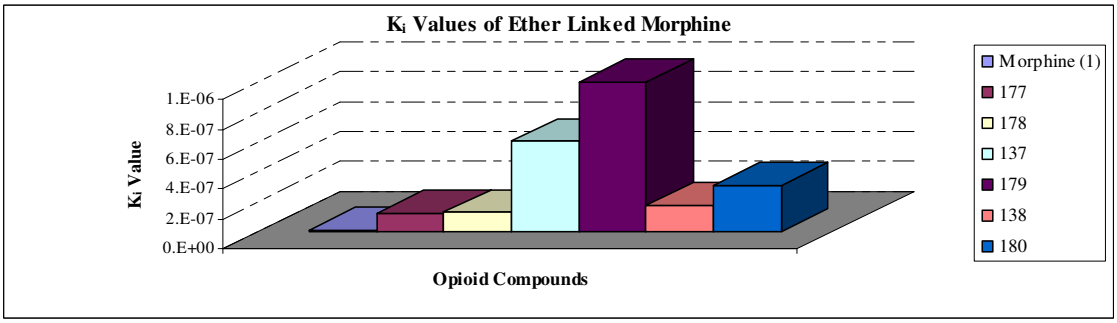

Graph 4.5 Comparison of K_i values for morphine (**1**) and ether linked morphine derivatives (**137**, **138**, **177**-**180**)

The "open" linked ether compounds **177**, **178** and **137** exhibited K_i values of 125 ± 15 nM, 128 ± 15 nM and 603 ± 87 nM respectively. A comparison of the "open" linked ether (**137**) and the closed macrocyclic derivatives (**138** and **180**) shows that closing the morphine scaffold increases the affinity for the receptor site (Graph 4.6). The calculated

K_i value for the "open" linked derivative, **137** was 603 ± 87 nM while the macrocyclic derivatives **138** and **180** were 309 ± 41 nM and 175 ± 15 nM respectively.

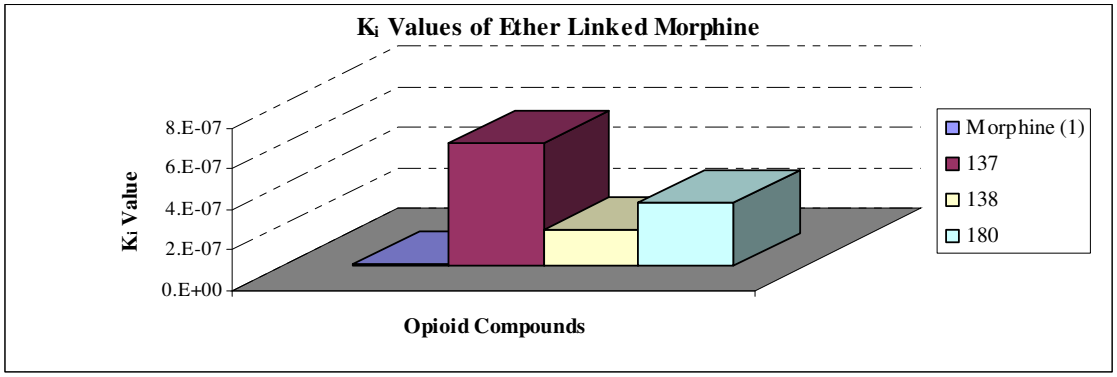

Graph 4.6 Comparison of K_i values for morphine (**1**) and ether linked morphine derivatives (**137**, **138** and **180**)

As expected, the diol model system macrocyclic structures displayed negligable affinity for the *mu* opioid receptor site (Table 4.7). The calculated K_i values for **181** and **182** were 90,800 ± 38,700 nM and 31,100 ± 5,240 nM respectively.

4.2.3 Discussion

The linked opioid compounds analysed as part of this project can be classed as "dual" or "twin" drugs due to the presence of two pharmacophoric groups covalently bonded to each other (Fig 4.12). They can be further classified as "identical twin drugs" or homodimer derivatives as the two pharmacophoric groups are identical. There is increasing interest in the potential benefits of twin and multiple ligand type drugs.[90-92] The administration of twin drugs can have favorable effects compared to the addition of the two separate drugs as the new twin drug will have its own distinct pharmacokinetic properties (absorption, distribution metabolism excretion and toxicity, ADMET).

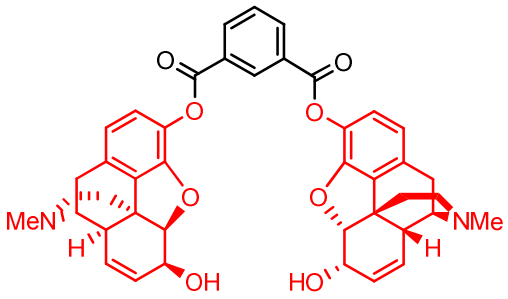

175

Fig 4.12 Compound **175** highlighting the two morphine pharmacophores

Previous studies on linked opioid compounds have lead to a variety of bivalent opioid derivatives[64, 65, 58, 59, 93] (for further information on bivalent opioid compounds see Chapter 1). Portoghese and co-workers have synthesised a variety of opioid bivalent ligands and analysed their opioid receptor affinities (Fig 4.13).[64]

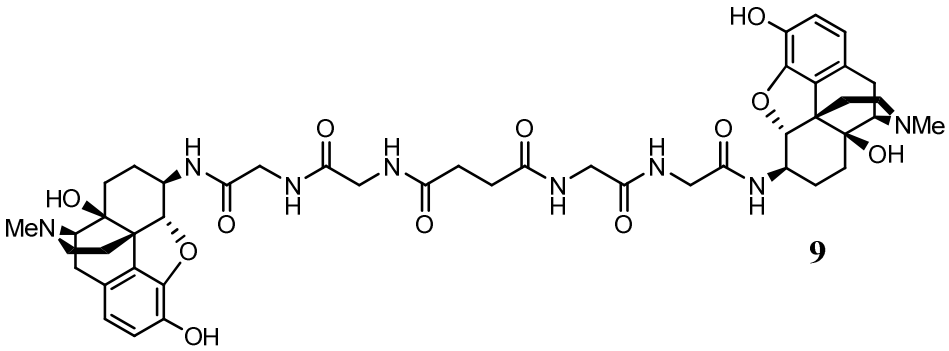

9

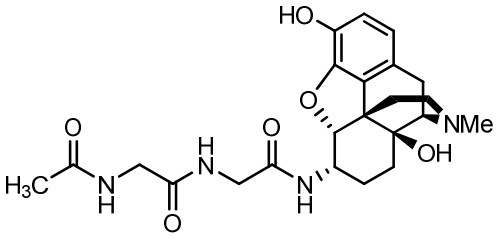

111

Fig 4.13 Structures of opioid compounds **9** and **111**

They have found that simultaneous interaction of both pharmacophores of the drug molecule is possible at the *mu* opioid receptor site. As the affinity of the bivalent ligand (**9**) is greater than double the affinity of the corresponding monovalent ligand (**111**)

(Table 4.9) then it can be concluded that the bivalent ligand must be interacting with more than one receptor site. By analogy it can be concluded that the novel linked opioid compounds analysed as part of this project may also interact with more than one *mu* receptor site.

Compound	K_i nM
9	14 ± 3
111	180 ± 41

Table 4.9 K_i values for compounds **9** and **111** to the *mu* opioid receptor

Before discussing the interactions of the novel linked opioids with the *mu* opioid receptor site we should discuss possible enzymatic degradation. An important aspect to consider for all drugs, but especially "twin" drugs is the role of enzymatic degradation in both *in vitro* and *in vivo* studies. It is known that both codeine and heroin exhibit their analgesic effects after being converted to morphine by enzymatic degradation. Codeine is *O*-demethylated to morphine in humans by cytochrome P450-2D6 (CYP-2D6).[32] By analogy it could be envisioned that the novel "linked" opioid compounds may also exhibit analgesic effects due to degradation to morphine. Both the ester (**119**, **126**-**128**, **144**, **145**, **174**-**176**) and ether (**137**, **138**, **177**-**180**) linked novel compounds would be susceptible to metabolism *in vivo*, *via* plasma esterases and enzymatic cytochrome P450. If the analgesic effect of the novel linked derivatives is dependent on conversion to morphine, the rate of conversion *in vivo* to morphine could potentially lead to slow-release type analgesics. It would be expected that the ester linked codeine (**119**, **126**-**128**, **144**, **145**) and morphine (**174**-**176**) derivatives would be more susceptible to *in vivo* degradation (*via* enzymatic hydrolysis) than the corresponding ether compounds. Mignat and co-workers have investigated the binding affinity and rate of hydrolysis of a selection of morphine-3-esters (Fig 4.14) (Table 4.10).[35]

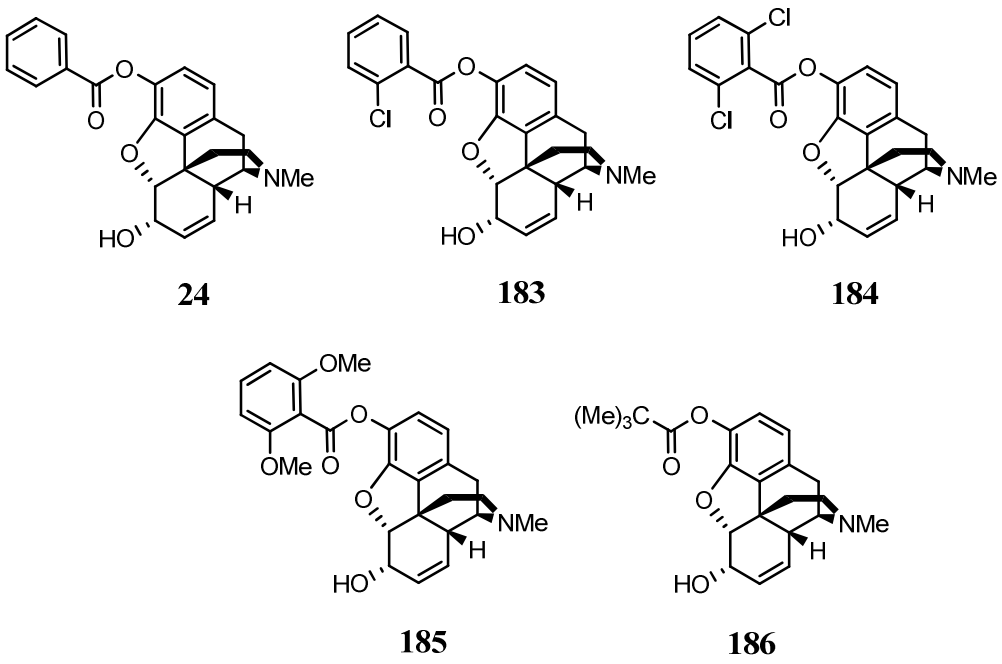

Fig 4.14 Structures of morphine-3-esters

		Hydrolysed % (Tris-Buffer 50 mM) 37 °C		Human Plasma 37 °C
Compound	**K_i (nM)**	**60 (min)**	**24 (h)**	**$t_{1/2}$ (h)**
Morphine, **1**	1.8			
24	29	3	35	0.62
183	160	0.6	9	0.94
184	8,200	0	0	>300
185	360	0	0	>300
186	52	1.1	4	8.3

Table 4.10 K_i values and hydrolysis data for morphine (**1**) and morphine-3-esters **24**, **183**-**186**

The rate of hydrolysis of the morphine-3-esters gives an indication of the stability of the ester bond which can be compared with the novel ester linked compounds analysed in this project. An examination of the stability of the ester bond in both buffer solution (Tris-Buffer 50 mM) and in human plasma (to measure plasma catalysed hydrolysis) was undertaken. In general the ester bond is stable to the aqueous buffer solution over

the experimental incubation time frame of 60 minutes. The highest percentage of hydrolysis to morphine was noted for compound **24** at only 3% after 60 minutes. If the compounds are incubated with the aqueous buffer solution for 24 hours there is an increase in hydrolysis with the highest corresponding to **24** at 35%.

In the presence of human plasma there is a much higher rate of hydrolysis for the ester bonds. Compound **24** is hydrolysed by 50% after 0.62 hours while compound **183** is hydrolysed by 50% after 0.94 hours. The experimental data also highlight that there is a large variance in hydrolysis rates depending on the particular ester formed. Thus choice of the ester functional group has a major effect on the rate of hydrolysis. It should also be noted that some of the morphine-3-esters exhibited no hydrolysis even after relatively harsh conditions. Compounds **184** and **185** displayed no degradation to morphine after incubation at 37 °C after 300 hours in the human plasma.

It can be concluded from the relatively low hydrolysis in the buffer solution compared to the much higher rate in the human plasma sample that most of the ester hydrolysis is due to enzymatic degradation. The rat brain tissue homogenate utilised in the experimental analysis of the linked opioid compounds in this project could be a source of enzymes for ester hydrolysis. Both the ester (**119**, **126**-**128**, **144**, **145**, **174**-**176**) and ether (**137**, **138**, **177**-**180**) linked opioid compounds could potentially be partly metabolised during the experimental *in vitro* analysis. It is important to note that enzymatic degradation of the linked opioid compounds would lead to 2 active units. If we consider compound **175**, enzymatic hydrolysis would lead to two morphine (**1**) derivatives (Fig 4.15).

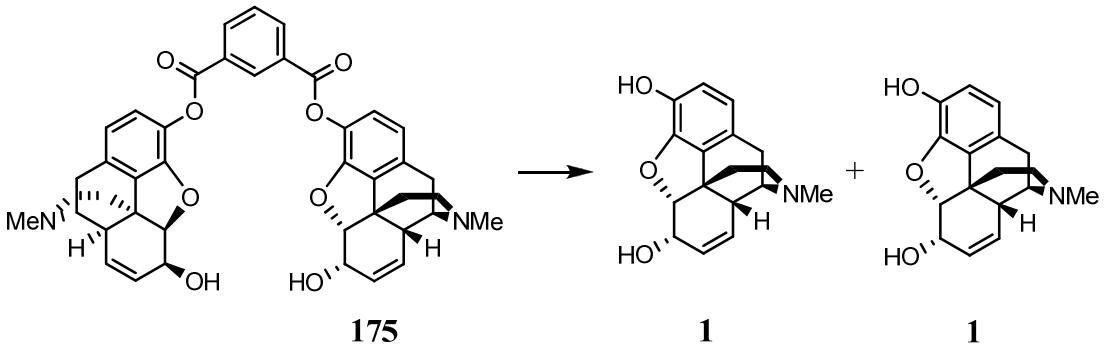

175 **1** **1**

Fig 4.15 Hydrolysis of compound **175** would result in two morphine (**1**) units

The calculated K_i for **175** was 41.2 ± 2 nM which is almost 4 times lower than morphine (**5**) at 10.9 ± 0.2 nM. The calculated value for **174** in comparison was 87.9 ± 18 nM. It is important to note that the difference in K_i values for compounds **174** and **175** could be due to their different rates of hydrolysis. If **175** is hydrolysed more rapidly then **174** then more "free" morphine will be present in the incubation tube resulting in a higher calculated affinity for compound **175**. Therefore the rate of enzymatic degradation for the linked opioid compounds should be considered when analysing the calculated K_i values. The rate of enzymatic degradation is an important factor to consider as it has important implications for *in vitro* testing and the potential use of the novel linked opioids as prodrugs in slow-release analgesics.

From the calculated K_i values, it is clear that we are not observing 100% enzymatic degradation to "free" morphine within the 60 minute incubation time frame. If there was 100% degradation to morphine the observed K_i values for **174** and **175** would be much lower than 41.2 ± 2 nM and 87.9 ± 18 nM respectively. Therefore, from the K_i values of the novel opioid derivatives we know that the linked opioid compounds are present in the incubation tube. If the linked opioid compounds are present within the incubation tube then by analogy with Portoghese and co-workers[64] we know that it is possible for the linked opioid derivatives to interact with more than one *mu* receptor site.

Further extensive studies would be required to examine the exact mechanism of interaction between the linked opioid compounds and the *mu* opioid receptor site; however we can deduce some factors from these preliminary studies. When discussing the possible structural factors which may influence multi-receptor binding to the *mu* opioid site, the rates of enzymatic degradation for the different linked opioids has been ignored. However as noted earlier, the *in vitro* rates of degradation may have an effect on the resulting K_i values

The aromatic ether linked opioids **177** and **178** exhibit identical affinity to the *mu* opioid receptor site with K_i values of 125 ± 15 nM and 128 ± 15 nM respectively. When the spacer length is increased in compound **137** the affinity to the receptor site decreases with a K_i value of 603 ± 87 nM. When the glycol linker is "locked" into position by the formation of the macrocyclic opioids (**138** and **180)** we observe a relative increase in affinity. The calculated K_i value for the "open" linked derivative, **137** was 603 ± 87 nM while the macrocyclic derivatives **138** and **180** were 175 ± 15 nM and 309 ± 41 nM respectively. A possible reason for the increased affinity for the macrocyclic opioids (**138**, **180**) relative to the "open" linked derivative (**137**) is formation of the macrocyclic opioid may "force" the two morphine pharmacophore units closer together (Fig 4.16). Therefore having the two morphine pharmacophores close together may aid binding to the *mu* opioid receptor site.

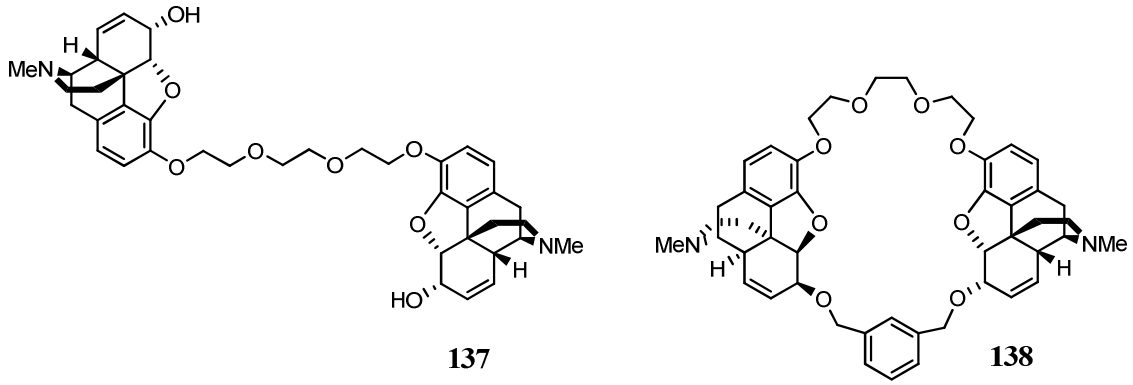

137 **138**

Fig 4.16 Structures of opioid compounds **137** and **138**

The most interesting compound from the ester linked codeine (**119**, **126**-**228**, **144**, **145**) and morphine (**174**-**176**) derivatives was compound **128**. The K_i value for **128** was calculated at 486 ± 61 nM, approximately 5 times lower than codeine (**2**, 2,500 ± 559 nM). As the affinity of the linked bivalent ligand (**128**) is greater than codeine (**2**) then it can be concluded that the bivalent ligand (**128**) may be interacting with more than one receptor site. In comparison to the aromatic ester linked codeine derivatives, **119** (9,750 ± 2,680 nM), **126** (21,800 ± 4,090 nM) and **127** (5,860 ± 654 nM), **128** exhibits a much higher affinity to the *mu* receptor. A possible reason for the increased affinity of **128** relative to the aromatic linked esters (**119**, **126**, **127**) is the linker group. If we consider that interaction of both pharmacophores in the molecule leads to increased affinity to the *mu* receptor site then any conformational restrictions due to the linker group will affect the K_i value.

The increased flexibility of **128** relative to the aromatic linked esters (**119**, **126**, **127**) may allow the compound to arrange both pharmacophoric units more favourably to the *mu* receptor. As noted for the ether linked morphine derivatives having the two opioid pharmacophores in close proximity may aid in binding to the *mu* opioid receptor. It is unclear at this stage if the increased binding is due to two separate and distinct *mu* opioid receptors or a single receptor and an accessory binding site. Further studies would be required to examine the exact interaction of the linked opioids and the *mu* receptor. It is also possible that the bivalent opioid compounds may be binding to *mu* opioid receptor homodimers.

Based on the data from this project some novel linked opioid targets, which may have promising *mu* receptor binding, are outlined in Fig 4.17. Formation of the linked opioids *via* the phenolic hydroxyl position lowers the affinity relative to morphine, as observed in the ester (**174**-**176**) and ether (**137**, **138**, **177**-**180**) linked morphine based opioids. It would be interesting to examine some of the corresponding ether (**187**, **188**) or ester linked morphine derivatives which are linked at the secondary alcohol instead of the phenolic position (**177**, **178**). If the two morphine pharmacophoric units are

linked through the secondary alcohol position the affinity of the linked derivative for the *mu* opioid receptor site could potentially be greater than morphine. This is assuming both morphine pharmacophores can interact with the receptor site which is plausible based on the calculated K_i values for the ester linked codeine derivative, **128**.

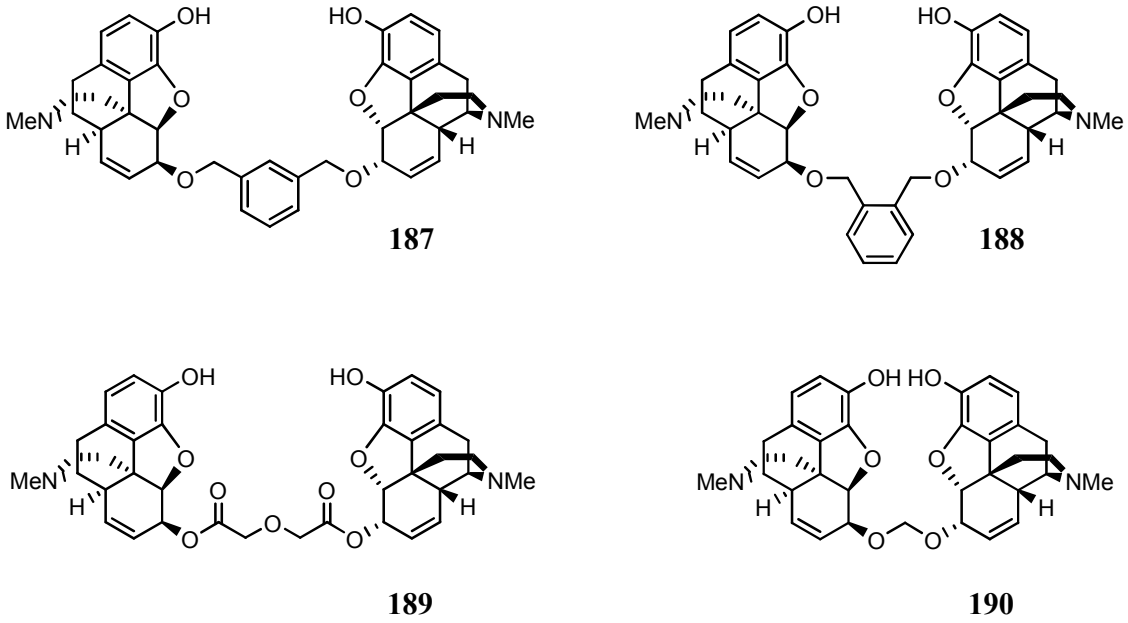

Fig 4.17 Possible targets for linked opioid derivatives

Interaction of the aromatic ring in the linker group may also have an effect on both pharmacophores interacting with the receptor thus analysis of **189** would be desirable. By analogy with **128**, which exhibits an affinity to the *mu* receptor over five times higher than codeine, compound **189** may display increased affinity for the *mu* opioid receptor site relative to morphine. From the preliminary data there is also some evidence that the close proximity of both opioid pharmacophores may improve binding to the *mu* receptor. Therefore it would be appropriate to analyse a linked opioid derivative such as **190** in which both morphine pharmacophores are closely bound to each other. Although the stability to hydrolysis is an important consideration and **190** may rapidly degrade.

4.3 Conclusion

The affinity ($1/K_i$) of 24 compounds (**1**, **2**, **75**, **76**, **119**, **126**-**128, 142**, **144**, **145**, **160**, **161**, **{174-176, 181}**[88], {**137**, **138**, **177**-**180**, **182}**[70]) for the *mu* opioid receptor was calculated by competitive radioligand binding techniques. Prior to the experimental analysis, a robust and reliable radioligand competitive binding method was developed. It was also shown that the addition of 0.1% TWEEN 80 to the stock solutions of opioid standards had no significant effect on the radioligand binding method. The general trend noted for the novel opioid compounds was that modification at the 1, 3 and 6 positions of the parent opioid structure lowered the affinity for the *mu* opioid receptor site. A selection of A ring modified codeine derivatives (**75**, **76**, **142**, **161**) were analysed along with ester linked codeine compounds (**119**, **126**-**128**, **144**, **145**). Also studied were a variety of ester (**174**-**176**) and ether (**137**, **138**, **177**-**180**) linked morphine based compounds.

For all the analysed A-ring modified codeine derivatives there was a higher K_i value, corresponding to lower affinity for the receptor site, relative to codeine. Thus, modification at the 1 position was shown to lower the affinity for the *mu* receptor. This is especially noticeable for **161** with a K_i value of 59,100 ± 12,000 nM compared to codeine (**2**) at 2,500 ± 559 nM. Therefore, *via* modification at this position of the opioid skeleton we can "block" binding to the receptor site if desired. This is especially important if we want to pursue the opioid derivatives in potential sensor applications (Chapter 5). If the opioid derivatives display potential uses as sensors then binding to the *mu* opioid receptor site would be an undesirable side effect. Thus through A ring modification we have a relatively simple process to nullify the analgesic activity.

In general the ester linked codeine compounds displayed lower affinity for the *mu* receptor site. The most interesting result from the analysis of the ester linked codeine structures was noted for the diglycol linked compound **128**. Compound **128** displayed a K_i value of 486 ± 61 nM, five times lower than codeine's calculated value at 2,500 ±

559 nM. Therefore it has been shown that formation of a "linked" codeine derivative can increase the binding affinity of opioid compounds for the *mu* opioid receptor site.

The ester and ether linked morphine derivatives in general displayed lower affinity than the parent morphine structure with the ester linked morphine derivatives (**174-176**) displaying higher affinity for the *mu* receptor site than the ether linked compounds (**137**, **138**, **177**-**180**). The calculated K_i values of the novel morphine derivatives ranged from 41.2 ± 2 nM (**174**) to 1070 ± 235 nM (**179**) in comparison to a K_i value for morphine (**1**) of 10.9 ± 0.2 nM. It should be noted that codeine (**2**) is a widely used opioid analgesic with an affinity of approximately 2,500 ± 559 nM.

Thus, a selection of linked opioid derivatives have been analysed which display a much higher affinity for the *mu* opioid receptor site than codeine. Therefore it is possible that they may have the potential to act as analgesic prodrugs. It should be noted that the results for the opioid binding have been generated *in vitro* with its corresponding limitations. It would be desirable to investigate these compounds and other opioid derivatives with *in vivo* experiments and thus parameters such as bioavailabilty and pharmokinetics could be examined.

4.4 Experimental

4.4.1 Tissue Membrane Preparation for Receptor Binding Protocol

Rats (Male Lister-hooded rats (250 g, Charles River UK) were killed by decapitation and the brain minus cerebellum rapidly removed. The brain was weighed and suspended in 8v/w ice cold buffer (buffer 50 mM Tris-HCl pH 7.4, ie 8 mL/g tissue). Brain tissue was homogenised at 1000 rpm/min for 20-30 sec at 4 °C. The sample was centrifuged at 40000 g at 4 °C for 20 min. Supernatant was discarded and the pellet was re-suspended in fresh buffer (8 v/w) using sonicator and vortex. The suspension was incubated at 37 °C for 30 min with shaking (to dissociate endogenous opioids from

receptors). The sample was centrifuged at 40000 g at 4 °C for 20 min. Supernatant was discarded and the pellet was re-suspended in fresh buffer (8 v/w) using sonicator and vortex. The sample was centrifuged at 40000 g at 4 °C for 20 min. The supernatant was discarded and the pellet was re-suspended in 10 mL of buffer solution using sonicator and vortex. The tissue membrane samples were stored as 1 mL aliquots at -80 °C.

4.4.2 Determination of Protein Concentration in Tissue Homogenate Protocol

Protein assay based on the Bradford-dye binding procedure, (solution, buffer 50 mM Tris-HCl pH 7.4). Stock solution of bovine serum albumin (BSA) 2 mg/mL, was prepared in buffer solution. Protein standards were prepared from stock bovine serum albumin (BSA), in buffer solution, in 6 concentration ranges, 0 ug/mL (blank), 100 µg/mL, 250 µg/mL, 500 µg/mL, 750 µg/mL, 1000 µg/mL to volumes of 200 µL. Tissue membrane samples were removed from -80 °C freezer and allowed to thaw. 1 mL aliquots of tissue samples were combined and vortexed / sonicated to ensure tissue sample was homogenous. Volume of tissue homogenate was removed and diluted by 1/10 in buffer (ie 15 µL in 135 µL buffer). Thawed tissue membrane homogenate was stored on ice. 25 µL of protein standards or unknown was added to analysis wells in triplicate. 1250 µL of Coomassie Blue reagent was added to each well and left for 10 min at room temp. Absorbance was read at 570 nm. Data was analysed using *excel* and *graphpad prism* software.

4.4.3 Dissociation Kinetics for ^{3}H DAMGO in Tissue Membrane Protocol

Membrane tissue homogenate prepared as outlined in membrane prep protocol. (Buffer solution, 50 mM Tris-HCl pH 7.4). ^{3}H DAMGO stock standard (Perkin Elmer), [Specific Activity 56.8 Ci/mmol, Conc. 1 mCi/mL] was made to stock solution of 10 nM in buffer solution to volume of 3 mL. Assays for total binding and non-specific binding over a range of incubation times were performed in duplicate and in LP3 tubes. For the analysis of total binding, to each vial was added, 100 µL of ^{3}H DAMGO, tissue

homogenate (corresponding to 400 µg protein) and made to final volume, 1 mL with buffer solution. (*The volume of tissue homogenate added to each LP3 tube is dependant on the protein concentration of the homogenous tissue sample used, which was calculated based on the Bradford-dye binding procedure*). For the analysis of non-specific binding, to each vial was added, 100 µL of ^{3}H DAMGO, 100 µL of NSB (non-specific binding) agent (naloxone, conc. 100 µM), 400 µg tissue homogenate and made to final volume, 1 mL with buffer solution. Assay vials were split into six groups with each group incubated for different times at 20 °C, 15 min, 30 min, 45 min, 60 min, 90 min and 120 min.

The reaction was terminated by the addition of 5 mL buffer solution to each assay tube. Tissue membrane samples were collected under vacuum using a Brandel Harvester. Tissue membrane samples were collected onto glass fibre filters (Whatman GF/B filters) which were pre-soaked in 0.2% polyethylenimine solution. Whatman GF/B filters were washed with 3 x 5 mL buffer solution to remove any unbound ^{3}H DAMGO from the tissue samples. Filter papers were then placed in scintillation vials to which 5 mL of scintillation cocktail was added to each (Ecoscint A). Vials were capped, vortexed for 30 sec. and left overnight. Vials were placed on scintillation counter and radioactivity was recorded. Data was analysed using *graphpad prism* software to calculate the time at which steady state binding has occurred.

4.4.4 Determination of K_d and B_{max} Values of ^{3}H DAMGO in Tissue Membrane Homogenate Protocol, (Saturation Binding Experiment)

Membrane tissue homogenate prepared as outlined in membrane prep protocol. (Buffer solution, 50 mM Tris-HCl pH 7.4). ^{3}H DAMGO stock standard (Perkin Elmer), [Specific Activity 56.8 Ci/mmol, Conc. 1 mCi/mL] made to stock solution of 200 nM in buffer solution to 1 mL. Serial 0.4 dilutions of stock ^{3}H DAMGO solution were made using buffer solution resulting in six concentrations, 200 nM, 80 nM, 32 nM, 12.8 nM (12.5 nM), 5.12 nM (5 nM), 2.048 nM (2 nM). Assays for total binding and non-

specific binding were performed in duplicate in LP3 glass tubes. For the analysis for total binding to each vial was added, 100 µL of ^{3}H DAMGO in 6 concentrations, 400 µg of tissue homogenate, and made up to final volume of 1 mL in buffer solution. For the analysis for non-specific binding to each vial was added, 100 µL of ^{3}H DAMGO in 6 concentrations, 100 µL of NSB (non-specific binding) agent (naloxone, conc. 100 µM), tissue homogenate (corresponding to 400 µg protein) and made to final volume, 1 mL with buffer solution. (*The volume of tissue homogenate added to each LP3 tube is dependant on the protein concentration of the homogenous tissue sample used, which was calculated based on the Bradford-dye binding procedure*). The vials were incubated at room temperature (20 °C) for 60 min. (*Incubation time is dependant on the association kinetics for the particular experiment. It is the time at which steady state binding has occurred. See association kinetics protocol for experimental method).*

Reaction was terminated by the addition of 5 mL buffer solution to each assay tube. Tissue membrane samples were collected under vacuum using a Brandel Harvester. Tissue membrane samples were collected onto glass fibre filters (Whatman GF/B filters) which were pre-soaked in 0.2% polyethylenimine solution. Whatman GF/B filters were washed with 3 x 5 mL buffer solution to remove any unbound ^{3}H DAMGO from the tissue samples. Filter papers were then placed in scintillation vials to which 5 mL of scintillation cocktail was added to each (Ecoscint A). Vials were capped, vortexed for 30 sec. and left overnight. Vials were placed on scintillation counter and radioactivity was recorded. Data was analysed using *graphpad prism* software to calculate the K_i and B_{max} parameters of ^{3}H DAMGO.

4.4.5 Determination of the K_i Values of Opioid Compounds Protocol (Competitive Binding Experiment)

Membrane tissue homogenate prepared as outlined in membrane prep protocol. (Buffer solution, 50 mM Tris-HCl pH 7.4). ^{3}H DAMGO stock standard (Perkin Elmer), [Specific Activity 56.8 Ci/mmol, Conc. 1 mCi/mL] made to stock solution of 20 nM in

buffer solution to final volume of 2.5 mL. (*The concentration of the competitive radioligand (^{3}H DAMGO) used for the experiment is dependant on its affinity for the tissue membrane sample, ie it's K_d value. For competitive binding experiments the concentration of radioligand used is usually 80% of its K_d. See determination of K_d and B_{max} values of ^{3}H DAMGO protocol for experimental method*). An opioid stock solution was prepared in buffer solution to a concentration of 10,000 µM. From the opioid stock standard solution a series of dilutions in buffer solution were performed resulting in a series of 10 opioid solutions in decreasing concentration, ie 3000 µM, 1000 µM, 300 µM, 100 µM, 30 µM, 10 µM, 3 µM, 1 µM, 0.3 µM and 0.1 µM. (*The concentration range used for the experiment is dependant on the affinity of the drug for the receptor site).*

The experimental assay was performed in 24 LP3 tubes. To the first 20 assay vials was added, 100 µL of the opioid stock solutions in each of the 10 concentrations, 100 µL ^{3}H DAMGO solution, tissue homogenate (corresponding to 400 µg protein) and made to final volume, 1 mL with buffer solution. (*The volume of tissue homogenate added to each LP3 tube is dependant on the protein concentration of the homogenous tissue sample used, which was calculated based on the Bradford-dye binding procedure*). To the next 2 assay vials was added, 100 µL naloxone solution (conc. 100 µM), 100 µL ^{3}H DAMGO, tissue homogenate (corresponding to 400 µg protein) and made to final volume, 1 mL with buffer solution. (*These assay vials, ie naloxone, are run in order to calculate the non-specific binding for the experiment*). To the final 2 assay vials was added, 100 µL buffer solution, 100 µL ^{3}H DAMGO, 400 µg tissue homogenate and made up to the final volume of 1 mL with buffer solution. *(These assay vials are run as the blank samples for the experiment).* The vials were incubated at room temperature (20 °C) for 60 min. *(Incubation time is dependant on the association kinetics for the particular experiment. It is the time at which steady state binding has occurred. See association kinetics protocol for experimental method).*

Reaction was terminated by the addition of 5 mL buffer solution to each assay tube. Tissue membrane samples were collected under vacuum using a Brandel Harvester. Tissue membrane samples were collected onto glass fibre filters (Whatman GF/B filters) which were pre-soaked in 0.2% polyethylenimine solution. Whatman GF/B filters were washed with 3 x 5 mL buffer solution to remove any unbound ^{3}H DAMGO from the tissue samples. Filter papers were then placed in scintillation vials to which 5 mL of scintillation cocktail was added to each (Ecoscint A). Vials were capped, vortexed for 30 sec and left overnight. Vials were placed on scintillation counter and radioactivity was recorded. Data was analysed using *graphpad prism* software to calculate the K_i parameters of the opioid compound.

Chapter 5

Metal Picrate Extraction Studies

5.1 Introduction

This chapter outlines the metal picrate binding studies performed on a series of opioid compounds. The aim is to investigate which metal cationic species may bind to the cavity site of the novel opioid derivatives (Fig 5.1). It could be possible that interactions between the metal cation species and the oxygen donor atoms could provide the stability required to form these complexes. This data provides important information relating to the novel opioid derivatives tested in relation to;

- Suitability of the novel opioid derivatives as potential pro-drugs (Chapter 4). If the compounds exhibit high binding to a variety of metal ion species this could inhibit their potential as novel opioid pro-drugs. High metal cation binding could lead to potential toxicity problems.
- Potential uses of the novel opioid compounds as metal ion sensors if significant metal binding is observed.

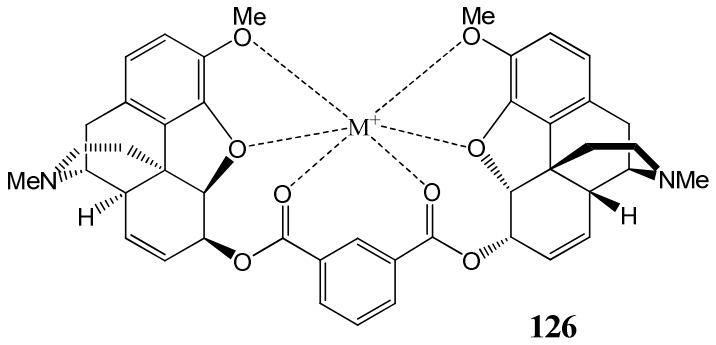

126

Fig 5.1 Metal cationic species binding to the opioid cavity for compound **126**

Metal picrate extraction studies are a well established technique performed to analyse the metal binding properties of a variety of host species.[94-96] The method is based on

measuring the relative distribution of a coloured metal salt (ie the metal picrate species) between water and an immiscible organic solvent containing the desired host species (Fig 5.2). If the complexing host compound has a high affinity to the metal species then a high percentage of the metal picrate salt will be "extracted" from the aqueous layer resulting in lower UV absorption. Conversly if there is little or no affinity between the host species and the metal cation the metal picrate salt will remain in the aqueous layer resulting in higher UV absorption. As a result, UV analysis of the absorption of the resulting aqueous layer provides an accurate measurement of metal binding affinities.

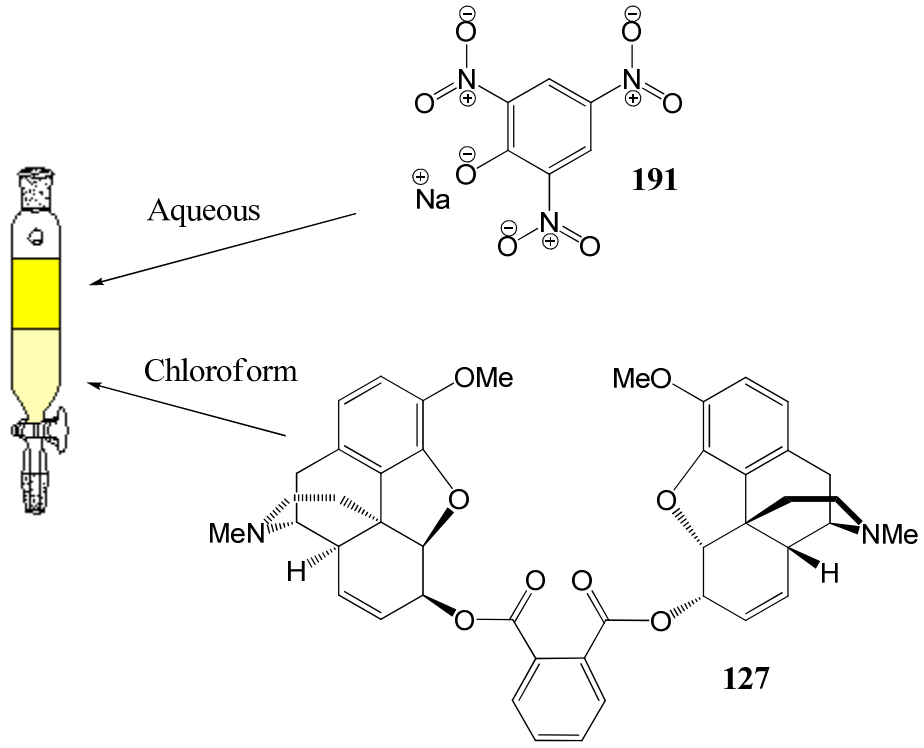

Fig 5.2 Partitioning of opioid species (**127**) and sodium picrate (**191**) between chloroform and water

An important factor to consider for the metal binding is the relationship between the diameter of the metal cation and the cavity size of the opioid species. The cation diameters of the metal compounds tested are outlined in Table 5.1.[95] From X-ray crystal analysis (Chapter 2, 2.5) information about the cavity size and orientation can be deduced. However, it must be remembered that this analysis is on solid state material while in solution different spatial orientations can be adopted.

Group I		Group II		Group III		Group IV	
Metal	Diameter (Å)	Metal	Diameter (Å)	Metal	Diameter (Å)	Metal	Diameter (Å)
Li^+	0.78	Mg^{2+}	0.78	La^{3+}	NA	Pb^{2+}	1.18
Na^+	0.98	Ca^{2+}	1.06				
K^+	1.33	Zn^{2+}	0.75				
		Co^{2+}	0.75				
		Cu^{2+}	0.73				

Table 5.1 Metal cation diameters from ionic radius[95]

5.2 Results and Discussion

The cation selectivity of a selection of opioid derivatives with modification of the linker moiety were analysed by metal picrate extraction studies. In total twelve opioid compounds were analysed with ten metal picrates with results presented in Tables 5.2-5.14. Also included are the results of a blank extraction study, with no host opioid compounds present in the chloroform layer. Furthermore it was decided to investigate if the A-ring modification on the opioid species would have an effect on the metal binding properties of the host compound. To this end a selection of four A-ring modified opioid derivatives were analysed against three metal picrate species, Na^+, Cu^{2+}, La^{3+}, presented in Tables 5.15-5.18.

The metal picrate extraction studies were performed by using host solutions of the opioid species in chloroform and picrate salt solutions in deionised water (Fig 5.2) according to the method by Pedersen.[94] The solutions were shaken for 15 min and the absorption of the resulting aqueous layer was measured at 356 nm. The absorbance of the aqueous layer for each particular metal picrate salt was then compared to calibration curves previously determined to calculate the concentration of the metal picrate in the aqueous layer (Fig 5.3).

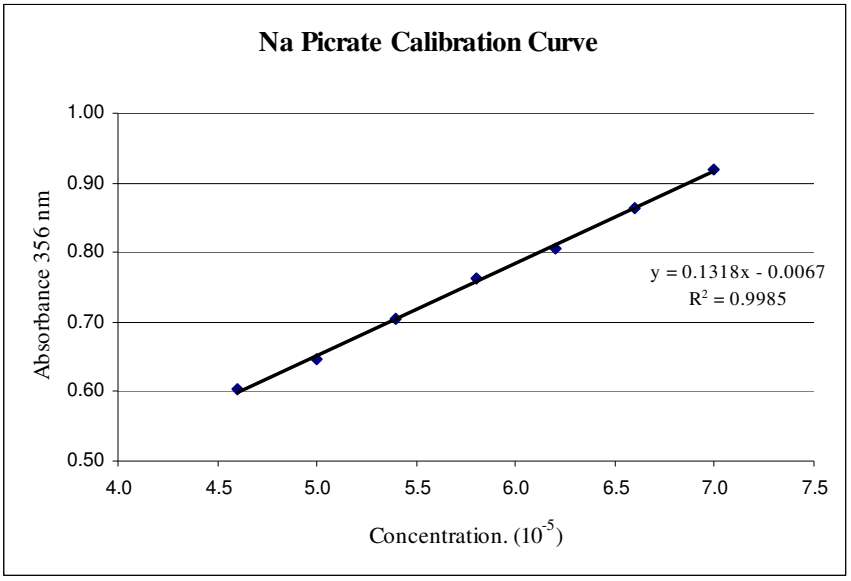

Fig 5.3 Calibration curve for sodium metal picrate

A calibration curve was determined for each of the ten metal picrate salts with the coefficient of determination (R^2 value) greater than 99% for each. Each host opioid species and metal picrate was analysed in triplicate with the average of the three results reported with standard deviation < 0.015

Opioid	Cation	% Extraction
BLANK	Li^+	-1.13
	Na^+	1.47
	K^+	0.84
	Ca^{2+}	1.80
	Mg^{2+}	1.56
	Zn^{2+}	1.67
	Co^{2+}	1.72
	Cu^{2+}	1.12
	Pb^{2+}	1.75
	La^{3+}	-1.79

Table 5.2 Extraction results with **Blank**

Opioid	Cation	% Extraction
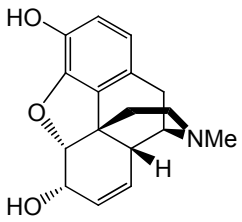 **1**	Li^+	0.71
	Na^+	2.10
	K^+	2.78
	Ca^{2+}	2.66
	Mg^{2+}	7.68
	Zn^{2+}	4.77
	Co^{2+}	7.43
	Cu^{2+}	12.44
	Pb^{2+}	5.75
	La^{3+}	7.21

Table 5.3 Extraction results with morphine (**1**)

Opioid	Cation	% Extraction
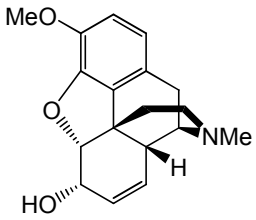 **2**	Li^+	2.70
	Na^+	0.81
	K^+	1.46
	Ca^{2+}	7.81
	Mg^{2+}	3.99
	Zn^{2+}	9.41
	Co^{2+}	7.35
	Cu^{2+}	1.89
	Pb^{2+}	2.68
	La^{3+}	-0.20

Table 5.4 Extraction results with codeine (**2**)

Opioid	Cation	% Extraction
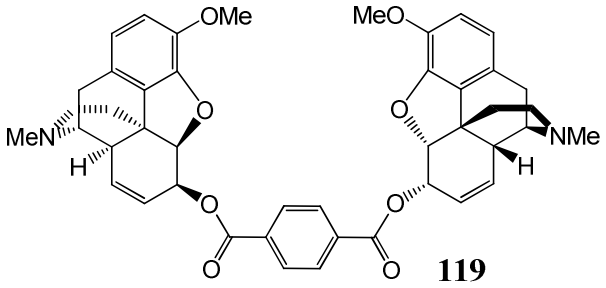 **119**	Li^+	0.11
	Na^+	-1.73
	K^+	1.03
	Ca^{2+}	12.61
	Mg^{2+}	17.20
	Zn^{2+}	7.54
	Co^{2+}	10.29
	Cu^{2+}	27.46
	Pb^{2+}	0.10
	La^{3+}	12.42

Table 5.5 Extraction results with **119**

Opioid	Cation	% Extraction
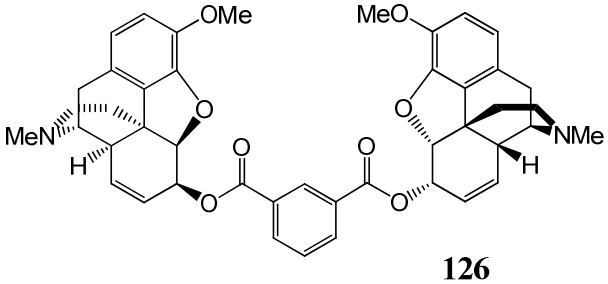 **126**	Li^+	-0.23
	Na^+	3.96
	K^+	2.36
	Ca^{2+}	8.49
	Mg^{2+}	10.17
	Zn^{2+}	9.61
	Co^{2+}	9.45
	Cu^{2+}	22.39
	Pb^{2+}	-0.07
	La^{3+}	16.21

Table 5.6 Extraction results with **126**

Opioid	Cation	% Extraction
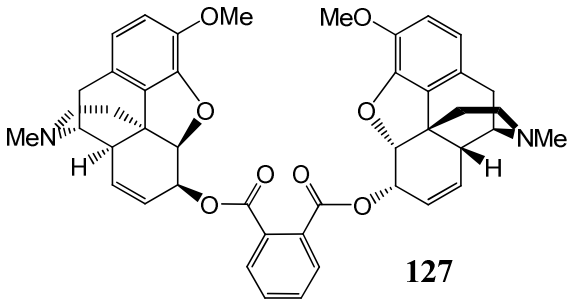 **127**	Li^+	-1.99
	Na^+	8.25
	K^+	5.17
	Ca^{2+}	8.21
	Mg^{2+}	10.95
	Zn^{2+}	10.14
	Co^{2+}	10.12
	Cu^{2+}	36.55
	Pb^{2+}	7.13
	La^{3+}	13.47

Table 5.7 Extraction results with **127**

Opioid	Cation	% Extraction
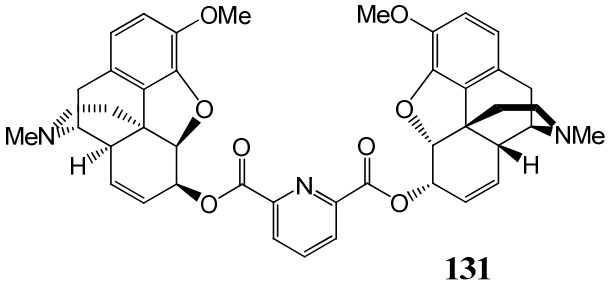 **131**	Li^+	-0.94
	Na^+	1.60
	K^+	1.03
	Ca^{2+}	6.11
	Mg^{2+}	7.72
	Zn^{2+}	7.98
	Co^{2+}	5.50
	Cu^{2+}	1.37
	Pb^{2+}	3.14
	La^{3+}	17.29

Table 5.8 Extraction results with **131**

Opioid	Cation	% Extraction
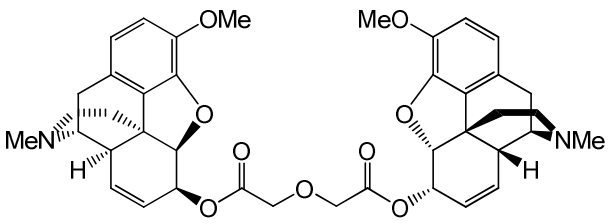 **128**	Li^+	-0.53
	Na^+	-1.17
	K^+	3.23
	Ca^{2+}	10.50
	Mg^{2+}	11.68
	Zn^{2+}	9.49
	Co^{2+}	12.19
	Cu^{2+}	2.83
	Pb^{2+}	4.04
	La^{3+}	20.33

Table 5.9 Extraction results with **128**

Opioid	Cation	% Extraction
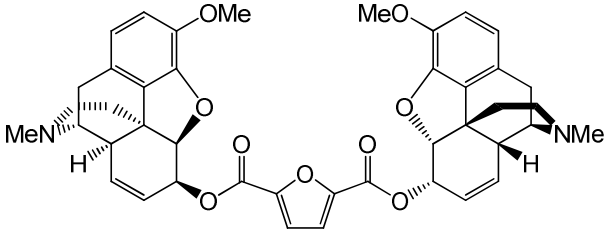 **130**	Li^+	-0.04
	Na^+	7.49
	K^+	2.29
	Ca^{2+}	10.08
	Mg^{2+}	10.11
	Zn^{2+}	7.48
	Co^{2+}	8.63
	Cu^{2+}	24.11
	Pb^{2+}	-1.34
	La^{3+}	15.04

Table 5.10 Extraction results with **130**

Opioid	Cation	% Extraction
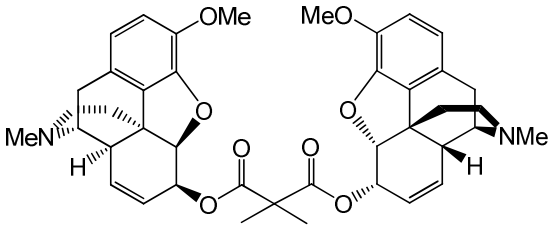 **129**	Li^+	1.05
	Na^+	0.81
	K^+	3.17
	Ca^{2+}	11.61
	Mg^{2+}	10.94
	Zn^{2+}	6.57
	Co^{2+}	9.51
	Cu^{2+}	21.45
	Pb^{2+}	4.59
	La^{3+}	18.73

Table 5.11 Extraction results with **129**

Opioid	Cation	% Extraction
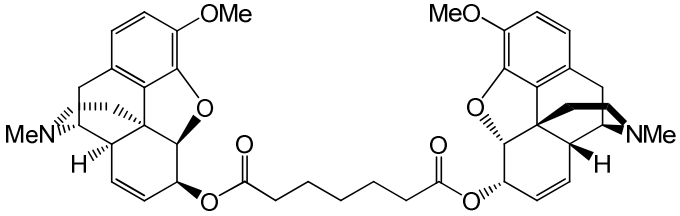 **132**	Li^+	0.30
	Na^+	4.00
	K^+	-1.55
	Ca^{2+}	12.10
	Mg^{2+}	8.06
	Zn^{2+}	2.93
	Co^{2+}	1.65
	Cu^{2+}	14.59
	Pb^{2+}	0.81
	La^{3+}	11.81

Table 5.12 Extraction results with **132**

Opioid	Cation	% Extraction
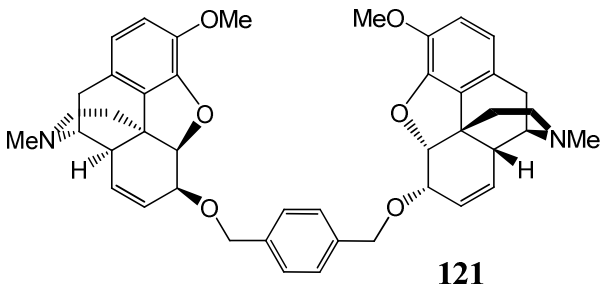 **121**	Li^+	-1.05
	Na^+	6.08
	K^+	-1.93
	Ca^{2+}	14.94
	Mg^{2+}	14.91
	Zn^{2+}	14.06
	Co^{2+}	15.72
	Cu^{2+}	20.85
	Pb^{2+}	13.21
	La^{3+}	20.64

Table 5.13 Extraction results with **121**

Opioid	Cation	% Extraction
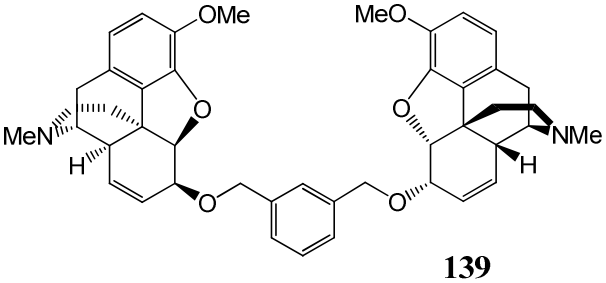 **139**	Li^+	2.82
	Na^+	-0.61
	K^+	11.46
	Ca^{2+}	12.30
	Mg^{2+}	17.19
	Zn^{2+}	9.59
	Co^{2+}	12.87
	Cu^{2+}	32.35
	Pb^{2+}	13.57
	La^{3+}	19.70

Table 5.14 Extraction results with **139**

Opioid	Cation	% Extraction
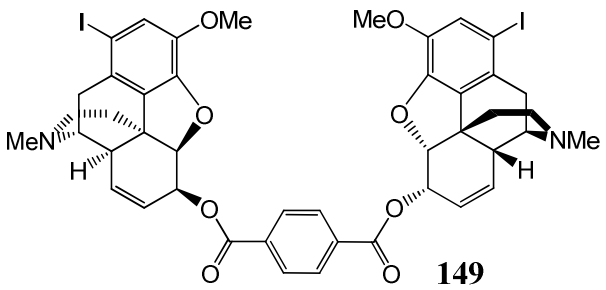 **149**	Na^{+}	0.64
	Cu^{2+}	34.49
	La^{3+}	16.35

Table 5.15 Extraction results with **149**

Opioid	Cation	% Extraction
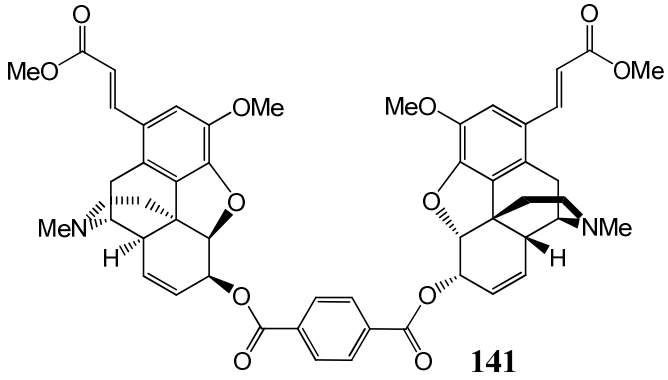 **141**	Na^{+}	3.11
	Cu^{2+}	28.66
	La^{3+}	17.95

Table 5.16 Extraction results with **141**

Opioid	Cation	% Extraction
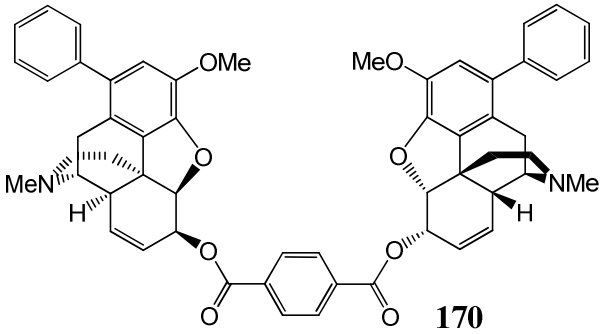 **170**	Na^+	1.19
	Cu^{2+}	32.86
	La^{3+}	16.50

Table 5.17 Extraction results with **170**

Opioid	Cation	% Extraction
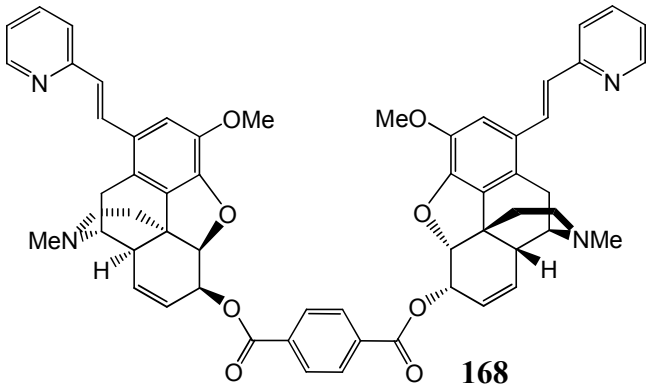 **168**	Na^+	-1.49
	Cu^{2+}	27.80
	La^{3+}	14.26

Table 5.18 Extraction results with **168**

From an examination of the blank samples investigated it is clear that there is no extraction of the metal picrate salts into the chloroform without the host opioid species.

However there is a small amount of variance from the expected zero percent binding, corresponding to ± 2%. This ± 2% deviation must be taken into account when analysing the extraction affinities of the host opioid species. Morphine (**1**) and codeine (**2**) were also analysed for their metal binding affinities. The data from these samples can then be directly correlated to the "linked" derivatives.

The extraction data showed that both morphine (**1**) and codeine (**2**), before any modification to form a "linked" derivative have binding to some of the metal picrates (Graph 5.1). The highest affinity for codeine was found for Zn^{2+} at 9.4 % while morphine showed the highest affinity for Cu^{2+} at 12.4%. Interestingly morphine showed a much higher affinity for Cu^{2+} than codeine which only resulted in an extraction of 1.9%. The only modification from morphine to codeine is the methoxy group at the 3 position which as a result must have some effect on the affinity of the opioid compounds to the metal picrate.

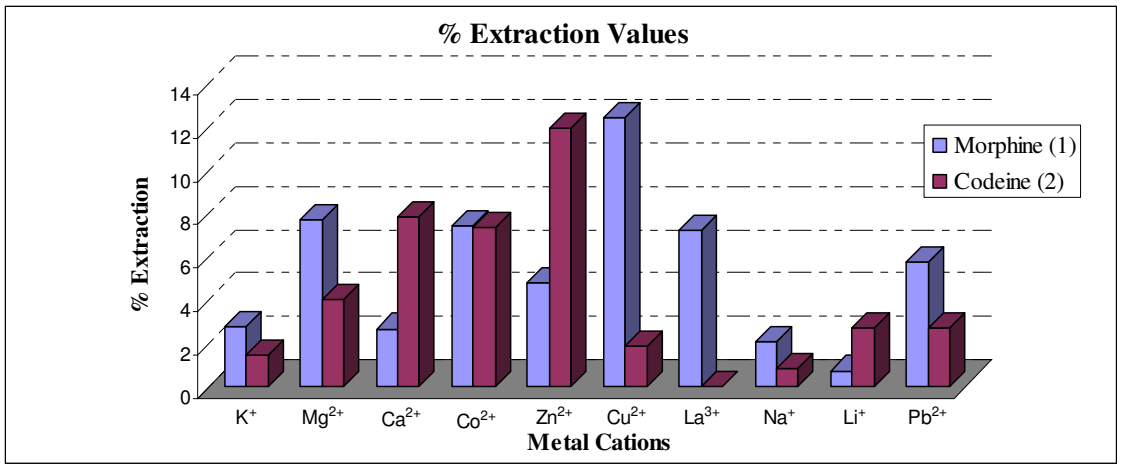

Graph 5.1 % Extraction values for morphine (**1**) and codeine (**2**)

Of more interest is the effect that modification at the six position of the opioids to form the "linked" derivatives has on the binding affinity to various metal picrates. As outlined previously the linked opioid compounds contain a cavity site which may form a host guest complex with various metal cationic species. An examination of the

extraction affinities for **119** compared to codeine shows that the linked compounds do show higher affinities for various metal cations especially Cu^{2+} and La^{3+} (Graph 5.2). For codeine the highest extraction was Zn^{2+} at 9.4% but **119** showed highest affinity for Cu^{2+} at 27.5%. Codeine only showed an extraction for Cu^{2+} at 1.9% which is over fourteen times lower than **119**. Therefore the presence of the cavity site in the "linked" opioid derivate appears to have an effect on the affinity of the opioid compounds to metal cations. Compound **119** also exhibited modest affinity to Mg^{2+}, Ca^{2+} and La^{3+} with extraction % values of 17.2%, 12.6% and 12.4% respectively.

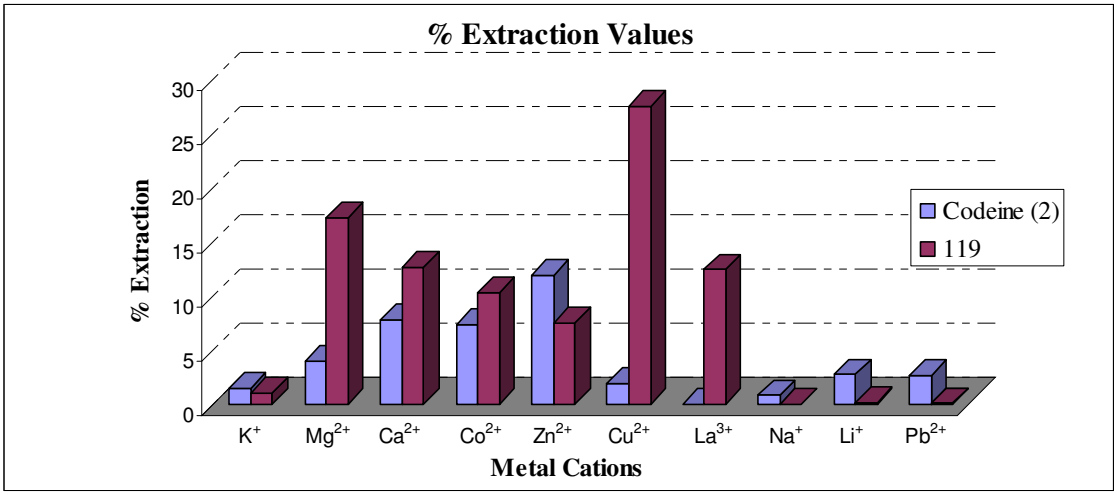

Graph 5.2 % Extraction values for codeine (**2**) and **119**

As the cavity site has been shown to have an effect on the affinity of various metal cations, especially Cu^{2+} and La^{3+}, to the opioid species it is important to investigate how modification at this site would affect the binding parameters. A comparison of the percentage extraction of the aromatic *para*-ester (**119**) derivative to the *meta* (**126**) and *ortho* (**127**) species shows that they are broadly similar (Graph 5.3). **119**, **126** and **127** display modest binding affinity to to Ca^{2+} Mg^{2+}, Co^{2+} and Zn^{2+} with generally higher binding to Cu^{2+} and La^{3+}. Each of the three compounds show the greatest affinity for Cu^{2+} with percentage extraction values of 27.5%, 22.4% and 36.6% for **119**, **126** and **127** respectively. They also exhibit modest binding to La^{3+} with percentage extraction values of 12.4%, 16.2% and 13.5% for **119**, **126** and **127** respectively. Analysis of the

other aromatic linked compounds tested, the furan (**130**) and pyridine (**131**) linked derivatives display similar results except (Graph 5.4) **131** which exhibits a percentage extraction of Cu^{2+} of 1.4%. The percentage extraction to La^{3+} for **130** and **131** was calculated at 15.0% and 17.3% % respectively.

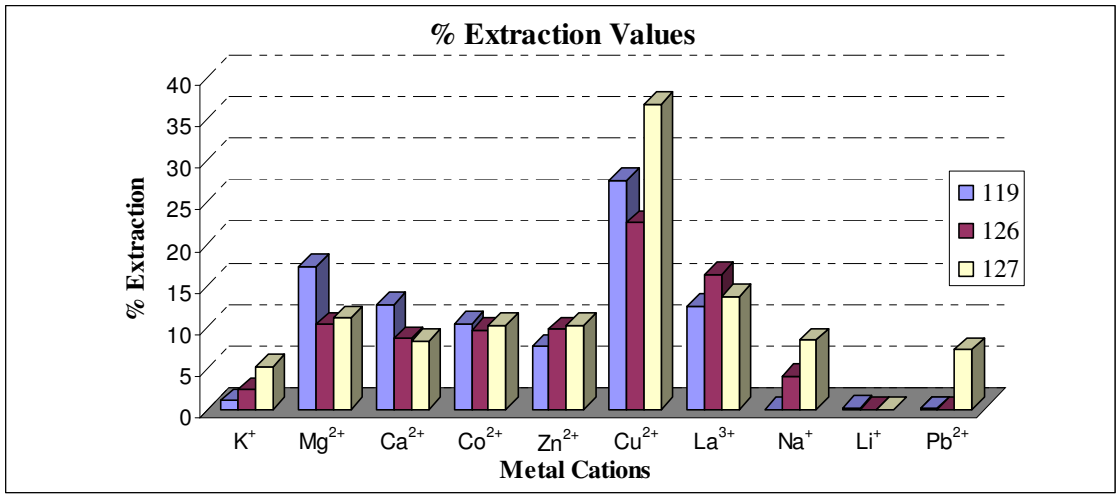

Graph 5.3 % Extraction values for **119**, **126** and **127**

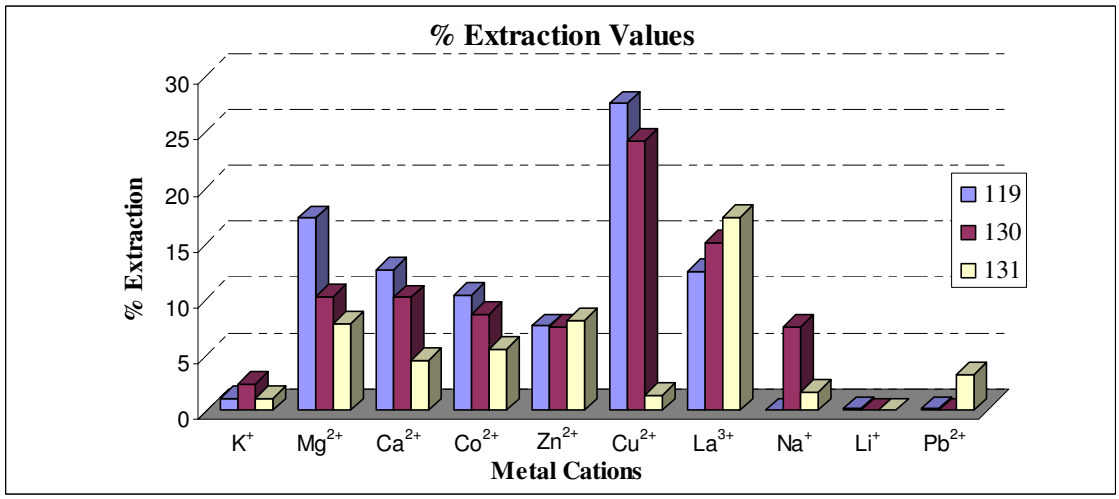

Graph 5.4 % Extraction values for **119**, **130** and **131**

Analysis of the non aromatic linked ester compounds **128**, **129** and **132** show generally similar results with modest binding affinities to Ca^{2+} Mg^{2+}, Co^{2+} and Zn^{2+} with typically higher binding to Cu^{2+} and La^{3+} (Graph 5.5). The percentage extraction values

for La^{3+} to **128**, **129** and **132** were calculated at 20.3%, 18.7% and 11.8% respectively. As in the case of the pyridine linked ester derivative (**131**), the percentage extraction value for Cu^{2+} of **128** was calculated at 2.8% which is significantly lower than the other derivatives. Due to the increased flexibility of the non aromatic linked compounds it could be envisioned that they are able to adopt a favourable conformation around the metal cation at least relative to the more structurally hindered aromatic linked derivatives. However, this increase flexibility could be offset by the loss of cation-π interactions which may be taking place between the metal cation and the aromatic-π electrons of the aromatic "bridging" moiety.

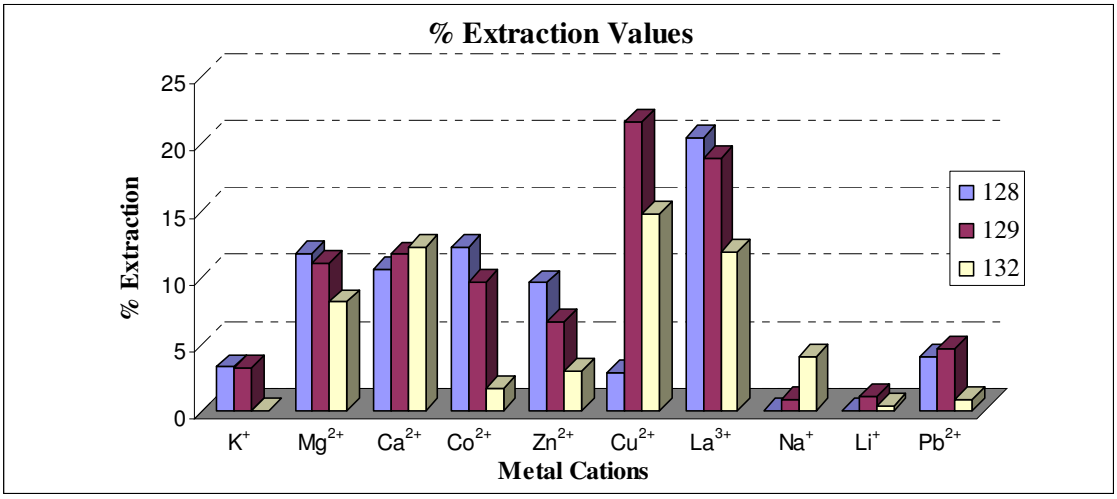

Graph 5.5 % Extraction values for **128**, **129** and **132**

Also examined were two ether linked compounds, the *para* (**121**) and *meta* (**139**) derivatives. It is interesting to note how the binding affinity is affected with the loss of two carbonyl groups on the "bridging" moiety. As with the ester linked compounds relatively modest extraction values were calculated for Ca^{2+} Mg^{2+}, Co^{2+} and Zn^{2+} with higher binding to Cu^{2+} and La^{3+} (Graph 5.6). The percentage extraction values for the ether linked compounds are comparable to the corresponding esters with binding to Cu^{2+} of 20.9% and 32.4% for **121** and **139** respectively. The percentage extraction for La^{3+} was calculated at 20.6% and 19.7% for **121** and **139** respectively.

Without the two donor atoms provided by the carbonyl groups in the ester linked derivatives it could be expected the there should be a significant decrease in the percentage extractions calculated. However, it must also be noted that the oxygen atom of the carbonyl group may interfere with binding to the cavity site through steric effects, thus removing them would vacate the cavity pocket. The ether linked derivatives exhibit significantly increased affinity for the Pb^{2+} cationic species. The percentage extractions for Pb^{2+} were calculated at 13.2% and 13.6% for **121** and **139** respectively. While this value is only a modest factor it should be noted that the highest percentage extraction value for the ester compounds was only 7.1% (**127**) with most values approximating to 0%.

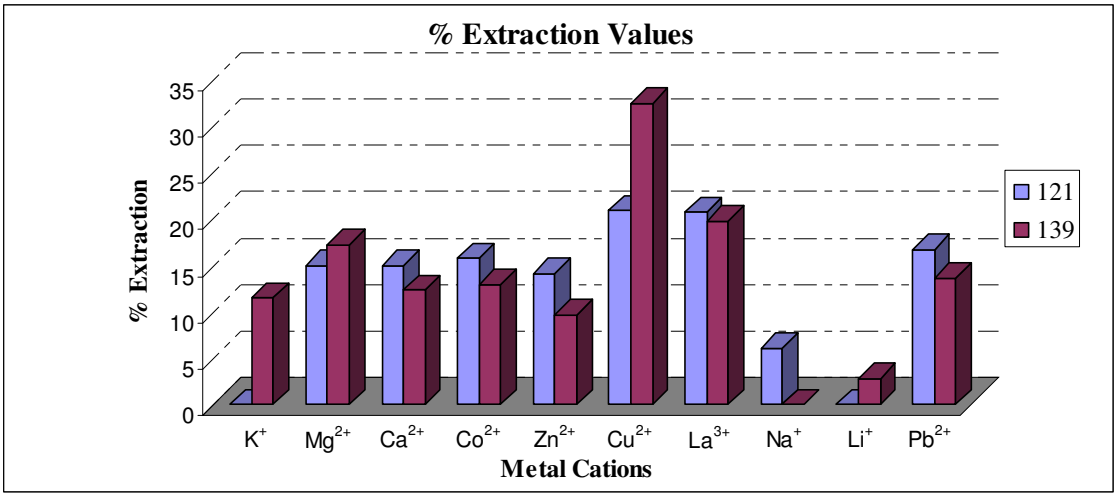

Graph 5.6 % Extraction values for **121** and **139**

The metal picrate binding data of the ether and ester linked codeine derivatives analysed as part of this project can be compared to some ether linked morphine derivatives that have been analysed previously within the research group (Tables 5.19-5.22).[70] In general the ether linked morphine compounds exhibited similar trends to the linked codeine compounds, with minimal binding to Li^{+} and Na^{+} and increased binding to Cu^{2+} and La^{3+} species. As with the ether linked codeine compounds the ether linked morphine derivatives showed increased binding to Pb^{2+} relative to the ester derivatives.

The most prominent comparison is for the macrocyclic opioid compounds **180** and **192**. Both of these compounds display much higher binding affinities to a variety of metal species especially Pb^{2+}, Cu^{2+} and La^{3+}. The percentage metal extraction values for compounds **180** and **192** towards Pb^{2+} were calculated at 78.0% and 48.2% respectively while Cu^{2+} exhibited 72.6% and 60.6% respectively. The percentage binding towards Zn^{2+} and Co^{2+} has also been shown to be much higher for **180** and **192** with values for Zn^{2+} of 41.8% and 23.5% respectively and for Co^{2+} 54.6% and 36.6% respectively. Due to the relatively high percentage binding of the morphine macrocycles they may be better targets for sensor applications. The relatively low binding of the linked codeine ester's on the other hand would lead them more towards use as prodrug candidates.

Opioid	Cation	% Extraction
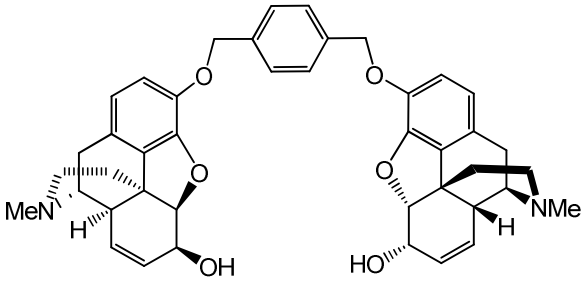 **136**	Li^{+}	0.0
	Na^{+}	0.2
	K^{+}	2.5
	Ca^{2+}	8.7
	Mg^{2+}	8.0
	Zn^{2+}	4.2
	Co^{2+}	8.1
	Cu^{2+}	8.9
	Pb^{2+}	24.7
	La^{3+}	17.6

Table 5.19 Extraction results with **136**[70]

Opioid	Cation	% Extraction
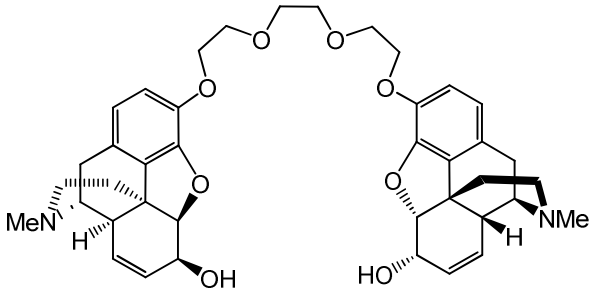 **137**	Li^+	1.9
	Na^+	4.2
	K^+	21.6
	Ca^{2+}	20.4
	Mg^{2+}	4.5
	Zn^{2+}	12.2
	Co^{2+}	28.6
	Cu^{2+}	45.7
	Pb^{2+}	40.4
	La^{3+}	16.5

Table 5.20 Extraction results with **137**[70]

Opioid	Cation	% Extraction
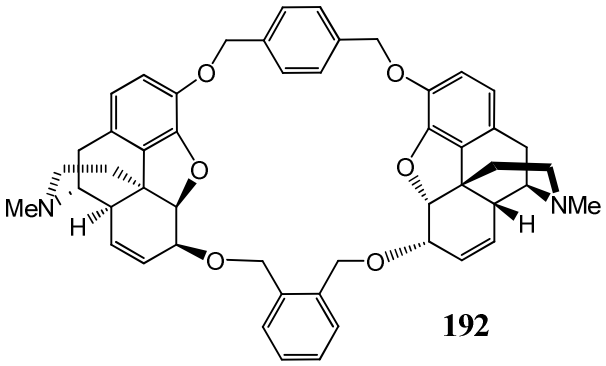 **192**	Li^+	0.4
	Na^+	0.4
	K^+	4.4
	Ca^{2+}	5.2
	Mg^{2+}	0.5
	Zn^{2+}	23.5
	Co^{2+}	36.6
	Cu^{2+}	60.6
	Pb^{2+}	48.2
	La^{3+}	39.8

Table 5.21 Extraction results with **192**[70]

Opioid	Cation	% Extraction
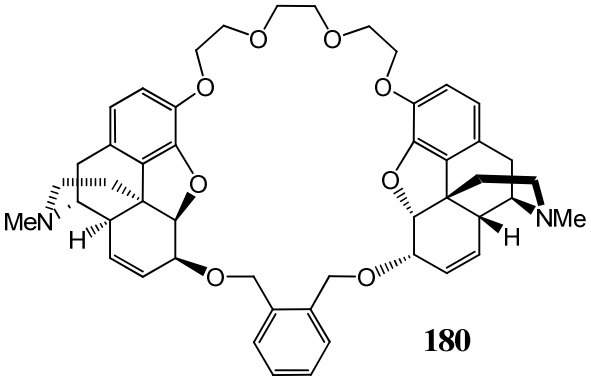 **180**	Li^+	3.1
	Na^+	11.9
	K^+	17.5
	Ca^{2+}	19.8
	Mg^{2+}	21.3
	Zn^{2+}	41.8
	Co^{2+}	54.6
	Cu^{2+}	72.6
	Pb^{2+}	78.0
	La^{3+}	43.2

Table 5.22 Extraction results with **180**[70]

On average the highest affinity of the opioid codeine derivatives tested was towards the Cu^{2+} cation. This was especially pronounced for the aromatic linked opioids with percentage extraction values for Cu^{2+} of 27.5%, 36.6% and 32.4% for **119**, **127** and **139** respectively. However, *vide supra* the morphine based ether linked opioids previously analysed within the research group[70] exhibit much higher binding affininty to Cu^{2+} (Graph 5.7)

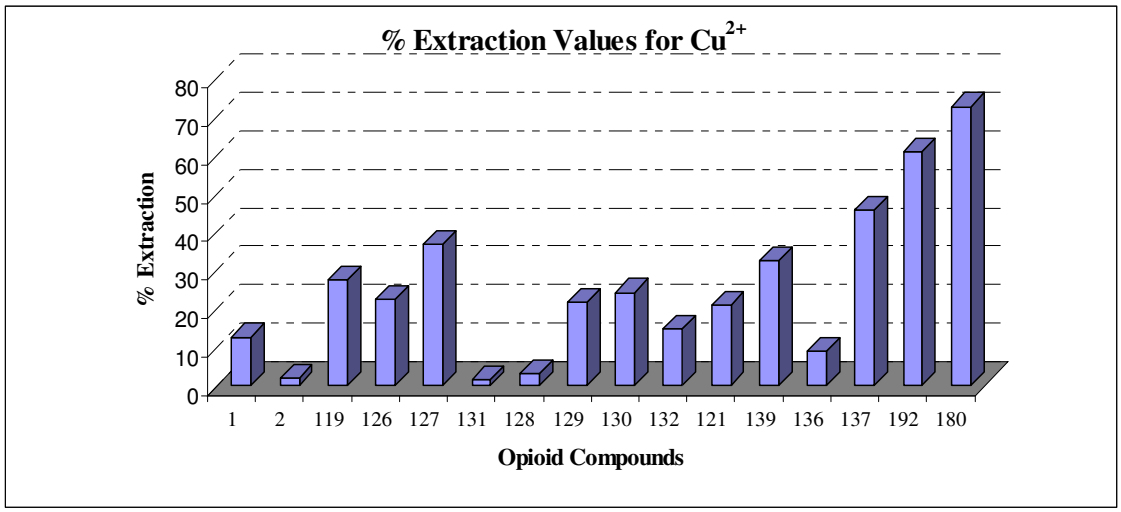

Graph 5.7 % Comparison of extraction values for opioid compounds to Cu^{2+}

Four A ring modified compounds were analysed (**141**, **149**, **168**, **170**) based on the *para*-ester linked derivative (**119**) against three metal picrates, Na^{+}, Cu^{2+} and La^{3+} (Graph 5.8). These opioid derivatives were chosen as a direct connection could then be made between A-ring modification (or lack thereof, **119**) and binding affinity. Previous analysis had shown that significant binding to **119** was calculated for Cu^{2+} and La^{3+} hence these metal picrates were chosen for analysis.

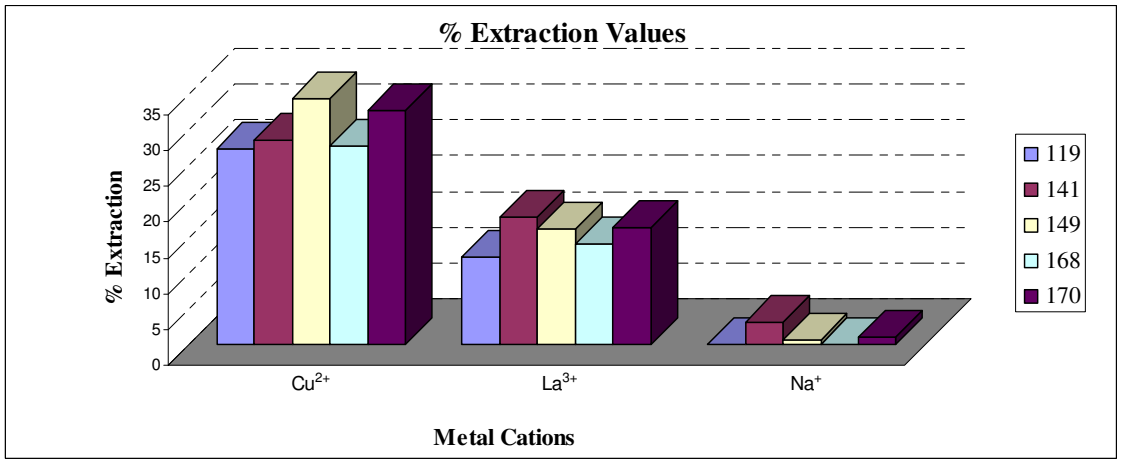

Graph 5.8 % Extraction values for **119**, **141**, **149**, **168** and **170** to Cu^{2+}, La^{3+} and Na^{+}

The Na^+ metal picrate had shown negligible binding to most opioid species and hence it was chosen as a minimal binding metal cation. The percentage extraction values calculated for the A-ring modified derivatives demonstrate that modification at the 1 position has little or no effect on the metal cationic binding to the cavity site. The calculated percentage extraction for Na^+ was minimal as expected while the values for Cu^{2+} were 28.7%, 34.5%, 27.8% and 32.9% for **141**, **149**, **168** and **170** respectively. The binding values for La^{3+} were, 18.0%, 16.4%, 14.3% and 16.5% for for **141**, **149**, **168** and **170** respectively.

5.3 Conclusion

The cation selectivity to ten metal picrates (Li^+, Na^+ K^+, Pb^{2+}, Ca^{2+}, Mg^{2+}, Zn^{2+}, Co^{2+}, Cu^{2+} and La^{3+}) of fourteen (**119**, **121**, **126-132**, **139**, **141**, **149**, **168**, **170**) novel opioid compounds were analysed by metal picrate extraction studies. Overall relatively low metal binding was exhibited by the codeine derivatives analysed. The general trend noted for the opioid compounds is that they showed minimal binding to Li^+, Na^+, K^+ and Pb^{2+}, modest binding to Ca^{2+}, Mg^{2+}, Zn^{2+} and Co^{2+} and highest binding to Cu^{2+} and La^{3+} cations. Investigation of the A-ring modified compounds (**141**, **149**, **168**, **170**) showed that alteration at the one position of the aromatic ring to a variety of functional groups had minimal effect on binding of the metal cation to the cavity site. The relatively low metal binding of the codeine derivatives to a variety of metal species implies that their use in sensor applications may be limited. However as these compounds have already displayed the potential as prodrug analgesic candidates low metal binding is desirable. High metal cationic binding to prodrug candidates can often lead to detrimental toxic side effects hence relatively low metal affinity for most of the "linked" codeine compounds is beneficial.

The most promising result in relation to their potential as sensors is the affinity for the Cu^{2+} cation. In general the highest binding for the codeine derivatives was noted for the Cu^{2+} metal cation. When the percentage extraction values of the linked compounds are

compared to morphine (**1**) and codeine (**2**) there is a general increase in binding to the Cu^{2+} metal cation. This would appear to suggest that formation of the cavity site in the linked opioid derivatives has an important role in the binding affinity of the Cu^{2+} cation. The highest percentage extraction value calculated for Cu^{2+} was for **127** at 36.6% while in contrast codeine (**2**) only exhibited an extraction value of 1.9%. Therefore the "linked" codeine compounds could have potential uses in sensor applications especially if further synthetic opioid derivatives are developed with increased Cu^{2+} binding.

It also has to be mentioned that for the purpose of this study the stoichiometric ratio of the complexes formed was assumed to be 1:1, complexing agent:metal picrate. However, it should be noted that other compounds may form containing 1:2 or 1:3 complexes. Future work on the potential use of opioid derivatives as sensors would focus on the ether linked morphine compounds (**136**, **137**, **180**, **192**) especially the macrocyclic derivatives (**180**, **192**). Previous work within the research group[70] has highlighted that the morphine macrocyclic compounds exhibit the highest affinity to a variety of metal cations especially especially Pb^{2+}, Cu^{2+} and La^{3+}. The binding affinity of the open chain linked codeine compounds analysed as part of this project were much lower in contrast and thus have more potential as potential analgesic pro-drug candidates (Chapter 4).

5.4 Experimental

5.4.1 General Method for Picrate Salt Synthesis

Picric acid (0.77 g, 65% suspension in water) was suspended in 20 mL of deionised water and warmed to 70 °C to make a saturated solution. The metal carbonate was added slowly to the hot solution with stirring until evolution of CO_2 gas ceased. The contents were allowed to cool slowly to RT and then further cooled to 0 °C until a yellow solid precipitated. The yellow solid picrate metal salt was isolated by gravity

filtration, washed with 5 mL of ice cold water and allowed to air dry. In consultation with the head of safety it was not permitted to completely dry the metal picrates and therefore accurate isolated yields products could not be recorded. The following ten metal picrate salts were synthesised according to the method outlined above, $LiC_6H_2N_3O_7$, $NaC_6H_2N_3O_7$, $KC_6H_2N_3O_7$,, $Ca(C_6H_2N_3O_7)_2$, $Mg(C_6H_2N_3O_7)_2$, $Zn(C_6H_2N_3O_7)_2$, $Co(C_6H_2N_3O_7)_2$, $Cu(C_6H_2N_3O_7)_2$, $Pb(C_6H_2N_3O_7)_2$, and $La(C_6H_2N_3O_7)_3$.

5.4.2 Picrate Extraction Studies

A sample of each picrate salt was dried *in vacuo*, weighed and made up to a 1000 mL, 7 x 10^{-5} M solution in deionised water. The solutions of the extracting opioid complexes were made up to a concentration of 1.75 x 10^{-5} M in chloroform. 6 mL of both the picrate solution and the opioid solution were transferred into a glass vial and shaken on an automatic shaker for 15 minutes at 600 oscillations per minute. Phases were allowed to separate at RT for 30 minutes before the UV absorption spectrum of the aqueous layer for each picrate salt sample was measured at 356 nm. All metal picrate extraction experiments were performed in triplicate with their mean UV absorbance values used for the calculations (standard deviation < 0.015).

For each metal picrate salt a calibration curve was generated by making up solutions in the range of 7 x 10^{-5} M to 4.6 x 10^{-5} M and recording their UV absorbance at 356 nm. The coefficient of determination (R^2 value) for each calibration curve was greater than 99%. The % extraction values for the metal cations were calculated using the following equation:

$$\% \text{ Extraction} = 100 \left\{ \frac{(\text{M Picrate})_0 - (\text{M Picrate})_e}{(\text{M Binding Agent})_{org}} \right\}$$

Where (M Picrate $)_0$ is the number of moles of metal picrate in the aqueous layer originally, (M Picrate $)_e$ is the number of moles of the picrate salt in the aqueous layer after extraction and (M Binding Agent $)_{org}$ is the number of moles of binding agent in the organic layer.

Chapter 6

Experimental

6.1 Experimental

All chemicals were purchased from Sigma-Aldrich, and used without further purification with the exception of codeine which was purchased from Johnson Matthey MacFarlan Smith, Edinburgh. THF was distilled under an atmosphere of nitrogen from sodium-benzophenone. DCM was distilled from CaH_2. All other solvents and reagents were used as supplied (Analytical or HPLC grade) without further purification. Thin layer chromatography (TLC) was performed on aluminium sheets coated with 60 F_{254} silica. TLC plates were visualised by UV (254 nm), iodine or aqueous potassium permanganate solution. Flash chromatography was performed on Davisil 60Å silica gel. Recrystallisations were performed *via* slow cooling technique for single solvent recrystallisations (acetone) and solvent diffusion for two solvent recrystallisations ($CHCl_3$:Hexane). Melting point determinations were carried out using a Stuart, SMP3 melting point apparatus. Infrared spectra were recorded on a Perkin Elmer FT-IR system, with ATR attachment. Optical rotations were measured on a Perkin Elmer 343 Polarimeter in HPLC grade chloroform. High Resolution Mass Spectrometry (HRMS) was carried out on a Waters Corp. Liquid Chromatography Time of flight mass spectrometer at the Microanalytical Laboratory, University College Dublin or a Waters Micromass LCT Premier mass spectrometer at ABCRF laboratory, University College Cork. NMR spectra were obtained on a Bruker AC 400 NMR spectrometer operating at 400 MHz for ^{1}H NMR and 100 MHz for ^{13}C NMR or where stated, on a Bruker AC 600 NMR spectrometer operating at 600 MHz for ^{1}H NMR and 150 MHz for ^{13}C NMR. The ^{1}H and ^{13}C NMR shifts (δ) are expressed in ppm relative to tetramethylsilane with coupling constants values (*J*) expressed in Hertz (Hz). Chemical-shift assignments for ^{1}H and ^{13}C spectra were assisted with COSY, DEPT, HMQC and HMBC experiments. The splitting patterns for NMR spectra are designated as follows:

s (singlet), d (doublet), t, (triplet), q, (quartet), p, (pentet), dd (doublet of doublets), ddd (doublet of doublet of doublets) and m (multiplet).

Compounds are named based on IUPAC nomenclature. Numbering for NMR assignment is based on molecular structures provided and as per NMR study, Chapter 2, 2.3.2.

6.2 Ester and Ether Linked Codeine Derivatives

Representative Procedure 1

A flask was charged with the appropriate opioid, anhydrous DCM and base and put under a nitrogen atmosphere. The acid dichloride was dissolved in anhydrous DCM and added dropwise to the reaction mixture. The reaction mixture was stired at RT under nitrogen for 18 h, washed with distilled water (3 x 10 mL), dried over anhydrous Na_2SO_4 and concentrated *in vacuo* before purification.

Representative Procedure 2

A flask was charged with the appropriate opioid, distilled THF, appropriate haloalkane, KI and KOH and heated under reflux for 18 h. After cooling THF was removed *via* rotary evaporation and contents re-dissolved in DCM. The resulting mixture was filtered through a thin layer of celite and the filtrate washed with distilled water (3 x 10 mL). The organic layer was dried over Na_2SO_4 and concentrated *in vacuo* before purification.

1,4-*bis*(1*S*,5*R*,13*R*,14*S*,17*R*)-10-methoxy-4-methyl-12-oxa-4-azapentacyclo[9.6.1.$0^{1,13}$.$0^{5,17}$.$0^{7,18}$]octadeca-7,9,11(18),15-tetraen-14-yl benzene-1,4-dicarboxylate, (119);

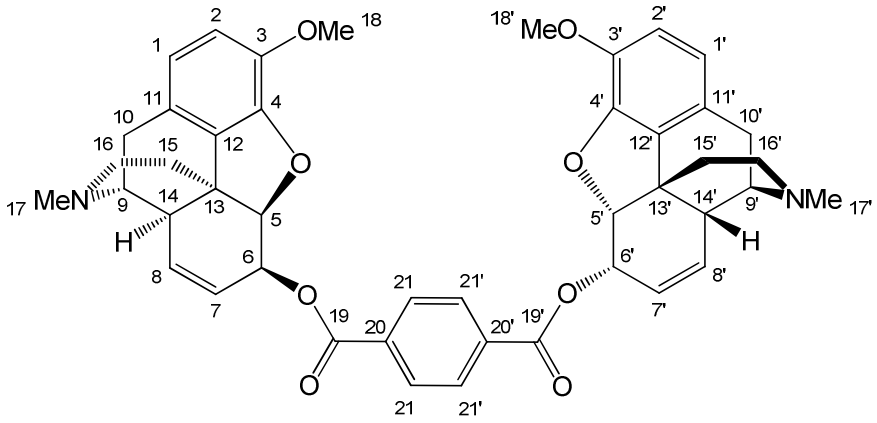

Following representative procedure 1, codeine (**2**) (0.291 g, 0.97 mmol), DMAP (0.131 g, 1.07 mmol, 1.1 Eq), DCM (10 mL) and terephthaloyl dichloride, (0.098 g, 0.48 mmol, 0.5 Eq) gave, after purification by column chromatography (SiO_2 10% MeOH/DCM, 1% NH_4OH), **119**, as a white solid in 73% yield (0.254 g, 0.35 mmol).

^{1}H NMR, ($CDCl_3$, 400 MHz) δ, 8.07 (s, 4H, (H21, H21')) 6.59 (d, *J* = 8.0 Hz, 2H, (H2, H2')), 6.50 (d, *J* = 8.0 Hz, 2H, (H1, H1')), 5.74-5.70 (m, 2H, (H7, H7')), 5.48-5.44 (m, 2H, (H8, H8')), 5.40-5.36 (m, 2H, (H6, H6')), 5.14 (d, *J* = 6.8 Hz, 2H, (H5, H5')), 3.64 (s, 6H, (H18, H18')) 3.33-3.31 (m, 2H, (H9, H9')), 2.99 (d, *J* = 18.4 Hz, 2H, (H10, H10')), 2.77-2.74 (m, 2H, (H14, H14')), 2.54 (dd, *J* = 12.0, 4.0 Hz, 2H, (H16, H16')), 2.39 (s, 6H, (H17, H17')), 2.35-2.23 (m, 4H, H16, H16', H10, H10')), 2.02 (ddd, *J* = 12.4, 12.4, 4.8 Hz, 2H, (H15, H15')), 1.83 (dd, *J* = 12.8, 2.0 Hz 2H, (H15, H15'))

^{13}C NMR, ($CDCl_3$, 100 MHz) δ, 165.34 (C19, C19'), 146.61 (C4, C4'), 142.21 (C3, C3'), 133.89 (C20, C20'), 130.71 (C12, C12'), 129.87 (C8, C8') 129.77 (C21, C21'), 128.28 (C7, C7'), 126.95 (C11, C11'), 119.34 (C1, C1') 114.30 (C2, C2'), 87.80 (C5, C5'), 68.84 (C6, C6'), 59.14 (C9, C9') 56.76 (C18, C18'), 46.76 (C16, C16'), 43.11

(C17, C17'), 42.60 (C13, C13'), 40.66 (C14, C14'), 35.36 (C15, C15'), 20.34 (C10, C10')

IR: υ (cm^{-1}), 2909, 1710 (C=O), 1503 (C-C, Ar), 1451, 1253, 1250, 1199, 1127, 1100, 1057, 1017

HRMS (EI, 70eV) Calculated for $[M+H]^+$, $C_{44}H_{45}N_2O_8^+$, requires: 729.3176, found 729.3176,

m.p. = 247-249 °C, $[\alpha]_D$ = -233° *c* = (0.10, $CHCl_3$, 589 nm, 20 °C)

1,3-*bis*(1*S*,5*R*,13*R*,14*S*,17*R*)-10-methoxy-4-methyl-12-oxa-4-azapentacyclo[9.6.1.$0^{1,13}$.$0^{5,17}$.$0^{7,18}$]octadeca-7,9,11(18),15-tetraen-14-yl benzene-1,3-dicarboxylate, (126);

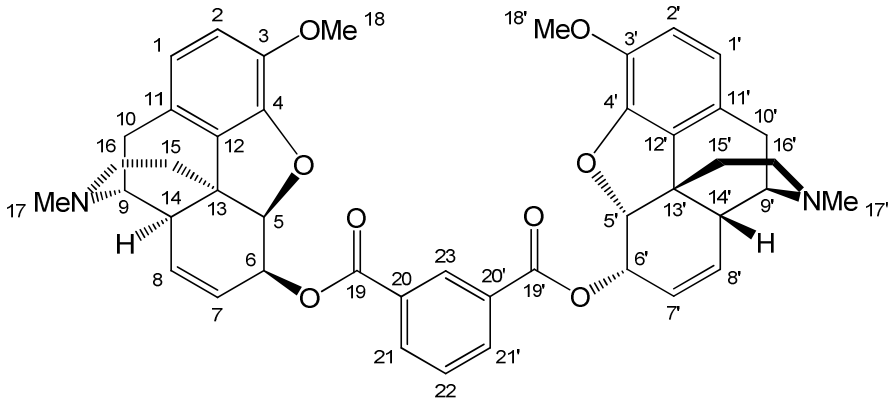

Following representative procedure 1, codeine (**2**) (0.451 g, 1.51 mmol), DMAP (0.203 g, 1.66 mmol, 1.1 Eq), DCM (15 mL) and isophthaloyl dichloride (0.153 g, 0.75 mmol, 0.5 Eq) gave, after purification by column chromatography (SiO_2 10% MeOH/DCM, 1% NH_4OH) followed by recrystallisation in acetone, **126** as white solid in 82% yield (0.449 g, 0.62 mmol).

^{1}H NMR, ($CDCl_3$, 400 MHz) δ, 8.65-8.64 (m, 1H, (H23)), 8.22 (dd, *J* = 7.6, 1.6 Hz, 2H, (H21, H21')), 7.46 (t, *J* = 7.6 Hz, 1H, (H22)), 6.57 (d, *J* = 8.4 Hz, 2H, (H2, H2')), 6.48 (d, *J* = 8.4 Hz, 2H, (H1, H1')), 5.74-5.71 (m, 2H, (H7, H7')), 5.46-5.43 (m, 2H,

(H8, H8')) 5.39-5.35 (m, 2H, (H6, H6')), 5.14 (dd, *J* = 6.8, 0.4 Hz, 2H, (H5, H5')), 3.61 (s, 6H, (H18, H18')) 3.33-3.30 (m, 2H, (H9, H9')), 2.98 (d, *J* = 18.4 Hz, 2H, (H10, H10')), 2.75-2.73 (m, 2H, (H14, H14')), 2.53 (dd, *J* = 12.0, 3.6 Hz 2H, (H16, H16')), 2.38 (s, 6H, (H17, H17')), 2.35-2.22 (m, 4H, (H16, H16', H10, H10')), 2.01 (ddd, *J* = 12.4, 12.4, 4.8 Hz, 2H, (H15, H15')), 1.82 (dd, *J* = 12.8, 1.6 Hz, 2H, (H15, H15'))

^{13}C NMR, ($CDCl_3$, 100 MHz) δ, 165.23 (C19, C19'), 146.73 (C4, C4'), 142.23 (C3, C3'), 134.34 (C21, C21'), 131.29 (C23), 130.71 (C12, C12'), 130.41 (C20, C20'), 129.74 (C8, C8'), 128.41 (C7, C7'), 128.40 (C22), 126.96 (C11, C11'), 119.29 (C1, C1'), 114.52 (C2, C2'), 87.84 (C5, C5'), 68.90 (C6, C6'), 59.16 (C9, C9'), 56.84 (C18, C18'), 46.78 (C16, C16'), 43.10 (C17, C17'), 42.64 (C13, C13'), 40.69 (C14, C14'), 35.36 (C15, C15'), 20.39 (C10, C10')

IR: υ (cm^{-1}), 2903, 1708 (C=O), 1505 (C-C, Ar), 1439, 1303, 1279, 1237, 1144, 1097, 1077, 1051, 1012

HRMS (EI, 70eV) Calculated for $[M+H]^+$, $C_{44}H_{45}N_2O_8^+$, requires: 729.3176, found 729.3165, m.p. = 256-258 °C, $[\alpha]_D$ = -189° *c* = (0.10, $CHCl_3$, 589 nm, 20 °C)

1,2-*bis*(1*S*,5*R*,13*R*,14*S*,17*R*)-10-methoxy-4-methyl-12-oxa-4-azapentacyclo[9.6.1.0^{1,13}.0^{5,17}.0^{7,18}]octadeca-7,9,11(18),15-tetraen-14-yl benzene-1,2-dicarboxylate, (127);

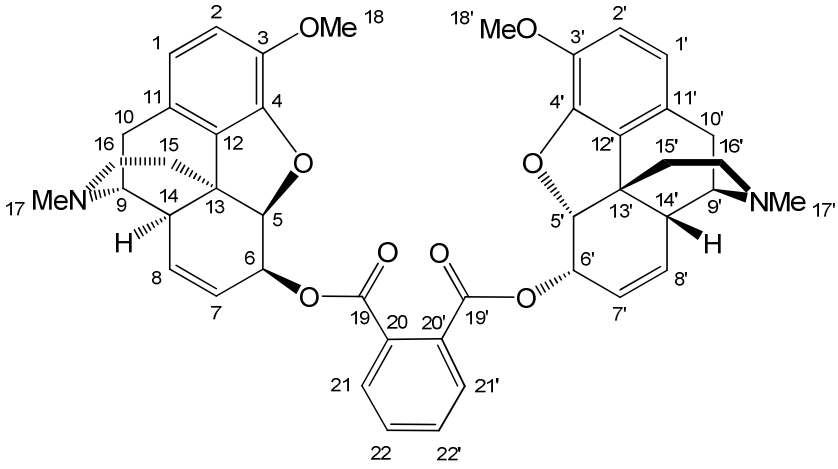

Following representative procedure 1, codeine (**2**) (0.352 g, 1.18 mmol), DMAP (0.159 g, 1.30 mmol, 1.1 Eq), DCM (10 mL) and phthaloyl dichloride (0.085 mL, 0.59 mmol, 0.5 Eq) gave, after purification by column chromatography (SiO_2 10% MeOH/DCM, 1% NH_4OH) followed by recrystallisation in $CHCl_3$:Hexane, **127** as a white solid in 72% yield (0.309 g, 0.42 mmol).

^{1}H NMR, ($CDCl_3$, 600 MHz) δ, 7.89-7.87 (m, 2H, (C21, C21')), 7.49-7.48 (m, 2H, (C22, C22')) 6.59 (d, *J* = 8.2 Hz, 2H, (H2, H2')), 6.48 (d, *J* = 8.2 Hz, 2H, (H1, H1')), 5.72-5.71 (m, 2H, (H7, H7')), 5.38-5.34 (m, 4H, (H8, H8', H6, H6')), 5.17 (d, *J* = 6.6 Hz, 2H, (H5, H5')), 3.70 (s, 6H, (H18, H18')), 3.39 (s, 2H, (H9, H9')), 2.99 (d, *J* = 18.6 Hz, 2H, (H10, H10')), 2.85 (s, 2H, (H14, H14')), 2.63 (d, *J* = 9.0 Hz, 2H, (H16, H16')), 2.45-2.38 (m, 8H, (H17, H17', H16, H16')), 2.33 (dd, *J* = 18.6, 6.0 Hz 2H, (H10, H10')), 2.11 (ddd, *J* = 12.6, 12.6, 3.6 Hz 2H, (H15, H15')), 1.84 (d, *J* = 10.8 Hz, 2H, (H15, H15'))

^{13}C NMR, ($CDCl_3$, 150 MHz) δ, 165.79 (C19, C19'), 145.80 (C4, C4'), 141.30 (C3, C3'), 130.90 (C20, C20'), 130.02 (C22, C22'), 129.45 (C12, C12'), 128.50 (C21, C21'), 127.86 (C8, C8'), 127.77 (C7, C7'), 125.27 (C11, C11'), 118.28 (C1, C1'), 113.40 (C2, C2'), 86.89 (C5, C5'), 68.19 (C6, C6'), 58.33 (C9, C9'), 55.76 (C18, C18'), 45.79 (C16, C16'), 41.81 (C17, C17'), 41.47 (C13, C13'), 39.06 (C14, C14'), 33.90 (C15, C15'), 19.60 (C10, C10')

IR: υ (cm^{-1}), 2906, 1725 (C=O), 1498 (C-C, Ar), 1442, 1288, 1269, 1255, 1242, 1205 1137, 1122, 1034, 1015

HRMS (EI, 70eV) Calculated for $[M+H]^+$, $C_{44}H_{45}N_2O_8^+$, requires: 729.3176, found 729.3199, m.p. = 231-233 °C, $[\alpha]_D$ = -185° *c* = (0.10, $CHCl_3$, 589 nm, 20 °C)

(1*S*,5*R*,13*R*,14*S*,17*R*)-10-methoxy-4-methyl-12-oxa-4-azapentacyclo[9.6.1.0^{1,13}.0^{5,17}.0^{7,18}]octadeca-7,9,11(18),15-tetraen-14-yl 2-(2-{[(1*S*,5*R*,13*R*,14*S*,17*R*)-10-methoxy-4-methyl-12-oxa-4-azapentacyclo[9.6.1.0^{1,13}.0^{5,17}.0^{7,18}]octadeca-7,9,11(18),15-tetraen-14-yl]oxy}-2-oxoethoxy)acetate, (128);

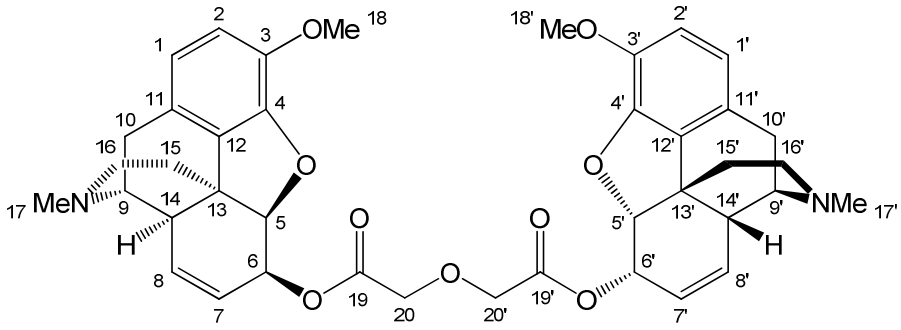

Following representative procedure 1, codeine (**2**) (0.331 g, 1.11 mmol), DMAP (0.149 g, 1.22 mmol, 1.1 Eq), DCM (10 mL) and diglycolyl dichloride (0.067 mL, 0.56 mmol, 0.5 Eq) gave, after purification by column chromatography (SiO_2 10% MeOH/DCM, 1% NH_4OH) followed by recrystallisation in $CHCl_3$:Hexane, **128** as a white solid in 40% yield (0.155 g, 0.22 mmol).

^{1}H NMR, ($CDCl_3$, 400 MHz) δ 6.57 (d, *J* = 8.4 Hz, 2H, (H2, H2')), 6.47 (d, *J* = 8.4 Hz, 2H, (H1, H1')), 5.58-5.55 (m, 2H, (H7, H7')), 5.40-5.36 (m, 2H, (H8, H8')) 5.22-5.19 (m, 2H, (H6, H6')), 5.02 (d, *J* = 6.8 Hz, 2H, (H5, H5')), 4.35 (d, *J* = 6.8 Hz, 4H, (H20, H20')), 3.73 (s, 6H, (H18, H18')) 3.29-3.27 (m, 2H, (H9, H9')), 2.96 (d, *J* = 18.4 Hz, 2H, (H10, H10')), 2.68-2.67 (m, 2H, (H14, H14')), 2.51 (dd, *J* = 12.0, 3.6 Hz 2H, (H16, H16')), 2.36 (s, 6H, (H17, H17')), 2.29 (ddd, *J* = 12.4, 12.4, 3.6 Hz, 2H, (H16, H16')), 2.21 (dd, *J* = 18.4, 6.0 Hz, 2H, (H10, H10')) 1.97 (ddd, *J* = 12.4, 12.4, 4.8 Hz, 2H, (H15, H15')), 1.78 (dd, *J* = 12.4, 1.2 Hz, 2H, (H15, H15'))

^{13}C NMR, ($CDCl_3$, 100 MHz) δ, 169.64 (C19 C19'), 146.53 (C4, C4'), 142.22 (C3, C3'), 130.50 (C12, C12'), 129.87 (C8, C8'), 127.97 (C7, C7'), 126.90 (C11, C11'), 119.27 (C1, C1'), 113.62 (C2, C2'), 87.60 (C5, C5'), 68.54 (C6, C6'), 68.06 (C20,

C20'), 59.08 (C9, C9'), 56.51 (C18, C18'), 46.69 (C16, C16'), 43.07 (C17, C17'), 42.59 (C13, C13'), 40.62 (C14, C14'), 35.35 (C15, C15'), 20.29 (C10, C10')

IR: υ (cm^{-1}), 2911, 1750 (C=O), 1500 (C-C, Ar), 1441, 1282, 1253, 1213, 1150, 1102, 1050, 1021

HRMS (EI, 70eV) Calculated for $[M+H]^+$, $C_{40}H_{45}N_2O_9^+$, requires: 697.3125, found 697.3128, m.p. = 183-185 °C, $[\alpha]_D$ = -175° *c* = (0.10, $CHCl_3$, 589 nm, 20 °C)

(1*S*,5*R*,13*R*,14*S*,17*R*)-10-methoxy-4-methyl-12-oxa-4-azapentacyclo[9.6.1.01,13.05,17.07,18]octadeca-7,9,11(18),15-tetraen-14-yl benzoate, (125);

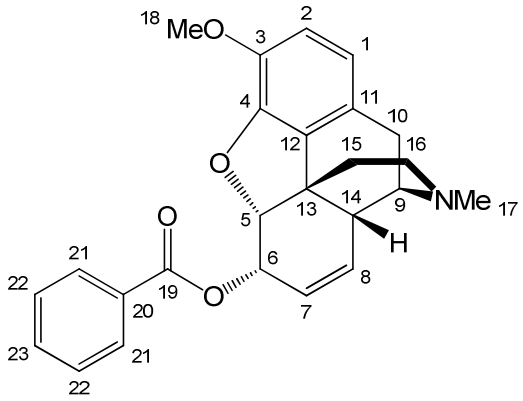

Following representative procedure 1, codeine (**2**) (0.305 g, 1.02 mmol), DMAP (0.137 g, 1.12 mmol, 1.1 Eq), DCM (10 mL) and benzoyl chloride (0.118 mL, 1.02 mmol, 1 Eq) gave, after purification by column chromatography (SiO_2 10% MeOH/DCM, 1% NH_4OH), **125** as a white solid in 92% yield (0.379 g, 0.94 mmol).

^1H and ^{13}C NMR data in agreement with literature[37]

^1H NMR, ($CDCl_3$, 400 MHz) δ 8.01 (dd, *J* = 7.6, 0.8 Hz 2H, (H21)), 7.50-7.46 (m, 1H, (H23)), 7.35 (t, *J* = 7.6 Hz, 2H, (H22)) 6.58 (d, *J* = 8.0 Hz, 1H, (H2), 6.47 (d, *J* = 8.0 Hz, 1H, (H1)), 5.71-5.68 (m, 1H, (H7)), 5.44-5.40 (m, 1H, (H8)) 5.40-5.34 (m, 1H, (H6)), 5.12 (dd, *J* = 6.8, 0.8 Hz, 1H, (H5)), 3.64 (s, 3H, (H18)) 3.32-3.30 (m, 1H, (H9)),

2.98 (d, *J* = 18.8 Hz, 1H, (H10)), 2.74-2.73 (m, 1H, (H14)), 2.52 (dd, *J* = 8.0 Hz 4.0 Hz 1H, (H16)), 2.37 (s, 3H, (H17)), 2.36-2.22 (m, 2H, (H16, H10)), 2.01 (ddd, *J* = 12.4, 12.4, 5.2 Hz, 1H, (H15)), 1.82 (dd, *J* = 12.8, 2.0 Hz, 1H, (H15))

^{13}C NMR, ($CDCl_3$, 100 MHz) δ, 166.08 (C19), 146.82 (C4), 142.15 (C3), 133.05 (C23), 130.88 (C20), 130.01 (C12), 129.93 (C21), 129.70 (C8), 128.56 (C7), 128.27 (C22), 127.09 (C11), 119.23 (C1), 114.59 (C2), 88.16 (C5), 68.62 (C6), 59.11 (C9), 56.90 (C18), 46.71 (C16), 43.12 (C17), 42.74 (C13), 40.75 (C14), 35.43 (C15), 20.38 (C10)

***Bis*(1*S*,5*R*,13*R*,14*S*,17*R*)-10-methoxy-4-methyl-12-oxa-4-azapentacyclo[9.6.1.0^{1,13}.0^{5,17}.0^{7,18}]octadeca-7,9,11(18),15-tetraen-14-yl 2,2-dimethylpropanedioate, (129);**

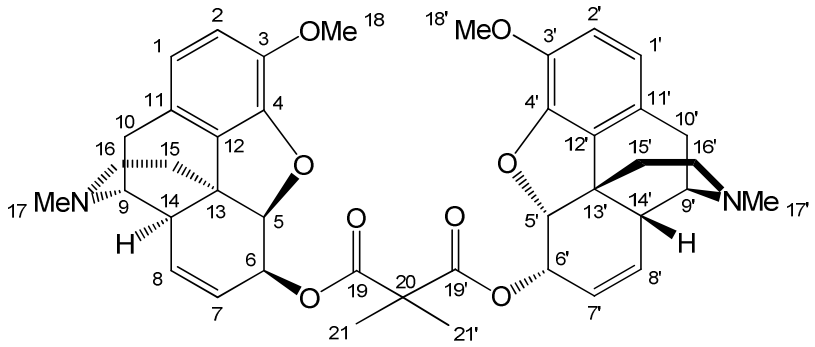

Following representative procedure 1, codeine (**2**) (0.329 g, 1.10 mmol), DMAP (0.148 g, 1.21 mmol, 1.1 Eq), DCM (10 mL) and dimethylmalonyl dichloride (0.073 mL, 0.55 mmol, 0.5 Eq) gave, after purification by column chromatography (SiO_2 10% MeOH/DCM, 1% NH_4OH) followed by recrystallisation in $CHCl_3$:Hexane, **129** as a white solid in 39% yield (0.149 g, 0.21 mmol).

^{1}H NMR, ($CDCl_3$, 400 MHz) δ, 6.56 (d, *J* = 8.4 Hz, 2H, (H2, H2')), 6.44 (*J* = 8.4 Hz, 2H, (H1, H1')), 5.47-5.43 (m, 2H, (H7, H7')), 5.32-5.28 (m, 2H, (H8, H8')), 5.09-5.06 (m, 2H, (H6, H6')), 5.03 (dd, *J* = 6.8, 0.8 Hz, 2H, (H5, H5')) 3.72 (s, 6H, (H18, H18'))

3.28-3.26 (m, 2H, (H9, H9')), 2.95 (d, *J* = 18.8 Hz, 2H, (H10, H10')), 2.67-2.65 (s, 2H, (H14, H14')), 2.51 (dd, *J* = 12.4, 4.0 Hz, 2H, (H16, H16')), 2.37 (s, 6H, (H17, H17')), 2.29 (ddd, *J* = 12.4, 12.4, 3.6 Hz, 2H, (H16, H16')), 2.20 (dd, *J* = 18.4, 6.0 Hz 2H, (H10, H10')) 1.97 (ddd, *J* = 12.4, 12.4, 4.8 Hz, 2H, (H15, H15')), 1.77 (dd, *J* = 12.8, 1.6 Hz 2H, (H15, H15')), 1.53 (s, 6H, (H21, H21'))

^{13}C NMR, ($CDCl_3$, 100 MHz) δ, 172.18 (C19, C19'), 146.83 (C4, C4'), 142.27 (C3, C3'), 130.60 (C12, C12'), 129.37 (C8, C8'), 128.39 (C7, C7'), 126.80 (C11, C11'), 119.04 (C1, C1'), 114.08 (C2, C2'), 87.80 (C5, C5'), 68.88 (C6, C6'), 59.10 (C9, C9'), 56.70 (C18, C18'), 50.02 (C20), 46.66 (C16, C16'), 43.07 (C17, C17'), 42.66 (C13, C13'), 40.56 (C14, C14'), 35.39 (C15, C15'), 22.70 (C21, C21'), 20.30 (C10, C10')

IR: υ (cm^{-1}), 2932, 1731 (C=O), 1497 (C-C, Ar), 1440, 1283, 1252, 1206, 1169, 1149, 1129, 1100, 1052, 1035, 1018

HRMS (EI, 70eV) Calculated for $[M+H]^+$, $C_{41}H_{47}N_2O_8^+$, requires: 695.3332, found 695.3351, m.p. = 203-205 °C, $[\alpha]_D$ = -131° *c* = (0.10, $CHCl_3$, 589 nm, 20 °C)

2,5-*bis*(1*S*,5*R*,13*R*,14*S*,17*R*)-10-methoxy-4-methyl-12-oxa-4-azapentacyclo[9.6.1.0^{1,13}.0^{5,17}.0^{7,18}]octadeca-7,9,11(18),15-tetraen-14-yl furan-2,5-dicarboxylate, (130);

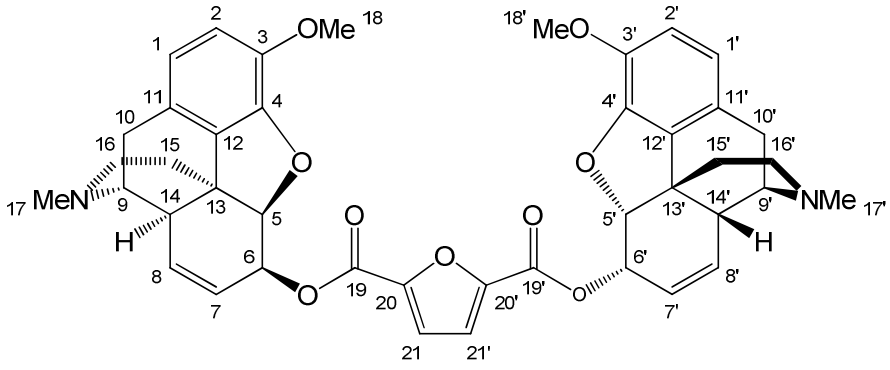

Following representative procedure 1, codeine (**2**) (0.396 g, 1.32 mmol), DMAP (0.178 g, 1.46 mmol, 1.1 Eq), DCM (10 mL) and 2,5 furan-dichloride (0.127 g, 0.66 mmol, 0.5 Eq) gave, after purification by column chromatography (SiO_2 10% MeOH/DCM, 1%

NH_4OH) followed by recrystallisation in $CHCl_3$:Hexane, **130** as a white solid in 51% yield (0.243 g, 0.34 mmol).

^{1}H NMR, ($CDCl_3$, 600 MHz) δ 7.19 (s, 2H, (H21, H21')) 6.60 (d, *J* = 7.8 Hz, 2H, (H2, H2')), 6.50 (d, *J* = 7.8 Hz, 2H, (H1, H1')), 5.72-5.70 (m, 2H, (H7, H7')), 5.45-5.42 (m, 2H, (H8, H8')) 5.36-5.34 (m, 2H, (H6, H6')), 5.12 (d, *J* = 7.2 Hz, 2H, (H5, H5')), 3.69 (s, 6H, (H18, H18')) 3.40 (s, 2H, (H9, H9')), 2.99 (d, *J* = 18.6 Hz, 2H, (H10, H10')), 2.84 (s, 2H, (H14, H14')), 2.63-2.62 (m, 2H, (H16, H16')), 2.44 (s, 6H, (H17, H17')), 2.41-2.31 (m, 4H, (H16, H16', H10, H10')), 2.11-2.07 (m, 2H, (H15, H15')), 1.84 (d, *J* = 13.2 Hz, 2H, (H15, H15'))

^{13}C NMR, ($CDCl_3$, 150 MHz) δ, 157.32 (C19, C19'), 146.74 (C20, C20'), 146.67 (C4, C4'), 142.41 (C3, C3') 130.42 (C12, C12'), 129.43 (C8, C8'), 128.31 (C7, C7'), 126.42 (C11, C11'), 119.46 (C1, C1'), 119.01 (C21, C21'), 114.85 (C2, C2'), 87.49 (C5, C5'), 68.99 (C6, C6'), 59.32 (C9, C9'), 56.98 (C18, C18'), 46.81 (C16, C16'), 42.92 (C17, C17'), 42.42 (C13, C13'), 40.19 (C14, C14'), 35.14 (C15, C15'), 20.81 (C10, C10')

IR: υ (cm^{-1}), 2933, 1719, 1706 (C=O), 1505, 1496 (C-C, Ar), 1439, 1298, 1276, 1253, 1167, 1157, 1139, 1047, 1008

HRMS (EI, 70eV) Calculated for $[M+H]^+$, $C_{42}H_{43}N_2O_9^+$, requires: 719.2969, found 719.2967, m.p. = 251-253 °C, $[\alpha]_D$ = -175° *c* = (0.10, $CHCl_3$, 589 nm, 20 °C)

2,6-*bis*(1*S*,5*R*,13*R*,14*S*,17*R*)-10-methoxy-4-methyl-12-oxa-4-azapentacyclo[9.6.1.$0^{1,13}$.$0^{5,17}$.$0^{7,18}$]octadeca-7,9,11(18),15-tetraen-14-yl pyridine-2,6-dicarboxylate, (131);

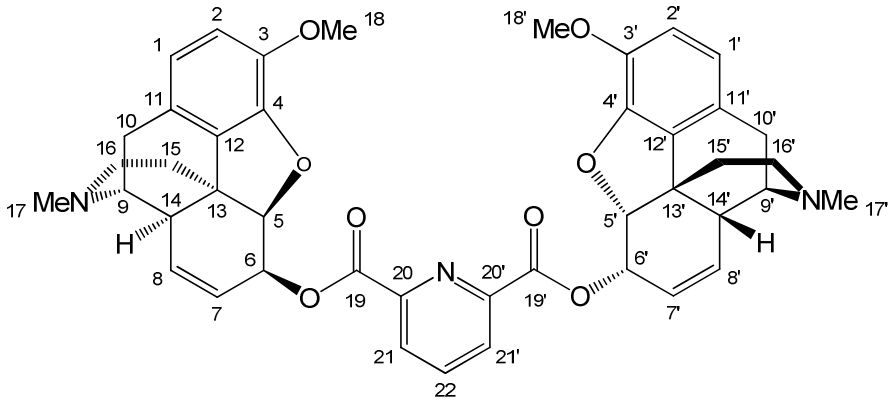

Following representative procedure 1, codeine (**2**) (0.398 g, 1.33 mmol), DMAP (0.178 g, 1.46 mmol, 1.1 Eq), DCM (8 mL) and 2,6-pyridinedicarbonyl dichloride (0.136 g, 0.67 mmol, 0.5 Eq) gave, after purification by column chromatography (SiO_2 10% MeOH/DCM, 1% NH_4OH) followed by recrystallisation in $CHCl_3$:Hexane, **131** as a white solid in 49% yield (0.238 g, 0.33 mmol).

^{1}H NMR, ($CDCl_3$, 400 MHz) δ, 8.24 (d, *J* = 7.6 Hz, 2H, (H21, H21')), 7.91 (t, *J* = 7.6 Hz, 1H, (H22)), 6.58 (d, *J* = 8.0 Hz, 2H, (H2, H2')), 6.48 (d, *J* = 8.0 Hz, 2H, (H1, H1')), 5.77-5.74 (m, 2H, (H7, H7')), 5.45-5.42 (m, 4H, (H8, H8', H6, H6')), 5.19 (d, *J* = 6.4 Hz, 2H, (H5, H5')), 3.65 (s, 6H, (H18, H18')) 3.35-3.33 (m, 2H, (H9, H9')), 2.99 (d, *J* = 18.8 Hz, 2H, (H10, H10')), 2.78-2.76 (m, 2H, (H14, H14')), 2.56 (dd, *J* = 12.0, 4.0 Hz, 2H, (H16, H16')), 2.40 (s, 6H, (H17, H17')), 2.34 (ddd, *J* = 12.0, 12.0, 3.2 Hz, 2H, (H16, H16')), 2.27 (dd, *J* = 18.8, 6.4 Hz 2H, (H10, H10')), 2.05 (ddd, *J* = 12.4, 12.4, 4.8 Hz, 2H, (H15, H15')), 1.83 (dd, *J* = 12.4, 1.6 Hz, 2H, (H15, H15'))

^{13}C NMR, ($CDCl_3$, 100 MHz) δ, 163.62 (C19, C19'), 148.57 (C20, C20'), 146.73 (C4, C4'), 142.20 (C3, C3'), 137.92 (C22, C22'), 130.70 (C12, C12'), 129.68 (C8, C8'), 128.23 (C7, C7'), 128.14 (C21, C21'), 126.96 (C11, C11'), 119.35 (C1, C1'), 114.58

(C2, C2'), 87.73 (C5, C5'), 69.56 (C6, C6'), 59.14 (C9, C9'), 56.94 (C18, C18'), 46.71 (C16, C16'), 43.02 (C17, C17'), 42.65 (C13, C13'), 40.50 (C14, C14'), 35.26 (C15, C15'), 20.42 (C10, C10)

IR: υ (cm^{-1}), 2910, 1748 (C=O), 1501 (C-C, Ar), 1445, 1281, 1231, 1172, 1147, 1048, 1020

HRMS (EI, 70eV) Calculated for $[M+H]^+$, $C_{43}H_{44}N_3O_8^+$, requires: 730.3128, found 730.3137, m.p. = 232-234 °C, $[\alpha]_D$ = -229° *c* = (0.10, $CHCl_3$, 589 nm, 20 °C)

***Bis*(1*S*,5*R*,13*R*,14*S*,17*R*)-10-methoxy-4-methyl-12-oxa-4-azapentacyclo[9.6.1.$0^{1,13}$.$0^{5,17}$.$0^{7,18}$]octadeca-7,9,11(18),15-tetraen-14-yl heptanedioate, (132);**

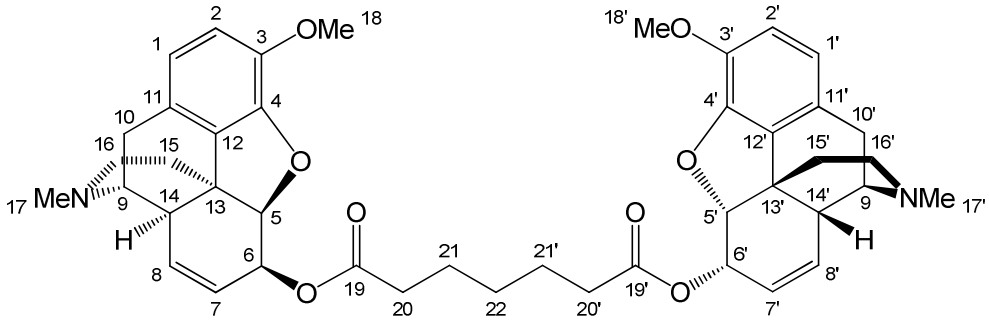

Following representative procedure 1, codeine (**2**) (0.301 g, 1.01 mmol), DMAP (0.136 g, 1.11 mmol, 1.1 Eq), DCM (8 mL) and heptanedioyl dichloride (0.083 mL, 0.51 mmol, 0.5 Eq) gave, after purification by column chromatography (SiO_2 10% MeOH/DCM, 1% NH_4OH) followed by recrystallisation in $CHCl_3$:Hexane, **132** as an off white solid in 63% yield (0.232 g, 0.32 mmol).

^{1}H NMR, ($CDCl_3$, 400 MHz) δ 6.58 (d, *J* = 8.4 Hz, 2H, (H2, H2')), 6.47 (d, *J* = 8.4 Hz, 2H, (H1, H1')), 5.57-5.40 (m, 2H, (H7, H7')), 5.38-5.34 (m, 2H, (H8, H8')) 5.12-5.09 (m, 2H, (H6, H6')), 5.01 (dd, *J* = 6.8, 0.8 Hz, 2H, (H5, H5')), 3.76 (s, 6H, (H18, H18')), 3.31-3.28 (m, 2H, (H9, H9')), 2.97 (d, *J* = 18.4 Hz, 2H, (H10, H10')), 2.69-2.67 (m, 2H, (H14, H14')), 2.52 (dd, *J* = 12.0, 4.0 Hz, 2H, (H16, H16')), 2.42-2.20 (m,

8H, (H16, H16', H10, H10', H20, H20')), 2.38 (s, 6H, (H17, H17')), 1.98 (ddd, *J* = 12.4, 12.4, 4.8 Hz, 2H, (H15, H15')), 1.79 (dd, *J* = 12.4, 1.6 Hz, 2H, (H15, H15')), 1.70-1.62 (m, 4H, (H21, H21')), 1.42-1.36 (m, 2H, (H22))

^{13}C NMR, ($CDCl_3$, 100 MHz) δ, 173.15 (C19 C19'), 146.75 (C4, C4'), 142.18 (C3, C3'), 130.59 (C12, C12'), 129.51 (C8, C8'), 128.59 (C7, C7'), 126.87 (C11, C11'), 119.10 (C1, C1'), 113.66 (C2, C2'), 88.05 (C5, C5'), 68.11 (C6, C6'), 59.07 (C9, C9'), 56.57 (C18, C18'), 46.69 (C16, C16'), 43.09 (C17, C17'), 42.74 (C13, C13'), 40.71 (C14, C14'), 35.41 (C15, C15'), 33.94 (C20, C20'), 28.72 (C21, C21') 24.60 (C22), 20.33 (C10, C10')

IR: υ (cm^{-1}), 2928, 1731 (C=O), 1504 (C-C, Ar), 1441, 1277, 1252, 1202, 1173, 1156, 1138, 1101, 1052, 1022

HRMS (EI, 70eV) Calculated for $[M+H]^+$, $C_{43}H_{51}N_2O_8^+$, requires: 723.3645, found 723.3647, m.p. = 55-57 °C, $[\alpha]_D$ = -233° *c* = (0.10, $CHCl_3$, 589 nm, 20 °C)

(1*S*,5*R*,13*R*,14*S*,17*R*)-10-methoxy-14-{[4-({[(1*S*,5*R*,13*R*,14*S*,17*R*)-10-methoxy-4-methyl-12-oxa-4-azapentacyclo[9.6.1.0^{1,13}.0^{5,17}.0^{7,18}]octadeca-7,9,11(18),15-tetraen-14-yl]oxy}methyl)phenyl]methoxy}-4-methyl-12-oxa-4-azapentacyclo[9.6.1.0^{1,13}.0^{5,17}.0^{7,18}]octadeca-7,9,11(18),15-tetraene, (121);

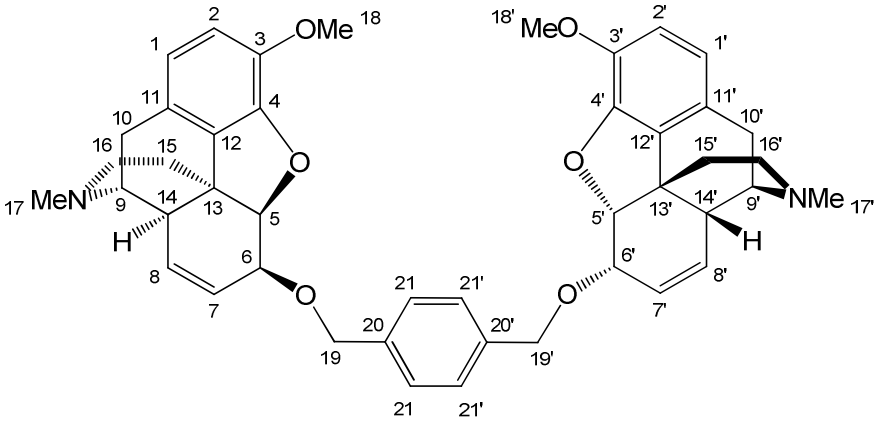

Following representative procedure 2, codeine (**2**) (0.653 g, 2.18 mmol), KOH (1.468 g, 26.16 mmol, 12 Eq), THF (10 mL), KI (0.073 g, 0.44 mmol, 0.2 Eq) and 1,4-

bis(bromomethyl)benzene (0.191 g, 1.09 mmol, 0.5 Eq) gave, after purification by column chromatography (SiO_2 10% MeOH/DCM, 1% NH_4OH) followed by recrystallisation in $CHCl_3$:Hexane, **121** as an off white solid in 55% yield (0.419 g, 0.60 mmol).

^{1}H NMR, ($CDCl_3$, 400 MHz) δ, 7.34 (s, 4H, (H21, H21')) 6.55 (d, *J* = 8.0 Hz, 2H, (H2, H2')), 6.43 (d, *J* = 8.0 Hz, 2H, (H1, H1')), 5.69-5.66 (m, *J* = 10.0 Hz, 2H, (H7, H7')), 5.25-5.22 (m, 2H, (H8, H8')), 4.91 (dd, *J* = 6.0, 0.8 Hz, 2H, (H5, H5')), 4.77 (d, *J* = 12.0 Hz, 2H, (H19, H19')), 4.57 (d, *J* = 12.0 Hz, 2H, (H19, H19')), 3.90-3.87 (m, 2H, (H6, H6')), 3.76 (s, 6H, (H18, H18')) 3.27-3.25 (m, 2H, (H9, H9')), 2.94 (d, *J* = 18.4 Hz, 2H, (H10, H10')), 2.56-2.55 (m, 2H, (H14, H14')), 2.49 (dd, *J* = 12.0, 3.6 Hz, 2H, (H16, H16')), 2.36-2.29 (m, 8H, (H17, H17', H16, H16')), 2.22 (dd, 18.4, 6.0 Hz, 2H, (H10, H10')), 1.94 (ddd, *J* = 12.4, 12.4, 4.8 Hz, 2H, (H15, H15')), 1.80 (dd, *J* = 12.4, 1.6 Hz, 2H, (H15, H15'))

^{13}C NMR, ($CDCl_3$, 100 MHz) δ, 147.46 (C4, C4'), 142.16 (C3, C3'), 137.65 (C20, C20'), 130.94 (C7, C7'), 130.84 (C12, C12') 128.71 (C8, C8'), 127.96 (C21, C21'), 126.94 (C11, C11'), 118.82 (C1, C1') 113.48 (C2, C2'), 89.59 (C5, C5'), 72.99 (C6, C6') 70.44 (C19, C19'), 58.96 (C9, C9') 56.56 (C18, C18'), 46.55 (C16, C16'), 43.34 (C13, C13'), 43.12 (C17, C17'), 41.00 (C14, C14'), 35.89 (C15, C15'), 20.50 (C10, C10')

IR: υ (cm^{-1}), 2907, 1499 (C-C, Ar), 1441, 1277, 1253, 1203, 1121, 1100, 1052, 1019

HRMS (EI, 70eV) Calculated for $[M+H]^+$, $C_{44}H_{49}N_2O_6^+$, requires: 701.3591, found 701.3571, m.p. = 179-181 °C, $[\alpha]_D$ = -240° *c* = (0.10, $CHCl_3$, 589 nm, 20 °C)

(1*S*,5*R*,13*R*,14*S*,17*R*)-10-methoxy-14-{[3-({[(1*S*,5*R*,13*R*,14*S*,17*R*)-10-methoxy-4-methyl-12-oxa-4-azapentacyclo[9.6.1.$0^{1,13}$.$0^{5,17}$.$0^{7,18}$]octadeca-7,9,11(18),15-tetraen-14-yl]oxy}methyl)phenyl]methoxy}-4-methyl-12-oxa-4-azapentacyclo[9.6.1.$0^{1,13}$.$0^{5,17}$.$0^{7,18}$]octadeca-7,9,11(18),15-tetraene, (139);

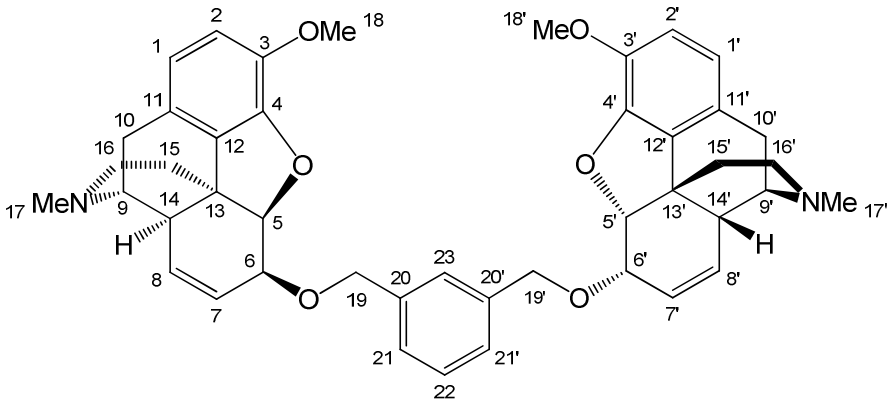

Following representative procedure 2, codeine (**2**) (0.667 g, 2.23 mmol), KOH (1.501 g, 26.76 mmol, 12 Eq), THF (10 mL), KI (0.075 g, 0.45 mmol, 0.2 Eq) and 1,3-*bis*(bromomethyl)benzene (0.196 g, 1.12 mmol, 0.5 Eq) gave, after purification by column chromatography (SiO_2 10% MeOH/DCM, 1% NH_4OH) followed by recrystallisation in $CHCl_3$:Hexane, **139** as an off white solid in 59% yield (0.461 g, 0.66 mmol).

^{1}H NMR, ($CDCl_3$, 400 MHz) δ, 7.38 (s, 1H, (H23)), 7.32-7.24 (m, 3H, (H22, H21, H21')), 6.56 (d, *J* = 8.4 Hz, 2H, (H2, H2')), 6.44 (d, *J* = 8.4 Hz, 2H, (H1, H1')), 5.72-5.68 (m, 2H, (H7, H7')), 5.27-5.23 (m, 2H, (H8, H8')), 4.93 (dd, *J* = 6.0, 1.2 Hz, 2H, (H5, H5')), 4.80 (d, *J* = 12.0 Hz, 2H, (H19, H19')), 4.59 (d, *J* = 12.0 Hz, 2H, (H19, H19')), 3.92-3.89 (m, 2H, (H6, H6')), 3.76 (s, 6H, (H18, H18')) 3.27-3.24 (m, 2H, (H9, H9')), 2.96 (d, *J* = 18.4 Hz, 2H, (H10, H10')), 2.56-2.55 (m, 2H, (H14, H14')), 2.49 (dd, *J* = 12.4, 4.4 Hz, 2H, (H16, H16')), 2.37-2.30 (m, 2H, (H16, H16')), 2.35 (s, 6H, (H17, H17')), 2.23 (dd, *J* = 18.4, 6.4 Hz, 2H, (H10, H10')), 1.93 (ddd, *J* = 12.4, 12.4, 4.8 Hz, 2H, (H15, H15')), 1.81 (dd, *J* = 12.4, 2.0 Hz, 2H, (H15, H15'))

^{13}C NMR, ($CDCl_3$, 100 MHz) δ, 146.43 (C4, C4'), 141.25 (C3, C3'), 137.25 (C20, C20'), 130.13 (C7, C7'), 129.51 (C12, C12'), 127.54 (C8, C8'), 127.18 (C22), 126.18 (C21, C21'), 126.16 (C23), 125.26 (C11, C11'), 117.87 (C1, C1'), 112.62 (C2, C2'), 88.41 (C5, C5'), 71.92 (C6, C6'), 69.58 (C19, C19'), 58.06 (C9, C9') 55.53 (C18, C18'), 45.53 (C16, C16'), 42.08 (C13, C13'), 41.76 (C17, C17'), 39.42 (C14, C14'), 34.34 (C15, C15'), 19.66 (C10, C10')

IR: υ (cm^{-1}), 2928, 1500 (C-C, Ar), 1441, 1277, 1254, 1156, 1120, 1100, 1084, 1052, 1019

HRMS (EI, 70eV) Calculated for $[M+H]^+$, $C_{44}H_{49}N_2O_6^+$, requires: 701.3591, found 701.3589, m.p. = 99-101 °C, $[\alpha]_D$ = -172° *c* = (0.10, $CHCl_3$, 589 nm, 20 °C)

6.3 Halogenated Codeine Derivatives

Representative Procedure 3

A flask was charged with the appropriate opioid, appropriate halogen succinimide, and 0.1M TFA aqueous solution. Contents stirred at corresponding temperature for 24 h. The pH of the reaction solution was adjusted to pH 8 *via* the addition of 10% NaOH solution and the aqueous phase was extracted with DCM. The organic phase was dried over anhydrous Na_2SO_4, filtered and concentrated *in vacuo* before purification.

(1*S*,5*R*,13*R*,14*S*,17*R*)-8-bromo-10-methoxy-4-methyl-12-oxa-4-azapentacyclo[9.6.1.0^{1,13}.0^{5,17}.0^{7,18}]octadeca-7,9,11(18),15-tetraen-14-ol, [1-bromocodeine], (75);

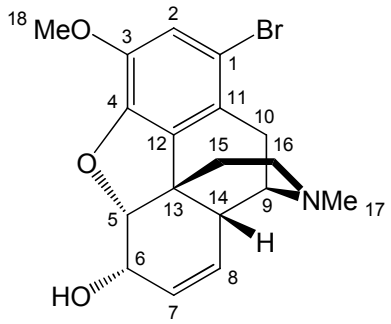

Following representative procedure 3 and stirring at RT, codeine (**2**) (1.244 g, 4.16 mmol), NBS (0.815 g, 4.58 mmol, 1.1 Eq) and TFA (150 mL) gave, after purification by column chromatography (SiO_2 10% MeOH/DCM, 1% NH_4OH) followed by recrystallisation in $CHCl_3$:Hexane, **75** as an off white solid in 83% yield (1.302 g, 3.45 mmol).

^{1}H NMR data in agreement with literature [97]

^{1}H NMR, ($CDCl_3$, 400 MHz) δ, 6.79 (s, 1H, (H2)), 5.66-5.64 (m, 1H, (H7)), 5.23-5.20 (m, 1H, (H8)), 4.83 (dd, *J* = 6.4, 0.8 Hz, 1H, (H5)), 4.13-4.10 (m, 1H, (H6)), 3.75 (s, 3H, (H18)), 3.36-3.34 (m, 1H, (H9)), 2.84 (d, *J* = 19.2 Hz, 1H, (H10)), 2.61-2.60 (m, 1H, (H14)), 2.54 (dd, *J* = 12.4, 4.0 Hz, 1H, (H16)), 2.39 (s, 3H, (H17)), 2.27 (ddd, *J* = 12.2, 12.2, 3.6 Hz, 1H, (H16)), 2.11 (dd, *J* = 19.2, 6.0 Hz, 1H, (H10)), 2.00 (ddd, *J* = 12.4, 12.4, 4.8 Hz, 1H, (H15)), 1.80 (dd, *J* = 12.4, 2.0 Hz, 1H, (H10))

^{13}C NMR, ($CDCl_3$, 100 MHz) δ, 145.85 (C4), 143.06 (C3), 133.62 (C12), 132.39 (C7), 128.10 (C8), 126.60 (C11), 115.64 (C1), 112.95 (C2), 91.66 (C5), 66.35 (C6), 58.78 (C9), 56.39 (C18), 46.19 (C16), 43.44 (C17), 43.11 (C13), 40.52 (C14), 35.71 (C15), 22.02 (C10)

(1*S*,5*R*,13*R*,14*S*,17*R*)-8-iodo-10-methoxy-4-methyl-12-oxa-4-azapentacyclo[9.6.1.0^{1,13}.0^{5,17}.0^{7,18}]octadeca-7,9,11(18),15-tetraen-14-ol, [1-iodocodeine], (142);

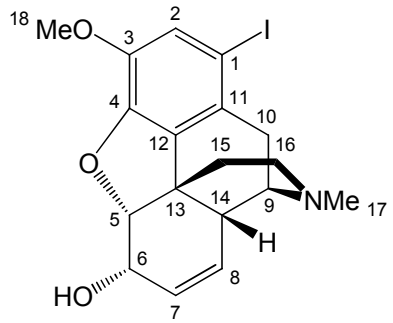

Following representative procedure 3 and stirring at RT, codeine (**2**) (1.238 g, 4.14 mmol), NIS (1.024 g, 4.55 mmol, 1.1 Eq) and TFA (150 mL) gave, after purification by column chromatography (SiO_2 10% MeOH/DCM, 1% NH_4OH) followed by recrystallisation in $CHCl_3$:Hexane, **142** as an orange solid in 89% yield (1.563 g, 3.68 mmol).

^{1}H NMR data in agreement with literature [98, 99]

^{1}H NMR, ($CDCl_3$, 400 MHz) δ, 7.02 (s, 1H, (H2)), 5.71-5.68 (m, 1H, (H7)), 5.22-5.18 (m, 1H, (H8)), 4.86 (d, *J* = 6.4 Hz, 1H, (H5)), 4.16-4.12 (m, 1H, (H6)), 3.77 (s, 3H, (H18)), 3.55-3.53 (m, 1H, (H9)), 2.86 (s, 1H, (H14)), 2.78-2.73 (m, 2H, (H10, H16)), 2.52 (s, 3H, (H17)), 2.40 (ddd, *J* = 12.4, 12.4, 3.6 Hz, 1H, (H16)), 2.24-2.14 (m, 2H, (H10, H15)), 1.85 (d, *J* = 11.6 Hz, 1H, (H15))

^{13}C NMR, ($CDCl_3$, 100 MHz) δ, 146.93 (C4), 143.54 (C3), 134.00 (C12), 131.79 (C7), 129.42 (C8), 127.43 (C11), 121.84 (C1), 91.28 (C2), 87.79 (C5), 66.23 (C6), 59.72 (C9), 56.42 (C18), 46.42 (C16), 43.36 (C17), 42.99 (C13), 40.04 (C14), 35.19 (C15), 26.78 (C10)

(1*S*,5*R*,13*R*,14*S*,17*R*)-8-chloro-10-methoxy-4-methyl-12-oxa-4-azapentacyclo[9.6.1.0^{1,13}.0^{5,17}.0^{7,18}]octadeca-7,9,11(18),15-tetraen-14-ol, [1-chlorocodeine], (76);

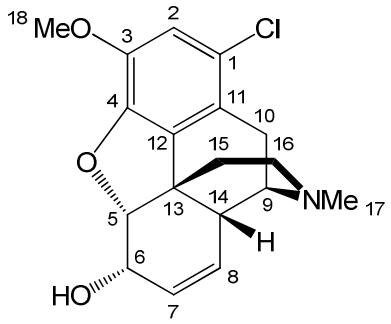

Following representative procedure 3 and stirring at 90°C, codeine (**2**) (0.585 g, 1.96 mmol), NCS (0.540 g, 4.04 mmol, 2.1 Eq) and TFA (40 mL) gave, after purification by

column chromatography (SiO_2 10% MeOH/DCM, 1% NH_4OH) followed by recrystallisation in $CHCl_3$:Hexane, **76** as an off white solid in 62% yield (0.405 g, 1.22 mmol).

^{1}H NMR data in agreement with literature [100]

^{1}H NMR, ($CDCl_3$, 400 MHz) δ, 6.63 (s, 1H (H2)), 5.67-5.65 (m, 1H, (H7)), 5.22-5.19 (m, 1H, (H8)), 4.85 (dd, *J* = 6.8, 1.2 Hz, 1H, (H5)), 4.14-4.10 (m, 1H, (H6)), 3.76 (s, 3H, (H18)), 3.43-3.41 (m, 1H, (H9)), 2.90 (d, *J* = 19.2 Hz, 1H, (H10)), 2.72 (s, 1H, (H14)), 2.61 (dd, *J* = 12.8, 4.4 Hz, 1H, (H16)), 2.43 (s, 3H, (H17)), 2.34 (ddd, *J* = 12.8, 12.8, 3.6 Hz 1H, (H16)), 2.22 (dd, *J* = 19.2 Hz, 6.4 Hz, 1H, (H10)), 2.08 (ddd, *J* = 12.8, 12.8, 5.6 Hz 1H, (H15)), 1.82 (dd, *J* = 12.8 Hz, 2.0 Hz, 1H, (H15))

^{13}C NMR, ($CDCl_3$, 100 MHz) δ, 145.28 (C4), 142.88 (C3), 133.80 (C12), 131.99 (C7), 127.62 (C8), 124.20 (C11), 123.91 (C1), 113.03 (C2), 91.59 (C5), 66.24 (C6), 58.71 (C9), 56.42 (C18), 46.31 (C16), 43.11 (C17), 42.91 (C13), 40.11 (C14), 35.31 (C15), 19.82 (C10)

1,4-*bis*(1*S*,5*R*,13*R*,14*S*,17*R*)-8-bromo-10-methoxy-4-methyl-12-oxa-4-azapentacyclo[9.6.1.0^{1,13}.0^{5,17}.0^{7,18}]octadeca-7,9,11(18),15-tetraen-14-yl benzene-1,4-dicarboxylate, (143);

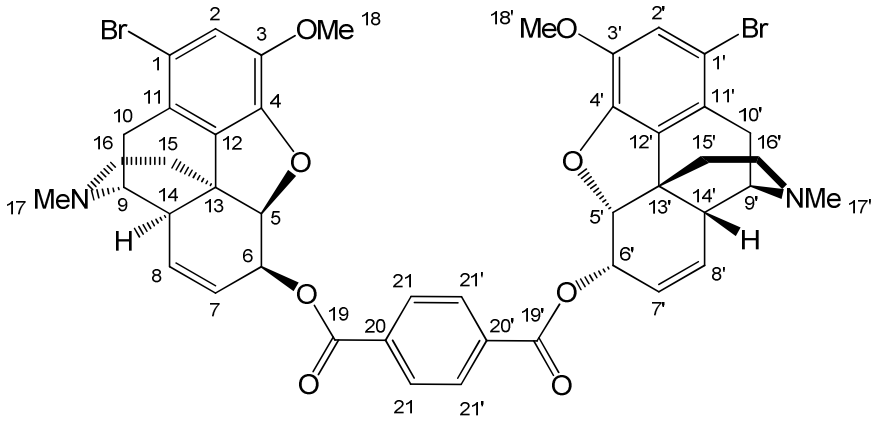

Following representative procedure 1, 1-bromocodeine (**75**) (0.200 g, 0.53 mmol) DMAP (0.071 g, 0.58 mmol, 1.1 Eq), DCM (8 mL) and terephthaloyl dichloride, (0.054 g, 0.27 mmol, 0.5 Eq) gave, after purification by column chromatography (SiO_2 10% MeOH/DCM, 1% NH_4OH) followed by recrystallisation in acetone, **143** as a white solid in 72% yield (0.172 g, 0.19 mmol).

^{1}H NMR, ($CDCl_3$, 400 MHz) δ, 8.05 (s, 4H, (H21, H21')) 6.80 (s, 2H, (H2, H2')), 5.76-5.73 (m, 2H, (H7, H7')), 5.47-5.43 (m, 2H, (H8, H8')), 5.40-5.37 (m, 2H, (H6, H6')), 5.17 (d, *J* = 6.8 Hz, 2H, (H5, H5')), 3.62 (s, 6H, (H18, H18')) 3.48-3.47 (m, 2H, (H9, H9')), 2.90-2.85 (m, 4H, (H10, H10', H14, H14')), 2.65 (dd, *J* = 12.0, 3.6 Hz, 2H, (H16, H16')), 2.46 (s, 6H, (H17, H17')), 2.32 (ddd, *J* = 12.0, 12.0, 3.2 Hz, 2H, (H16, H16')), 2.23 (dd, *J* = 19.2, 6.0 Hz, 2H, (H10, H10')) 2.11 (ddd, *J* = 12.4, 12.4, 4.8 Hz, 2H, (H15, H15')), 1.85 (d, *J* = 11.2 Hz, 2H, (H15, H15'))

^{13}C NMR, ($CDCl_3$, 100 MHz) δ, 164.18 (C19, C19'), 145.10 (C4, C4'), 142.19 (C3, C3'), 132.78 (C20, C20'), 130.92 (C12, C12'), 128.73 (C21, C21'), 128.29 (C8, C8), 127.60 (C7, C7'), 125.06 (C11, C11'), 116.04 (C2, C2'), 111.65 (C1, C1') 86.88 (C5, C5'), 67.40 (C6, C6'), 58.12 (C9, C9'), 55.73 (C18, C18'), 45.52 (C16, C16'), 41.89 (C17, C17'), 41.86 (C13, C13') 39.03 (C14, C14'), 33.97 (C15, C15'), 20.92 (C10, C10')

IR: υ (cm^{-1}), 2912, 1717 (C=O), 1488 (C-C, Ar), 1437, 1280, 1255, 1201, 1175, 1159, 1123, 1107, 1054, 1019

HRMS (EI, 70eV) Calculated for $[M+H]^+$, $C_{44}H_{43}Br^{79}Br^{79}N_2O_8^+$, requires: 885.1386, found 885.1427. Calculated for $[M+H]^+$, $C_{44}H_{43}Br^{79}Br^{81}N_2O_8^+$, requires: 887.1366, found 887.1541, m.p. = 233-235 °C, $[\alpha]_D$ = -213° *c* = (0.10, $CHCl_3$, 589 nm, 20 °C)

1,3-*bis*(1*S*,5*R*,13*R*,14*S*,17*R*)-8-bromo-10-methoxy-4-methyl-12-oxa-4-azapentacyclo[9.6.1.$0^{1,13}$.$0^{5,17}$.$0^{7,18}$]octadeca-7,9,11(18),15-tetraen-14-yl benzene-1,3-dicarboxylate, (144);

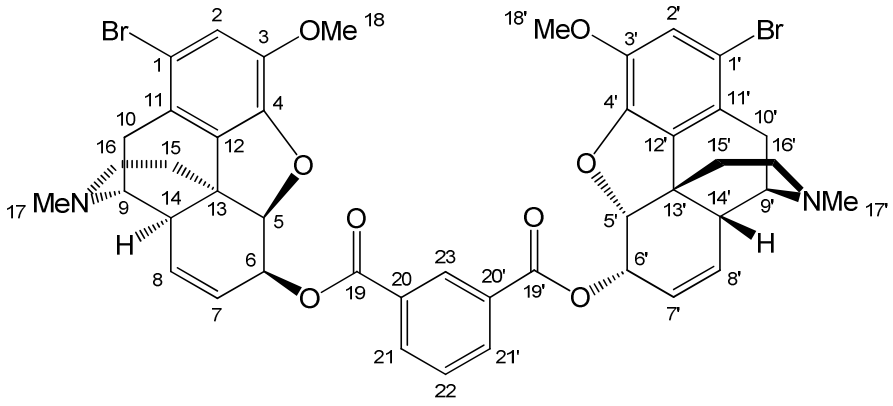

Following representative procedure 1, 1-bromocodeine (**75**) (0.247 g, 0.65 mmol), DMAP (0.089 g, 0.72 mmol, 1.1 Eq), DCM (8 mL) and isophthaloyl dichloride (0.067 g, 0.33 mmol, 0.5 Eq) gave, after purification by column chromatography (SiO_2 10% MeOH/DCM, 1% NH_4OH) followed by recrystallisation in $CHCl_3$:Hexane, **144** as a white solid in 75% yield (0.218 g, 0.25 mmol).

^{1}H NMR, ($CDCl_3$, 400 MHz) δ, 8.62 (s, 1H, (H23)), 8.21 (dd, *J* = 7.6, 2.0 Hz, 2H, (H21, H21')), 7.46 (t, *J* = 7.6 Hz, 1H, (H22)), 6.78 (s, 2H, (H2)), 5.75-5.73 (m, 2H, (H7, H7')), 5.47-5.43 (m, 2H, (H8, H8')) 5.39-5.35 (m, 2H, (H6, H6')), 5.16 (d, *J* = 6.0 Hz, 2H, (H5, H5')), 3.59 (s, 6H, (H18, H18')) 3.41-3.39 (m, 2H, (H9, H9')), 2.87 (d, *J* = 18.8 Hz, 2H, (H10, H10')), 2.77-2.76 (m, 2H, (H14, H14)), 2.56 (dd, *J* = 12.0, 4.8 Hz 2H, (H16, H16')), 2.41 (s, 6H, (H17, H17')), 2.26 (ddd, *J* = 12.0, 12.0, 3.6 Hz, 2H, (H16, H16')), 2.14 (dd, *J* = 18.8, 6.4 Hz, 2H, (H10, H10')), 2.03 (ddd, *J* = 12.4, 12.4, 4.8 Hz, 2H, (H15, H15')), 1.82 (d, *J* = 12.4 Hz, 2H, (H15, H15'))

^{13}C NMR, ($CDCl_3$, 100 MHz) δ, 164.09 (C19, C19'), 145.16 (C4, C4'), 142.14 (C3, C3'), 133.30 (C21, C21'), 131.03 (C12, C12'), 130.24 (C23), 129.28 (C20, C20'), 128.40 (C8, C8'), 127.62 (C7, C7'), 127.38 (C22), 125.28 (C11, C11'), 116.03 (C2,

C2'), 111.57 (C1, C1'), 86.96 (C5, C5'), 67.49 (C6, C6'), 58.05 (C9, C9'), 55.74 (C18, C18'), 45.47 (C16, C16'), 42.00 (C17, C17'), 41.98 (C13, C13'), 39.25 (C14, C14'), 34.17 (C15, C15'), 20.85 (C10, C10')

IR: υ (cm^{-1}), 2909, 1723 (C=O), 1487 (C-C, Ar), 1435, 1281, 1252, 1230, 1201, 1175, 1158, 1115, 1080, 1051, 1017

HRMS (EI, 70eV) Calculated for $[M+H]^+$, $C_{44}H_{43}Br^{79}Br^{79}N_2O_8^+$, requires: 885.1386, found 885.1407. Calculated for $[M+H]^+$, $C_{44}H_{43}Br^{79}Br^{81}N_2O_8^+$, requires: 887.1366, found 887.1531, m.p. = 227-229 °C, $[\alpha]_D$ = -168° *c* = (0.10, $CHCl_3$, 589 nm, 20 °C)

1,2-*bis*(1*S*,5*R*,13*R*,14*S*,17*R*)-8-bromo-10-methoxy-4-methyl-12-oxa-4-azapentacyclo[9.6.1.$0^{1,13}$.$0^{5,17}$.$0^{7,18}$]octadeca-7,9,11(18),15-tetraen-14-yl benzene-1,2-dicarboxylate, (145);

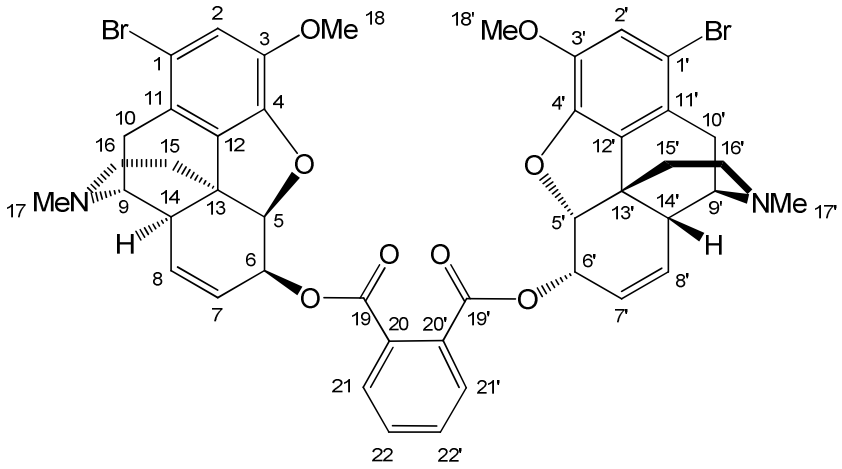

Following representative procedure 1, 1-bromocodeine (**75**) (0.200 g, 0.53 mmol), DMAP (0.071 g, 0.58 mmol, 1.1 Eq), DCM (8 mL) and phthaloyl dichloride (0.038 mL, 0.27 mmol, 0.5 Eq) gave, after purification by column chromatography (SiO_2 10% MeOH/DCM, 1% NH_4OH) followed by recrystallisation in $CHCl_3$:Hexane, **145** as a white solid in 71% yield (0.170 g, 0.19 mmol).

^{1}H NMR, ($CDCl_3$, 600 MHz) δ, 7.85-7.83 (m, 2H, (H21, H21')), 7.50-7.48 (m, 2H, (H22, H22')), 6.79 (s, 2H, (H2, H2')), 5.72-5.71 (m, 2H, (H7, H7')), 5.36-5.33 (m, 4H,

(H8, H8', H6, H6')), 5.17 (d, *J* = 6.6 Hz, 2H, (H5, H5')), 3.68 (s, 6H, (H18, H18')) 3.49 (s, 2H, (H9, H9')), 2.91 (s, 2H, (H14, H14')), 2.86 (d, *J* = 19.8 Hz, 2H, (H10, H10')), 2.68 (s, 2H, (H16, H16')), 2.49 (s, 6H, (H17, H17')), 2.38-2.34 (m, 2H, (H16, H16')), 2.24-2.19 (m, 4H, (H10, H10', H15',H15')), 1.85 (d, *J* = 12.6 Hz, 2H, (H15, H15'))

^{13}C NMR, ($CDCl_3$, 150 MHz) δ, 166.72 (C19, C19'), 146.38 (C4, C4'), 143.32 (C3, C3'), 131.79 (C20, 20'), 131.75 (C12, C12'), 131.12 (C22, C22'), 129.51 (C21, C21'), 129.19 (C7, C7'), 129.14 (C8, C8'), 128.47 (C11, C11'), 117.10 (C2, C2'), 112.58 (C1, C1'), 88.12 (C5, C5'), 68.91 (C6, C6'), 59.33 (C9, C9'), 56.76 (C18, C18'), 46.63 (C16, C16'), 42.87 (C13, C13'), 42.75 (C17, C17'), 39.60 (C14, C14'), 34.69 (C15, C15'), 22.19 (C10, C10')

IR: υ (cm^{-1}), 2898, 1718 (C=O), 1489 (C-C, Ar), 1438, 1268, 1256, 1201, 1177, 1124, 1101, 1083, 1054, 1032

HRMS (EI, 70eV) Calculated for $[M+H]^+$, $C_{44}H_{43}Br^{79}Br^{79}N_2O_8^+$, requires: 885.1386, found 885.1367. Calculated for $[M+H]^+$, $C_{44}H_{43}Br^{79}Br^{81}N_2O_8^+$, requires: 887.1366, found 887.1376, m.p. = 240-242 °C, $[\alpha]_D$ = -219° *c* = (0.10, $CHCl_3$, 589 nm, 20 °C)

(1*S*,5*R*,13*R*,14*S*,17*R*)-8-bromo-10-methoxy-4-methyl-12-oxa-4-azapentacyclo[9.6.1.0^{1,13}.0^{5,17}.0^{7,18}]octadeca-7,9,11(18),15-tetraen-14-yl 2-(2-{[(1*S*,5*R*,13*R*,14*S*,17*R*)-8-bromo-10-methoxy-4-methyl-12-oxa-4-azapentacyclo[9.6.1.0^{1,13}.0^{5,17}.0^{7,18}]octadeca-7,9,11(18),15-tetraen-14-yl]oxy}-2-oxoethoxy)acetate, (146);

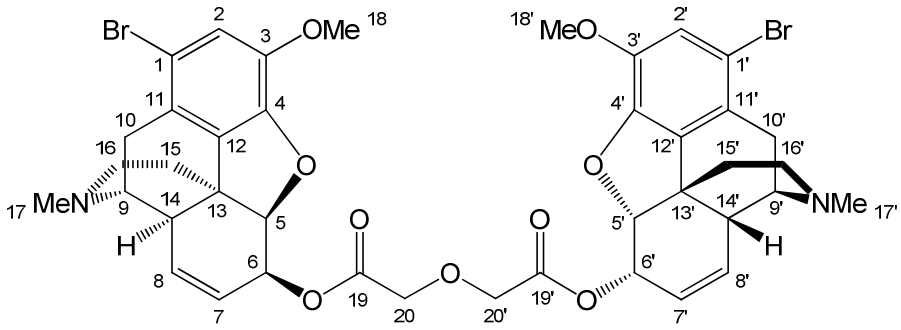

Following representative procedure 1, 1-bromocodeine (**75**) (0.259 g, 0.69 mmol), DMAP (0.093 g, 0.76 mmol, 1.1 Eq), DCM (8 mL) and diglycolyl dichloride (0.042 mL, 0.35 mmol, 0.5 Eq) gave, after purification by column chromatography (SiO_2 10% MeOH/DCM, 1% NH_4OH) followed by recrystallisation in $CHCl_3$:Hexane, **146** as a white solid in 39% yield (0.114 g, 0.13 mmol).

^{1}H NMR, ($CDCl_3$, 400 MHz) δ 6.79 (s, 2H, (H2, H2')), 5.60-5.57 (m, 2H, (H7, H7')), 5.40-5.36 (m, 2H, (H8, H8')), 5.21-5.18 (m, 2H, (H6, H6')), 5.05 (dd, *J* = 6.8, 0.8 Hz, 2H, (H5, H5')), 4.34 (d, *J* = 5.2 Hz, 4H, (H20, H20')), 3.73 (s, 6H, (H18, H18')) 3.37 (s, 2H, (H9, H9')), 2.84 (d, *J* = 19.2 Hz, 2H, (H10, H10')), 2.73-2.72 (m, 2H, (H14, H14')), 2.55 (d, *J* = 9.6 Hz, 2H, (H16, H16')), 2.40 (s, 6H, (H17, H17')), 2.25 (ddd, *J* = 12.4, 12.4, 3.2 Hz, 2H, (H16, H16')), 2.11 (dd, *J* = 19.2, 6.0 Hz 2H, (H10, H10')), 2.00 (ddd, *J* = 12.4, 12.4, 4.0 Hz, 2H, (H15, H15')), 1.79 (dd, *J* = 12.4, 1.6 Hz, 2H, (H15, H15'))

^{13}C NMR, ($CDCl_3$, 100 MHz) δ, 169.53 (C19, C19'), 146.06 (C4, C4'), 143.11 (C3, C3'), 131.89 (C12, C12'), 129.63 (C8, C8'), 128.17 (C7, C7'), 126.38 (C11, C11'), 116.41 (C2, C2'), 112.60 (C1, C1'), 87.83 (C5, C5'), 68.28 (C6, C6'), 68.05 (C20, C20'), 59.00 (C9, C9'), 56.58 (C18, C18'), 46.44 (C16, C16'), 43.05 (C17, C17'), 43.03 (C13, C13') 40.31 (C14, C14'), 35.24 (C15, C15'), 21.82 (C10, C10')

IR: υ (cm^{-1}), 2927, 1753 (C=O), 1735, 1486 (C-C, Ar), 1431, 1273, 1251, 1203, 1157, 1143, 1109, 1051, 1030, 1019

HRMS (EI, 70eV) Calculated for $[M+H]^+$, $C_{44}H_{43}Br^{79}Br^{79}N_2O_8^+$, requires: 853.1335, found 853.1331. Calculated for $[M+H]^+$, $C_{44}H_{43}Br^{79}Br^{81}N_2O_8^+$, requires: 855.1315, found 855.1323, m.p. = 210-212 °C, $[\alpha]_D$ = -199° *c* = (0.10, $CHCl_3$, 589 nm, 20 °C)

(1*S*,5*R*,13*R*,14*S*,17*R*)-8-bromo-10-methoxy-4-methyl-12-oxa-4-azapentacyclo[9.6.1.0^{1,13}.0^{5,17}.0^{7,18}]octadeca-7,9,11(18),15-tetraen-14-yl benzoate, (147);

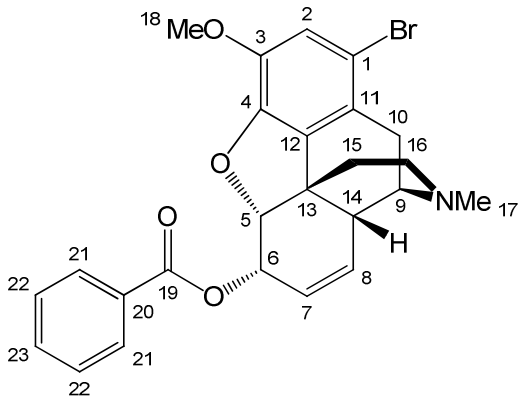

Following representative procedure 1, 1-bromocodeine (**75**) (0.181 g, 0.48 mmol), DMAP (0.065 g, 0.53 mmol, 1.1 Eq), DCM (8 mL) and benzoyl chloride (0.056 mL, 0.48 mmol, 1 Eq) gave, after purification by column chromatography (SiO_2 10% MeOH/DCM, 1% NH_4OH) followed by recrystallisation in $CHCl_3$:Hexane, **147** as a white solid in 89% yield (0.205 g, 0.43 mmol).

^{1}H NMR, ($CDCl_3$, 400 MHz) δ 7.98 (dd, *J* = 8.0, 0.8 Hz, 2H, (H21)), 7.50 (t, *J* = 8.0 Hz, 1H, (H23)), 7.36 (t, *J* = 8.0 Hz, 2H, (H22)) 6.80 (s, 1H, (H2)), 5.77-5.73 (m, 1H, (H7)), 5.43-5.39 (m, 1H, (H8)), 5.37-5.34 (m, 1H, (H6)), 5.18 (d, *J* = 6.4 Hz, 1H, (H5)), 3.60 (s, 4H, (H18, H9)), 2.95 (s, 1H, (H14)), 2.88 (d, *J* = 19.2 Hz, 1H, (H10)), 2.79 (dd, *J* = 12.0, 4.0 Hz, 1H, (H16)), 2.53 (s, 3H, (H17)), 2.40 (ddd, *J* = 12.0, 12.0, 4.0 Hz, 1H, (H16)), 2.30 (dd, *J* = 19.2, 6.0 Hz, 1H, (H10)), 2.16 (ddd, *J* = 12.8, 12.8, 4.8 Hz, 1H, (H15)), 1.86 (dd, *J* = 12.8, 1.6 Hz, 1H, (H15))

^{13}C NMR, ($CDCl_3$, 100 MHz) δ, 165.92 (C19), 146.25 (C4), 143.41 (C3), 133.21 (C23), 131.55 (C12), 129.91 (C21), 129.70 (C20), 129.46 (C7), 128.32 (C22), 128.19 (C8), 125.01 (C11), 117.37 (C2), 112.66 (C1), 87.91 (C5), 67.83 (C6), 59.30 (C9), 56.79 (C18), 46.63 (C16), 42.52 (C13), 42.45 (C17), 39.25 (C14), 34.26 (C15), 22.28 (C10)

IR: υ (cm^{-1}), 2929, 1714 (C=O), 1487 (C-C, Ar), 1436, 1280, 1264, 1201, 1173, 1158, 1117, 1107, 1058, 1028

HRMS (EI, 70eV) Calculated for $[M+H]^+$, $C_{25}H_{25}Br^{79}NO_4^+$, requires: 482.0967, found 482.0967, m.p. = 161-163 °C, $[\alpha]_D$ = -228° *c* = (0.10, $CHCl_3$, 589 nm, 20 °C)

2,6-*bis*(1*S*,5*R*,13*R*,14*S*,17*R*)-8-bromo-10-methoxy-4-methyl-12-oxa-4-azapentacyclo[9.6.1.$0^{1,13}$.$0^{5,17}$.$0^{7,18}$]octadeca-7,9,11(18),15-tetraen-14-yl pyridine-2,6-dicarboxylate, (148);

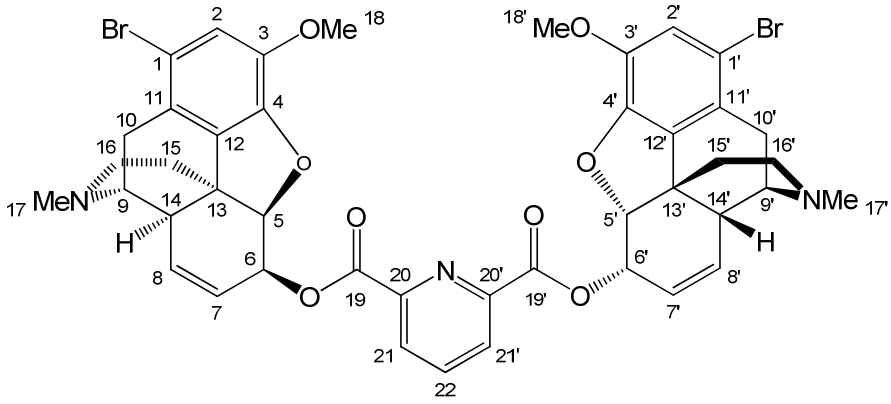

Following representative procedure 1, 1-bromocodeine (**75**) (0.458 g, 1.21 mmol), DMAP (0.162 g, 1.33 mmol, 1.1 Eq), DCM (10 mL) and 2,6-pyridinedicarbonyl dichloride (0.123 g, 0.61 mmol, 0.5 Eq) gave, after purification by column chromatography (SiO_2 10% MeOH/DCM, 1% NH_4OH) followed by recrystallisation in $CHCl_3$:Hexane, **148** as a white solid in 51% yield (0.274 g, 0.31 mmol).

^{1}H NMR, ($CDCl_3$, 400 MHz) δ, 8.23 (d, *J* = 8.0 Hz, 2H, (H21, H21')), 7.93 (t, *J* = 8.0 Hz, 1H, (H22), 6.79 (s, 2H, (H2, H2')) 5.82-5.78 (m, 2H, (H7, H7')), 5.44-5.41 (m, 4H, (H8, H8', H6, H6')), 5.22 (d, *J* = 6.4 Hz, 2H, (H5, H5')), 3.63 (s, 6H, (H18, H18')) 3.51-3.50 (m, 2H, (H9, H9')), 2.90-2.85 (m, 4H, (H10, H10', H14, H14')), 2.68 (dd, *J* = 12.0, 4.0 Hz, 2H, (H16, H16')), 2.48 (s, 6H, (H17, H17')), 2.35 (ddd, *J* = 12.0, 12.0, 3.2 Hz, 2H, (H16, H16')), 2.23 (dd, *J* = 19.2, 6.4 Hz, (H10, H10')) 2.15 (ddd, *J* = 12.4, 12.4, 3.2 Hz, 2H, (H15, H15')), 1.88 (dd, *J* = 12.4, 1.6 Hz, 2H, (H15, H15'))

^{13}C NMR, ($CDCl_3$, 100 MHz) δ, 163.59 (C19, C19'), 148.34 (C20, C20'), 146.26 (C4, C4'), 143.28 (C3, C3'), 137.98 (C22), 131.77 (C12, C12'), 128.94 (C8, C8'), 128.70 (C7, C7'), 128.31 (C21, C21'), 125.72 (C11, C11'), 117.33 (C2, C2'), 112.71 (C1, C1'), 87.81 (C5, C5'), 69.28 (C6, C6'), 59.24 (C9, C9'), 56.91 (C18, C18'), 46.58 (C16, C16'), 42.88 (C13, C13'), 42.77 (C17, C17'), 39.72 (C14, C14'), 34.72 (C15, C15'), 22.13 (C10, C10')

IR: υ (cm^{-1}), 2910, 1746 (C=O), 1721, 1486 (C-C, Ar), 1435, 1281, 1235, 1202, 1174, 1143, 1114, 1051, 1017

HRMS (EI, 70eV) Calculated for $[M+H]^+$, $C_{44}H_{43}Br^{79}Br^{79}N_2O_8^+$, requires: 886.1339, found 886.1354. Calculated for $[M+H]^+$, $C_{44}H_{43}Br^{79}Br^{81}N_2O_8^+$, requires: 888.1318, found 888.1494, m.p. = 182-183 °C, $[\alpha]_D$ = -196° *c* = (0.10, $CHCl_3$, 589 nm, 20 °C)

1,4-*bis*(1*S*,5*R*,13*R*,14*S*,17*R*)-8-iodo-10-methoxy-4-methyl-12-oxa-4-azapentacyclo[9.6.1.0^{1,13}.0^{5,17}.0^{7,18}]octadeca-7,9,11(18),15-tetraen-14-yl benzene-1,4-dicarboxylate, (149);

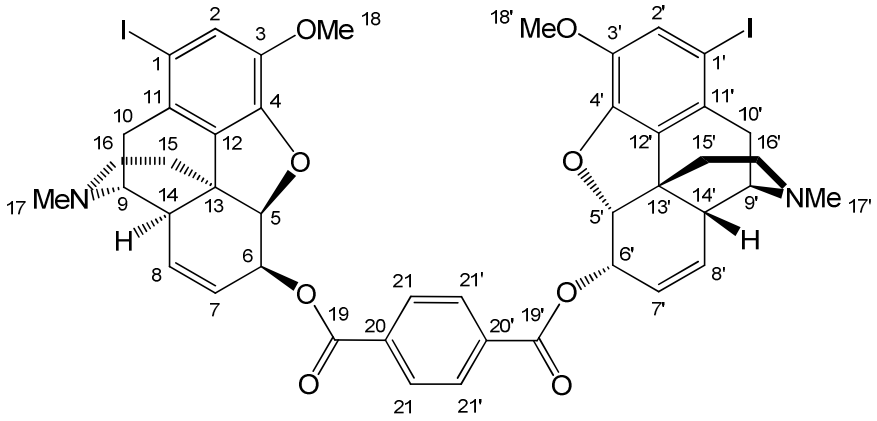

Following representative procedure 1, 1-iodocodeine (**142**) (0.438 g, 1.03 mmol), DMAP (0.138 g, 1.13 mmol, 1.1 Eq), DCM (8 mL) and terephthaloyl dichloride, (0.106 g, 0.52 mmol, 0.5 Eq) gave, after purification by column chromatography (SiO_2 10% MeOH/DCM, 1% NH_4OH) followed by recrystallisation in acetone, **149** as an off white solid in 76% yield (0.386 g, 0.39 mmol).

^{1}H NMR, ($CDCl_3$, 400 MHz) δ, 8.05 (s, 4H, (H21, H21')) 7.02 (s, 2H, (H2, H2')), 5.77-5.73 (m, 2H, (H7, H7')), 5.46-5.44 (m, 2H, (H8, H8')), 5.39-5.37 (m, 2H, (H6, H6')), 5.16 (d, *J* = 6.8 Hz, 2H, (H5, H5')), 3.61 (s, 6H, (H18, H18')) 3.54-3.52 (m, 2H, (H9, H9')), 2.87 (s, 2H, (H14, H14')), 2.78 (d, *J* = 18.8 Hz, 2H, (H10, H10')), 2.70 (dd, *J* = 12.0, 3.6 Hz, 2H, (H16, H16')), 2.49 (s, 6H, (H17, H17')), 2.32 (ddd, *J* = 12.0, 12.0, 3.6 Hz, 2H, (H16, H16')), 2.18-2.09 (m, 4H (H10, H10', H15, H15')), 1.84 (d, *J* = 11.6 Hz, 2H, (H15, H15'))

^{13}C NMR, ($CDCl_3$, 100 MHz) δ, 165.18 (C19, C19'), 147.15 (C4, C4'), 143.64 (C3, C3'), 133.76 (C20, C20'), 131.47 (C12, C12'), 129.77 (C21, C21'), 129.22 (C11, C11'), 128.93 (C7, C7') 128.89 (C8, C8'), 123.13 (C2, C2'), 87.59 (C5, C5'), 86.49 (C1, C1'), 68.28 (C6, C6'), 59.77 (C9, C9'), 56.74 (C18, C18'), 46.58 (C16, C16'), 42.86 (C13, C13'), 42.70 (C17, C17') 39.65 (C14, C14'), 34.63 (C15, C15'), 26.55 (C10, C10')

IR: υ (cm^{-1}), 2909, 1714 (C=O), 1481 (C-C, Ar), 1436, 1279, 1252, 1200, 1173, 1157, 1121, 1053, 1019

HRMS (EI, 70eV) Calculated for $[M+H]^+$, $C_{44}H_{43}I_2N_2O_8^+$, requires: 981.1109, found 981.1118, m.p. = 222-223 °C, $[\alpha]_D$ = -206° *c* = (0.10, $CHCl_3$, 589 nm, 20 °C)

1,3-*bis*(1*S*,5*R*,13*R*,14*S*,17*R*)-8-iodo-10-methoxy-4-methyl-12-oxa-4-azapentacyclo[9.6.1.0^{1,13}.0^{5,17}.0^{7,18}]octadeca-7,9,11(18),15-tetraen-14-yl benzene-1,3-dicarboxylate, (150);

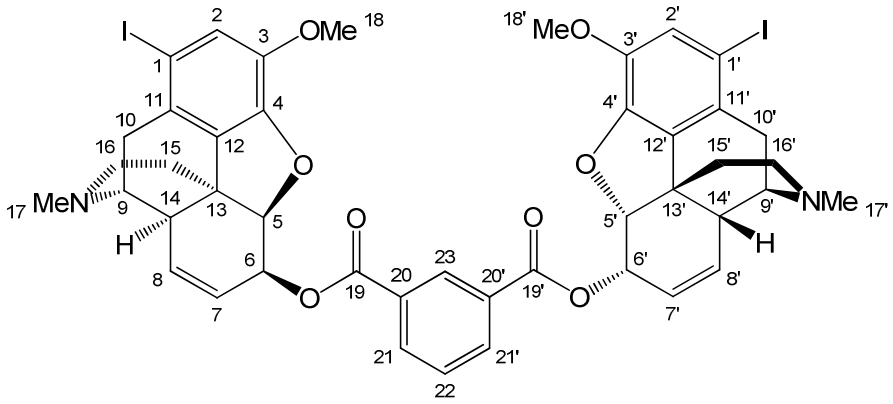

Following representative procedure 1, 1-iodocodeine (**142**) (0.449 g, 1.05 mmol), DMAP (0.142 g, 1.16 mmol, 1.1 Eq), DCM (8 mL) and isophthaloyl dichloride (0.108 g, 0.53 mmol, 0.5 Eq) gave, after purification by column chromatography (SiO_2 10% MeOH/DCM, 1% NH_4OH) followed by recrystallisation in $CHCl_3$:Hexane, **150** as an off white solid in 79% yield (0.410 g, 0.42 mmol).

^{1}H NMR, ($CDCl_3$, 400 MHz) δ, 8.56 (s, 1H, (H23)), 8.17 (dd, *J* = 8.0, 2.0 Hz, 2H, (H21, H21')), 7.45 (t, *J* = 8.0 Hz, 1H, (H22)), 7.02 (s, 2H, (H2, H2')), 5.81-5.77 (m, 2H, (H7, H7')), 5.46-5.42 (m, 2H, (H8, H8')) 5.39-5.36 (m, 2H, (H6, H6')), 5.19 (d, *J* = 6.8 Hz, 2H, (H5, H5')), 3.78-3.75 (m, 2H, (H9, H9')) 3.56 (s, 6H, (H18, H18')), 3.14 (s, 2H, (H14, H14')), 2.94 (dd, *J* = 12.4, 3.6 Hz, 2H, (H16, H16')), 2.79 (d, *J* = 19.2 Hz, 2H, (H10, H10')), 2.63 (s, 6H, (H17, H17')), 2.49 (ddd, *J* = 12.4, 12.4, 3.6 Hz, 2H, (H16, H16'), 2.36-2.27 (m, 4H, (H10, H10', H15, H15')), 1.90 (dd, *J* = 13.6, 2.0 Hz, 2H, (H15, H15'))

^{13}C NMR, ($CDCl_3$, 100 MHz) δ, 164.95 (C19, C19'), 147.18 (C4, C4'), 144.03 (C3, C3'), 134.39 (C21, C21'), 131.27 (C23), 130.80 (C12, C12'), 130.11 (C20, C20'), 129.75 (C7, C7'), 128.48 (C22), 127.59 (C11, C11'), 127.48 (C8, C8'), 123.53 (C2, C2'), 87.17 (C5, C5'), 86.43 (C1, C1'), 67.84 (C6, C6'), 60.38 (C9, C9'), 56.73 (C18, C18'), 47.01 (C16, C16'), 42.31 (C17, C17'), 42.27 (C13, C13'), 38.63 (C14, C14'), 33.63 (C15, C15'), 26.98 (C10, C10')

IR: υ (cm^{-1}), 2929, 1717 (C=O), 1481 (C-C, Ar), 1431, 1278, 1232, 1200, 1173, 1157, 1115, 1096, 1050, 1017

HRMS (EI, 70eV) Calculated for $[M+H]^+$, $C_{44}H_{43}I_2N_2O_8^+$, requires: 981.1109, found 981.1109, m.p. = 215-216 °C, $[\alpha]_D$ = -132° *c* = (0.10, $CHCl_3$, 589 nm, 20 °C)

(1*S*,5*R*,13*R*,14*S*,17*R*)-8-bromo-14-{[4-({[(1*S*,5*R*,13*R*,14*S*,17*R*)-8-bromo-10-methoxy-4-methyl-12-oxa-4-azapentacyclo[9.6.1.0^{1,13}.0^{5,17}.0^{7,18}]octadeca-7,9,11(18),15-tetraen-14-yl]oxy}methyl)phenyl]methoxy}-10-methoxy-4-methyl-12-oxa-4-azapentacyclo[9.6.1.0^{1,13}.0^{5,17}.0^{7,18}]octadeca-7,9,11(18),15-tetraene, (151):

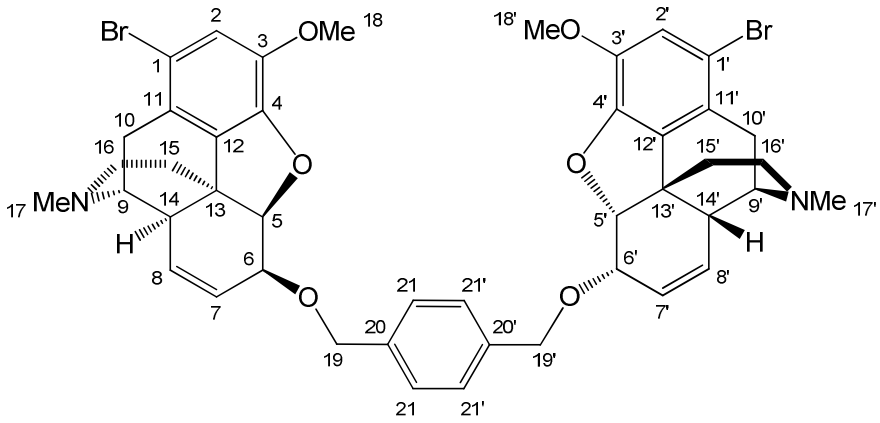

Following representative procedure 2, 1-bromocodeine (**75**) (0.400 g, 1.06 mmol), KOH (0.714 g, 12.72 mmol, 12 Eq), THF (10 mL), KI (0.035 g, 0.21 mmol, 0.2 Eq) and 1,4-*bis*(bromomethyl)benzene (0.140 g, 0.53 mmol, 0.5 Eq) gave, after purification by column chromatography (SiO_2 10% MeOH/DCM, 1% NH_4OH), **151** as an off white solid in 53% yield (0.239 g, 0.28 mmol).

^{1}H NMR, ($CDCl_3$, 400 MHz) δ, 7.33 (s, 4H, (H21, H21')) 6.76 (s, 2H, (H2, H2')), 5.72-5.68 (m, 2H, (H7, H7')), 5.25-5.22 (m, 2H, (H8, H8')), 4.93 (dd, *J* = 6.0, 1.2 Hz, 2H, (H5, H5')), 4.76 (d, *J* = 12.0 Hz, 2H, (H19, H19')), 4.57 (d, *J* = 12.0 Hz, 2H, (H19, H19')), 3.90-3.87 (m, 2H, (H6, H6')), 3.76 (s, 6H, (H18, H18')), 3.36-3.34 (m, 2H, (H9, H9')), 2.82 (d, *J* = 18.8 Hz, 2H, (H10, H10')), 2.59-2.58 (m, 2H, (H14, H14') 2.38 (dd, *J* = 12.0, 4.0 Hz, 2H, (H16, H16')), 2.39 (s, 6H, (H17, H17')), 2.29 (ddd, *J* = 12.0, 12.0, 3.6 Hz 2H, (H16, H16')), 2.13 (dd, *J* = 18.8, 6.4 Hz, 2H, (H10, H10')), 1.96 (ddd, *J* = 12.4, 12.4, 4.8 Hz, 2H, (H15, H15')), 1.81 (dd, *J* = 12.4, 1.6 Hz, 2H, (H15, H15'))
^{13}C NMR, ($CDCl_3$, 100 MHz) δ, 146.98 (C4, C4'), 143.11 (C3, C3'), 137.56 (C20, C20'), 132.11 (C12, C12'), 131.22 (C7, C7'), 128.37 (C8, C8') 128.00 (C21, C21'),

126.15 (C11, C11'), 116.20 (C2, C2') 112.12 (C1, C1'), 88.87 (C5, C5'), 72.76 (C6, C6'), 70.57 (C19, C19'), 58.93 (C9, C9') 56.58 (C18, C18'), 46.33 (C16, C16'), 43.73 (C13, C13'), 43.04 (C17, C17'), 40.60 (C14, C14'), 35.67 (C15, C15'), 22.11 (C10, C10')

IR: υ (cm^{-1}), 2907, 1487 (C-C, Ar), 1435, 1280, 1254, 1202, 1175, 1156, 1120, 1085, 1052, 1018

HRMS (EI, 70eV) Calculated for $[M+H]^+$, $C_{44}H_{47}Br^{79}Br^{79}N_2O_6^+$, requires: 857.1801, found 857.1800. Calculated for $[M+H]^+$, $C_{44}H_{47}Br^{79}Br^{81}N_2O_6^+$, requires: 859.1780, found 859.1800, m.p. = 131-133 °C, $[\alpha]_D$ = -220° *c* = (0.10, $CHCl_3$, 589 nm, 20 °C)

(1*S*,5*R*,13*R*,14*S*,17*R*)-8-bromo-14-{[3-({[(1*S*,5*R*,13*R*,14*S*,17*R*)-8-bromo-10-methoxy-4-methyl-12-oxa-4-azapentacyclo[9.6.1.$0^{1,13}$.$0^{5,17}$.$0^{7,18}$]octadeca-7,9,11(18),15-tetraen-14-yl]oxy}methyl)phenyl]methoxy}-10-methoxy-4-methyl-12-oxa-4-azapentacyclo[9.6.1.$0^{1,13}$.$0^{5,17}$.$0^{7,18}$]octadeca-7,9,11(18),15-tetraene, (152);

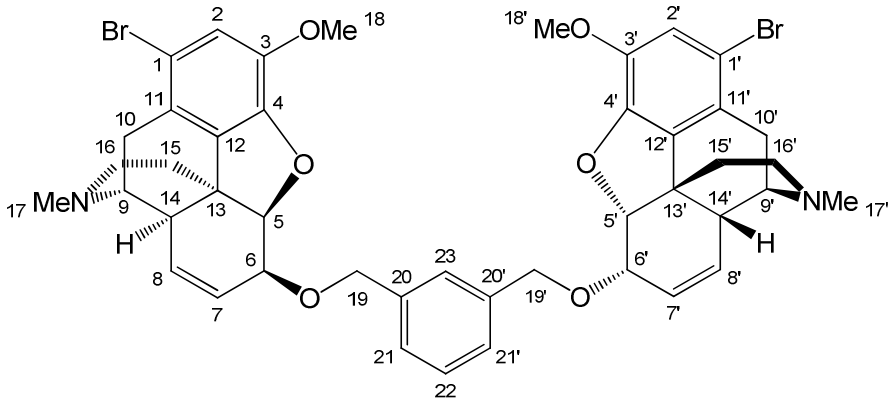

Following representative procedure 2, 1-bromocodeine (**75**) (0.400 g, 1.06 mmol), KOH (0.714 g, 12.72 mmol, 12 Eq), THF (10 mL), KI (0.035 g, 0.21 mmol, 0.2 Eq) and 1,4-*bis*(bromomethyl)benzene (0.140 g, 0.53 mmol, 0.5 Eq) gave, after purification by column chromatography (SiO_2 10% MeOH/DCM, 1% NH_4OH), **152** as in an off white solid in 59% yield (0.270 g, 0.31 mmol).

^1H NMR, ($CDCl_3$, 400 MHz) δ, 7.36 (s, 1H, (H23)), 7.29-7.25 (m, 3H, (H22, H21,

H21')), 6.76 (s, 2H, (H2, H2')), 5.72-5.68 (m, 2H, (H7, H7')), 5.25-5.22 (m, 2H, (H8, H8')), 4.93 (dd, *J* = 6.0, 0.8 Hz, 2H, (H5, H5')), 4.77 (d, *J* = 12.0 Hz, 2H (H19, H19')), 4.58 (d, *J* = 12.0 Hz, 2H (H19, H19')), 3.91-3.87 (m, 2H, (H6, H6')), 3.74 (s, 6H, (H18, H18')) 3.34-3.32 (m, 2H, (H9, H9')), 2.82 (d, *J* = 19.2 Hz, 2H, (H10, H10')), 2.58-2.55 (m, 2H, (H14, H14')), 2.51 (dd, *J* = 12.0, 4.0 Hz, 2H, (H16, H16')), 2.37 (s, 6H, (H17, H17')), 2.28 (ddd, *J* = 12.0, 12.0, 3.6 Hz, 2H (H16, H16')), 2.11 (dd, *J* = 19.2, 6.0 Hz, 2H, (H10, H10')), 1.94 (ddd, *J* = 12.8, 12.8, 5.2 Hz, 2H, (H15, H15')), 1.80 (dd, *J* = 12.8, 1.2 Hz, 2H, (H15, H15'))

^{13}C NMR, ($CDCl_3$, 100 MHz) δ, 146.99 (C4, C4'), 143.09 (C3, C3'), 138.24 (C20, C20'), 132.15 (C12, C12'), 131.17 (C7, C7'), 128.57 (C22), 128.47 (C8, C8'), 127.24 (C21, C21'), 127.21 (C23), 126.25 (C21, C21'), 116.22 (C2, C2') 112.11 (C1, C1'), 89.88 (C5, C5'), 72.92 (C6, C6'), 70.69 (C19, C19'), 58.90 (C9, C9') 56.59 (C18, C18'), 46.31 (C16, C16'), 43.77 (C13, C13'), 43.08 (C17, C17'), 40.69 (C14, C14'), 35.75 (C15, C15'), 22.07 (C10, C10')

IR: υ (cm^{-1}), 2930, 1487 (C-C, Ar), 1435, 1280, 1254, 1202, 1175, 1156, 1120, 1083, 1052, 1017

HRMS (EI, 70eV) Calculated for $[M+H]^+$, $C_{44}H_{47}Br^{79}Br^{79}N_2O_6^+$, requires: 857.1801, found 857.1808. Calculated for $[M+H]^+$, $C_{44}H_{47}Br^{79}Br^{81}N_2O_6^+$, requires: 859.1780, found 859.1792, m.p. = 110-111 °C, $[\alpha]_D$ = -163° *c* = (0.10, $CHCl_3$, 589 nm, 20 °C)

(1*S*,5*R*,13*R*,14*S*,17*R*)-8-iodo-14-{[4-({[(1*S*,5*R*,13*R*,14*S*,17*R*)-8-iodo-10-methoxy-4-methyl-12-oxa-4-azapentacyclo[9.6.1.$0^{1,13}$.$0^{5,17}$.$0^{7,18}$]octadeca-7,9,11(18),15-tetraen-14-yl]oxy}methyl)phenyl]methoxy}-10-methoxy-4-methyl-12-oxa-4-azapentacyclo[9.6.1.$0^{1,13}$.$0^{5,17}$.$0^{7,18}$]octadeca-7,9,11(18),15-tetraene, (153);

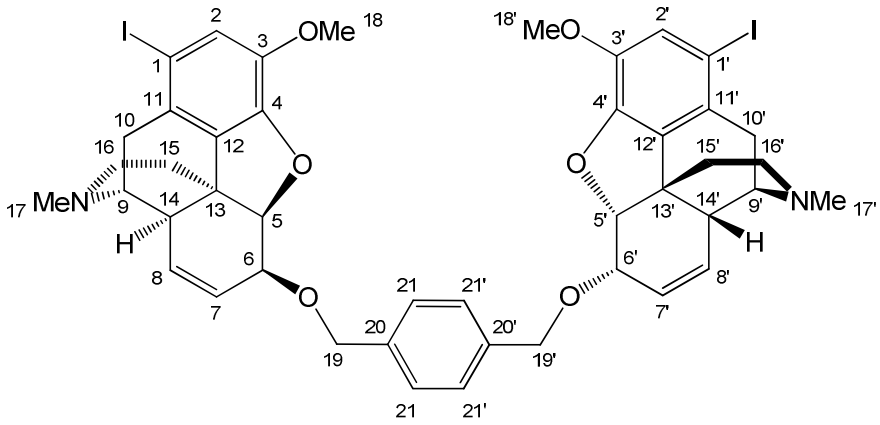

Following representative procedure 2, 1-iodocodeine (**142**) (0.601 g, 1.41 mmol), KOH (0.949 g, 16.92 mmol, 12 Eq), THF (10 mL), KI (0.046 g, 0.28 mmol, 0.2 Eq) and 1,4-*bis*(bromomethyl)benzene (0.187 g, 0.71 mmol, 0.5 Eq) gave, after purification by column chromatography (SiO_2 10% MeOH/DCM, 1% NH_4OH), **153** as an off white solid in 60% yield (0.403 g, 0.42 mmol).

^{1}H NMR, ($CDCl_3$, 400 MHz) δ, 7.33 (s, 4H, (H21, H21')) 6.98 (s, 2H, (H2, H2')), 5.71-5.69 (m, 2H, (H7, H7')), 5.25-5.21 (m, 2H, (H8, H8')), 4.91 (dd, *J* = 6.0, 0.8 Hz, 2H, (H5, H5')), 4.75 (d, *J* = 12.0 Hz, 2H, (H19, H19')), 4.57 (d, *J* = 12.0 Hz, 2H, (H19, H19')), 3.91-3.87 (m, 2H, (H6, H6')), 3.75 (s, 6H, (H18, H18')), 3.36-3.34 (m, 2H, (H9, H9')), 2.72 (d, *J* = 18.8 Hz, 2H, (H10, H10')), 2.58-2.52 (m, 4H, (H14, H14', H16, H16')), 2.39 (s, 6H, (H17, H17')), 2.27 (ddd, *J* = 12.4, 12.4, 3.6 Hz 2H, (H16, H16')), 2.04 (dd, *J* = 18.8, 6.4 Hz, 2H, (H10, H10')), 1.96 (ddd, *J* = 12.4, 12.4, 4.8 Hz, 2H, (H15, H15')), 1.79 (dd, *J* = 12.4, 1.6 Hz, 2H, (H15, H15'))

^{13}C NMR, ($CDCl_3$, 100 MHz) δ, 148.02 (C4, C4'), 143.45 (C3, C3'), 137.55 (C20, C20'), 131.86 (C12, C12'), 131.29 (C7, C7'), 129.71 (C11, C11') 128.31 (C8, C8'),

128.00 (C21, C21') 122.21 (C2, C2') 89.70 (C5, C5'), 85.86 (C1, C1'), 72.73 (C6, C6'), 70.59 (C19, C19'), 59.55 (C9, C9') 56.60 (C18, C18'), 46.35 (C16, C16'), 43.88 (C13, C13'), 43.04 (C17, C17'), 40.59 (C14, C14'), 35.62 (C15, C15'), 26.62 (C10, C10')

IR: υ (cm^{-1}), 2930, 1481 (C-C, Ar), 1433, 1279, 1252, 1201, 1175, 1157, 1120, 1086, 1051, 1018

HRMS (EI, 70eV) Calculated for $[M+H]^+$, $C_{44}H_{47}I_2N_2O_6^+$, requires: 953.1523, found 953.1536, m.p. = 140-141 °C, $[\alpha]_D$ = -210° *c* = (0.10, $CHCl_3$, 589 nm, 20 °C)

(13*R*,14*S*)-8-iodo-14-{[3-({[(1*R*,5*S*,13*S*,14*R*)-8-iodo-10-methoxy-4-methyl-12-oxa-4-azapentacyclo[9.6.1.0^{1,13}.0^{5,17}.0^{7,18}]octadeca-7(18),8,10,15-tetraen-14-yl]oxy}methyl)phenyl]methoxy}-10-methoxy-4-methyl-12-oxa-4-azapentacyclo[9.6.1.0^{1,13}.0^{5,17}.0^{7,18}]octadeca-7(18),8,10,15-tetraene, (154);

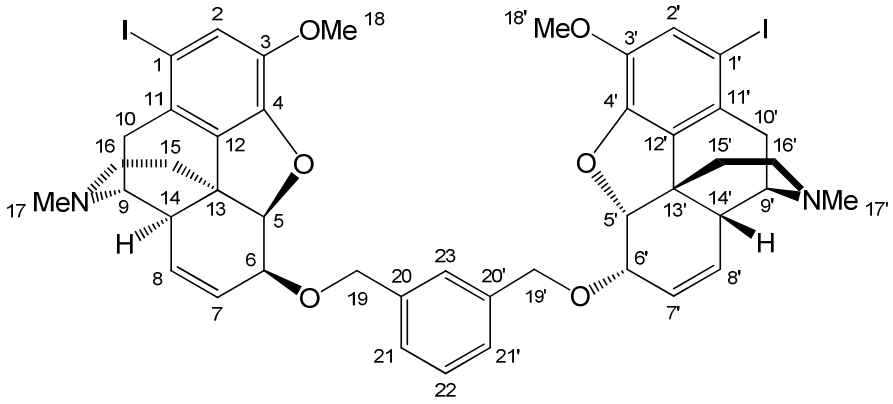

Following representative procedure 2, 1-iodocodeine (**142**) (0.731 g, 1.72 mmol), KOH (1.158 g, 20.64 mmol, 12 Eq), THF (10 mL), KI (0.056 g, 0.34 mmol, 0.2 Eq) and 1,3-*bis*(bromomethyl)benzene (0.227 g, 0.86 mmol, 0.5 Eq) gave, after purification by column chromatography (SiO_2 10% MeOH/DCM, 1% NH_4OH), **154** as an off white solid in 45% yield (0.369 g, 0.39 mmol).

^{1}H NMR, ($CDCl_3$, 400 MHz) δ, 7.36 (s, 1H, (H23)), 7.30-7.28 (m, 3H, (H22, H21, H21')), 6.98 (s, 2H, (H2, H2')), 5.74-5.70 (m, 2H, (H7, H7')), 5.25-5.21 (m, 2H, (H8,

H8')), 4.93 (dd, *J* = 6.4, 0.8 Hz, 2H, (H5, H5')), 4.77 (d, *J* = 12.0 Hz, 2H (H19, H19')), 4.58 (d, *J* = 12.0 Hz, 2H (H19, H19')), 3.91-3.89 (m, 2H, (H6, H6')), 3.75 (s, 6H, (H18, H18')) 3.44-3.42 (m, 2H, (H9, H9')), 2.73 (d, *J* = 18.8 Hz, 2H, (H10, H10')), 2.68 (s, 2H, (H14, H14')), 2.62 (dd, *J* = 12.0, 4.0 Hz, 2H, (H16, H16')), 2.45 (s, 6H, (H17, H17')), 2.33 (ddd, *J* = 12.0, 12.0, 3.6 Hz, 2H (H16, H16')), 2.13-2.00 (m, 4H, (H10, H10', H15, H15')), 1.83 (dd, *J* = 12.8, 1.6 Hz, 2H, (H15, H15'))

^{13}C NMR, ($CDCl_3$, 100 MHz) δ, 148.05 (C4, C4'), 143.56 (C3, C3'), 138.18 (C20, C20'), 131.65 (C12, C12'), 131.52 (C7, C7'), 129.21 (C11, C11'), 128.61 (C8, C8'), 127.91 (C22), 127.29 (C21, C21'), 127.23 (C23), 122.40 (C2, C2') 89.58 (C5, C5'), 85.82 (C1, C1'), 72.73 (C6, C6'), 70.77 (C19, C19'), 59.71 (C9, C9') 56.62 (C18, C18'), 46.45 (C16, C16'), 43.70 (C13, C13'), 42.88 (C17, C17'), 40.24 (C14, C14'), 35.29 (C15, C15'), 26.74 (C10, C10')

IR: υ (cm^{-1}), 2929, 1481 (C-C, Ar), 1433, 1278, 1253, 1201, 1175, 1156, 1120, 1083, 1051, 1018

HRMS (EI, 70eV) Calculated for $[M+H]^+$, $C_{44}H_{47}I_2N_2O_6^+$, requires: 953.1523, found 953.1539, m.p. = 74-75 °C, $[\alpha]_D$ = -170° *c* = (0.10, $CHCl_3$, 589 nm, 20 °C)

6.4 Palladium Coupled Codeine Derivatives

Representative Procedure 4

A flask was charged with the appropriate opioid, imidazole, *t*-butyldimethylsilyl chloride and anhydrous DMF and stirred under a nitrogen atmosphere at RT for 20 h. The reaction mixture was diluted with DCM, washed with distilled water (3 x 10 mL), dried over anhydrous Na_2SO_4 and concentrated *in vacuo* before purification.

Representative Procedure 5

A flask was charged with the appropriate opioid, palladium acetate, phosphine ligand, anhydrous DMF, anhydrous NEt_3 and appropriate alkene and stirred under a nitrogen atmosphere at 100 °C for 24 h. After cooling the mixture was diluted with diethyl ether, filtered and concentrated *in vacuo* before purification.

Representative Procedure 6

A flask was charged with the appropriate TBDMS protected opioid, TBAF (1 M solution in THF) and THF and stirred for at RT for 24 h. THF was removed from the reaction mixture *via* rotary evaporation and contents redissolved in DCM. The resulting mixture was washed with distilled water (3 x 10 mL), dried over Na_2SO_4 and concentrated *in vacuo* before purification.

(1*S*,5*R*,13*R*,14*S*,17*R*)-14-[(tert-butyldimethylsilyl)oxy]-10-methoxy-4-methyl-12-oxa-4-azapentacyclo[9.6.1.$0^{1,13}$.$0^{5,17}$.$0^{7,18}$]octadeca-7,9,11(18),15-tetraene, (160);

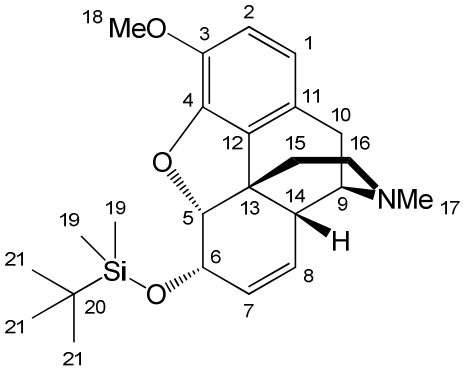

Following representative procedure 4, codeine (**2**) (0.301 g, 1.01 mmol), imidazole (0.082 g, 1.21 mmol, 1.2 Eq), *t*-butyldimethylsilyl chloride (0.183 g, 1.21 mmol, 1.2 Eq) and anhydrous DMF (2 mL), gave, after purification by column chromatography (SiO_2 10% MeOH/DCM) followed by recrystallisation in EtOH, **160** as a white solid in 87% yield (0.365 g, 0.88 mmol).

^{1}H NMR data in agreement with literature[101]

^{1}H NMR, ($CDCl_3$, 400 MHz) δ, 6.60 (d, *J* = 8.2 Hz, 1H, (H2, H2')), 6.46 (d, *J* = 8.2 Hz, 1H, (H1, H1')), 5.65-5.62 (m, 1H, (H7)), 5.13-5.09 (m, 1H, (H8)), 4.69 (d, *J* = 6.4 Hz, 1H, (H5)), 4.24-4.20 (m, 1H, (H6)), 3.90-3.87 (m, 1H, (H9)), 3.78 (s, 3H, (H18)), 3.37 (m, 1H, (H14)), 3.16 (dd, *J* = 12.4, 4.0 Hz, 1H, (H16)), 2.70 (*J* = 18.8 Hz, 1H, (H10)), 2.85-2.70 (m, 5H, (H17, H16, H10)), 2.53 (ddd, *J* = 13.6, 13.6, 4.8 Hz, 1H, (H15)),

1.92 (dd, *J* = 13.6, 2.8 Hz, 1H, (H15), 0.82 (s, 9H, (H21)), 0.05 (s, 3H, (H19)), 0.02 (s, 3H, (H19)),

^{13}C NMR, ($CDCl_3$, 100 MHz) δ, 147.76 (C4), 142.98 (C3), 135.94 (C7), 129.18 (C12), 124.24 (C8), 122.58 (C11), 119.24 (C1), 115.98 (C2), 90.97 (C5), 67.45 (C6), 60.57 (C9), 57.21 (C18), 47.26 (C16), 41.72 (C13), 41.59 (C17), 37.63 (C14), 32.84 (C15), 25.81 (C20), 21.92 (C10), 18.29 (C21), -4.59 (C19), -4.86 (C19)

(1*S*,5*R*,13*R*,14*S*,17*R*)-8-bromo-14-[(tert-butyldimethylsilyl)oxy]-10-methoxy-4-methyl-12-oxa-4-azapentacyclo[9.6.1.0^{1,13}.0^{5,17}.0^{7,18}]octadeca-7,9,11(18),15-tetraene, (158);

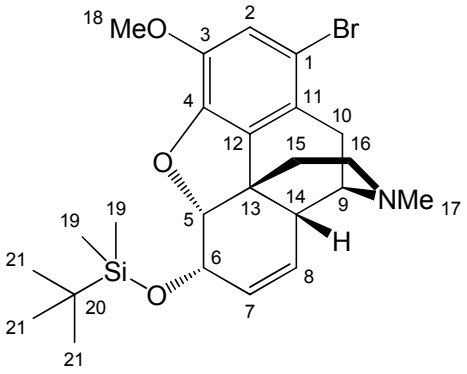

Following representative procedure 4, 1-bromocodeine (**75**) (0.784 g, 2.07 mmol), imidazole (0.169 g, 2.48 mmol, 1.2 Eq), *t*-butyldimethylsilyl chloride (0.374 g, 2.48 mmol, 1.2 Eq) and anhydrous DMF (2 mL) gave, after purification by column chromatography (SiO_2 10% MeOH/DCM) followed by recrystallisation in $CHCl_3$:Hexane, **158** as a white solid in 89% yield (0.905 g, 1.84 mmol).

^{1}H and ^{13}C NMR data in agreement with literature[74]

^{1}H NMR, ($CDCl_3$, 400 MHz) δ, 6.76 (s, 1H, (H2)), 5.60-5.58 (m, 1H, (H7)), 5.20-5.16 (m, 1H, (H8)), 4.64 (dd, *J* = 6.4, 1.2 Hz, 1H, (H5)), 4.20-4.16 (m, 1H, (H6)), 3.77 (s, 3H, (H18)), 3.33-3.31 (m, 1H, (H9)), 2.82 (*J* = 18.8 Hz, 1H, (H10)), 2.57 (s, 1H, (H14)), 2.51 (dd, *J* = 12.0, 4.0 Hz, 1H, (H16)), 2.38 (s, 3H, (H17)), 2.27 (ddd, *J* = 12.4, 12.4, 3.6 Hz, 1H, (H16)), 2.10 (dd, *J* = 18.8, 6.4 Hz 1H, (H10)), 1.94 (ddd, *J* = 12.4,

12.4, 5.2 Hz, 1H, (H15)), 1.77 (dd, *J* = 12.4, 1.6 Hz, 1H, (H15)), 0.85 (s, 9H, (H21), 0.06 (s, 3H, (H19)), 0.05 (s, 3H, (H19))

^{13}C NMR, ($CDCl_3$, 100 MHz) δ, 146.28 (C4), 141.92 (C3), 133.18 (C7), 131.52 (C8), 126.68 (C12), 125.54 (C11), 116.26 (C1), 110.83 (C2), 91.44 (C5), 67.27 (C6), 57.86 (C9), 56.07 (C18), 45.27 (C16), 42.73 (C17), 42.11 (C13), 39.72 (C14), 34.85 (C15), 24.85 (C20), 21.07 (C10), 17.35 (C21), -5.59 (C19), -5.78 (C19)

(1*S*,5*R*,13*R*,14*S*,17*R*)-8-iodo-14-[(tert-butyldimethylsilyl)oxy]-10-methoxy-4-methyl-12-oxa-4-azapentacyclo[9.6.1.0^{1,13}.0^{5,17}.0^{7,18}]octadeca-7,9,11(18),15-tetraene, (159);

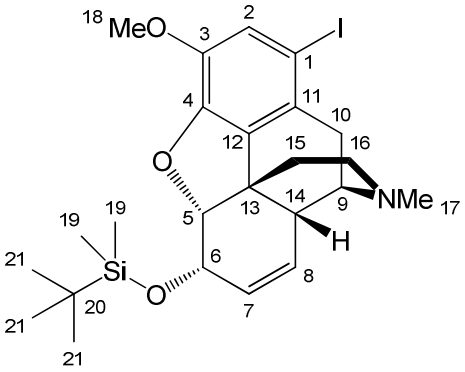

Following representative procedure 4, 1-iodocodeine (**142**) (0.477 g, 1.12 mmol), imidazole (0.091 g, 1.34 mmol, 1.2 Eq), *t*-butyldimethylsilyl chloride (0.202 g, 1.34 mmol, 1.2 Eq) and anhydrous DMF (2 mL) gave, after purification by column chromatography (SiO_2 10% MeOH/DCM) followed by recrystallisation in $CHCl_3$:Hexane, **159** as a white solid in 86% yield (0.520 g, 0.96 mmol).

^{1}H NMR data in agreement with literature[99]

^{1}H NMR, ($CDCl_3$, 400 MHz) δ, 7.00 (s, 1H, (H2)), 5.64-5.61 (m, 1H, (H7)), 5.16-5.12 (m, 1H, (H8)), 4.67 (dd, *J* = 6.4, 0.8 Hz, 1H, (H5)), 4.22-4.18 (m, 1H, (H6)), 3.77 (s, 3H, (H18)), 3.65-3.63 (m, 1H, (H9)), 2.91-2.86 (m, 2H, (H14, H16)), 2.73 (d, *J* = 19.2 Hz, (H10)), 2.60 (s, 3H, (H17)), 2.49 (ddd, *J* = 12.4, 12.4, 3.6 Hz, 1H, (H16)), 2.30-

2.18 (m, 2H, (H10, H15)), 1.84 (dd, *J* = 13.2, 2.0 Hz, 1H, (H15)), 0.84 (s, 9H, (H21)), 0.06 (s, 3H, (H19)), 0.04 (s, 3H, (H19))

^{13}C NMR, ($CDCl_3$, 100 MHz) δ, 148.33 (C4), 143.80 (C3), 135.37 (C7), 131.35 (C8), 127.82 (C12), 125.67 (C11), 123.94 (C2), 91.58 (C5), 85.48 (C1), 67.66 (C6), 60.22 (C9), 57.16 (C18), 46.71 (C16), 43.01 (C17), 42.37 (C13), 39.04 (C14), 34.27 (C15), 27.17 (C20), 25.84 (C10), 18.33 (C21), -4.57 (C19), -4.80 (C19)

Methyl (2*E*)-3-[(1*S*,5*R*,13*R*,14*S*,17*R*)-14-[(tert-butyldimethylsilyl)oxy]-10-methoxy-4-methyl-12-oxa-4-azapentacyclo[9.6.1.0^{1,13}.0^{5,17}.0^{7,18}]octadeca-7,9,11(18),15-tetraen-8-yl]prop-2-enoate, (161);

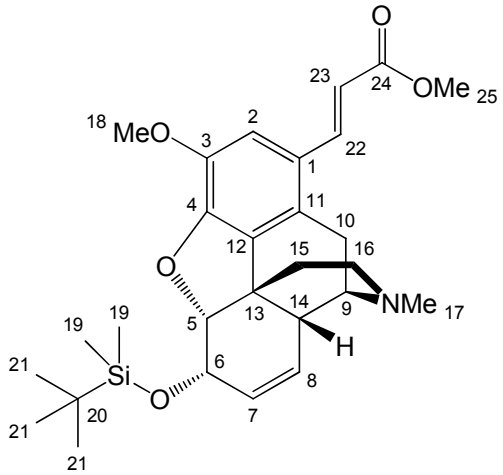

Following representative procedure 5, **159** (0.505 g, 0.94 mmol, 1 Eq), palladium acetate (0.011 g, 5 mol%), triphenylphosphine (0.049 g, 20 mol%), DMF (1 mL), NEt_3 (0.46 mL, 3.29 mmol, 3.5 Eq) and methyl acrylate (0.34 mL, 3.76 mmol, 4 Eq) gave, after purification by column chromatography (SiO_2 10% MeOH/DCM) followed by recrystallisation in EtOH, **161** as white solid in 85% yield (0.399 g, 0.80 mmol).

^{1}H and ^{13}C NMR data in agreement with literature[74]

^{1}H NMR, ($CDCl_3$, 400 MHz) δ, 7.74 (d, *J* = 16.0 Hz, 1H, (H22)), 6.89 (s, 1H, (H2)), 6.14 (d, *J* = 16.0 Hz, 1H, (H23)), 5.62-5.58 (m, 1H, (H7)), 5.21-5.18 (m, 1H, (H8)),

4.69 (dd, *J* = 6.0, 1.2 Hz, 1H, (H5)), 4.23-4.19 (m, 1H, (H6)), 3.80 (s, 3H, (H18)), 3.73 (s, 3H, (H25)) 3.36-3.34 (m, 1H, (H9)), 3.06 (d, *J* = 18.8 Hz, 1H, (H10)), 2.61-2.60 (m, 1H, (H14), 2.53 (dd, *J* = 12.0, 4.0 Hz, 1H, (H16)), 2.40 (s, 3H, (H17)), 2.32-2.25 (m, 2H, (H16, H10)), 1.97 (ddd, *J* = 12.8, 12.8, 5.2 Hz, 1H, (H15)), 1.77 (dd, *J* = 12.8, 1.6 Hz, 1H, (H15)), 0.86 (s, 9H, (H21)), 0.07 (s, 3H, (H19)), 0.05 (s, 3H, (H19))

^{13}C NMR, ($CDCl_3$, 100 MHz) δ, 167.98 (C24), 150.43 (C4), 142.61 (C3), 141.04 (C22), 134.15 (C7), 131.67 (C8), 127.92 (C23), 127.87 (C12), 124.30 (C11), 115.09 (C1), 112.21 (C2), 93.00 (C5), 68.38 (C6), 58.61 (C9), 56.83 (C18), 51.61 (C25), 46.26 (C16), 43.28 (C13) 43.17 (C17), 40.53 (C14), 35.84 (C15), 25.98 (C21), 19.35 (C10), 18.37 (C20), -4.57 (C19), -4.77 (C19)

Methyl (2*E*)-3-[(1*S*,5*R*,13*R*,14*S*,17*R*)-14-hydroxy-10-methoxy-4-methyl-12-oxa-4-azapentacyclo[9.6.1.0^{1,13}.0^{5,17}.0^{7,18}]octadeca-7,9,11(18),15-tetraen-8-yl]prop-2-enoate, (140);

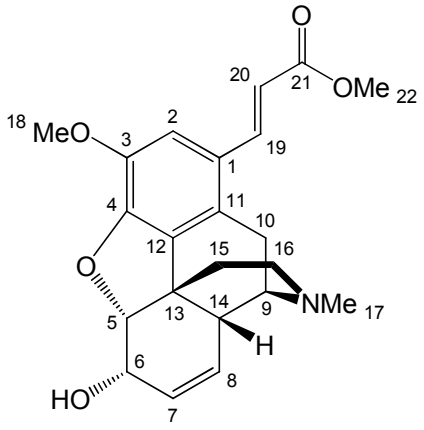

Following representative procedure 5, **159** (0.631 g, 1.17 mmol, 1 Eq), palladium acetate (0.013 g, 5 mol%), triphenylphosphine (0.061 g, 20 mol%), DMF (1 mL), NEt_3 (0.568 mL, 4.10 mmol, 3.5 Eq) and methyl acrylate (0.419 mL, 4.68 mmol, 4 Eq) gave, after treatment with TBAF (1 M solution in THF, 2.34 mL, 2.34 mmol, 2 Eq) in THF (5 mL) according to representative procedure 6 and purification by column

chromatography (SiO_2 10% MeOH/DCM, 1% NH_4OH) followed by recrystallisation in $CHCl_3$:Hexane, **140** as a white solid in 63% yield (0.283 g, 0.74 mmol).

^1H and ^{13}C NMR data in agreement with literature[74]

^1H NMR, ($CDCl_3$, 400 MHz) δ, 7.73 (d, *J* = 15.6 Hz, 1H, (H22)), 6.88 (s, 1H, (H2)), 6.17 (d, *J* = 15.6 Hz, 1H, (H23)), 5.67-5.63 (m, 1H, (H7)), 5.23-5.20 (m, 1H, (H8)), 4.87 (dd, *J* = 6.4, 1.2 Hz, 1H, (H5)), 4.14 (s, 1H, (H6)), 3.78 (s, 3H, (H18)), 3.73 (s, 3H, (H25)) 3.39-3.38 (m, 1H, (H9)), 3.08 (d, *J* = 18.8 Hz, 1H, (H10)), 2.68 (s, 1H, (H14), 2.57 (dd, *J* = 12.0, 4.4 Hz, 1H, (H16)), 2.41 (s, 3H, (H17)), 2.34-2.26 (m, 2H, (H16, H10)), 2.05 (ddd, *J* = 12.8, 12.8, 4.8 Hz, 1H, (H15)), 1.79 (dd, *J* = 12.8, 1.6 Hz, 1H, (H15))

^{13}C NMR, ($CDCl_3$, 100 MHz) δ, 167.80 (C21), 148.91 (C4), 142.80 (C3), 140.75 (C19), 133.67 (C7), 131.52 (C12), 128.12 (C8), 127.63 (C1), 125.20 (C11), 115.84 (C20), 110.47 (C2), 92.19 (C5), 66.54 (C6), 58.62 (C9), 56.15 (C18), 51.73 (C22), 46.24 (C16), 43.10 (C17) 42.96 (C13), 40.19 (C14), 35.55 (C15), 19.36 (C10)

(1*S*,5*R*,13*R*,14*S*,17*R*)-10-methoxy-4-methyl-8-[(*E*)-2-phenylethenyl]-12-oxa-4-azapentacyclo[9.6.1.$0^{1,13}$.$0^{5,17}$.$0^{7,18}$]octadeca-7,9,11(18),15-tetraen-14-ol, (155);

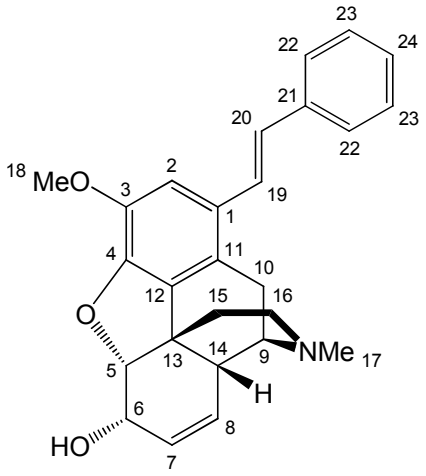

Following representative procedure 5, **159** (0.410 g, 0.76 mmol, 1 Eq), palladium acetate (0.009 g, 5 mol%), triphenylphosphine (0.040 g, 20 mol%), DMF (1 mL), NEt_3 (0.369 mL, 2.66 mmol, 3.5 Eq) and styrene (0.348 mL, 3.04 mmol, 4 Eq) gave, after treatment with TBAF (1 M solution in THF, 1.52 mL, 1.52 mmol, 2 Eq) in THF (5 mL) according to representative procedure 6 and purification by column chromatography (SiO_2 10% MeOH/DCM, 1% NH_4OH) followed by recrystallisation in $CHCl_3$:Hexane, **155** as an off white solid in 62% yield (0.188 g, 0.47 mmol).

^1H and ^{13}C NMR data in agreement with literature[74]

^1H NMR, ($CDCl_3$, 400 MHz) δ, 7.44-7.43 (m, 2H, (H22)), 7.31-7.28 (m, 2H, (H23)), 7.24.7.23 (m, 1H, (H24)), 7.05 (d, *J* = 16.0 Hz, 1H, (H19)), 6.95 (s, 1H, (H2)), 6.85 (d, *J* = 16.0 Hz, 1H, (H20)), 5.73-5.71 (m, 1H, (H7)), 5.22-5.20 (m, 1H, (H8)), 4.90 (d, *J* = 6.0 Hz, 1H, (H5)), 4.19-4.17 (m, 1H, (H6)), 3.85 (s, 3H, (H18)), 3.74 (s, 1H, (H9)), 3.10 (d, *J* = 18.8 Hz, 1H, (H10)), 3.06 (s, 1H, (H14)), 2.93 (d, *J* = 14.4 Hz, 1H, (H16)), 2.66-2.56 (m, 5H, (H17, H16, H10)), 2.34 (ddd, *J* = 12.4, 12.4, 3.6 Hz, 1H, (H15)), 1.91 (d, *J* = 12.4 Hz, 1H, (H15))

^{13}C NMR, ($CDCl_3$, 100 MHz) δ, 146.54 (C4), 142.83 (C3), 137.57 (C21), 133.91 (C7), 130.82 (C12), 128.74 (C23), 128.59 (C1), 128.19 (C8), 127.54 (C20), 126.68 (C24), 126.38 (C22), 124.51 (C19), 124.27 (C11), 109.31 (C2), 91.51 (C5), 66.35 (C6), 59.07 (C9), 56.30 (C18), 46.49 (C16), 42.83 (C17), 42.81 (C13), 39.70 (C14), 35.11 (C15), 19.72 (C10)

(1*S*,5*R*,13*R*,14*S*,17*R*)-10-methoxy-4-methyl-8-(2-phenylethynyl)-12-oxa-4-azapentacyclo[9.6.1.0^{1,13}.0^{5,17}.0^{7,18}]octadeca-7,9,11(18),15-tetraen-14-ol, (156);

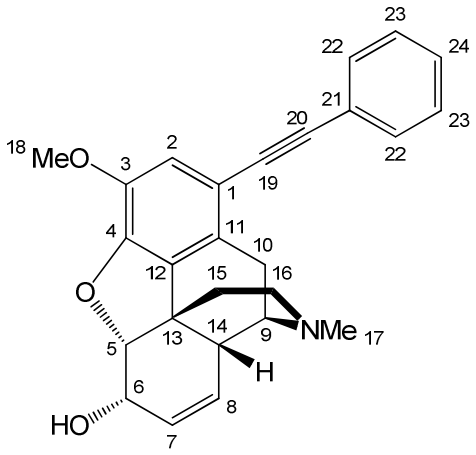

Following representative procedure 5, **159** (0.523 g, 0.97 mmol), palladium acetate (0.011 g, 5 mol%), triphenylphosphine (0.051 g, 20 mol%), DMF (1 mL), NEt_3 (0.471 mL, 3.40 mmol, 3.5 Eq) and tributyl(phenylethynyl)tin (0.407 mL, 1.16 mmol, 1.2 Eq) gave, after treatment with TBAF (1 M solution in THF, 1.94 mL, 1.94 mmol, 2 Eq) in THF (5 mL) according to representative procedure 6 and purification by column chromatography (SiO_2 10% MeOH/DCM, 1% NH_4OH) followed by recrystallisation in $CHCl_3$:Hexane, **156** as an off white solid in 48% yield (0.192 g, 0.48 mmol).

^{1}H and ^{13}C NMR data in agreement with literature[74]

^{1}H NMR, ($CDCl_3$, 400 MHz) δ, 7.45-7.43 (m, 2H, (H22), 7.29-7.23 (m, 3H, (H23, H24)), 6.80 (s, 1H, (H2)), 5.63-5.61 (m, 1H, (H7)), 5.22-5.18 (m, (H8)), 4.85 (dd, *J* = 6.4, 0.8 Hz, 1H, (H5)), 4.14-4.10 (m, 1H, (H6)), 3.74 (s, 3H, (H18)), 3.39-3.37 (m, 1H, (H9)), 3.05 (d, *J* = 19.2 Hz, 1H, (H10)), 2.66-2.64 (m, 1H, (H14)), 2.57 (dd, *J* = 12.0, 4.0 Hz, 1H, (H16)), 2.40 (s, 3H, (H17)), 2.37-2.30 (m, 2H, (H16, H10)), 2.03 (ddd *J* = 12.0, 12.0, 4.8 Hz, 1H, (H15)), 1.79 (d, *J* = 12.0 Hz, 1H, (H15))

^{13}C NMR, ($CDCl_3$, 100 MHz) δ, 147.42 (C4), 142.15 (C3), 133.52 (C7), 131.41 (C22), 131.23 (C12), 129.65 (C21), 128.42 (C23), 128.18 (C24), 128.14 (C8), 123.47 (C11),

115.84 (C2), 113.79 (C1), 92.50 (C20), 92.17 (C5), 87.42 (C19), 66.64 (C6), 58.73 (C9), 56.18 (C18), 46.24 (C16), 43.09 (C13), 42.99 (C17), 40.39 (C14), 35.41 (C15), 20.42 (C10)

(1*S*,5*R*,13*R*,14*S*,17*R*)-10-methoxy-4-methyl-8-phenyl-12-oxa-4-azapentacyclo[9.6.1.0^{1,13}.0^{5,17}.0^{7,18}]octadeca-7,9,11(18),15-tetraen-14-ol, (157);

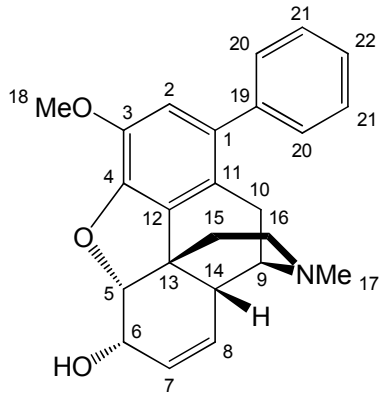

A flask was charged with **159** (0.674 g, 1.25 mmol), palladium acetate (0.014 g, 5 mol%), triphenylphosphine (0.066 g, 20 mol%), DMF (1 mL), Na_2CO_3 (0.464 g, 4.38 mmol, 3.5 Eq) and phenylboronic acid (0.305 g, 2.50 mmol, 2 Eq) and stirred under a nitrogen atmosphere at 100 °C for 20 h. After cooling the mixture was diluted with diethyl ether (5 mL), filtered and concentrated *in vacuo*. Following representative procedure 6, TBAF (1 M solution in THF, 2.50 mL, 2.5 mmol, 2 Eq) in THF (5 mL) gave, after purification by column chromatography (SiO_2 10% MeOH/DCM, 1% NH_4OH) followed by recrystallisation in $CHCl_3$:Hexane, **157** as an off white solid in 80% yield (0.375 g, 1.00 mmol).

^{1}H and ^{13}C NMR data in agreement with literature[74]

^{1}H NMR, ($CDCl_3$, 400 MHz) δ, 7.37-7.26 (m, 5H, (H20, H21, H22), 6.57 (s, 1H, (H2)), 5.72-5.69 (m, 1H, (H7)), 5.21-5.17 (m, 1H, (H8)), 4.88 (dd, *J* = 6.4, 0.8 Hz, 1H, (H5)), 4.17-4.15 (m, 1H, (H6)), 3.79 (s, 3H, (H18)), 3.33 (s, 1H, (H9)), 2.98 (d, *J* = 19.2 Hz, 1H, (H10)), 2.75-2.70 (m, 2H, (H14, H16)), 2.56-2.51 (m, 1H, (H16)), 2.42 (s, 3H,

(H17)), 2.12-2.09 (m, 2H, (H10, H15)), 1.90 (dd, *J* = 12.8, 1.6 Hz, 1H, (H15))

^{13}C NMR, ($CDCl_3$, 100 MHz) δ, 145.81 (C4), 142.06 (C3), 140.62 (C19), 134.16 (C12), 133.69 (C7), 131.13 (C11), 129.17 (C20), 128.39 (C21), 127.99 (C8), 126.93 (C22), 123.96 (C1), 114.12 (C2), 91.44 (C5), 66.46 (C6), 59.02 (C9), 56.24 (C18), 46.64 (C16), 43.22 (C13), 43.07 (C17), 40.15 (C14), 35.54 (C15), 20.42 (C10)

(1*S*,5*R*,13*R*,14*S*,17*R*)-14-[(tert-butyldimethylsilyl)oxy]-10-methoxy-4-methyl-8-[(*E*)-2-(pyridin-4-yl)ethenyl]-12-oxa-4-azapentacyclo[9.6.1.0^{1,13}.0^{5,17}.0^{7,18}]octadeca-7,9,11(18),15-tetraene, (164);

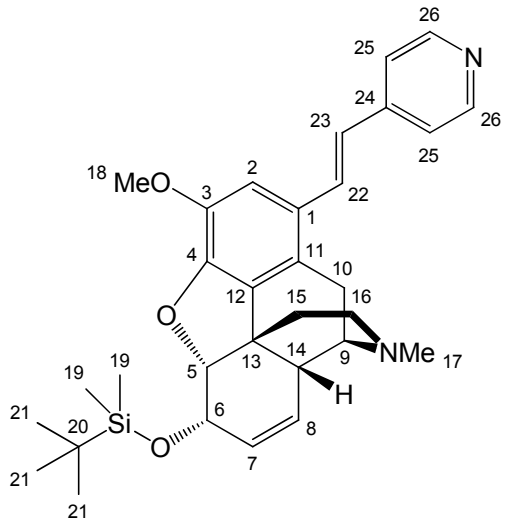

Following representative procedure 5, **159** (0.537 g, 1.00 mmol, palladium acetate (0.011 g, 5 mol%), triphenylphosphine (0.052 g, 20 mol%), DMF (1 mL), NEt_3 (0.49 mL, 3.5 mmol, 3.5 Eq) and 4-vinylpyridine (0.431 mL, 4.00 mmol, 4 Eq) gave, after purification by column chromatography (SiO_2 10% MeOH/DCM) followed by recrystallisation in $CHCl_3$:Hexane, **164** as an orange solid in 92% yield (0.475 g, 0.92 mmol).

^{1}H NMR, ($CDCl_3$, 400 MHz) δ, 8.47-8.45 (m, 2H, (H26)), 7.30 (d, *J* = 16.0 Hz, 1H, (H22)), 7.26-7.24 (m, 2H, (H25)), 6.92 (s, 1H, (H2)), 6.70 (d, *J* = 16.0 Hz, 1H, (H23)), 5.61-5.58 (m, 1H, (H7)), 5.22-5.18 (m, 1H, (H8)), 4.67 (dd, *J* = 6.4, 1.2 Hz, 1H, (H5)),

4.22-4.19 (m, 1H, (H6)), 3.84 (s, 3H, (H18)), 3.37-3.35 (m, 1H, (H9)), 3.04 (d, *J* = 18.8 Hz, 1H, (H10)), 2.61 (s, 1H, (H14)), 2.53 (dd, *J* = 12.0, 4.0 Hz, 1H, (H16)), 2.41 (s, 3H, (H17)), 2.37-2.27 (m, 2H, (H16, H10), 1.97 (ddd, *J* = 12.4, 12.4, 4.8 Hz, 1H, (H15)), 1.79 (dd, *J* = 12.4, 1.6 Hz, 1H, (H15)), 0.92 (s, 9H, (H21)), 0.13 (s, 3H, (H19)), 0.11 (s, 3H, (H19))

^{13}C NMR, ($CDCl_3$, 100 MHz) δ, 150.11 (C26), 149.07 (C24), 145.21 (C4), 142.63 (C3), 134.19 (C7), 131.65 (C12), 129.27 (C22), 127.83 (C8), 126.27 (C11), 126.18 (C1), 124.28 (C23), 120.64 (C25), 111.59 (C2), 92.75 (C5), 68.42 (C6), 58.77 (C9), 57.13 (C18), 46.37 (C16), 43.37 (C13), 43.21 (C17), 40.55 (C14), 35.84 (C15), 25.88 (C21), 19.45 (C10), 18.37 (C20), -4.54 (C19), -4.74 (C19)

IR: υ (cm^{-1}), 2928, 2854, 1589, 1325, 1252, 1201, 1174, 1129, 1117, 1101, 1084

HRMS (EI, 70eV) Calculated for $[M+H]^+$, $C_{31}H_{41}N_2O_3Si^+$, requires: 517.2886, found 517.2869, m.p. = 220-221 °C, $[\alpha]_D$ = -72° *c* = (0.10, $CHCl_3$, 589 nm, 20 °C)

(1*S*,5*R*,13*R*,14*S*,17*R*)-10-methoxy-4-methyl-8-[(*E*)-2-(pyridin-4-yl)ethenyl]-12-oxa-4-azapentacyclo[9.6.1.0^{1,13}.0^{5,17}.0^{7,18}]octadeca-7,9,11(18),15-tetraen-14-ol, (162);

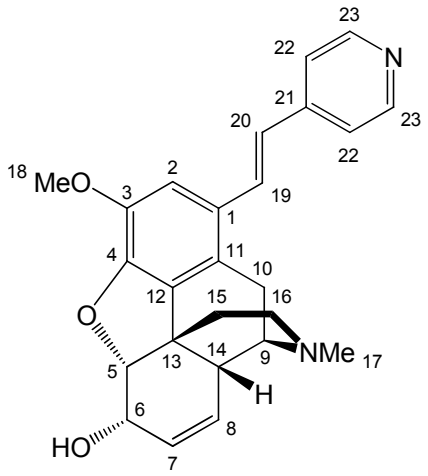

Following representative procedure 5, **159** (0.508 g, 0.94 mmol), palladium acetate (0.011 g, 5 mol%), triphenylphosphine (0.049 g, 20 mol%), DMF (1 mL), NEt_3 (0.456 mL, 3.29 mmol, 3.5 Eq) and 4-vinylpyridine (0.405 mL, 3.76 mmol, 4 Eq) gave, after

treatment with TBAF (1 M solution in THF, 1.88 mL, 1.88 mmol, 2 Eq) in THF (5 mL) according to representative procedure 6 and purification by column chromatography (SiO_2 10% MeOH/DCM, 1% NH_4OH) followed by recrystallisation in $CHCl_3$:Hexane, **162** as an off white solid in 79% yield (0.298 g, 0.74 mmol).

^{1}H NMR, ($CDCl_3$, 400 MHz) δ, 8.48-8.46 (m, 2H, (H23)), 7.31 (d, *J* = 16.0 Hz, 1H, (H19)), 7.28-7.26 (m, 2H, (H22)), 6.92 (s, 1H, (H2)), 6.72 (d, *J* = 16.0 Hz, 1H, (H20)) 5.68-5.66 (m, 1H, (H7)), 5.25-5.21 (m, 1H, (H8)), 4.86 (dd, *J* = 6.4, 1.2 Hz, 1H, (H5)), 4.15-4.12 (m, 1H, (H6)), 3.83 (s, 3H, (H18)), 3.39-3.37 (m, 1H, (H9)), 3.05 (d, *J* = 18.8 Hz, 1H, (H10)), 2.99 (s, 1H (OH)), 2.65-2.64 (m, 1H, (H14)), 2.56 (dd, *J* = 12.0, 4.0 Hz, 1H, (H16)), 2.41 (s, 3H, (H17)), 2.37-2.27 (m, 2H, (H16, H10), 2.02 (ddd, *J* = 12.4, 12.4, 5.2 Hz, 1H, (H15)), 1.81 (dd, *J* = 12.4, 1.6 Hz, 1H, (H15))

^{13}C NMR, ($CDCl_3$, 100 MHz) δ, 150.10 (C23), 147.60 (C4), 145.06 (C21), 142.78 (C3), 133.66 (C7), 131.50 (C12), 129.15 (C19), 128.19 (C8), 127.13 (C1), 126.04 (C11), 124.83 (C20), 120.71 (C22), 109.62 (C2), 92.00 (C5), 66.54 (C6), 58.69 (C9), 56.32 (C18), 46.29 (C16), 43.16 (C17), 43.10 (C13), 40.30 (C14), 35.65 (C15), 19.40 (C10)

IR: υ (cm^{-1}), 2932, 2901, 1589, 1488, 1443, 1354, 1319, 1173, 1116, 1063

HRMS (EI, 70eV) Calculated for $[M+H]^+$, $C_{25}H_{27}N_2O_3^+$, requires: 403.2016, found 403.2008, m.p. = 224-225 °C, $[\alpha]_D$ = -27° *c* = (0.10, $CHCl_3$, 589 nm, 20 °C)

(1*S*,5*R*,13*R*,14*S*,17*R*)-14-[(tert-butyldimethylsilyl)oxy]-10-methoxy-4-methyl-8-[(*E*)-2-(pyridin-2-yl)ethenyl]-12-oxa-4-azapentacyclo[9.6.1.$0^{1,13}$.$0^{5,17}$.$0^{7,18}$]octadeca-7,9,11(18),15-tetraene, (163);

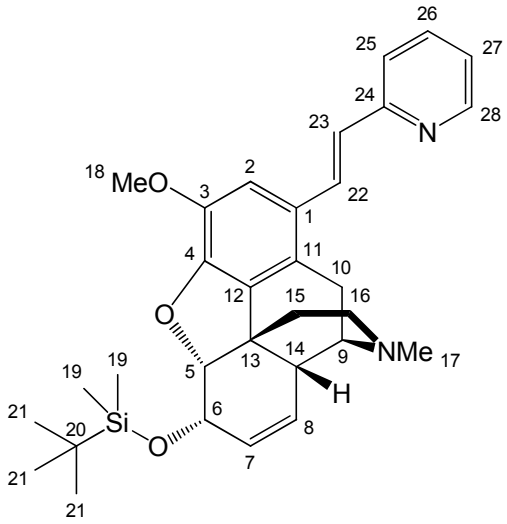

Following representative procedure 5, **159** (0.540 g, 1.00 mmol), palladium acetate (0.011 g, 5 mol%), triphenylphosphine (0.052 g, 20 mol%), DMF (1 mL), NEt_3 (0.49 mL, 3.5 mmol, 3.5 Eq) and 2-vinylpyridine (0.431 mL, 4.00 mmol, 4 Eq) gave, after purification by column chromatography (SiO_2 10% MeOH/DCM) followed by recrystallisation in $CHCl_3$:Hexane, **163** as an orange solid in 81% yield (0.419 g, 0.81 mmol).

^{1}H NMR, ($CDCl_3$, 400 MHz) δ, 8.50-8.49 (m, 1H, (H28)), 7.65 (d, *J* = 16.0 Hz, 1H (H22)), 7.55 (ddd, *J* = 7.6, 7.6, 1.6 Hz, 1H (H26)), 7.25 (d, *J* = 8.0 Hz, 1H, (H25)), 7.05-7.02 (m, 1H, (H27)), 6.98 (s, 1H, (H2)), 6.86 (d, *J* = 16.0 Hz, 1H, (H23)), 5.61-5.58 (m, 1H, (H7)), 5.20-5.16 (m, 1H, (H8)), 4.67 (dd, *J* = 6.0, 0.8 Hz, 1H, (H5)), 4.22-4.19 (m, 1H, (H6)), 3.83 (s, 3H, (H18)), 3.42-3.39 (m, 1H, (H9)), 3.12 (d, *J* = 18.8 Hz, 1H, (H10)), 2.69 (s, 1H, (H14)), 2.58 (dd, *J* = 12.0, 4.0 Hz, 1H, (H16)), 2.44 (s, 3H, (H17)), 2.42-2.35 (m, 2H, (H16, H10)), 2.03 (ddd, *J* = 12.0, 12.0, 4.8 Hz 1H, (H15)), 1.81 (d, *J* = 12.0 Hz, 1H, (H15)), 0.85 (s, 9H, (H21)), 0.07 (s, 3H, (H19)), 0.05 (s, 3H,

(H19))

^{13}C NMR, ($CDCl_3$, 100 MHz) δ, 156.00 (C24), 149.61 (C28), 148.72 (C4), 142.62 (C3), 136.53 (C26), 134.26 (C7), 131.21 (C12), 128.69 (C22), 127.53 (C8), 126.82 (C11), 126.36 (C23), 125.83 (C1), 122.07 (C25), 121.68 (C27), 111.44 (C2), 92.58 (C5), 68.41 (C6), 59.01 (C9), 56.98 (C18), 46.49 (C16), 43.25 (C13), 43.12 (C17), 40.35 (C14), 35.64 (C15), 25.90 (C21), 19.76 (C10), 18.37 (C20), -4.55 (C19), -4.75 (C19)

IR: υ (cm^{-1}), 2929, 2854, 1585, 1471, 1436, 1316, 1251, 1121

HRMS (EI, 70eV) Calculated for $[M+H]^+$, $C_{31}H_{41}N_2O_3Si^+$, requires: 517.2881, found 517.2886, m.p. = 102-104 °C, $[\alpha]_D$ = -76° *c* = (0.10, $CHCl_3$, 589 nm, 20 °C)

(1*S*,5*R*,13*R*,14*S*,17*R*)-10-methoxy-4-methyl-8-[(*E*)-2-(pyridin-2-yl)ethenyl]-12-oxa-4-azapentacyclo[9.6.1.0^{1,13}.0^{5,17}.0^{7,18}]octadeca-7,9,11(18),15-tetraen-14-ol, (165);

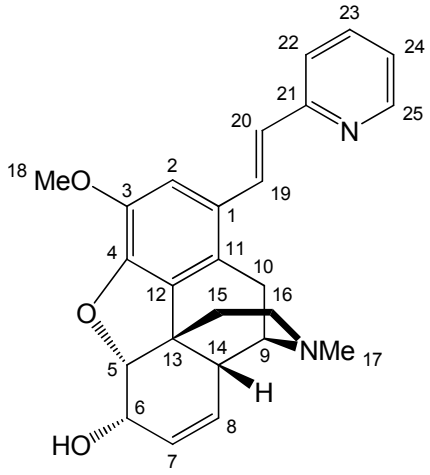

Following representative procedure 5, **159** (0.506 g, 0.94 mmol), palladium acetate (0.011 g, 5 mol%), triphenylphosphine (0.049 g, 20 mol%), DMF (1 mL), NEt_3 (0.456 mL, 3.29 mmol, 3.5 Eq) and 2-vinylpyridine (0.405 mL, 3.76 mmol, 4 Eq) gave, after treatment with TBAF (1 M solution in THF, 1.88 mL, 1.88 mmol, 2 Eq) in THF (5 mL) according to representative procedure 6 and purification by column chromatography

(SiO_2 10% MeOH/DCM, 1% NH_4OH) followed by recrystallisation in $CHCl_3$:Hexane, **165** as an off white solid in 64% yield (0.241 g, 0.60 mmol).

^{1}H NMR, ($CDCl_3$, 400 MHz) δ, 8.53-8.51 (m, 1H, (H25)), 7.67 (d, *J* = 16.0 Hz, 1H (H19)), 7.59 (ddd, *J* = 7.6, 7.6, 1.6 Hz, 1H, (H23)), 7.29 (d, *J* = 7.6 Hz, 1H, (H22)), 7.09-7.05 (m, 1H, (H24)), 7.00 (s, 1H, (H2)), 6.91 (d, *J* = 16.0 Hz, 1H, (H20)), 5.68-5.65 (m, 1H, (H7)), 5.24-5.20 (m, 1H, (H8)), 4.87 (dd, *J* = 6.4, 1.2 Hz, 1H, (H5)), 4.15-4.13 (m, 1H, (H6)), 3.83 (s, 3H, (H18)), 3.43-3.40 (m, 1H, (H9)), 3.14 (d, *J* = 18.8 Hz, 1H, (H10)), 2.70-2.68 (m, 1H, (H14)), 2.60 (dd, *J* = 12.0, 4.0 Hz, 1H, (H16)), 2.44 (s, 3H, (H17)), 2.42-2.33 (m, 2H, (H16, H10)), 2.06 (ddd, *J* = 12.8, 12.8, 5.2 Hz 1H, (H15)), 1.83 (dd, *J* = 12.8, 1.6 Hz, 1H, (H15))

^{13}C NMR, ($CDCl_3$, 100 MHz) δ, 155.82 (C21), 149.67 (C25), 147.19 (C4), 142.73 (C3), 136.61 (C23), 133.65 (C7), 131.16 (C12), 128.57 (C19), 128.04 (C8), 127.69 (C1), 126.88 (C20), 125.89 (11), 122.07 (C22), 121.88 (C24), 109.50 (C2), 91.82 (C5), 66.49 (C6), 58.85 (C9), 56.21 (C18), 46.37 (C16), 43.09 (C17), 43.00 (C13), 40.20 (C14), 35.56 (C15), 19.62 (C10)

IR: υ (cm^{-1}), 2932, 1584, 1493, 1468, 1445, 1318, 1120, 1089, 1066

HRMS (EI, 70eV) Calculated for $[M+H]^+$, $C_{25}H_{27}N_2O_3^+$, requires: 403.2022, found 403.2006, m.p. = 105-106 °C, $[\alpha]_D$ = -31° *c* = (0.10, $CHCl_3$, 589 nm, 20 °C)

6.5 Palladium Coupled "Linked" Codeine Derivatives

1,4-*bis*(1*S*,5*R*,13*R*,14*S*,17*R*)-10-methoxy-8-[(1*E*)-3-methoxy-3-oxoprop-1-en-1-yl]-4-methyl-12-oxa-4-azapentacyclo[9.6.1.0^{1,13}.0^{5,17}.0^{7,18}]octadeca-7,9,11(18),15-tetraen-14-yl benzene-1,4-dicarboxylate, (141);

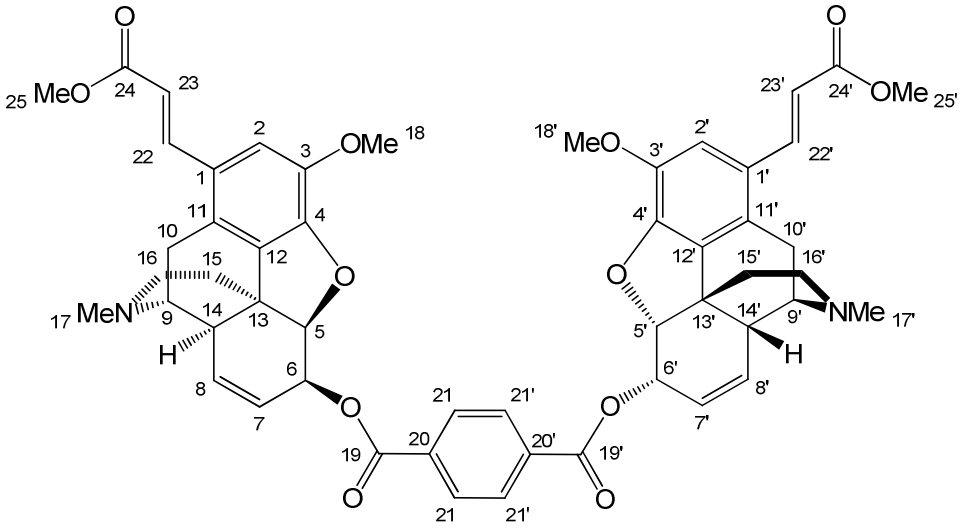

Following representative procedure 1, **140** (0.314 g, 0.82 mmol), DMAP (0.110 g, 0.90 mmol, 1.1 Eq), DCM (8 mL) and terephthaloyl dichloride, (0.083 g, 0.41 mmol, 0.5 Eq) gave, after purification by column chromatography (SiO_2 10% MeOH/DCM, 1% NH_4OH) followed by recrystallisation in acetone, **141** as a white solid in 65% yield (0.238 g, 0.27 mmol).

^{1}H NMR, ($CDCl_3$, 400 MHz) δ, 8.07 (s, 4H, (H21, H21')), 7.76 (d, *J* = 16.0 Hz, 2H, (H22, H22')), 6.91 (s, 2H, (H2, H2')), 6.18 (d, *J* = 16.0 Hz, 2H, (H23, H23')), 5.75-5.72 (m, 2H, (H7, H7')), 5.48-5.44 (m, 2H, (H8, H8')), 5.41-5.38 (m, 2H, (H6, H6')), 5.20 (d, *J* = 6.8 Hz, 2H, (H5, H5')), 3.73 (s, 6H, (H25, H25')), 3.67 (s, 6H, (H18, H18')), 3.42-3.40 (m, 2H, (H9, H9')), 3.10 (d, *J* = 18.8 Hz, 2H, (H10, H10')), 2.78 (s, 2H, (H14, H14')), 2.56 (dd, *J* = 12.0, 3.6 Hz, 2H, (H16, H16')), 2.41 (s, 6H, (H17, H17')), 2.35-2.23 (m, 4H, (H10, H10', H16, H16')), 2.04 (ddd, *J* = 12.4, 12.4, 4.8 Hz,

2H, (H15, H15')), 1.82 (d, *J* = 11.2 Hz, 2H, (H15, H15'))

^{13}C NMR, ($CDCl_3$, 100 MHz) δ(ppm), 167.84 (C24, C24'), 165.21 (C19, C19'), 149.14 (C4, C4'), 142.77 (C3, C3'), 140.82 (C22, C22'), 133.80 (C20, C20'), 131.29 (C12, C12'), 129.80 (C8, C8'), 129.78 (C21, C21'), 128.44 (C7, C7'), 127.69 (C11, C11'), 125.04 (C1, C1'), 115.73 (C23, C23'), 111.87 (C2, C2'), 88.55 (C5, C5'), 68.73 (C6, C6'), 58.78 (C9, C9'), 56.53 (C18, C18'), 51.68 (C25, C25'), 46.47 (C16, C16'), 43.14 (C17, C17), 42.67 (C13, C13'), 40.23 (C14, C14'), 35.30 (C15, C15'), 19.16 (C10, C10')

IR: υ (cm^{-1}), 2939, 1710 (C=O), 1496 (C-C, Ar), 1438, 1267, 1169, 1161, 1120, 1103, 1047, 1018

HRMS (EI, 70eV) Calculated for $[M+H]^+$, $C_{52}H_{53}N_2O_{12}^+$, requires: 897.3599, found 897.3622, m.p. = 221-223 °C, $[\alpha]_D$ = -307° *c* = (0.10, $CHCl_3$, 589 nm, 20 °C)

1,4-*bis*(1*S*,5*R*,13*R*,14*S*,17*R*)-10-methoxy-4-methyl-8-[(*E*)-2-phenylethenyl]-12-oxa-4-azapentacyclo[9.6.1.0^{1,13}.0^{5,17}.0^{7,18}]octadeca-7,9,11(18),15-tetraen-14-yl benzene-1,4-dicarboxylate, (166);

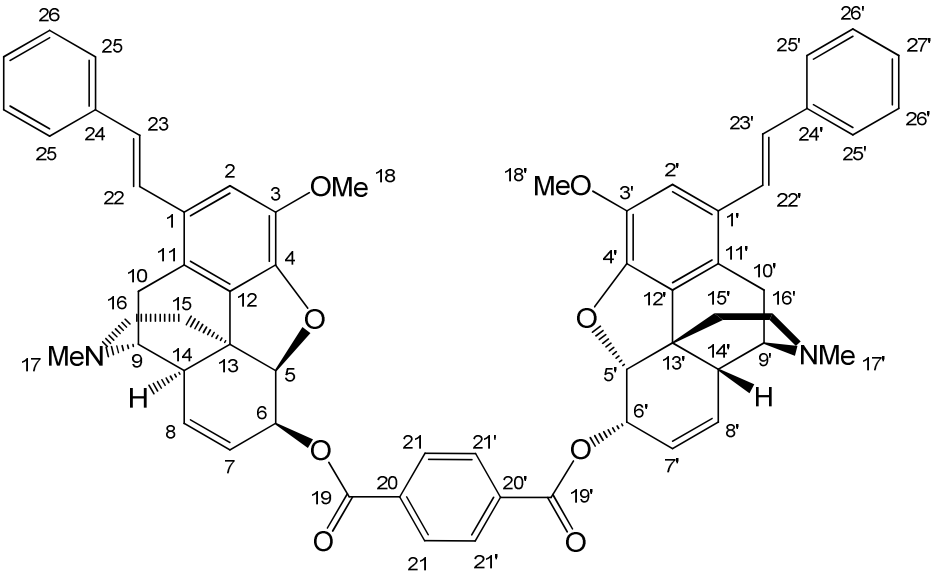

Route A;

Following representative procedure 1, **155** (0.280 g, 0.70 mmol), DMAP (0.094 g, 0.77 mmol, 1.1 Eq), DCM (8 mL) and terephthaloyl dichloride, (0.071 g, 0.35 mmol, 0.5 Eq) gave, after purification by column chromatography (SiO_2 10% MeOH/DCM, 1% NH_4OH) followed by recrystallisation in acetone, **166** as an off white solid in 56% yield (0.183 g, 0.20 mmol).

Route B;

Following representative procedure 5, **149** (0.317 g, 0.32 mmol), palladium acetate (0.007 g, 10 mol%), triphenylphosphine (0.034 g, 40 mol%), DMF (1 mL), NEt_3 (0.311 mL, 2.24 mmol, 7 Eq) and styrene (0.293 mL, 2.56 mmol, 8 Eq) gave, after purification by column chromatography (SiO_2 10% MeOH/DCM, 1% NH_4OH) followed by recrystallisation in acetone, **166** as an off white solid in 42% yield (0.126 g, 0.14 mmol).

^{1}H NMR, ($CDCl_3$, 400 MHz) δ(ppm), 8.08 (s, 4H, (H21, H21')) 7.44-7.42 (m, 4H, (H25, H25')), 7.30-7.26 (m, 4H, (H26, H26')), 7.19-7.17 (m, 2H, (H27, H27')), 7.11 (d, *J* = 16.4 Hz, 2H, (H22, H22')), 6.94 (s, 2H, (H2, H2')), 6.84 (d, *J* = 16.4 Hz, 2H, (H23, H23')), 5.75-5.73 (m, 2H, (H7, H7')), 5.48-5.45 (m, 2H, (H8, H8')), 5.40-5.38 (m, 2H, (H6, H6')), 5.17 (d, *J* = 6.8 Hz, 2H, (H5, H5')), 3.70 (s, 6H, (H18, H18')), 3.41-3.40 (m, 2H, (H9, H9')), 3.07 (d, *J* = 18.8 Hz, 2H, (H10, H10')), 2.78 (s, 2H, (H14, H14')), 2.57 (dd, *J* = 12.0 Hz, 4.0 Hz 2H, (H16, H16')) 2.42 (s, 6H, (H17, H17')), 2.37-2.29 (m, 4H, (H16, H16', H10, H10')), 2.04-2.00 (m, 2H, (H15, H15')), 1.84 (d, *J* = 12.4 Hz, 2H, (H15, H15'))

^{13}C NMR, ($CDCl_3$, 100 MHz) δ(ppm), 165.34 (C19, C19'), 146.82 (C4, C4'), 142.70 (C3, C3'), 137.78 (C24, C24'), 133.89 (C20, C20'), 130.91 (C12, C12'), 129.81 (C21, C21'), 129.78 (C8, C8'), 128.73 (C26, C26'), 128.43 (C7, C7'), 128.24 (C1, C1'), 127.85 (C23, C23'), 127.42 (C27, C27'), 126.37 (C25, C25'), 125.05 (C11, C11'), 124.72 (C22, C22'), 110.58 (C2, C2'), 88.07 (C5, C5'), 68.77 (C6, C6'), 59.05 (C9,

C9'), 56.73 (C18, C18'), 46.67 (C16, C16'), 43.14 (C17, C17'), 42.70 (C13, C13'), 40.25 (C14, C14), 35.30 (C15, C15'), 19.28 (C10, C10')

IR: υ (cm^{-1}), 2909, 1713 (C=O), 1498 (C-C, Ar), 1444, 1267, 1121, 1104, 1050, 1018

HRMS (EI, 70eV) Calculated for $[M+H]^+$, $C_{60}H_{57}N_2O_8H^+$, requires: 933.4115, found 933.4141, m.p. = 217-219 °C, $[\alpha]_D$ = -161° *c* = (0.10, $CHCl_3$, 589 nm, 20 °C)

1,4-*bis*(1*S*,5*R*,13*R*,14*S*,17*R*)-10-methoxy-4-methyl-8-[(*E*)-2-(pyridin-4-yl)ethenyl]-12-oxa-4-azapentacyclo[9.6.1.$0^{1,13}$.$0^{5,17}$.$0^{7,18}$]octadeca-7,9,11(18),15-tetraen-14-yl benzene-1,4-dicarboxylate, (167);

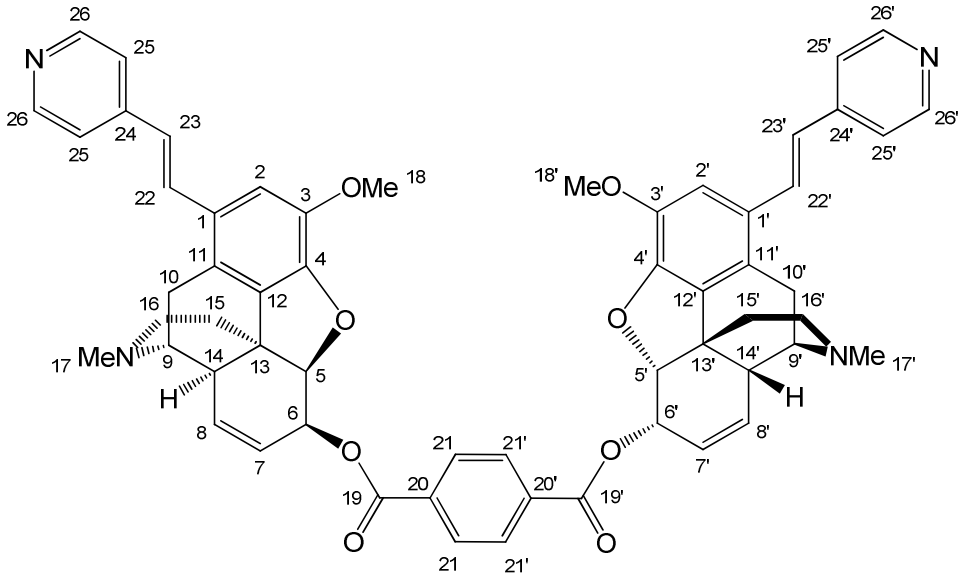

Route A;

Following representative procedure 1, **164** (0.297 g, 0.74 mmol), DMAP (0.099 g, 0.81 mmol, 1.1 Eq), DCM (8 mL) and terephthaloyl dichloride, (0.075 g, 0.37 mmol, 0.5 Eq) gave, after purification by column chromatography (SiO_2 10% MeOH/DCM, 1% NH_4OH) followed by recrystallisation in acetone, **167** as an off white solid in 57% yield (0.197 g, 0.21 mmol).

Route B;

Following representative procedure 5, **149** (0.301 g, 0.31 mmol), palladium acetate (0.007 g, 10 mol%), triphenylphosphine (0.033 g, 40 mol%), DMF (1 mL), NEt_3 (0.301 mL, 2.17 mmol, 7 Eq) and 4-vinylpyridine (0.267 mL, 2.48 mmol, 8 Eq) gave, after purification by column chromatography (SiO_2 10% MeOH/DCM, 1% NH_4OH) followed by recrystallisation in acetone, **167** as an off white solid in 49% yield (0.143 g, 0.15 mmol).

^{1}H NMR, ($CDCl_3$, 400 MHz) δ(ppm), 8.49-8.48 (m, 4H, (H26, H26')), 8.08 (s, 4H, (H21, H21')), 7.33 (d, *J* = 16.0 Hz, 2H, (H22, H22')), 7.29-7.28 (m, 4H, (H25, H25')), 6.95 (s, 2H, (H2, H2')), 6.75 (d, *J* = 16.0 Hz, 2H, (H23, H23')), 5.77-5.73 (m, 2H, (H7, H7')), 5.50-5.46 (m, 2H, (H8, H8')), 5.42-5.39 (m, 2H, (H6, H6')), 5.20 (d, *J* = 6.4 Hz, 2H, (H5, H5')), 3.70 (s, 6H, (H18, H18')), 3.48-3.45 (m, 2H, (H9, H9')), 3.09 (d, *J* = 18.4 Hz, 2H, (H10, H10')), 2.83-2.81 (s, 2H, (H14, H14')), 2.61 (dd, *J* = 12.0, 4.0 Hz 2H, (H16, H16')) 2.45 (s, 6H, (H17, H17')), 2.41-2.30 (m, 4H, (H16, H16', H10, H10')), 2.07 (ddd, *J* = 12.0, 12.0, 4.8 Hz 2H, (H15, H15')), 1.88 (d, *J* = 12.0 Hz, 2H, (H15, H15'))

^{13}C NMR, ($CDCl_3$, 100 MHz) δ(ppm), 165.26 (C19, C19'), 150.06 (C26, C26'), 147.76 (C4, C4'), 145.11 (C24, C24'), 142.83 (C3, C3'), 133.83 (C20, C20'), 131.12 (C12, C12'), 129.79 (C21, C21'), 129.65 (C8, C8'), 129.08 (C22, C22'), 128.52 (C7, C7'), 127.05 (C11, C11'), 125.74 (C1, C1'), 124.86 (C23, C23'), 120.74 (C25, C25'), 111.08 (C2, C2'), 88.21 (C5, C5'), 68.69 (C6, C6'), 58.90 (C9, C9'), 56.73 (C18, C18'), 46.55 (C16, C16'), 43.02 (C17, C17'), 42.63 (C13, C13'), 40.01 (C14, C14'), 35.11 (C15, C15'), 19.31 (C10, C10')

IR: υ (cm^{-1}), 2937, 1709 (C=O), 1589, 1489 (C-C, Ar), 1439, 1267, 1120, 1104, 1050, 1016

HRMS (EI, 70eV) Calculated for $[M+H]^+$, $C_{58}H_{55}N_4O_8^+$, requires: 935.4020, found 935.4038, m.p. = 264-266 °C, $[\alpha]_D$ = -112° *c* = (0.10, $CHCl_3$, 589 nm, 20 °C)

1,4-*bis*(1*S*,5*R*,13*R*,14*S*,17*R*)-10-methoxy-4-methyl-8-[(*E*)-2-(pyridin-2-yl)ethenyl]-12-oxa-4-azapentacyclo[9.6.1.$0^{1,13}$.$0^{5,17}$.$0^{7,18}$]octadeca-7,9,11(18),15-tetraen-14-yl benzene-1,4-dicarboxylate, (168);

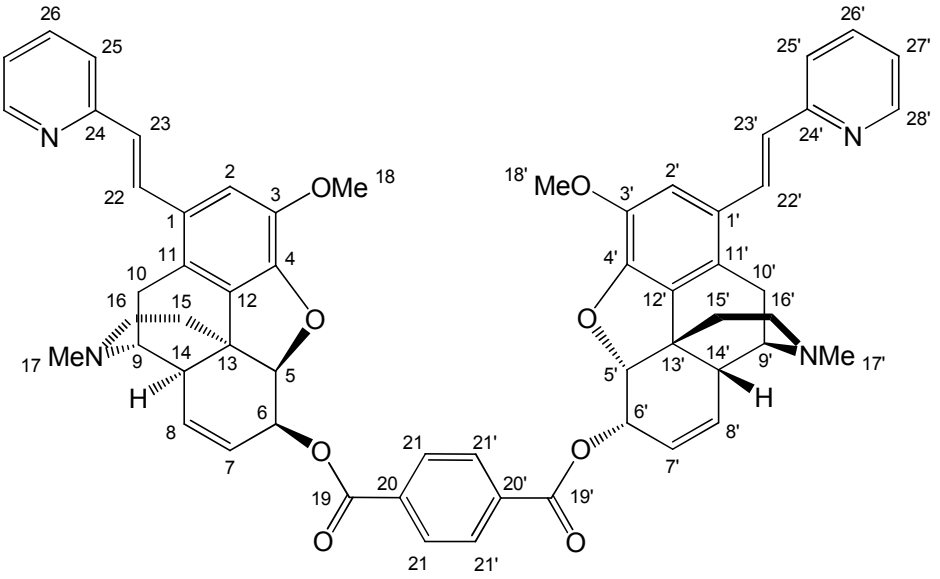

Route A;

Following representative procedure 1, **165** (0.298 g, 0.74 mmol), DMAP (0.099 g, 0.81 mmol, 1.1 Eq), DCM (8 mL) and terephthaloyl dichloride, (0.075 g, 0.37 mmol, 0.5 Eq) gave, after purification by column chromatography (SiO_2 10% MeOH/DCM, 1% NH_4OH) followed by recrystallisation in acetone, **168** as an off white solid in 49% yield (0.169 g, 0.18 mmol).

Route B;

Following representative procedure 5, **149** (0.307 g, 0.31 mmol), palladium acetate (0.007 g, 10 mol%), triphenylphosphine (0.033 g, 40 mol%), DMF (1 mL), NEt_3 (0.301 mL, 2.17 mmol, 7 Eq) and 4-vinylpyridine (0.267 mL, 2.48 mmol, 8 Eq) gave, after purification by column chromatography (SiO_2 10% MeOH/DCM, 1% NH_4OH) followed by recrystallisation in acetone, **168** as an off white solid in 44% yield (0.127 g, 0.14 mmol).

^{1}H NMR, ($CDCl_3$, 400 MHz) δ, 8.53-8.52 (m, 2H, (H28, H28')), 8.09 (s, 4H, (H21, H21')), 7.69, (d, *J* = 16.0 Hz, 2H (H22, H22')), 7.59 (ddd, *J* = 7.6, 7.6, 1.6 Hz, 2H (H26, H26')), 7.29 (d, *J* = 8.0 Hz, 2H, (H25, H25')), 7.08-7.05 (m, 2H, (H27, H27')), 7.01 (s, 2H, (H2, H2')), 6.91 (d, *J* = 16.0 Hz, 2H (H23, H23')), 5.76-5.73 (m, 2H, (H7, H7')), 5.48-5.45 (m, 2H, (H8, H8')), 5.42-5.39 (m, 2H, (H6, H6')), 5.19 (d, *J* = 6.8 Hz, 2H, (H5, H5')), 3.71 (s, 6H, (H18, H18')) 3.46-3.44 (m, 2H, (H9, H9')), 3.17 (d, *J* = 18.8 Hz, 2H, (H10, H10')), 2.83 (s, 2H, (H14, H14')), 2.60 (dd, *J* = 12.0, 4.0 Hz, 2H, (H16, H16')), 2.45 (s, 6H, (H17, H17')), 2.40-2.31 (m, 4H, (H16, H16', H10, H10')), 2.08 (ddd, *J* = 12.4, 12.4, 4.8 Hz, 2H, (H15, H15')), 1.86 (d, *J* = 11.6 Hz, 2H, (H15, H15'))

^{13}C NMR, ($CDCl_3$, 100 MHz) δ, 165.32 (C19, C19'), 155.87 (C24, C24'), 149.67 (C28, C28'), 147.46 (C4, C4'), 142.72 (C3, C3'), 136.62 (C26, C26'), 133.85 (C20, C20'), 130.90 (C12, C12'), 129.81 (C21, C21'), 129.74 (C8, C8'), 128.59 (C22, C22'), 128.42 (C7, C7'), 127.49 (C11, C11'), 126.75 (C23, C23'), 125.93 (C1, C1'), 122.16 (C25, C25'), 121.84 (C27, C27'), 110.79 (C2, C2'), 88.22 (C5, C5'), 68.80 (C6, C6'), 58.99 (C9, C9'), 56.59 (C18, C18')), 46.61 (C16, C16'), 43.13 (C17, C17'), 42.70 (C13, C13'), 40.22 (C14, C14'), 35.27 (C15, C15'), 19.42 (C10, C10')

IR: υ (cm^{-1}), 2907, 1717 (C=O), 1584, 1485 (C-C, Ar), 1469, 1443, 1248, 1120, 1102, 1049, 1018

HRMS (EI, 70eV) Calculated for $[M+H]^+$, $C_{58}H_{55}N_4O_8^+$, requires: 935.4020, found 935.4033, m.p. = 192-194 °C, $[\alpha]_D$ = -140° *c* = (0.10, $CHCl_3$, 589 nm, 20 °C)

1,4-*bis*(1*S*,5*R*,13*R*,14*S*,17*R*)-10-methoxy-4-methyl-8-(2-phenylethynyl)-12-oxa-4-azapentacyclo[9.6.1.0^{1,13}.0^{5,17}.0^{7,18}]octadeca-7,9,11(18),15-tetraen-14-yl benzene-1,4-dicarboxylate, (169);

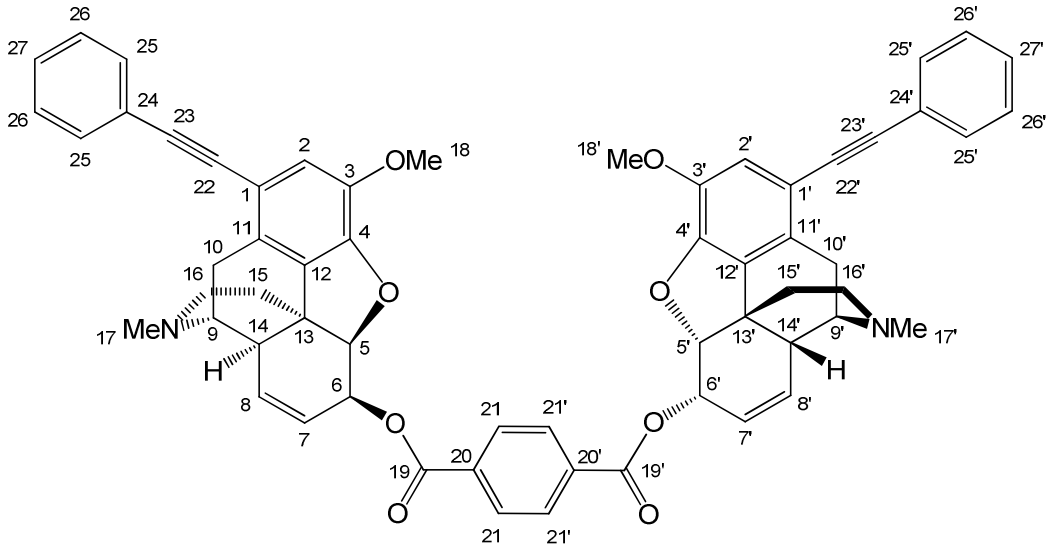

Following representative procedure 1, **156** (0.140 g, 0.35 mmol), DMAP (0.048 g, 0.39 mmol, 1.1 Eq), DCM (6 mL) and terephthaloyl dichloride, (0.037 g, 0.18 mmol, 0.5 Eq) gave, after purification by column chromatography (SiO_2 10% MeOH/DCM, 1% NH_4OH) followed by recrystallisation in acetone, **169** as an off white solid in 53% yield (0.089 g, 0.10 mmol).

^{1}H NMR Data, ($CDCl_3$, 400 MHz) δ, 8.06 (s, 4H, (H21, H21')), 7.47-7.44 (m, 4H, (H25, H25')), 7.27-7.24 (m, 6H, (H26, H26', H27, H27')), 6.81 (s, 2H, (H2, H2')), 5.72-5.68 (m, 2H, (H7, H7')), 5.47-5.43 (m, 2H, (H8, H8')), 5.41-5.38 (m, 2H, (H6, H6')), 5.17 (d, *J* = 6.4 Hz, 2H, (H5, H5')), 3.66 (s, 6H, (H18, H18')) 3.39-3.37 (m, 2H, (H9, H9')), 3.09 (d, *J* = 18.8 Hz, 2H, (H10, H10')), 2.76-2.75 (m, 2H, (H14, H14')), 2.54 (dd, *J* = 12.0, 4.0 Hz, 2H, (H16, H16')), 2.40 (s, 6H, (H17, H17')), 2.37-2.27 (H16, H16', H10, H10')) 2.02 (ddd, *J* = 12.4, 12.4, 4.8 Hz, 2H, (H15, H15')), 1.82 (d, *J* = 11.2 Hz, 2H, (H15, H15'))

^{13}C NMR, ($CDCl_3$, 100 MHz) δ(ppm), 165.30 (C19, C19'), 147.59 (C4, C4'), 142.24 (C3, C3'), 133.87 (C20, C20'), 131.44 (C25, C25'), 131.00 (C12, C12'), 129.96 (C8, C8'), 129.80 (C21, C21'), 129.75 (C24, C24'), 128.39 (C26, C26'), 128.23 (C27, C27'), 128.06 (C7, C7'), 123.62 (C11, C11'), 117.11 (C2, C2'), 113.68 (C1, C1'), 92.31 (C23, C23'), 88.42 (C5, C5'), 87.52 (C22, C22'), 68.82 (C6, C6'), 58.97 (C9, C9'), 56.57 (C18, C18'), 46.53 (C16, C16'), 43.15 (C17, C17'), 42.85 (C13, C13'), 40.62 (C14, C14'), 35.33 (C15, C15'), 20.21 (C10, C10')

IR: υ (cm^{-1}), 2908, 2204 (C≡C) 1712 (C=O), 1500 (C-C, Ar), 1440, 1267, 1248, 1204, 1120, 1104, 1050, 1019

HRMS (EI, 70eV) Calculated for $[M+H]^+$, $C_{60}H_{53}N_2O_8^+$, requires: 929.3802, found 929.3829, m.p. = 236-238 °C, $[\alpha]_D$ = -281° *c* = (0.10, $CHCl_3$, 589 nm, 20 °C)

1,4-*bis*(1*S*,5*R*,13*R*,14*S*,17*R*)-10-methoxy-4-methyl-8-phenyl-12-oxa-4-azapentacyclo[9.6.1.0^{1,13}.0^{5,17}.0^{7,18}]octadeca-7,9,11(18),15-tetraen-14-yl benzene-1,4-dicarboxylate, (170);

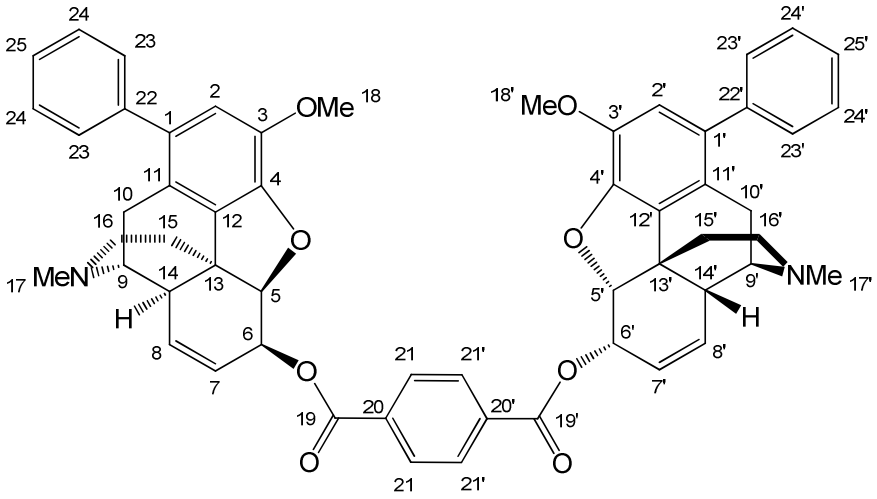

Following representative procedure 1, **157** (0.462 g, 1.23 mmol), DMAP (0.165 g, 1.35 mmol, 1.1 Eq), DCM (8 mL) and terephthaloyl dichloride, (0.126 g, 0.62 mmol, 0.5 Eq) gave, after purification by column chromatography (SiO_2 10% MeOH/DCM, 1%

NH_4OH) followed by recrystallisation in acetone, **170** as an off white solid in 61% yield (0.332 g, 0.38 mmol).

^{1}H NMR, ($CDCl_3$, 400 MHz) δ, 8.11 (s, 4H, (H21, H21')), 7.37-7.24 (m, 10H, (H23, H23', H24, H24', H25, H25')), 6.57 (s, 2H, (H2, H2')), 5.79-5.77 (m, (H7, H7')), 5.46-5.40 (m, 4H, (H8, H8', H6, H6')), 5.19 (d, *J* = 7.2 Hz, 2H, (H5, H5')), 3.67 (s, 6H, (H18, H18')) 3.33-3.31 (m, 2H, (H9, H9')), 3.00 (d, *J* = 18.4 Hz, 2H, (H10, H10')), 2.81 (s, 2H, (H14, H14')), 2.66 (dd, *J* = 12.0, 4.0 Hz, 2H, (H16, H16')), 2.46 (ddd, *J* = 12.0, 12.0, 3.2 Hz, 2H, (H16, H16')), 2.39 (s, 6H, (H17, H17')), 2.16-2.06 (m, 4H, (H10, H10', H15, H15')), 1.90 (dd, *J* = 12.8, 2.0 Hz, 2H, (H15, H15'))

^{13}C NMR, ($CDCl_3$, 100 MHz) δ(ppm), 165.37 (C19, C19'), 146.03 (C4, C4'), 142.13 (C3, C3'), 140.65 (C22, C22'), 133.91 (C20, C20'), 133.85 (C12, C12'), 130.73 (C11, C11'), 129.84 (C21, C21'), 129.63 (C8, C8'), 129.14 (C23, C23'), 128.57 (C7, C7'), 128.37 (C24, C24'), 126.86 (C25, C25'), 123.81 (C1, C1'), 115.53 (C2, C2'), 87.89 (C5, C5'), 68.85 (C6, C6'), 59.23 (C9, C9'), 56.67 (C18, C18'), 46.90 (C16, C16'), 43.05 (C17, C17'), 42.91 (C13, C13'), 40.03 (C14, C14')), 35.16 (C15, C15'), 20.29 (C10, C10')

IR: υ (cm^{-1}), 2929, 1715 (C=O), 1484 (C-C, Ar), 1448, 1339, 1265, 1242, 1149, 1123, 1104, 1051, 1018

HRMS (EI, 70eV) Calculated for $[M+H]^+$, $C_{56}H_{53}N_2O_8^+$, requires: 881.3802, found 881.3809, m.p. = 218-220 °C, $[\alpha]_D$ = -279° *c* = (0.10, $CHCl_3$, 589 nm, 20 °C)

1,3-*bis*(1*S*,5*R*,13*R*,14*S*,17*R*)-10-methoxy-4-methyl-8-phenyl-12-oxa-4-azapentacyclo[9.6.1.$0^{1,13}$.$0^{5,17}$.$0^{7,18}$]octadeca-7,9,11(18),15-tetraen-14-yl benzene-1,3-dicarboxylate, (171);

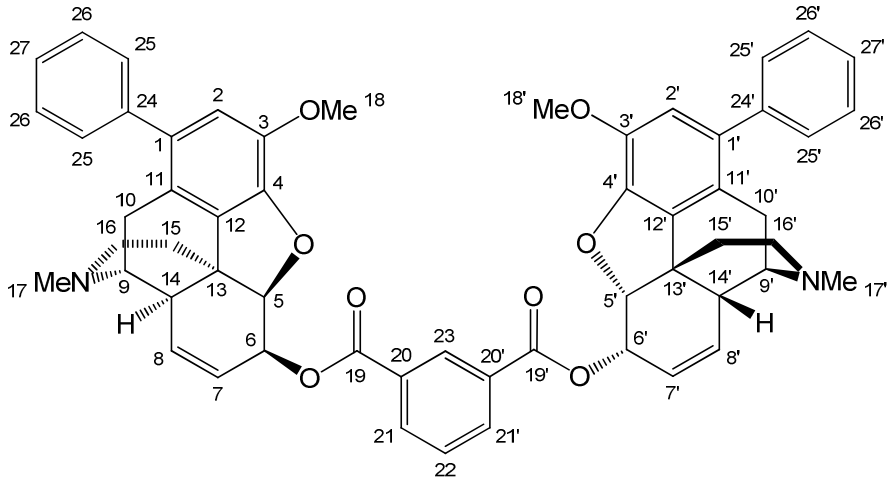

Following representative procedure 1, **157** (0.512 g, 1.36 mmol), DMAP (0.183 g, 1.50 mmol, 1.1 Eq), DCM (8 mL) and terephthaloyl dichloride, (0.138 g, 0.68 mmol, 0.5 Eq) gave, after purification by column chromatography (SiO_2 10% MeOH/DCM, 1% NH_4OH) followed by recrystallisation in $CHCl_3$:Hexane, **171** as an off white solid in 39% yield (0.236 g, 0.27 mmol).

^{1}H NMR, ($CDCl_3$, 400 MHz) δ, 8.69-8.68 (m, 1H, (H23)), 8.25 (dd, *J* = 8.0, 2.0 Hz, 2H, (H21, H21')), 7.48 (t, *J* = 8.0 Hz, 1H, (H22)), 7.36-7.24 (m, 10H, (H25, H25', H26, H26', H27, H27')), 6.57 (s, 2H, (H2)), 5.82-5.78 (m, 2H, (H7, H7')), 5.43-5.40 (m, 4H, (H8, H8', H6, H6')), 5.19 (d, *J* = 6.4 Hz, 2H, (H5, H5')), 3.64 (s, 6H, (H18, H18')) 3.36-3.34 (m, 2H, (H9, H9')), 2.98 (d, *J* = 18.8 Hz, 2H, (H10, H10')), 2.87 (s, 2H, (H14, H14)), 2.69 (dd, *J* = 12.0, 4.0 Hz 2H, (H16, H16')), 2.48 (ddd, *J* = 12.0, 12.0, 3.6 Hz, 2H, (H16, H16')), 2.41 (s, 6H, (H17, H17')), 2.20-2.10 (m, 4H, (H10, H10', H15, H15')), 1.90 (dd, *J* = 12.4, 1.6 Hz, 2H, (H15, H15'))

^{13}C NMR, ($CDCl_3$, 100 MHz) δ(ppm), 165.25 (C19, C19'), 146.07 (C4, C4'), 142.21 (C3, C3'), 140.61 (C24, C24'), 134.42 (C21, C21'), 133.85 (C20, C20'), 131.32 (C23),

130.58 (C12, C12'), 130.38 (C11, C11'), 129.24 (C8, C8') 129.14 (C26, C26'), 128.84 (C7, C7'), 128.47 (C22, C22'), 128.37 (C25, C25'), 126.86 (C27, C27'), 123.45 (C1, C1'), 115.68 (C2, C2'), 87.80 (C5, C5'), 68.77 (C6, C6'), 59.35 (C9, C9'), 56.68 (C18, C18'), 46.98 (C16, C16'), 42.95 (C17, C17'), 42.79 (C13, C13'), 39.82 (C14, C14')), 34.96 (C15, C15'), 20.37 (C10, C10')

IR: υ (cm^{-1}), 2930, 1721 (C=O), 1480 (C-C, Ar), 1446, 1230, 1142, 1049, 1018

HRMS (EI, 70eV) Calculated for $[M+H]^+$, $C_{56}H_{53}N_2O_8^+$, requires: 881.3802, found 881.3824, m.p. = 152-154 °C, $[\alpha]_D$ = -223° *c* = (0.10, $CHCl_3$, 589 nm, 20 °C)

Bibliography

1. Brownstein, M. J., *Proc. Natl. Acad. Sci. USA*, **1993**, 90, (12), 5391-5393
2. Seymour, J., Clark, D. and Winslow, M., *J. Pain Symptom Manag.*, **2005**, 29, (1), 2-13
3. Power, I., *Brit. J. Anaesth.*, **2005**, 95, (1), 43-51
4. Ballantyne, J. C., *Pain Physician.*, **2007**, 10, 479-491
5. Braenden, O. J., Eddy, N. B. and Halbach, H., *Bulletin W.H.O.***1955**, 13, 937-998
6. Eddy, N. B., Halbach, H. and Braenden, O. J., *Bulletin W.H.O.*, **1956**, 14, 353-402
7. Martin, W. R., Eades, C. G., Thompson, J. A., Huppler, R. E. and Gilbert, P. E., *J. Pharmacol. Exp. Ther.*, **1976**, 197, (3), 517-532
8. Goldstein, A. and Naidu, A., *Mol. Pharmacol.*, **1989**, 36, 265-272
9. Minami, M. and Satoh, M., *Neurosci. Res.*, **1995**, 23, 121-145
10. Cvejic, S. and Devi, L. A, *J. Biol. Chem.*, **1997**, 272, (43), 26959-26964
11. George, S. R., Fan, T., Xie, Z., Tse, R., Tam, V., Varghese, G. and O'Dowd, B. F., *J. Biol. Chem.*, **2000**, 275, 26128-26135
12. Filizola, M. and Weinstein, H., *Biopolymers*, **2002**, 66, 317-325
13. Jordan, B. A. and Devi, L. A., *Nature*, **1999**, 399, 697-700
14. Gomes J., Jordan, B. A., Gupta, J. A., Trapaidze, N., Nagy, V. and Devi, L. A., *J Neurosci.*, **2000**, 20, (RC110), 1-5
15. Gupta, A., Decaillot, F., M. and Devi, L. A., *AAPS J*, **2006**, 8, (1), E153-159
16. Pasternak, G. W., *J. Pain Symptom Manag.*, **2005**, 29, (5), 2-9
17. McFadyen, I. J., Houshyar, H., Liu-Chen, L., Woods, J. H. and Traynor, J. R., *Mol. Pharmacol.*, **2000**, 58, 669-676
18. Cepeda, M. S., Farrar, J. T., Baumgarten, M., Boston, R., Carr, D. B. and Strom, B. L., *Clin. Pharmacol. Ther.*, **2003**, 74, (2), 102-112
19. Glare, P., Walsh, D. and Sheehan, D., *Am. J. Hosp. Palliat. Me.*, **2006**, 23, 229-235
20. White, J. M. and Irvine, R. J., *Addiction*, **1999**, 94, (7), 961-972

21. Giran, L., Gyulai, Z., Antus, S., Berenyi, S. and Sipos, A., *Monatsh Chem*., **2010**, 141, 1135-1143

22. Pasquinucci, L., Prezzavento, O., Marrazzo, A., Amata, E., Ronsisvalle, S., Georgoussi, Z., Fourla, D-D., Scoto, G. M., Parenti, C., Arico, G. and Ronsisvalle, G., *Bioorg. Med. Chem*., **2010**, 18, 4975-4982

23. Chen, Z., Davies, E., Miller, W. S., Shan, S., Valenzaro, K. J. and Kyle, D. J., *Bioorg. Med. Chem. Lett*., **2004**, 14, 5275-5279

24. Duax, W. L., Smith, G. D., Griffin, J. F. and Portoghese, P. S., *Science*, **1982**, 220, 417-418

25. Sasaki, Y., Hirabuki, M., Ambo, A., Ouchi, H. and Yamamoto, Y., *Bioorg. Med. Chem. Lett*., **2001**, 11, 327-329

26. Staniszewska, R., Fichna, J., Gach, K., Toth, G., Poels, J., Broeck, J. V. and Janecka, A., *Chem. Biol. Drug Des*., **2008**, 72, 91-94

27. Eddy, N. B., *J. Pharmacol. Exp. Ther.*, **1933**, 49, (3), 319-328

28. Portoghese, P. S., *J. Med. Chem*., **1965**, 8, 609-616

29. Loew, G. H. and Berkowitz, D. S., *J. Med. Chem*., **1975**, 18, (7), 656-662

30. Osei-Gyimah, P. and Archer, S., *J. Med. Chem*., **1981**, 24, (2), 212-214

31. Bertalmio, A. J., Medzihradsky, F., Winger, G. and Woods, J. H., *J. Pharmacol. Exp. Ther.*, **1992**, 261, (1), 278-284

32. Thompson, C. M., Wojno, H., Greiner, E., May, E. L., Rice, K. C. and Selley, D. E., *J. Pharmacol. Exp. Ther.*, **2004**, 308, (2), 547-554

33. Hart, E. R. and McCawley, E. L., *J. Pharmacol*, **1944**, 82, 339-348

34. Mohacsi, E., Leimgruber, W. and Baruth, H., *J. Med. Chem*. **1982**, 25 1264-1268

35. Mignat, C., Heber, D., Schlicht, H. and Ziegler, A., *J. Pharm. Sci*., **1996**, 85, (7), 690-694

36. Cunningham, C. W., Mercer, S. L., Hassan, H. E., Traynor, H. E., Eddington, N. D. and Coop, A., *J. Med. Chem*., **2008**, 51, 2316-2320

37. Marples, B. A. and Traynor, J. R., *Pat. WO 96/16063*, **1996**

38. Reden, J., Reich, M. F., Rice, K. C., Jacobson, A. E., Brossi, A., Streaty, R. A. and Klee, W. A., *J. Med. Chem*., **1979**, 22, 256-259

39. Wentland, M. P., Duan, W., Cohen, D. J. and Bidlack, J. M., *J. Med. Chem.*, **2000**, 43, 3558-3565

40. Decker, M., Si, Y-G., Knapp, B. I., Bidlack, J. M. and Neumeyer, J. L., *J. Med. Chem.*, **2010**, 53, 402-418

41. Zhang, A., Xiong, W., Hilbert, E., DeVita, E. K., Bidlack, J. M. and Neumeyer, J. L., *J. Med. Chem.*, **2004**, 47, 1886-1888

42. Carliss, R., *WO 092337 A1*, **2005**

43. Bostros, S., Lipkowski, A. W., Larson, D. L., Stark, P. A., Takemori, A. E. and Portoghese, P. S., *J. Med. Chem*, **1989**, 32, 2068-2071

44. Derrick, I., Moynihan, H. A., Broadbear, J., Woods, J. H. and Lewis, J. W., *Bioorg. Med. Chem. Lett.*, **1996**, 6, (2), 167-172

45. Ghirmai, S., Azar, M. R. and Cashman, J. R., *Bioorg. Med. Chem.*, **2009**, 17, 6671-6681

46. Pasternak, G. W. and Hahn, E. F., *J. Med. Chem.*, **1980**, 23, 674-676

47. Hahn, E. F., Itzhak, Y., Nishimura, S., Johnson, N. and Pasternak, G. W., *J. Pharmacol. Exp. Ther.*, **1985**, 235, (3), 846-850

48. Lousberg., R. J. J. and Weiss, U., *Experientia*, **1974**, 30, (12), 1440-1441

49. Mohacsi, E., O'Brien, J., Bount, J. and Sepinwall, J., *J. Med. Chem.*, **1985**, 28, (9), 1177-1180

50. Peng, X., Knapp, B. I., Bidlack, J. M. and Neumeyer, J. L., *Bioorg. Med. Chem.*, **2007**, 15, 4106-4112

51. Messer, W. S., *Curr. Pharm. Design*, **2004**, 10, 2015-2020

52. Portoghese, P. S., *J. Med. Chem.*, **2001**, 44, (14), 2259-2269

53. Ballet, S., Pietsch, M. and Abell, A. D., *Protein Peptide Lett.*, **2008**, 15, 668-682

54. Lenard, N. R., Daniels, D. J., Portoghese, P. S. and Roerig S. C., *Eur. J. Pharmacol.*, **2007**, 566, 75-82

55. Gao, Y., Liu, X., Wei, J., Zhu, B., Chen, Q. and Wang, R., *Bioorg. Med. Chem. Lett.* **2005**, 15, 1847-1850

56. Daniel, D. J., Kulkarni, A., Xie, Z., Bhushan, R. G. and Portoghese, P. S., *J. Med. Chem.*, **2005**, 48, 1713-1716

57. Mathews, J. L., Fulton, B. S., Negus, S. S., Neumeyer, J. L. and Bidlack, J. M., *Neurochem. Res*., **2008**, 33, 2142-2150

58. Neumeyer, J. L., Zhang, A., Xiong, W., Gu, X-H., Hilbert, J. E., Knapp, B. I., Negus, S. S., Mello, N. K. and Bidlack, J. M., *J. Med. Chem*., **2003**, 46, 5162-5170

59. Fulton, B. S., Knapp, B. L., Bidlack, J. M. and Neumeyer, J. L., *Bioorg. Med. Chem. Lett*., **2010**, 20, 1507-1509

60. Decker, M., Fulton, B. S., Zhang, B., Knapp, B. I., Bidlack, J. M. and Neumeyer, J. L., *J. Med. Chem*., **2009**, 52, 7389-7396

61. Peng, X., Knapp, B. I., Bidlack, J. M. and Neumeyer, J. L., *J. Med. Chem*., **2006**, 49, 256-262

62. Erez, M., Takemori, A. E. and Portoghese, P. S.*, J. Med. Chem*. **1982**, 25, 847-849

63. Portoghese, P. S., Ronsisvalle, G., Larson, D. L. and Takemori, A. E., *J. Med. Chem*. **1986**, 29, 1650-1653

64. Portoghese, P. S., Larson, D. L., Sayre, L. M., Yim, C. B., Ronsisvalle, G., Tam, S. W. and Takemori, A. E., *J. Med. Chem*., **1986**, 29, 1855-1861

65. Hahn, E. F., Carrol-Buatti, M. and Pasternak, G. W., *J. Neurosci*., **1982**, 2, (5), 572-576

66. Hahn, E. F., Nishimura, S., Goodman, R. R. and Pasternak, G. W., *J. Pharmacol. Exp. Ther.*, **1985**, 235, (3), 839-845

67. Fishburn, J., Simone, C., Riely, T. A., Zacarias, A. and Gursahani, H., *PCT, WO 2010/033195 A1*, **2010**

68. Hartmann, M., Stimmeder, D., Engelsen, S., Koch, A., Rovenszky, F., Kremminger, P. and Hutzinger, M., *PCT WO 97/22606*, **1997**

69. Frensch, K., Voegtle, F., *Liebigs Ann. Chem.*, **1979**, 12, 2118-2120

70. Kowalska, E., *Thesis*, *Dublin City University*, Chiral Macrocycles based on the Morphine Scaffold, **2008**

71. Canfield, D. V., Barrick, J. and Giessen, B. C., *Acta Cryst. (Section C)*, **1987**, C43, (5), 977

72. Mackay, M. and Hodgkin, D. C., *Jou. Chem. Soc*., **1955**, 3261-3267

73. Wilson, M. L., Carroll, P. J. and Dalton, D. R., *J. Org. Chem*., **2005**, 70, 6492-6495

74. Davies, S. G., Goodwin, C. J., Pyatt, D. and Smith, A. D., *J. Chem. Soc. Perkin Trans. 1*, **2001**, 1413-1420

75. Heck, R. F. and Nolley, J. P., *J. Org. Chem.*, **1972** 37, (14), 2320-2322

76. Milstein, D. and Stille, J. K., *J. Am. Chem. Soc.,* **1978** 100, (11), 3636-3638

77. Miyaura, N., Yamada, K. and Suzuki, A., *Tetrahedron. Lett.*, **1979**, (36), 3437-3440

78. Jenkins, S. M., Ehman, K. and Barone, S., *Dev. Brain Res*., **2004**, 151, 1-12

79. Yang, Y., Su., C., Huang, X. and Liu, Q., *Tetrahedron Lett*., **2009**, 50, 5754-5756

80. Carless, H. A. J. and Haywood, D. J., *J. Chem. Soc. Chem. Commun*., **1980**, 980-981

81. Ferguson, J. R., Hollis, S. J., Johnston, G. A., Lumbard, K. W. and Stachulski, A. V., *J. Label. Compd. Radiopharm*., **2002**, 45, 107-113

82. Unterwald, E. M., Rubenfeld, J. M., Imai, Y., Wang, J-B., Uhi, G. R. and Kreek, M. J., *Mol. Brain Res.*, **1995**, 33, 351-355

83. Ioja, E., Toth, G., Benyhe, S., Tourwe, D., Peter, A., Tomboly, C. and Borsodi, A., *Neurosignals*, **2005**, 14, 317-328

84. Martin, T. J., Dworkin, S. J. and Smith, J. E., *J. Pharmacol. Exp. Ther.*, **1993**, 267, 506-514

85. Pasternak, G. W., Wilson, H. A. and Snyder, S. H., *Mol. Pharmacol.,* **1975**, 11, 340-351

86. Benyhe, S., Farkas, J., Toth, G. and Wollenmann, M., *J. Neurosci. Res*, **1997**, 48, 249-258

87. Bradford, M. M., *Anal. Biochem*., **1976**, 72, 248-254

88. Deegan, B., *Thesis*, *Dublin City University*, Working Towards Alkaloid Macrocycles, **2009**

89. Chen, Z. R., Irvine, R. J., Somogyi, A. A. and Bochner, F., *Life Sci.*, **1991**, 48, (22), 2165-2171

90. Morphy, R., Kay, C. and Rankovic, Z., *Drug Discov. Today*, **2004**, 9, (15), 641-651

91. Morphy, R. and Rankovic, Z., *J. Med. Chem*., **2005**, 48, (21), 6523-6543

92. Espinoza-Fonseca, M. L., *Bioorg. Med. Chem*., **2006**, 14, 896-879

93. Daniels, D. J., Kulkarni, A., Xie, Z., Bhushan, R. G. and Portoghese, P. S., *J. Med. Chem*, **2005**, 48, 1713-1716

94. Pedersen, C. J., *J. Am. Chem. Soc.*, **1970**, 92, (2), 391-394

95. Marcos, P. M., Ascenso, J. R. and Cragg, P. J., *Suprmol.. Chem*., **2007**, 19, (3), 199-206

96. Nazarenko, A. Y., Baulin, V. L., Lamb, J. D., Volkova, T. A., Varnek, A. A. and Wipff, G., *Solvent Extr. Ion. Exc*, **1999**, 17, (3), 495-523

97. Hosztafi, S. and Makleit, S., *Synthetic Commun.*, **1994**, 24, (21), 3031-3045

98. Liebman, A. A., Malarek, D. H., Blount, J. F., Nelson, N. R. and Delaney, C. M., *J. Org. Chem.*, **1978**, 43, (4), 737-739

99. Seltzman, H. H., Roche, M., Laudeman, C. P., Wyrick, C. D. J. and Carroll, F. I., *J. Labelled Compd. Rad*., **1998**, XLI, 811-821

100. Singh, B. B., Chauhan, R. S., Madyastha, K. M., Bhatnagar, S. P., Kirk, K. L. and Weiss, U., *Heterocycles*, **1982**, 19, (5), 837-847

101. Arenzo, H. B., Barton, D. H. R., Davies, S. G., Lusinchi, X., Meunier, B. and Pascard, C., *Nouv. J. Chim.*, **1980**, 4, (6), 369-375

Appendix A

A.1 X-ray crystal data of 126

1,3-*bis*(1*S*,5*R*,13*R*,14*S*,17*R*)-10-methoxy-4-methyl-12-oxa-4-azapentacyclo[9.6.1.$0^{1,13}$.$0^{5,17}$.$0^{7,18}$]octadeca-7,9,11(18),15-tetraen-14-yl benzene-1,3-dicarboxylate, (126);

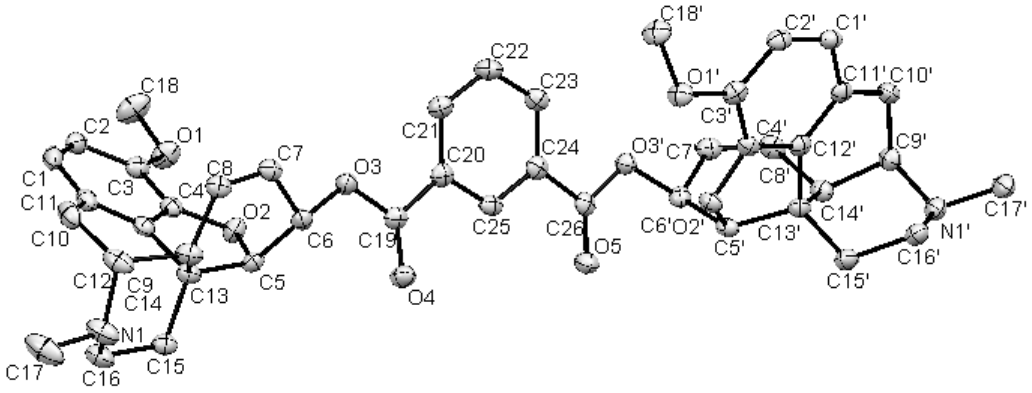

Fig A.1 ORTEP diagram of **126** with atom labels

Formula	$C_{44}H_{44}N_2O_8$
Space Group	P 2_1
Cell Lengths (Å)	**a** 8.7535(4) **b** 12.4059(5) **c** 16.6518(7)
Cell Angles (°)	**α** 90 **β** 100 **γ** 90
Cell Volume (Å^3)	1780.83
Z, Z’	**Z**: 2 **Z'**: 0
R-Factor (%)	3.3

Table A.1 X-ray crystal data for **126**

Number	Atom1	Atom2	Length (Å)
1	C1	H1	0.949(2)
2	C1	C2	1.405(2)
3	C1	C11	1.394(2)
4	C2	H2	0.951(2)
5	C2	C3	1.405(3)
6	C3	C4	1.387(2)
7	C3	O1	1.365(2)
8	C4	O2	1.381(2)
9	C4	C12	1.373(2)
10	O2	C5	1.465(2)
11	C5	H5	1.000(2)
12	C5	C6	1.544(2)
13	C5	C13	1.548(2)
14	C6	H6	1.001(2)
15	C6	C7	1.505(2)
16	C6	O3	1.445(2)
17	C7	H7	0.950(2)
18	C7	C8	1.322(2)
19	C8	H8	0.950(2)
20	C8	C14	1.506(2)
21	C9	H9	1.000(2)
22	C9	C10	1.555(3)
23	C9	C14	1.537(3)
24	C9	N1	1.474(2)
25	C10	H10A	0.990(2)
26	C10	H10B	0.990(2)
27	C10	C11	1.517(2)
28	C11	C12	1.381(2)
29	C12	C13	1.494(2)
30	C13	C14	1.551(2)
31	C13	C15	1.538(2)
32	C14	H14	1.000(2)
33	C15	H15A	0.991(2)
34	C15	H15B	0.991(2)
35	C15	C16	1.517(3)
36	C16	H16A	0.990(2)
37	C16	H16B	0.990(2)
38	C16	N1	1.459(2)
39	N1	C17	1.447(3)
40	C17	H17A	0.980(2)
41	C17	H17B	0.980(2)
42	C17	H17C	0.980(3)

43	O1	C18	1.423(2)
44	C18	H18A	0.981(2)
45	C18	H18B	0.980(2)
46	C18	H18C	0.980(2)
47	O3	C19	1.347(2)
48	C19	O4	1.206(2)
49	C19	C20	1.490(2)
50	C20	C21	1.393(2)
51	C20	C25	1.392(2)
52	C21	H21	0.949(2)
53	C21	C22	1.392(3)
54	C22	H22	0.950(2)
55	C22	C23	1.388(3)
56	C23	H23	0.950(2)
57	C23	C24	1.393(2)
58	C24	C25	1.389(2)
59	C24	C26	1.490(2)
60	C25	H25	0.950(1)
61	C1'	H1'	0.950(2)
62	C1'	C2'	1.386(3)
63	C1'	C11'	1.398(2)
64	C2'	H2'	0.950(2)
65	C2'	C3'	1.408(2)
66	C3'	C4'	1.393(2)
67	C3'	O1'	1.368(2)
68	C4'	O2'	1.382(2)
69	C4'	C12'	1.374(2)
70	O2'	C5'	1.463(2)
71	C5'	H5'	1.000(2)
72	C5'	C6'	1.564(2)
73	C5'	C13'	1.544(2)
74	C6'	H6'	1.000(2)
75	C6'	C7'	1.491(2)
76	C6'	O3'	1.455(2)
77	C7'	H7'	0.951(2)
78	C7'	C8'	1.328(2)
79	C8'	H8'	0.950(2)
80	C8'	C14'	1.500(2)
81	C9'	H9'	1.000(2)
82	C9'	C10'	1.552(2)
83	C9'	C14'	1.547(2)
84	C9'	N1'	1.476(2)
85	C10'	H10C	0.990(2)
86	C10'	H10D	0.990(2)
87	C10'	C11'	1.508(2)

88	C11'	C12'	1.384(2)
89	C12'	C13'	1.507(2)
90	C13'	C14'	1.537(2)
91	C13'	C15'	1.534(2)
92	C14'	H14'	1.001(1)
93	C15'	H15C	0.991(2)
94	C15'	H15D	0.990(2)
95	C15'	C16'	1.521(3)
96	C16'	H16C	0.991(2)
97	C16'	H16D	0.990(2)
98	C16'	N1'	1.469(2)
99	N1'	C17'	1.462(2)
100	C17'	H17D	0.980(2)
101	C17'	H17E	0.980(2)
102	C17'	H17F	0.980(2)
103	O1'	C18'	1.432(2)
104	C18'	H18D	0.980(2)
105	C18'	H18E	0.980(2)
106	C18'	H18F	0.980(2)
107	O3'	C26	1.346(2)
108	C26	O5	1.201(2)

Table A.2 Bond length data for **126**

Number	**Atom1**	**Atom2**	**Atom3**	**Angle (°)**
1	H1	C1	C2	119.3(2)
2	H1	C1	C11	119.3(2)
3	C2	C1	C11	121.5(2)
4	C1	C2	H2	119.4(2)
5	C1	C2	C3	121.3(2)
6	H2	C2	C3	119.3(2)
7	C2	C3	C4	116.1(2)
8	C2	C3	O1	126.2(2)
9	C4	C3	O1	117.6(1)
10	C3	C4	O2	126.0(1)
11	C3	C4	C12	121.3(1)
12	O2	C4	C12	112.6(1)
13	C4	O2	C5	106.7(1)
14	O2	C5	H5	109.0(1)
15	O2	C5	C6	111.6(1)
16	O2	C5	C13	106.7(1)
17	H5	C5	C6	109.0(1)
18	H5	C5	C13	109.0(1)
19	C6	C5	C13	111.4(1)
20	C5	C6	H6	107.8(1)

21	C5	C6	C7	114.3(1)
22	C5	C6	O3	112.3(1)
23	H6	C6	C7	107.7(1)
24	H6	C6	O3	107.8(1)
25	C7	C6	O3	106.6(1)
26	C6	C7	H7	119.9(2)
27	C6	C7	C8	120.2(1)
28	H7	C7	C8	119.9(2)
29	C7	C8	H8	120.1(2)
30	C7	C8	C14	119.7(1)
31	H8	C8	C14	120.2(2)
32	H9	C9	C10	107.3(2)
33	H9	C9	C14	107.2(2)
34	H9	C9	N1	107.3(2)
35	C10	C9	C14	112.7(1)
36	C10	C9	N1	115.8(2)
37	C14	C9	N1	106.2(1)
38	C9	C10	H10A	108.4(2)
39	C9	C10	H10B	108.3(2)
40	C9	C10	C11	115.5(2)
41	H10A	C10	H10B	107.5(2)
42	H10A	C10	C11	108.3(2)
43	H10B	C10	C11	108.4(2)
44	C1	C11	C10	126.5(2)
45	C1	C11	C12	115.6(2)
46	C10	C11	C12	117.6(1)
47	C4	C12	C11	123.4(2)
48	C4	C12	C13	109.8(1)
49	C11	C12	C13	126.6(1)
50	C5	C13	C12	100.5(1)
51	C5	C13	C14	116.8(1)
52	C5	C13	C15	111.2(1)
53	C12	C13	C14	106.8(1)
54	C12	C13	C15	111.2(1)
55	C14	C13	C15	109.9(1)
56	C8	C14	C9	115.2(1)
57	C8	C14	C13	109.1(1)
58	C8	C14	H14	108.6(1)
59	C9	C14	C13	106.5(1)
60	C9	C14	H14	108.6(2)
61	C13	C14	H14	108.6(1)
62	C13	C15	H15A	109.2(1)
63	C13	C15	H15B	109.2(1)
64	C13	C15	C16	112.2(1)
65	H15A	C15	H15B	107.9(2)

66	H15A	C15	C16	109.1(1)
67	H15B	C15	C16	109.2(1)
68	C15	C16	H16A	109.4(2)
69	C15	C16	H16B	109.4(2)
70	C15	C16	N1	111.1(1)
71	H16A	C16	H16B	108.0(2)
72	H16A	C16	N1	109.4(2)
73	H16B	C16	N1	109.4(2)
74	C9	N1	C16	112.5(1)
75	C9	N1	C17	113.5(2)
76	C16	N1	C17	111.3(2)
77	N1	C17	H17A	109.5(2)
78	N1	C17	H17B	109.5(2)
79	N1	C17	H17C	109.4(2)
80	H17A	C17	H17B	109.5(2)
81	H17A	C17	H17C	109.5(2)
82	H17B	C17	H17C	109.5(2)
83	C3	O1	C18	116.8(1)
84	O1	C18	H18A	109.5(2)
85	O1	C18	H18B	109.5(2)
86	O1	C18	H18C	109.4(2)
87	H18A	C18	H18B	109.5(2)
88	H18A	C18	H18C	109.5(2)
89	H18B	C18	H18C	109.5(2)
90	C6	O3	C19	116.5(1)
91	O3	C19	O4	123.5(2)
92	O3	C19	C20	111.9(1)
93	O4	C19	C20	124.5(2)
94	C19	C20	C21	122.4(1)
95	C19	C20	C25	117.6(1)
96	C21	C20	C25	119.8(2)
97	C20	C21	H21	120.2(2)
98	C20	C21	C22	119.7(2)
99	H21	C21	C22	120.2(2)
100	C21	C22	H22	119.6(2)
101	C21	C22	C23	120.6(2)
102	H22	C22	C23	119.7(2)
103	C22	C23	H23	120.2(2)
104	C22	C23	C24	119.5(2)
105	H23	C23	C24	120.3(2)
106	C23	C24	C25	120.2(2)
107	C23	C24	C26	123.3(1)
108	C25	C24	C26	116.5(1)
109	C20	C25	C24	120.1(2)
110	C20	C25	H25	119.9(2)

111	C24	C25	H25	119.9(2)
112	H1'	C1'	C2'	119.1(2)
113	H1'	C1'	C11'	119.2(2)
114	C2'	C1'	C11'	121.7(2)
115	C1'	C2'	H2'	119.0(2)
116	C1'	C2'	C3'	121.9(2)
117	H2'	C2'	C3'	119.1(2)
118	C2'	C3'	C4'	116.0(1)
119	C2'	C3'	O1'	125.5(1)
120	C4'	C3'	O1'	118.4(1)
121	C3'	C4'	O2'	126.9(1)
122	C3'	C4'	C12'	121.0(1)
123	O2'	C4'	C12'	111.9(1)
124	C4'	O2'	C5'	104.8(1)
125	O2'	C5'	H5'	109.8(1)
126	O2'	C5'	C6'	109.3(1)
127	O2'	C5'	C13'	104.9(1)
128	H5'	C5'	C6'	109.8(1)
129	H5'	C5'	C13'	109.9(1)
130	C6'	C5'	C13'	113.1(1)
131	C5'	C6'	H6'	107.8(1)
132	C5'	C6'	C7'	116.3(1)
133	C5'	C6'	O3'	110.1(1)
134	H6'	C6'	C7'	107.7(1)
135	H6'	C6'	O3'	107.8(1)
136	C7'	C6'	O3'	106.8(1)
137	C6'	C7'	H7'	118.1(2)
138	C6'	C7'	C8'	123.8(1)
139	H7'	C7'	C8'	118.1(2)
140	C7'	C8'	H8'	118.9(2)
141	C7'	C8'	C14'	122.0(1)
142	H8'	C8'	C14'	119.0(2)
143	H9'	C9'	C10'	107.0(1)
144	H9'	C9'	C14'	106.9(1)
145	H9'	C9'	N1'	107.0(1)
146	C10'	C9'	C14'	112.4(1)
147	C10'	C9'	N1'	115.4(1)
148	C14'	C9'	N1'	107.7(1)
149	C9'	C10'	H10C	108.7(1)
150	C9'	C10'	H10D	108.6(1)
151	C9'	C10'	C11'	114.7(1)
152	H10C	C10'	H10D	107.6(2)
153	H10C	C10'	C11'	108.5(1)
154	H10D	C10'	C11'	108.6(1)
155	C1'	C11'	C10'	126.3(1)

156	C1'	C11'	C12'	115.4(1)
157	C10'	C11'	C12'	118.1(1)
158	C4'	C12'	C11'	123.8(1)
159	C4'	C12'	C13'	109.0(1)
160	C11'	C12'	C13'	126.8(1)
161	C5'	C13'	C12'	98.8(1)
162	C5'	C13'	C14'	118.0(1)
163	C5'	C13'	C15'	111.6(1)
164	C12'	C13'	C14'	108.1(1)
165	C12'	C13'	C15'	112.0(1)
166	C14'	C13'	C15'	108.0(1)
167	C8'	C14'	C9'	113.2(1)
168	C8'	C14'	C13'	110.8(1)
169	C8'	C14'	H14'	108.6(1)
170	C9'	C14'	C13'	106.6(1)
171	C9'	C14'	H14'	108.8(1)
172	C13'	C14'	H14'	108.7(1)
173	C13'	C15'	H15C	109.5(1)
174	C13'	C15'	H15D	109.4(1)
175	C13'	C15'	C16'	110.8(1)
176	H15C	C15'	H15D	108.1(2)
177	H15C	C15'	C16'	109.4(2)
178	H15D	C15'	C16'	109.6(2)
179	C15'	C16'	H16C	109.3(2)
180	C15'	C16'	H16D	109.3(2)
181	C15'	C16'	N1'	111.7(1)
182	H16C	C16'	H16D	107.9(2)
183	H16C	C16'	N1'	109.3(1)
184	H16D	C16'	N1'	109.3(1)
185	C9'	N1'	C16'	113.9(1)
186	C9'	N1'	C17'	112.6(1)
187	C16'	N1'	C17'	109.4(1)
188	N1'	C17'	H17D	109.5(2)
189	N1'	C17'	H17E	109.4(2)
190	N1'	C17'	H17F	109.5(2)
191	H17D	C17'	H17E	109.5(2)
192	H17D	C17'	H17F	109.5(2)
193	H17E	C17'	H17F	109.4(2)
194	C3'	O1'	C18'	115.9(1)
195	O1'	C18'	H18D	109.5(2)
196	O1'	C18'	H18E	109.5(2)
197	O1'	C18'	H18F	109.4(2)
198	H18D	C18'	H18E	109.4(2)
199	H18D	C18'	H18F	109.5(2)
200	H18E	C18'	H18F	109.5(2)

201	C6'	O3'	C26	114.1(1)
202	C24	C26	O3'	112.4(1)
203	C24	C26	O5	124.0(1)

Table A.3 Bond angle data for **126**

Number	Atom1	Atom2	Atom3	Atom4	Torsion (°)
1	H1	C1	C2	H2	-3.8(3)
2	H1	C1	C2	C3	176.2(2)
3	C11	C1	C2	H2	176.2(2)
4	C11	C1	C2	C3	-3.9(3)
5	H1	C1	C11	C10	-6.5(3)
6	H1	C1	C11	C12	180.0(2)
7	C2	C1	C11	C10	173.6(2)
8	C2	C1	C11	C12	0.0(2)
9	C1	C2	C3	C4	0.7(2)
10	C1	C2	C3	O1	-178.1(2)
11	H2	C2	C3	C4	-179.3(2)
12	H2	C2	C3	O1	1.9(3)
13	C2	C3	C4	O2	-172.6(1)
14	C2	C3	C4	C12	6.2(2)
15	O1	C3	C4	O2	6.3(2)
16	O1	C3	C4	C12	-174.9(1)
17	C2	C3	O1	C18	5.7(2)
18	C4	C3	O1	C18	-173.1(2)
19	C3	C4	O2	C5	172.5(2)
20	C12	C4	O2	C5	-6.4(2)
21	C3	C4	C12	C11	-10.7(3)
22	C3	C4	C12	C13	174.5(1)
23	O2	C4	C12	C11	168.3(1)
24	O2	C4	C12	C13	-6.6(2)
25	C4	O2	C5	H5	133.7(1)
26	C4	O2	C5	C6	-105.7(1)
27	C4	O2	C5	C13	16.1(2)
28	O2	C5	C6	H6	-152.9(1)
29	O2	C5	C6	C7	87.4(2)
30	O2	C5	C6	O3	-34.3(2)
31	H5	C5	C6	H6	-32.4(2)
32	H5	C5	C6	C7	-152.1(1)
33	H5	C5	C6	O3	86.2(2)
34	C13	C5	C6	H6	88.0(2)
35	C13	C5	C6	C7	-31.8(2)
36	C13	C5	C6	O3	-153.4(1)
37	O2	C5	C13	C12	-18.8(1)
38	O2	C5	C13	C14	-133.8(1)

39	O2	C5	C13	C15	99.0(1)
40	H5	C5	C13	C12	-136.4(1)
41	H5	C5	C13	C14	108.6(2)
42	H5	C5	C13	C15	-18.6(2)
43	C6	C5	C13	C12	103.2(1)
44	C6	C5	C13	C14	-11.8(2)
45	C6	C5	C13	C15	-139.0(1)
46	C5	C6	C7	H7	-137.3(2)
47	C5	C6	C7	C8	42.7(2)
48	H6	C6	C7	H7	102.9(2)
49	H6	C6	C7	C8	-77.1(2)
50	O3	C6	C7	H7	-12.6(2)
51	O3	C6	C7	C8	167.4(1)
52	C5	C6	O3	C19	-76.8(2)
53	H6	C6	O3	C19	41.8(2)
54	C7	C6	O3	C19	157.2(1)
55	C6	C7	C8	H8	176.8(2)
56	C6	C7	C8	C14	-3.2(2)
57	H7	C7	C8	H8	-3.2(3)
58	H7	C7	C8	C14	176.8(2)
59	C7	C8	C14	C9	-160.6(2)
60	C7	C8	C14	C13	-40.9(2)
61	C7	C8	C14	H14	77.4(2)
62	H8	C8	C14	C9	19.4(2)
63	H8	C8	C14	C13	139.1(2)
64	H8	C8	C14	H14	-102.6(2)
65	H9	C9	C10	H10A	-88.6(2)
66	H9	C9	C10	H10B	27.8(2)
67	H9	C9	C10	C11	149.7(2)
68	C14	C9	C10	H10A	153.7(2)
69	C14	C9	C10	H10B	-89.9(2)
70	C14	C9	C10	C11	31.9(2)
71	N1	C9	C10	H10A	31.1(2)
72	N1	C9	C10	H10B	147.5(2)
73	N1	C9	C10	C11	-90.7(2)
74	H9	C9	C14	C8	-58.2(2)
75	H9	C9	C14	C13	-179.3(1)
76	H9	C9	C14	H14	63.9(2)
77	C10	C9	C14	C8	59.6(2)
78	C10	C9	C14	C13	-61.6(2)
79	C10	C9	C14	H14	-178.4(1)
80	N1	C9	C14	C8	-172.6(1)
81	N1	C9	C14	C13	66.2(2)
82	N1	C9	C14	H14	-50.6(2)
83	H9	C9	N1	C16	178.5(1)

84	H9	C9	N1	C17	51.0(2)
85	C10	C9	N1	C16	58.8(2)
86	C10	C9	N1	C17	-68.7(2)
87	C14	C9	N1	C16	-67.2(2)
88	C14	C9	N1	C17	165.4(2)
89	C9	C10	C11	C1	-176.7(2)
90	C9	C10	C11	C12	-3.3(2)
91	H10A	C10	C11	C1	61.5(2)
92	H10A	C10	C11	C12	-125.1(2)
93	H10B	C10	C11	C1	-54.9(2)
94	H10B	C10	C11	C12	118.5(2)
95	C1	C11	C12	C4	7.2(2)
96	C1	C11	C12	C13	-178.9(2)
97	C10	C11	C12	C4	-167.0(2)
98	C10	C11	C12	C13	7.0(2)
99	C4	C12	C13	C5	15.5(2)
100	C4	C12	C13	C14	137.8(1)
101	C4	C12	C13	C15	-102.4(2)
102	C11	C12	C13	C5	-159.2(2)
103	C11	C12	C13	C14	-36.9(2)
104	C11	C12	C13	C15	83.0(2)
105	C5	C13	C14	C8	47.5(2)
106	C5	C13	C14	C9	172.4(1)
107	C5	C13	C14	H14	-70.8(2)
108	C12	C13	C14	C8	-64.0(2)
109	C12	C13	C14	C9	61.0(2)
110	C12	C13	C14	H14	177.8(1)
111	C15	C13	C14	C8	175.3(1)
112	C15	C13	C14	C9	-59.7(2)
113	C15	C13	C14	H14	57.1(2)
114	C5	C13	C15	H15A	-56.6(2)
115	C5	C13	C15	H15B	61.1(2)
116	C5	C13	C15	C16	-177.8(1)
117	C12	C13	C15	H15A	54.5(2)
118	C12	C13	C15	H15B	172.3(1)
119	C12	C13	C15	C16	-66.6(2)
120	C14	C13	C15	H15A	172.5(1)
121	C14	C13	C15	H15B	-69.7(2)
122	C14	C13	C15	C16	51.4(2)
123	C13	C15	C16	H16A	71.9(2)
124	C13	C15	C16	H16B	-170.0(1)
125	C13	C15	C16	N1	-49.1(2)
126	H15A	C15	C16	H16A	-49.3(2)
127	H15A	C15	C16	H16B	68.9(2)
128	H15A	C15	C16	N1	-170.2(1)

129	H15B	C15	C16	H16A	-167.0(2)
130	H15B	C15	C16	H16B	-48.9(2)
131	H15B	C15	C16	N1	72.0(2)
132	C15	C16	N1	C9	58.0(2)
133	C15	C16	N1	C17	-173.4(2)
134	H16A	C16	N1	C9	-62.9(2)
135	H16A	C16	N1	C17	65.7(2)
136	H16B	C16	N1	C9	178.9(2)
137	H16B	C16	N1	C17	-52.5(2)
138	C9	N1	C17	H17A	-48.2(2)
139	C9	N1	C17	H17B	-168.2(2)
140	C9	N1	C17	H17C	71.8(2)
141	C16	N1	C17	H17A	-176.3(2)
142	C16	N1	C17	H17B	63.7(2)
143	C16	N1	C17	H17C	-56.3(2)
144	C3	O1	C18	H18A	-59.5(2)
145	C3	O1	C18	H18B	-179.5(2)
146	C3	O1	C18	H18C	60.5(2)
147	C6	O3	C19	O4	2.9(2)
148	C6	O3	C19	C20	-174.4(1)
149	O3	C19	C20	C21	11.8(2)
150	O3	C19	C20	C25	-171.9(1)
151	O4	C19	C20	C21	-165.5(2)
152	O4	C19	C20	C25	10.8(3)
153	C19	C20	C21	H21	-5.4(3)
154	C19	C20	C21	C22	174.6(2)
155	C25	C20	C21	H21	178.4(2)
156	C25	C20	C21	C22	-1.6(3)
157	C19	C20	C25	C24	-177.0(2)
158	C19	C20	C25	H25	3.0(2)
159	C21	C20	C25	C24	-0.7(2)
160	C21	C20	C25	H25	179.4(2)
161	C20	C21	C22	H22	-178.1(2)
162	C20	C21	C22	C23	1.9(3)
163	H21	C21	C22	H22	1.9(3)
164	H21	C21	C22	C23	-178.1(2)
165	C21	C22	C23	H23	179.9(2)
166	C21	C22	C23	C24	-0.0(3)
167	H22	C22	C23	H23	-0.0(3)
168	H22	C22	C23	C24	180.0(2)
169	C22	C23	C24	C25	-2.3(3)
170	C22	C23	C24	C26	177.2(2)
171	H23	C23	C24	C25	177.8(2)
172	H23	C23	C24	C26	-2.8(3)
173	C23	C24	C25	C20	2.6(2)

174	C23	C24	C25	H25	-177.4(2)
175	C26	C24	C25	C20	-176.9(1)
176	C26	C24	C25	H25	3.1(2)
177	C23	C24	C26	O3'	-2.7(2)
178	C23	C24	C26	O5	178.6(2)
179	C25	C24	C26	O3'	176.8(1)
180	C25	C24	C26	O5	-2.0(2)
181	H1'	C1'	C2'	H2'	-0.8(3)
182	H1'	C1'	C2'	C3'	179.2(2)
183	C11'	C1'	C2'	H2'	179.2(2)
184	C11'	C1'	C2'	C3'	-0.8(3)
185	H1'	C1'	C11'	C10'	-10.0(3)
186	H1'	C1'	C11'	C12'	176.5(2)
187	C2'	C1'	C11'	C10'	170.0(2)
188	C2'	C1'	C11'	C12'	-3.6(2)
189	C1'	C2'	C3'	C4'	3.5(2)
190	C1'	C2'	C3'	O1'	-174.6(2)
191	H2'	C2'	C3'	C4'	-176.5(2)
192	H2'	C2'	C3'	O1'	5.4(3)
193	C2'	C3'	C4'	O2'	-176.4(1)
194	C2'	C3'	C4'	C12'	-1.7(2)
195	O1'	C3'	C4'	O2'	1.8(2)
196	O1'	C3'	C4'	C12'	176.5(1)
197	C2'	C3'	O1'	C18'	18.6(2)
198	C4'	C3'	O1'	C18'	-159.5(1)
199	C3'	C4'	O2'	C5'	155.7(2)
200	C12'	C4'	O2'	C5'	-19.4(2)
201	C3'	C4'	C12'	C11'	-2.9(2)
202	C3'	C4'	C12'	C13'	-176.5(1)
203	O2'	C4'	C12'	C11'	172.6(1)
204	O2'	C4'	C12'	C13'	-1.1(2)
205	C4'	O2'	C5'	H5'	149.4(1)
206	C4'	O2'	C5'	C6'	-90.1(1)
207	C4'	O2'	C5'	C13'	31.4(1)
208	O2'	C5'	C6'	H6'	-128.9(1)
209	O2'	C5'	C6'	C7'	110.1(1)
210	O2'	C5'	C6'	O3'	-11.5(2)
211	H5'	C5'	C6'	H6'	-8.4(2)
212	H5'	C5'	C6'	C7'	-129.4(1)
213	H5'	C5'	C6'	O3'	109.0(1)
214	C13'	C5'	C6'	H6'	114.7(1)
215	C13'	C5'	C6'	C7'	-6.3(2)
216	C13'	C5'	C6'	O3'	-127.9(1)
217	O2'	C5'	C13'	C12'	-30.4(1)
218	O2'	C5'	C13'	C14'	-146.5(1)

219	O2'	C5'	C13'	C15'	87.7(1)
220	H5'	C5'	C13'	C12'	-148.4(1)
221	H5'	C5'	C13'	C14'	95.5(2)
222	H5'	C5'	C13'	C15'	-30.3(2)
223	C6'	C5'	C13'	C12'	88.6(1)
224	C6'	C5'	C13'	C14'	-27.5(2)
225	C6'	C5'	C13'	C15'	-153.4(1)
226	C5'	C6'	C7'	H7'	-155.2(1)
227	C5'	C6'	C7'	C8'	24.8(2)
228	H6'	C6'	C7'	H7'	83.7(2)
229	H6'	C6'	C7'	C8'	-96.3(2)
230	O3'	C6'	C7'	H7'	-31.8(2)
231	O3'	C6'	C7'	C8'	148.2(2)
232	C5'	C6'	O3'	C26	-66.8(2)
233	H6'	C6'	O3'	C26	50.6(2)
234	C7'	C6'	O3'	C26	166.1(1)
235	C6'	C7'	C8'	H8'	173.5(2)
236	C6'	C7'	C8'	C14'	-6.5(3)
237	H7'	C7'	C8'	H8'	-6.5(3)
238	H7'	C7'	C8'	C14'	173.5(1)
239	C7'	C8'	C14'	C9'	-147.4(2)
240	C7'	C8'	C14'	C13'	-27.7(2)
241	C7'	C8'	C14'	H14'	91.6(2)
242	H8'	C8'	C14'	C9'	32.6(2)
243	H8'	C8'	C14'	C13'	152.3(2)
244	H8'	C8'	C14'	H14'	-88.3(2)
245	H9'	C9'	C10'	H10C	-83.8(2)
246	H9'	C9'	C10'	H10D	33.0(2)
247	H9'	C9'	C10'	C11'	154.6(1)
248	C14'	C9'	C10'	H10C	159.2(1)
249	C14'	C9'	C10'	H10D	-84.1(2)
250	C14'	C9'	C10'	C11'	37.6(2)
251	N1'	C9'	C10'	H10C	35.1(2)
252	N1'	C9'	C10'	H10D	151.9(1)
253	N1'	C9'	C10'	C11'	-86.5(2)
254	H9'	C9'	C14'	C8'	-58.7(2)
255	H9'	C9'	C14'	C13'	179.2(1)
256	H9'	C9'	C14'	H14'	62.2(2)
257	C10'	C9'	C14'	C8'	58.4(2)
258	C10'	C9'	C14'	C13'	-63.7(2)
259	C10'	C9'	C14'	H14'	179.3(1)
260	N1'	C9'	C14'	C8'	-173.4(1)
261	N1'	C9'	C14'	C13'	64.5(2)
262	N1'	C9'	C14'	H14'	-52.5(2)
263	H9'	C9'	N1'	C16'	-174.7(1)

264	H9'	C9'	N1'	C17'	60.0(2)
265	C10'	C9'	N1'	C16'	66.4(2)
266	C10'	C9'	N1'	C17'	-58.9(2)
267	C14'	C9'	N1'	C16'	-60.1(2)
268	C14'	C9'	N1'	C17'	174.7(1)
269	C9'	C10'	C11'	C1'	179.8(2)
270	C9'	C10'	C11'	C12'	-6.8(2)
271	H10C	C10'	C11'	C1'	58.1(2)
272	H10C	C10'	C11'	C12'	-128.5(2)
273	H10D	C10'	C11'	C1'	-58.5(2)
274	H10D	C10'	C11'	C12'	114.9(2)
275	C1'	C11'	C12'	C4'	5.4(2)
276	C1'	C11'	C12'	C13'	177.9(1)
277	C10'	C11'	C12'	C4'	-168.7(1)
278	C10'	C11'	C12'	C13'	3.8(2)
279	C4'	C12'	C13'	C5'	19.6(2)
280	C4'	C12'	C13'	C14'	143.0(1)
281	C4'	C12'	C13'	C15'	-98.1(2)
282	C11'	C12'	C13'	C5'	-153.8(2)
283	C11'	C12'	C13'	C14'	-30.4(2)
284	C11'	C12'	C13'	C15'	88.5(2)
285	C5'	C13'	C14'	C8'	44.4(2)
286	C5'	C13'	C14'	C9'	168.0(1)
287	C5'	C13'	C14'	H14'	-74.9(2)
288	C12'	C13'	C14'	C8'	-66.5(2)
289	C12'	C13'	C14'	C9'	57.1(2)
290	C12'	C13'	C14'	H14'	174.1(1)
291	C15'	C13'	C14'	C8'	172.0(1)
292	C15'	C13'	C14'	C9'	-64.4(2)
293	C15'	C13'	C14'	H14'	52.7(2)
294	C5'	C13'	C15'	H15C	-49.8(2)
295	C5'	C13'	C15'	H15D	68.5(2)
296	C5'	C13'	C15'	C16'	-170.6(1)
297	C12'	C13'	C15'	H15C	60.0(2)
298	C12'	C13'	C15'	H15D	178.3(1)
299	C12'	C13'	C15'	C16'	-60.8(2)
300	C14'	C13'	C15'	H15C	179.0(1)
301	C14'	C13'	C15'	H15D	-62.7(2)
302	C14'	C13'	C15'	C16'	58.2(2)
303	C13'	C15'	C16'	H16C	69.4(2)
304	C13'	C15'	C16'	H16D	-172.8(1)
305	C13'	C15'	C16'	N1'	-51.7(2)
306	H15C	C15'	C16'	H16C	-51.5(2)
307	H15C	C15'	C16'	H16D	66.3(2)
308	H15C	C15'	C16'	N1'	-172.6(1)

309	H15D	C15'	C16'	H16C	-169.8(2)
310	H15D	C15'	C16'	H16D	-52.0(2)
311	H15D	C15'	C16'	N1'	69.1(2)
312	C15'	C16'	N1'	C9'	53.7(2)
313	C15'	C16'	N1'	C17'	-179.4(1)
314	H16C	C16'	N1'	C9'	-67.4(2)
315	H16C	C16'	N1'	C17'	59.5(2)
316	H16D	C16'	N1'	C9'	174.7(1)
317	H16D	C16'	N1'	C17'	-58.4(2)
318	C9'	N1'	C17'	H17D	74.9(2)
319	C9'	N1'	C17'	H17E	-45.2(2)
320	C9'	N1'	C17'	H17F	-165.1(1)
321	C16'	N1'	C17'	H17D	-52.8(2)
322	C16'	N1'	C17'	H17E	-172.8(1)
323	C16'	N1'	C17'	H17F	67.2(2)
324	C3'	O1'	C18'	H18D	-69.3(2)
325	C3'	O1'	C18'	H18E	170.8(1)
326	C3'	O1'	C18'	H18F	50.8(2)
327	C6'	O3'	C26	C24	170.6(1)
328	C6'	O3'	C26	O5	-10.6(2)

Table A.4 Torsion Angle data for **126**

A.2 X-ray crystal data of 127

1,2-*bis*(1*S*,5*R*,13*R*,14*S*,17*R*)-10-methoxy-4-methyl-12-oxa-4-azapentacyclo[9.6.1.0^{1,13}.0^{5,17}.0^{7,18}]octadeca-7,9,11(18),15-tetraen-14-yl benzene-1,2-dicarboxylate, (127);

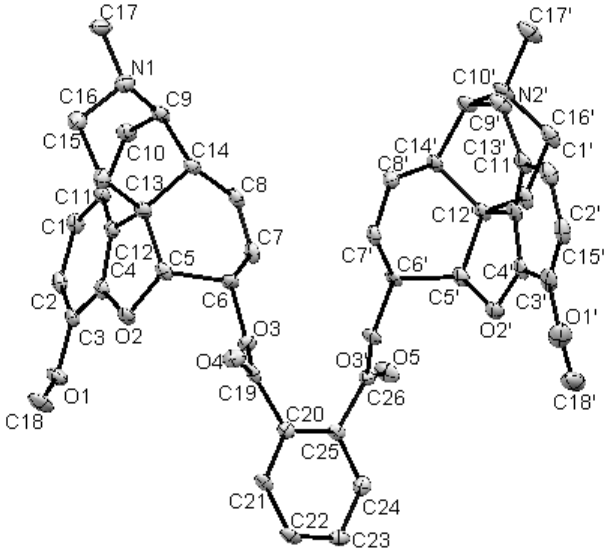

Fig A.2 ORTEP diagram of **127** with atom labels

Formula	$C_{44}H_{44}N_2O_8$
Space Group	P 2_1 2_1 2_1
Cell Lengths (Å)	**a** 7.5800(2) **b** 8.2045(2) **c** 56.9797(18)
Cell Angles (°)	**α** 90 **β** 90 **γ** 90
Cell Volume (Å^3)	3543.57
Z, Z'	**Z**: 4 **Z'**: 0
R-Factor (%)	4.19

Table A.5 X-ray crystal data for **127**

Number	Atom1	Atom2	Length (Å)
1	C1	H1	0.948(2)
2	C1	C2	1.378(2)
3	C1	C11	1.405(3)
4	C2	H2	0.950(2)

5	C2	C3	1.401(3)
6	C3	C4	1.394(3)
7	C3	O1	1.375(2)
8	C4	O2	1.383(3)
9	C4	C12	1.373(2)
10	O2	C5	1.464(3)
11	C5	H5	1.000(2)
12	C5	C6	1.537(3)
13	C5	C13	1.558(2)
14	C6	H6	1.000(2)
15	C6	C7	1.509(2)
16	C6	O3	1.450(2)
17	C7	H7	0.950(2)
18	C7	C8	1.315(2)
19	C8	H8	0.950(2)
20	C8	C14	1.505(2)
21	C9	H9	0.999(2)
22	C9	C10	1.555(3)
23	C9	C14	1.542(3)
24	C9	N1	1.469(2)
25	C10	H10A	0.988(2)
26	C10	H10B	0.990(2)
27	C10	C11	1.509(2)
28	C11	C12	1.382(2)
29	C12	C13	1.510(3)
30	C13	C14	1.545(2)
31	C13	C15	1.534(2)
32	C14	H14	0.999(2)
33	C15	H15A	0.990(2)
34	C15	H15B	0.990(2)
35	C15	C16	1.520(2)
36	C16	H16A	0.988(2)
37	C16	H16B	0.990(2)
38	C16	N1	1.468(2)
39	N1	C17	1.461(2)
40	C17	H17A	0.983(2)
41	C17	H17B	0.981(2)
42	C17	H17C	0.980(2)
43	O1	C18	1.441(2)
44	C18	H18A	0.979(2)
45	C18	H18B	0.981(3)
46	C18	H18C	0.979(3)
47	O3	C19	1.340(2)
48	C19	O4	1.203(2)
49	C19	C20	1.496(2)

50	C20	C21	1.392(2)
51	C20	C25	1.397(2)
52	C21	H21	0.951(2)
53	C21	C22	1.385(2)
54	C22	H22	0.950(2)
55	C22	C23	1.384(2)
56	C23	H23	0.950(2)
57	C23	C24	1.386(2)
58	C24	H24	0.949(2)
59	C24	C25	1.383(2)
60	C25	C26	1.490(2)
61	C1'	H1'	0.949(2)
62	C1'	C2'	1.381(2)
63	C1'	C11'	1.405(3)
64	C2'	H2'	0.951(2)
65	C2'	C3'	1.401(3)
66	C3'	C4'	1.386(3)
67	C3'	O1'	1.379(2)
68	C4'	O2'	1.388(3)
69	C4'	C12'	1.374(2)
70	O2'	C5'	1.461(3)
71	C5'	H5'	1.001(2)
72	C5'	C6'	1.536(3)
73	C5'	C13'	1.553(2)
74	C6'	H6'	1.001(2)
75	C6'	C7'	1.499(2)
76	C6'	O3'	1.455(2)
77	C7'	H7'	0.950(2)
78	C7'	C8'	1.322(2)
79	C8'	H8'	0.950(2)
80	C8'	C14'	1.504(2)
81	C9'	H9'	0.999(2)
82	C9'	C10'	1.558(3)
83	C9'	C14'	1.536(3)
84	C9'	N2'	1.478(2)
85	C10'	H10C	0.991(2)
86	C10'	H10D	0.990(2)
87	C10'	C11'	1.512(2)
88	C11'	C12'	1.380(3)
89	C12'	C13'	1.510(3)
90	C13'	C14'	1.544(3)
91	C13'	C15'	1.535(2)
92	C14'	H14'	1.000(2)
93	C15'	H15C	0.991(2)
94	C15'	H15D	0.989(2)

95	C15'	C16'	1.516(2)
96	C16'	H16C	0.991(2)
97	C16'	H16D	0.990(2)
98	C16'	N2'	1.468(2)
99	N2'	C17'	1.466(3)
100	C17'	H17D	0.981(2)
101	C17'	H17E	0.981(3)
102	C17'	H17F	0.980(2)
103	O1'	C18'	1.434(4)
104	C18'	H18D	0.979(3)
105	C18'	H18E	0.979(3)
106	C18'	H18F	0.980(3)
107	O3'	C26	1.344(2)
108	C26	O5	1.207(2)

Table A.6 Bond length data for **127**

Number	Atom1	Atom2	Atom3	Angle (°)
1	H1	C1	C2	119.7(2)
2	H1	C1	C11	119.5(2)
3	C2	C1	C11	120.8(2)
4	C1	C2	H2	118.9(2)
5	C1	C2	C3	122.2(2)
6	H2	C2	C3	118.9(2)
7	C2	C3	C4	116.4(2)
8	C2	C3	O1	117.8(2)
9	C4	C3	O1	125.8(2)
10	C3	C4	O2	126.7(2)
11	C3	C4	C12	120.7(2)
12	O2	C4	C12	112.4(2)
13	C4	O2	C5	106.9(1)
14	O2	C5	H5	109.1(2)
15	O2	C5	C6	111.9(1)
16	O2	C5	C13	106.7(1)
17	H5	C5	C6	109.0(2)
18	H5	C5	C13	109.0(2)
19	C6	C5	C13	111.1(1)
20	C5	C6	H6	107.3(2)
21	C5	C6	C7	114.3(1)
22	C5	C6	O3	114.1(1)
23	H6	C6	C7	107.3(2)
24	H6	C6	O3	107.3(2)
25	C7	C6	O3	106.1(1)
26	C6	C7	H7	120.0(2)
27	C6	C7	C8	120.0(2)

28	H7	C7	C8	120.0(2)
29	C7	C8	H8	120.1(2)
30	C7	C8	C14	119.8(2)
31	H8	C8	C14	120.1(2)
32	H9	C9	C10	106.6(2)
33	H9	C9	C14	106.8(2)
34	H9	C9	N1	106.7(2)
35	C10	C9	C14	112.9(1)
36	C10	C9	N1	115.6(1)
37	C14	C9	N1	107.7(1)
38	C9	C10	H10A	108.5(2)
39	C9	C10	H10B	108.7(2)
40	C9	C10	C11	114.5(1)
41	H10A	C10	H10B	107.5(2)
42	H10A	C10	C11	108.8(2)
43	H10B	C10	C11	108.6(2)
44	C1	C11	C10	124.7(2)
45	C1	C11	C12	116.2(2)
46	C10	C11	C12	118.7(2)
47	C4	C12	C11	123.1(2)
48	C4	C12	C13	110.0(2)
49	C11	C12	C13	126.2(2)
50	C5	C13	C12	99.8(1)
51	C5	C13	C14	116.7(1)
52	C5	C13	C15	111.9(1)
53	C12	C13	C14	106.4(1)
54	C12	C13	C15	112.9(1)
55	C14	C13	C15	108.9(1)
56	C8	C14	C9	114.2(1)
57	C8	C14	C13	109.3(1)
58	C8	C14	H14	109.0(2)
59	C9	C14	C13	106.4(1)
60	C9	C14	H14	108.9(2)
61	C13	C14	H14	108.9(2)
62	C13	C15	H15A	109.2(2)
63	C13	C15	H15B	109.2(2)
64	C13	C15	C16	112.1(1)
65	H15A	C15	H15B	107.9(2)
66	H15A	C15	C16	109.2(2)
67	H15B	C15	C16	109.2(2)
68	C15	C16	H16A	109.4(2)
69	C15	C16	H16B	109.4(2)
70	C15	C16	N1	111.0(1)
71	H16A	C16	H16B	108.1(2)
72	H16A	C16	N1	109.4(2)

73	H16B	C16	N1	109.5(2)
74	C9	N1	C16	112.5(1)
75	C9	N1	C17	113.0(1)
76	C16	N1	C17	110.4(1)
77	N1	C17	H17A	109.5(2)
78	N1	C17	H17B	109.4(2)
79	N1	C17	H17C	109.5(2)
80	H17A	C17	H17B	109.5(2)
81	H17A	C17	H17C	109.4(2)
82	H17B	C17	H17C	109.5(2)
83	C3	O1	C18	115.4(2)
84	O1	C18	H18A	109.5(2)
85	O1	C18	H18B	109.4(2)
86	O1	C18	H18C	109.5(2)
87	H18A	C18	H18B	109.6(2)
88	H18A	C18	H18C	109.3(2)
89	H18B	C18	H18C	109.5(2)
90	C6	O3	C19	117.8(1)
91	O3	C19	O4	125.3(2)
92	O3	C19	C20	109.9(1)
93	O4	C19	C20	124.8(2)
94	C19	C20	C21	118.6(2)
95	C19	C20	C25	121.9(2)
96	C21	C20	C25	119.4(2)
97	C20	C21	H21	119.9(2)
98	C20	C21	C22	120.2(2)
99	H21	C21	C22	119.9(2)
100	C21	C22	H22	120.0(2)
101	C21	C22	C23	120.1(2)
102	H22	C22	C23	119.9(2)
103	C22	C23	H23	120.0(2)
104	C22	C23	C24	120.1(2)
105	H23	C23	C24	119.9(2)
106	C23	C24	H24	119.9(2)
107	C23	C24	C25	120.1(2)
108	H24	C24	C25	119.9(2)
109	C20	C25	C24	120.1(2)
110	C20	C25	C26	123.0(2)
111	C24	C25	C26	116.9(2)
112	H1'	C1'	C2'	119.8(2)
113	H1'	C1'	C11'	119.5(2)
114	C2'	C1'	C11'	120.7(2)
115	C1'	C2'	H2'	119.0(2)
116	C1'	C2'	C3'	122.0(2)
117	H2'	C2'	C3'	119.1(2)

118	C2'	C3'	C4'	116.8(2)
119	C2'	C3'	O1'	117.4(2)
120	C4'	C3'	O1'	125.6(2)
121	C3'	C4'	O2'	127.3(2)
122	C3'	C4'	C12'	120.3(2)
123	O2'	C4'	C12'	112.3(2)
124	C4'	O2'	C5'	107.3(1)
125	O2'	C5'	H5'	109.5(2)
126	O2'	C5'	C6'	112.0(1)
127	O2'	C5'	C13'	106.9(1)
128	H5'	C5'	C6'	109.2(2)
129	H5'	C5'	C13'	109.4(2)
130	C6'	C5'	C13'	109.7(1)
131	C5'	C6'	H6'	107.3(2)
132	C5'	C6'	C7'	113.8(2)
133	C5'	C6'	O3'	114.0(1)
134	H6'	C6'	C7'	107.2(2)
135	H6'	C6'	O3'	107.2(2)
136	C7'	C6'	O3'	106.9(1)
137	C6'	C7'	H7'	120.8(2)
138	C6'	C7'	C8'	118.4(2)
139	H7'	C7'	C8'	120.8(2)
140	C7'	C8'	H8'	120.6(2)
141	C7'	C8'	C14'	118.9(2)
142	H8'	C8'	C14'	120.6(2)
143	H9'	C9'	C10'	106.9(2)
144	H9'	C9'	C14'	107.1(2)
145	H9'	C9'	N2'	107.0(2)
146	C10'	C9'	C14'	112.6(1)
147	C10'	C9'	N2'	115.0(1)
148	C14'	C9'	N2'	107.8(1)
149	C9'	C10'	H10C	108.8(2)
150	C9'	C10'	H10D	108.8(2)
151	C9'	C10'	C11'	114.2(1)
152	H10C	C10'	H10D	107.6(2)
153	H10C	C10'	C11'	108.6(2)
154	H10D	C10'	C11'	108.6(2)
155	C1'	C11'	C10'	124.1(2)
156	C1'	C11'	C12'	116.1(2)
157	C10'	C11'	C12'	119.4(2)
158	C4'	C12'	C11'	123.3(2)
159	C4'	C12'	C13'	110.0(2)
160	C11'	C12'	C13'	125.6(2)
161	C5'	C13'	C12'	100.4(1)
162	C5'	C13'	C14'	116.3(1)

163	C5'	C13'	C15'	111.4(1)
164	C12'	C13'	C14'	106.3(1)
165	C12'	C13'	C15'	113.3(1)
166	C14'	C13'	C15'	109.0(1)
167	C8'	C14'	C9'	113.8(1)
168	C8'	C14'	C13'	109.2(1)
169	C8'	C14'	H14'	109.0(2)
170	C9'	C14'	C13'	106.9(1)
171	C9'	C14'	H14'	108.9(2)
172	C13'	C14'	H14'	109.0(2)
173	C13'	C15'	H15C	109.3(2)
174	C13'	C15'	H15D	109.3(2)
175	C13'	C15'	C16'	111.6(1)
176	H15C	C15'	H15D	108.0(2)
177	H15C	C15'	C16'	109.3(2)
178	H15D	C15'	C16'	109.3(2)
179	C15'	C16'	H16C	109.4(2)
180	C15'	C16'	H16D	109.4(2)
181	C15'	C16'	N2'	111.3(1)
182	H16C	C16'	H16D	107.9(2)
183	H16C	C16'	N2'	109.4(2)
184	H16D	C16'	N2'	109.4(2)
185	C9'	N2'	C16'	112.6(1)
186	C9'	N2'	C17'	112.0(2)
187	C16'	N2'	C17'	110.3(2)
188	N2'	C17'	H17D	109.5(2)
189	N2'	C17'	H17E	109.4(2)
190	N2'	C17'	H17F	109.5(2)
191	H17D	C17'	H17E	109.6(2)
192	H17D	C17'	H17F	109.4(2)
193	H17E	C17'	H17F	109.5(2)
194	C3'	O1'	C18'	115.8(2)
195	O1'	C18'	H18D	109.5(3)
196	O1'	C18'	H18E	109.5(3)
197	O1'	C18'	H18F	109.5(3)
198	H18D	C18'	H18E	109.4(3)
199	H18D	C18'	H18F	109.4(3)
200	H18E	C18'	H18F	109.5(3)
201	C6'	O3'	C26	116.7(2)
202	C25	C26	O3'	111.5(2)
203	C25	C26	O5	124.3(2)
204	O3'	C26	O5	124.2(2)

Table A.7 Bond angle data for **127**

Number	Atom1	Atom2	Atom3	Atom4	Torsion (°)
1	H1	C1	C2	H2	-4.3(3)
2	H1	C1	C2	C3	175.8(2)
3	C11	C1	C2	H2	175.8(2)
4	C11	C1	C2	C3	-4.1(3)
5	H1	C1	C11	C10	-6.7(3)
6	H1	C1	C11	C12	-178.9(2)
7	C2	C1	C11	C10	173.2(2)
8	C2	C1	C11	C12	1.0(3)
9	C1	C2	C3	C4	0.6(3)
10	C1	C2	C3	O1	-177.2(2)
11	H2	C2	C3	C4	-179.3(2)
12	H2	C2	C3	O1	2.9(3)
13	C2	C3	C4	O2	-169.3(2)
14	C2	C3	C4	C12	5.9(3)
15	O1	C3	C4	O2	8.3(3)
16	O1	C3	C4	C12	-176.5(2)
17	C2	C3	O1	C18	-148.0(2)
18	C4	C3	O1	C18	34.4(3)
19	C3	C4	O2	C5	166.7(2)
20	C12	C4	O2	C5	-8.8(2)
21	C3	C4	C12	C11	-9.4(3)
22	C3	C4	C12	C13	179.2(2)
23	O2	C4	C12	C11	166.5(2)
24	O2	C4	C12	C13	-4.9(2)
25	C4	O2	C5	H5	136.0(2)
26	C4	O2	C5	C6	-103.3(2)
27	C4	O2	C5	C13	18.4(2)
28	O2	C5	C6	H6	-154.3(2)
29	O2	C5	C6	C7	86.9(2)
30	O2	C5	C6	O3	-35.5(2)
31	H5	C5	C6	H6	-33.6(2)
32	H5	C5	C6	C7	-152.4(2)
33	H5	C5	C6	O3	85.2(2)
34	C13	C5	C6	H6	86.6(2)
35	C13	C5	C6	C7	-32.2(2)
36	C13	C5	C6	O3	-154.6(1)
37	O2	C5	C13	C12	-19.9(2)
38	O2	C5	C13	C14	-133.9(2)
39	O2	C5	C13	C15	99.8(2)
40	H5	C5	C13	C12	-137.5(2)
41	H5	C5	C13	C14	108.5(2)
42	H5	C5	C13	C15	-17.8(2)
43	C6	C5	C13	C12	102.3(2)
44	C6	C5	C13	C14	-11.7(2)

45	C6	C5	C13	C15	-138.0(2)
46	C5	C6	C7	H7	-136.1(2)
47	C5	C6	C7	C8	44.0(2)
48	H6	C6	C7	H7	105.0(2)
49	H6	C6	C7	C8	-74.9(2)
50	O3	C6	C7	H7	-9.5(2)
51	O3	C6	C7	C8	170.6(2)
52	C5	C6	O3	C19	-77.4(2)
53	H6	C6	O3	C19	41.4(2)
54	C7	C6	O3	C19	155.9(2)
55	C6	C7	C8	H8	175.4(2)
56	C6	C7	C8	C14	-4.6(3)
57	H7	C7	C8	H8	-4.5(3)
58	H7	C7	C8	C14	175.5(2)
59	C7	C8	C14	C9	-159.0(2)
60	C7	C8	C14	C13	-40.0(2)
61	C7	C8	C14	H14	78.9(2)
62	H8	C8	C14	C9	21.0(3)
63	H8	C8	C14	C13	140.0(2)
64	H8	C8	C14	H14	-101.1(2)
65	H9	C9	C10	H10A	-89.4(2)
66	H9	C9	C10	H10B	27.2(2)
67	H9	C9	C10	C11	148.9(2)
68	C14	C9	C10	H10A	153.6(2)
69	C14	C9	C10	H10B	-89.7(2)
70	C14	C9	C10	C11	31.9(2)
71	N1	C9	C10	H10A	29.0(2)
72	N1	C9	C10	H10B	145.6(2)
73	N1	C9	C10	C11	-92.7(2)
74	H9	C9	C14	C8	-59.4(2)
75	H9	C9	C14	C13	180.0(1)
76	H9	C9	C14	H14	62.7(2)
77	C10	C9	C14	C8	57.4(2)
78	C10	C9	C14	C13	-63.2(2)
79	C10	C9	C14	H14	179.6(1)
80	N1	C9	C14	C8	-173.7(1)
81	N1	C9	C14	C13	65.7(2)
82	N1	C9	C14	H14	-51.6(2)
83	H9	C9	N1	C16	-178.8(1)
84	H9	C9	N1	C17	55.5(2)
85	C10	C9	N1	C16	62.9(2)
86	C10	C9	N1	C17	-62.8(2)
87	C14	C9	N1	C16	-64.4(2)
88	C14	C9	N1	C17	169.8(1)
89	C9	C10	C11	C1	-172.9(2)

90	C9	C10	C11	C12	-0.9(2)
91	H10A	C10	C11	C1	65.5(2)
92	H10A	C10	C11	C12	-122.5(2)
93	H10B	C10	C11	C1	-51.2(2)
94	H10B	C10	C11	C12	120.8(2)
95	C1	C11	C12	C4	5.7(3)
96	C1	C11	C12	C13	175.6(2)
97	C10	C11	C12	C4	-167.0(2)
98	C10	C11	C12	C13	3.0(3)
99	C4	C12	C13	C5	15.2(2)
100	C4	C12	C13	C14	136.9(2)
101	C4	C12	C13	C15	-103.7(2)
102	C11	C12	C13	C5	-155.9(2)
103	C11	C12	C13	C14	-34.2(2)
104	C11	C12	C13	C15	85.2(2)
105	C5	C13	C14	C8	47.3(2)
106	C5	C13	C14	C9	171.1(1)
107	C5	C13	C14	H14	-71.7(2)
108	C12	C13	C14	C8	-62.9(2)
109	C12	C13	C14	C9	60.8(2)
110	C12	C13	C14	H14	178.1(2)
111	C15	C13	C14	C8	175.1(1)
112	C15	C13	C14	C9	-61.1(2)
113	C15	C13	C14	H14	56.1(2)
114	C5	C13	C15	H15A	-53.8(2)
115	C5	C13	C15	H15B	64.0(2)
116	C5	C13	C15	C16	-174.9(1)
117	C12	C13	C15	H15A	57.9(2)
118	C12	C13	C15	H15B	175.6(2)
119	C12	C13	C15	C16	-63.3(2)
120	C14	C13	C15	H15A	175.8(1)
121	C14	C13	C15	H15B	-66.5(2)
122	C14	C13	C15	C16	54.6(2)
123	C13	C15	C16	H16A	70.0(2)
124	C13	C15	C16	H16B	-171.8(2)
125	C13	C15	C16	N1	-50.8(2)
126	H15A	C15	C16	H16A	-51.1(2)
127	H15A	C15	C16	H16B	67.1(2)
128	H15A	C15	C16	N1	-171.9(2)
129	H15B	C15	C16	H16A	-168.9(2)
130	H15B	C15	C16	H16B	-50.6(2)
131	H15B	C15	C16	N1	70.3(2)
132	C15	C16	N1	C9	56.2(2)
133	C15	C16	N1	C17	-176.6(1)
134	H16A	C16	N1	C9	-64.6(2)

135	H16A	C16	N1	C17	62.5(2)
136	H16B	C16	N1	C9	177.1(2)
137	H16B	C16	N1	C17	-55.7(2)
138	C9	N1	C17	H17A	67.4(2)
139	C9	N1	C17	H17B	-52.6(2)
140	C9	N1	C17	H17C	-172.6(2)
141	C16	N1	C17	H17A	-59.4(2)
142	C16	N1	C17	H17B	-179.5(2)
143	C16	N1	C17	H17C	60.5(2)
144	C3	O1	C18	H18A	-77.2(2)
145	C3	O1	C18	H18B	162.8(2)
146	C3	O1	C18	H18C	42.7(3)
147	C6	O3	C19	O4	16.4(3)
148	C6	O3	C19	C20	-164.5(1)
149	O3	C19	C20	C21	-133.3(2)
150	O3	C19	C20	C25	43.3(2)
151	O4	C19	C20	C21	45.8(3)
152	O4	C19	C20	C25	-137.6(2)
153	C19	C20	C21	H21	-4.9(3)
154	C19	C20	C21	C22	174.9(2)
155	C25	C20	C21	H21	178.4(2)
156	C25	C20	C21	C22	-1.7(3)
157	C19	C20	C25	C24	-173.2(2)
158	C19	C20	C25	C26	10.2(3)
159	C21	C20	C25	C24	3.3(3)
160	C21	C20	C25	C26	-173.2(2)
161	C20	C21	C22	H22	178.4(2)
162	C20	C21	C22	C23	-1.5(3)
163	H21	C21	C22	H22	-1.7(3)
164	H21	C21	C22	C23	178.4(2)
165	C21	C22	C23	H23	-176.8(2)
166	C21	C22	C23	C24	3.1(3)
167	H22	C22	C23	H23	3.3(3)
168	H22	C22	C23	C24	-176.8(2)
169	C22	C23	C24	H24	178.5(2)
170	C22	C23	C24	C25	-1.5(3)
171	H23	C23	C24	H24	-1.6(3)
172	H23	C23	C24	C25	178.4(2)
173	C23	C24	C25	C20	-1.8(3)
174	C23	C24	C25	C26	175.0(2)
175	H24	C24	C25	C20	178.3(2)
176	H24	C24	C25	C26	-5.0(3)
177	C20	C25	C26	O3'	43.2(2)
178	C20	C25	C26	O5	-139.7(2)
179	C24	C25	C26	O3'	-133.5(2)

180	C24	C25	C26	O5	43.7(3)
181	H1'	C1'	C2'	H2'	-4.3(3)
182	H1'	C1'	C2'	C3'	175.8(2)
183	C11'	C1'	C2'	H2'	175.8(2)
184	C11'	C1'	C2'	C3'	-4.1(3)
185	H1'	C1'	C11'	C10'	-7.7(3)
186	H1'	C1'	C11'	C12'	179.9(2)
187	C2'	C1'	C11'	C10'	172.2(2)
188	C2'	C1'	C11'	C12'	-0.3(3)
189	C1'	C2'	C3'	C4'	0.9(3)
190	C1'	C2'	C3'	O1'	-175.2(2)
191	H2'	C2'	C3'	C4'	-179.0(2)
192	H2'	C2'	C3'	O1'	4.9(3)
193	C2'	C3'	C4'	O2'	-168.4(2)
194	C2'	C3'	C4'	C12'	6.6(3)
195	O1'	C3'	C4'	O2'	7.2(3)
196	O1'	C3'	C4'	C12'	-177.7(2)
197	C2'	C3'	O1'	C18'	-151.2(2)
198	C4'	C3'	O1'	C18'	33.2(3)
199	C3'	C4'	O2'	C5'	167.9(2)
200	C12'	C4'	O2'	C5'	-7.5(2)
201	C3'	C4'	C12'	C11'	-11.5(3)
202	C3'	C4'	C12'	C13'	179.9(2)
203	O2'	C4'	C12'	C11'	164.2(2)
204	O2'	C4'	C12'	C13'	-4.3(2)
205	C4'	O2'	C5'	H5'	134.2(2)
206	C4'	O2'	C5'	C6'	-104.4(2)
207	C4'	O2'	C5'	C13'	15.8(2)
208	O2'	C5'	C6'	H6'	-160.5(2)
209	O2'	C5'	C6'	C7'	81.0(2)
210	O2'	C5'	C6'	O3'	-42.1(2)
211	H5'	C5'	C6'	H6'	-39.1(2)
212	H5'	C5'	C6'	C7'	-157.5(2)
213	H5'	C5'	C6'	O3'	79.4(2)
214	C13'	C5'	C6'	H6'	80.9(2)
215	C13'	C5'	C6'	C7'	-37.6(2)
216	C13'	C5'	C6'	O3'	-160.7(1)
217	O2'	C5'	C13'	C12'	-17.2(2)
218	O2'	C5'	C13'	C14'	-131.3(2)
219	O2'	C5'	C13'	C15'	103.1(2)
220	H5'	C5'	C13'	C12'	-135.7(2)
221	H5'	C5'	C13'	C14'	110.2(2)
222	H5'	C5'	C13'	C15'	-15.4(2)
223	C6'	C5'	C13'	C12'	104.5(2)
224	C6'	C5'	C13'	C14'	-9.6(2)

225	C6'	C5'	C13'	C15'	-135.2(2)
226	C5'	C6'	C7'	H7'	-130.5(2)
227	C5'	C6'	C7'	C8'	49.5(2)
228	H6'	C6'	C7'	H7'	111.1(2)
229	H6'	C6'	C7'	C8'	-69.0(2)
230	O3'	C6'	C7'	H7'	-3.6(2)
231	O3'	C6'	C7'	C8'	176.3(2)
232	C5'	C6'	O3'	C26	-75.1(2)
233	H6'	C6'	O3'	C26	43.4(2)
234	C7'	C6'	O3'	C26	158.1(2)
235	C6'	C7'	C8'	H8'	173.8(2)
236	C6'	C7'	C8'	C14'	-6.3(3)
237	H7'	C7'	C8'	H8'	-6.3(3)
238	H7'	C7'	C8'	C14'	173.6(2)
239	C7'	C8'	C14'	C9'	-160.7(2)
240	C7'	C8'	C14'	C13'	-41.4(2)
241	C7'	C8'	C14'	H14'	77.5(2)
242	H8'	C8'	C14'	C9'	19.2(3)
243	H8'	C8'	C14'	C13'	138.6(2)
244	H8'	C8'	C14'	H14'	-102.5(2)
245	H9'	C9'	C10'	H10C	-89.9(2)
246	H9'	C9'	C10'	H10D	27.0(2)
247	H9'	C9'	C10'	C11'	148.5(2)
248	C14'	C9'	C10'	H10C	152.7(2)
249	C14'	C9'	C10'	H10D	-90.4(2)
250	C14'	C9'	C10'	C11'	31.1(2)
251	N2'	C9'	C10'	H10C	28.7(2)
252	N2'	C9'	C10'	H10D	145.6(2)
253	N2'	C9'	C10'	C11'	-92.8(2)
254	H9'	C9'	C14'	C8'	-59.9(2)
255	H9'	C9'	C14'	C13'	179.4(1)
256	H9'	C9'	C14'	H14'	61.9(2)
257	C10'	C9'	C14'	C8'	57.3(2)
258	C10'	C9'	C14'	C13'	-63.3(2)
259	C10'	C9'	C14'	H14'	179.1(1)
260	N2'	C9'	C14'	C8'	-174.8(1)
261	N2'	C9'	C14'	C13'	64.6(2)
262	N2'	C9'	C14'	H14'	-53.0(2)
263	H9'	C9'	N2'	C16'	-178.2(1)
264	H9'	C9'	N2'	C17'	56.7(2)
265	C10'	C9'	N2'	C16'	63.1(2)
266	C10'	C9'	N2'	C17'	-61.9(2)
267	C14'	C9'	N2'	C16'	-63.3(2)
268	C14'	C9'	N2'	C17'	171.6(2)
269	C9'	C10'	C11'	C1'	-172.0(2)

270	C9'	C10'	C11'	C12'	0.2(2)
271	H10C	C10'	C11'	C1'	66.3(2)
272	H10C	C10'	C11'	C12'	-121.5(2)
273	H10D	C10'	C11'	C1'	-50.4(2)
274	H10D	C10'	C11'	C12'	121.8(2)
275	C1'	C11'	C12'	C4'	8.0(3)
276	C1'	C11'	C12'	C13'	174.8(2)
277	C10'	C11'	C12'	C4'	-164.8(2)
278	C10'	C11'	C12'	C13'	1.9(3)
279	C4'	C12'	C13'	C5'	13.2(2)
280	C4'	C12'	C13'	C14'	134.7(2)
281	C4'	C12'	C13'	C15'	-105.7(2)
282	C11'	C12'	C13'	C5'	-155.1(2)
283	C11'	C12'	C13'	C14'	-33.6(2)
284	C11'	C12'	C13'	C15'	86.1(2)
285	C5'	C13'	C14'	C8'	48.5(2)
286	C5'	C13'	C14'	C9'	172.1(1)
287	C5'	C13'	C14'	H14'	-70.4(2)
288	C12'	C13'	C14'	C8'	-62.2(2)
289	C12'	C13'	C14'	C9'	61.4(2)
290	C12'	C13'	C14'	H14'	178.9(2)
291	C15'	C13'	C14'	C8'	175.3(1)
292	C15'	C13'	C14'	C9'	-61.1(2)
293	C15'	C13'	C14'	H14'	56.4(2)
294	C5'	C13'	C15'	H15C	-54.4(2)
295	C5'	C13'	C15'	H15D	63.6(2)
296	C5'	C13'	C15'	C16'	-175.4(1)
297	C12'	C13'	C15'	H15C	57.9(2)
298	C12'	C13'	C15'	H15D	175.9(2)
299	C12'	C13'	C15'	C16'	-63.1(2)
300	C14'	C13'	C15'	H15C	176.0(1)
301	C14'	C13'	C15'	H15D	-66.0(2)
302	C14'	C13'	C15'	C16'	55.1(2)
303	C13'	C15'	C16'	H16C	69.4(2)
304	C13'	C15'	C16'	H16D	-172.7(2)
305	C13'	C15'	C16'	N2'	-51.6(2)
306	H15C	C15'	C16'	H16C	-51.6(2)
307	H15C	C15'	C16'	H16D	66.4(2)
308	H15C	C15'	C16'	N2'	-172.6(2)
309	H15D	C15'	C16'	H16C	-169.6(2)
310	H15D	C15'	C16'	H16D	-51.6(2)
311	H15D	C15'	C16'	N2'	69.4(2)
312	C15'	C16'	N2'	C9'	56.4(2)
313	C15'	C16'	N2'	C17'	-177.7(2)
314	H16C	C16'	N2'	C9'	-64.6(2)

315	H16C	C16'	N2'	C17'	61.4(2)
316	H16D	C16'	N2'	C9'	177.3(1)
317	H16D	C16'	N2'	C17'	-56.7(2)
318	C9'	N2'	C17'	H17D	69.0(2)
319	C9'	N2'	C17'	H17E	-51.1(2)
320	C9'	N2'	C17'	H17F	-171.1(2)
321	C16'	N2'	C17'	H17D	-57.2(2)
322	C16'	N2'	C17'	H17E	-177.4(2)
323	C16'	N2'	C17'	H17F	62.6(2)
324	C3'	O1'	C18'	H18D	-77.4(3)
325	C3'	O1'	C18'	H18E	162.7(2)
326	C3'	O1'	C18'	H18F	42.6(3)
327	C6'	O3'	C26	C25	-172.0(1)
328	C6'	O3'	C26	O5	10.9(3)

Table A.8 Torsion Angle data for **127**

A.3 X-ray crystal data of 162

(1*S*,5*R*,13*R*,14*S*,17*R*)-10-methoxy-4-methyl-8-[(*E*)-2-(pyridin-4-yl)ethenyl]-12-oxa-4-azapentacyclo[9.6.1.$0^{1,13}$.$0^{5,17}$.$0^{7,18}$]octadeca-7,9,11(18),15-tetraen-14-ol, (162);

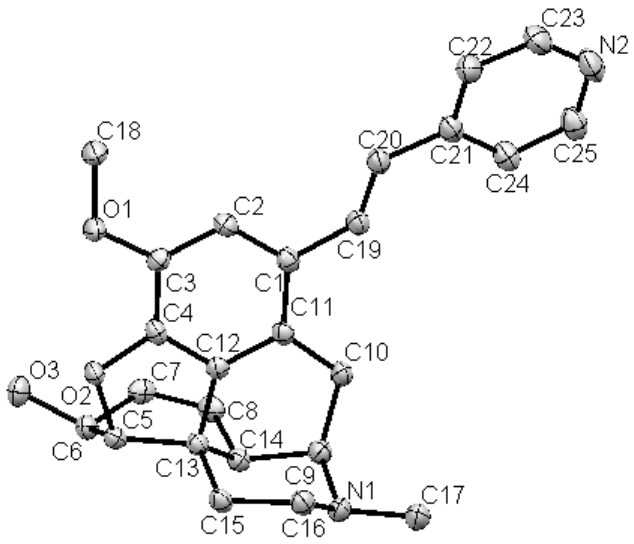

Fig A.3 ORTEP diagram of **162** with atom labels

Formula	$C_{25}H_{26}N_2O_3$
Space Group	P 2_1
Cell Lengths (Å)	**a** 7.0000(6) **b** 7.4627(7) **c** 19.2449(17)
Cell Angles (°)	**α** 90 **β** 98.251(5) **γ** 90
Cell Volume ($Å^3$)	994.926
Z, Z'	**Z**: 2 **Z'**: 0
R-Factor (%)	3.17

Table A.9 X-ray crystal data for 1**62**

Number	**Atom1**	**Atom2**	**Length (Å)**
1	O1	C3	1.361(2)
2	O1	C18	1.436(2)
3	O2	C4	1.376(2)
4	O2	C5	1.479(2)
5	O3	H3	0.840(1)
6	O3	C6	1.419(2)
7	N1	C9	1.468(2)
8	N1	C16	1.462(2)
9	N1	C17	1.461(2)
10	N2	C23	1.335(2)
11	N2	C25	1.347(2)
12	C1	C2	1.412(2)
13	C1	C11	1.415(2)
14	C1	C19	1.465(2)
15	C2	H2	0.951(2)
16	C2	C3	1.394(2)
17	C3	C4	1.391(2)
18	C4	C12	1.369(2)
19	C5	H5	1.000(1)
20	C5	C6	1.538(2)
21	C5	C13	1.536(2)
22	C6	H6	1.000(2)
23	C6	C7	1.512(2)
24	C7	H7	0.950(1)
25	C7	C8	1.323(2)
26	C8	H8	0.951(1)
27	C8	C14	1.503(2)
28	C9	H9	1.000(1)
29	C9	C10	1.561(2)

30	C9	C14	1.537(2)
31	C10	H10A	0.990(2)
32	C10	H10B	0.990(1)
33	C10	C11	1.515(2)
34	C11	C12	1.381(2)
35	C12	C13	1.507(2)
36	C13	C14	1.548(2)
37	C13	C15	1.531(2)
38	C14	H14	0.999(2)
39	C15	H15A	0.990(1)
40	C15	H15B	0.991(2)
41	C15	C16	1.521(2)
42	C16	H16A	0.991(2)
43	C16	H16B	0.990(1)
44	C17	H17A	0.980(2)
45	C17	H17B	0.979(2)
46	C17	H17C	0.980(2)
47	C18	H18A	0.980(2)
48	C18	H18B	0.980(2)
49	C18	H18C	0.980(2)
50	C19	H19	0.950(1)
51	C19	C20	1.340(2)
52	C20	H20	0.950(1)
53	C20	C21	1.463(2)
54	C21	C22	1.394(2)
55	C21	C24	1.399(2)
56	C22	H22	0.950(2)
57	C22	C23	1.378(3)
58	C23	H23	0.950(2)
59	C24	H24	0.950(2)
60	C24	C25	1.378(2)
61	C25	H25	0.950(2)

Table A.10 Bond length data for **162**

Number	**Atom1**	**Atom2**	**Atom3**	**Angle (°)**
1	C3	O1	C18	117.1(1)
2	C4	O2	C5	106.4(1)
3	H3	O3	C6	109.5(1)
4	C9	N1	C16	112.7(1)
5	C9	N1	C17	113.1(1)
6	C16	N1	C17	110.4(1)
7	C23	N2	C25	115.2(2)
8	C2	C1	C11	119.5(1)
9	C2	C1	C19	121.6(1)

10	C11	C1	C19	118.9(1)
11	C1	C2	H2	119.0(1)
12	C1	C2	C3	121.9(1)
13	H2	C2	C3	119.0(1)
14	O1	C3	C2	126.8(1)
15	O1	C3	C4	116.2(1)
16	C2	C3	C4	117.0(1)
17	O2	C4	C3	125.6(1)
18	O2	C4	C12	112.8(1)
19	C3	C4	C12	121.4(1)
20	O2	C5	H5	109.4(1)
21	O2	C5	C6	108.2(1)
22	O2	C5	C13	106.2(1)
23	H5	C5	C6	109.4(1)
24	H5	C5	C13	109.4(1)
25	C6	C5	C13	114.1(1)
26	O3	C6	C5	110.4(1)
27	O3	C6	H6	106.6(1)
28	O3	C6	C7	113.0(1)
29	C5	C6	H6	106.5(1)
30	C5	C6	C7	113.2(1)
31	H6	C6	C7	106.5(1)
32	C6	C7	H7	119.7(1)
33	C6	C7	C8	120.5(1)
34	H7	C7	C8	119.8(1)
35	C7	C8	H8	119.5(1)
36	C7	C8	C14	121.0(1)
37	H8	C8	C14	119.5(1)
38	N1	C9	H9	106.9(1)
39	N1	C9	C10	114.9(1)
40	N1	C9	C14	107.9(1)
41	H9	C9	C10	106.9(1)
42	H9	C9	C14	106.8(1)
43	C10	C9	C14	113.0(1)
44	C9	C10	H10A	108.5(1)
45	C9	C10	H10B	108.6(1)
46	C9	C10	C11	114.8(1)
47	H10A	C10	H10B	107.5(1)
48	H10A	C10	C11	108.5(1)
49	H10B	C10	C11	108.6(1)
50	C1	C11	C10	124.8(1)
51	C1	C11	C12	117.0(1)
52	C10	C11	C12	117.8(1)
53	C4	C12	C11	122.9(1)
54	C4	C12	C13	109.5(1)

55	C11	C12	C13	127.0(1)
56	C5	C13	C12	100.7(1)
57	C5	C13	C14	116.0(1)
58	C5	C13	C15	112.1(1)
59	C12	C13	C14	106.6(1)
60	C12	C13	C15	112.4(1)
61	C14	C13	C15	108.8(1)
62	C8	C14	C9	114.6(1)
63	C8	C14	C13	109.0(1)
64	C8	C14	H14	108.9(1)
65	C9	C14	C13	106.3(1)
66	C9	C14	H14	108.9(1)
67	C13	C14	H14	109.0(1)
68	C13	C15	H15A	109.2(1)
69	C13	C15	H15B	109.2(1)
70	C13	C15	C16	112.0(1)
71	H15A	C15	H15B	107.9(1)
72	H15A	C15	C16	109.2(1)
73	H15B	C15	C16	109.2(1)
74	N1	C16	C15	110.8(1)
75	N1	C16	H16A	109.4(1)
76	N1	C16	H16B	109.5(1)
77	C15	C16	H16A	109.5(1)
78	C15	C16	H16B	109.5(1)
79	H16A	C16	H16B	108.0(1)
80	N1	C17	H17A	109.5(2)
81	N1	C17	H17B	109.5(2)
82	N1	C17	H17C	109.5(2)
83	H17A	C17	H17B	109.4(2)
84	H17A	C17	H17C	109.5(2)
85	H17B	C17	H17C	109.4(2)
86	O1	C18	H18A	109.5(1)
87	O1	C18	H18B	109.5(1)
88	O1	C18	H18C	109.4(1)
89	H18A	C18	H18B	109.5(2)
90	H18A	C18	H18C	109.5(2)
91	H18B	C18	H18C	109.5(2)
92	C1	C19	H19	116.1(1)
93	C1	C19	C20	127.9(1)
94	H19	C19	C20	116.0(1)
95	C19	C20	H20	117.5(1)
96	C19	C20	C21	125.0(1)
97	H20	C20	C21	117.5(1)
98	C20	C21	C22	120.4(1)
99	C20	C21	C24	124.0(1)

100	C22	C21	C24	115.6(1)
101	C21	C22	H22	119.9(2)
102	C21	C22	C23	120.2(2)
103	H22	C22	C23	119.9(2)
104	N2	C23	C22	124.6(2)
105	N2	C23	H23	117.6(2)
106	C22	C23	H23	117.7(2)
107	C21	C24	H24	120.0(2)
108	C21	C24	C25	120.1(2)
109	H24	C24	C25	120.0(2)
110	N2	C25	C24	124.2(2)
111	N2	C25	H25	117.9(2)
112	C24	C25	H25	117.9(2)

Table A.11 Bond angle data for **162**

Number	Atom1	Atom2	Atom3	Atom4	Torsion
1	C18	O1	C3	C2	2.1(2)
2	C18	O1	C3	C4	-175.0(1)
3	C3	O1	C18	H18A	60.2(2)
4	C3	O1	C18	H18B	-59.8(2)
5	C3	O1	C18	H18C	-179.8(1)
6	C5	O2	C4	C3	164.1(1)
7	C5	O2	C4	C12	-10.4(2)
8	C4	O2	C5	H5	137.5(1)
9	C4	O2	C5	C6	-103.4(1)
10	C4	O2	C5	C13	19.5(1)
11	H3	O3	C6	C5	32.8(2)
12	H3	O3	C6	H6	148.2(1)
13	H3	O3	C6	C7	-95.2(1)
14	C16	N1	C9	H9	-179.0(1)
15	C16	N1	C9	C10	62.6(2)
16	C16	N1	C9	C14	-64.4(2)
17	C17	N1	C9	H9	54.9(2)
18	C17	N1	C9	C10	-63.5(2)
19	C17	N1	C9	C14	169.5(1)
20	C9	N1	C16	C15	56.5(2)
21	C9	N1	C16	H16A	-64.4(2)
22	C9	N1	C16	H16B	177.4(1)
23	C17	N1	C16	C15	-176.0(1)
24	C17	N1	C16	H16A	63.1(2)
25	C17	N1	C16	H16B	-55.1(2)
26	C9	N1	C17	H17A	-171.9(1)
27	C9	N1	C17	H17B	68.2(2)
28	C9	N1	C17	H17C	-51.8(2)

29	C16	N1	C17	H17A	60.9(2)
30	C16	N1	C17	H17B	-59.1(2)
31	C16	N1	C17	H17C	-179.0(1)
32	C25	N2	C23	C22	-0.8(3)
33	C25	N2	C23	H23	179.2(2)
34	C23	N2	C25	C24	1.0(3)
35	C23	N2	C25	H25	-179.0(2)
36	C11	C1	C2	H2	178.7(1)
37	C11	C1	C2	C3	-1.4(2)
38	C19	C1	C2	H2	-1.4(2)
39	C19	C1	C2	C3	178.6(1)
40	C2	C1	C11	C10	168.7(1)
41	C2	C1	C11	C12	-3.4(2)
42	C19	C1	C11	C10	-11.2(2)
43	C19	C1	C11	C12	176.6(1)
44	C2	C1	C19	H19	-161.9(1)
45	C2	C1	C19	C20	18.0(2)
46	C11	C1	C19	H19	18.0(2)
47	C11	C1	C19	C20	-162.0(2)
48	C1	C2	C3	O1	-174.7(1)
49	C1	C2	C3	C4	2.3(2)
50	H2	C2	C3	O1	5.3(2)
51	H2	C2	C3	C4	-177.7(1)
52	O1	C3	C4	O2	4.9(2)
53	O1	C3	C4	C12	178.9(1)
54	C2	C3	C4	O2	-172.5(1)
55	C2	C3	C4	C12	1.6(2)
56	O2	C4	C12	C11	168.0(1)
57	O2	C4	C12	C13	-3.4(2)
58	C3	C4	C12	C11	-6.7(2)
59	C3	C4	C12	C13	-178.1(1)
60	O2	C5	C6	O3	-36.6(2)
61	O2	C5	C6	H6	-152.0(1)
62	O2	C5	C6	C7	91.2(1)
63	H5	C5	C6	O3	82.5(1)
64	H5	C5	C6	H6	-32.8(2)
65	H5	C5	C6	C7	-149.6(1)
66	C13	C5	C6	O3	-154.6(1)
67	C13	C5	C6	H6	90.1(1)
68	C13	C5	C6	C7	-26.7(2)
69	O2	C5	C13	C12	-20.3(1)
70	O2	C5	C13	C14	-134.8(1)
71	O2	C5	C13	C15	99.4(1)
72	H5	C5	C13	C12	-138.2(1)
73	H5	C5	C13	C14	107.3(1)

74	H5	C5	C13	C15	-18.5(2)
75	C6	C5	C13	C12	98.8(1)
76	C6	C5	C13	C14	-15.7(2)
77	C6	C5	C13	C15	-141.5(1)
78	O3	C6	C7	H7	-13.5(2)
79	O3	C6	C7	C8	166.6(1)
80	C5	C6	C7	H7	-140.0(1)
81	C5	C6	C7	C8	40.1(2)
82	H6	C6	C7	H7	103.2(2)
83	H6	C6	C7	C8	-76.7(2)
84	C6	C7	C8	H8	174.6(1)
85	C6	C7	C8	C14	-5.4(2)
86	H7	C7	C8	H8	-5.3(2)
87	H7	C7	C8	C14	174.7(1)
88	C7	C8	C14	C9	-157.1(1)
89	C7	C8	C14	C13	-38.1(2)
90	C7	C8	C14	H14	80.7(2)
91	H8	C8	C14	C9	22.9(2)
92	H8	C8	C14	C13	141.9(1)
93	H8	C8	C14	H14	-99.4(2)
94	N1	C9	C10	H10A	30.1(2)
95	N1	C9	C10	H10B	146.7(1)
96	N1	C9	C10	C11	-91.5(2)
97	H9	C9	C10	H10A	-88.3(2)
98	H9	C9	C10	H10B	28.3(2)
99	H9	C9	C10	C11	150.1(1)
100	C14	C9	C10	H10A	154.5(1)
101	C14	C9	C10	H10B	-88.9(2)
102	C14	C9	C10	C11	32.8(2)
103	N1	C9	C14	C8	-174.3(1)
104	N1	C9	C14	C13	65.3(1)
105	N1	C9	C14	H14	-52.0(2)
106	H9	C9	C14	C8	-59.7(2)
107	H9	C9	C14	C13	179.9(1)
108	H9	C9	C14	H14	62.6(2)
109	C10	C9	C14	C8	57.6(2)
110	C10	C9	C14	C13	-62.9(1)
111	C10	C9	C14	H14	179.8(1)
112	C9	C10	C11	C1	-174.6(1)
113	C9	C10	C11	C12	-2.5(2)
114	H10A	C10	C11	C1	63.8(2)
115	H10A	C10	C11	C12	-124.2(1)
116	H10B	C10	C11	C1	-52.8(2)
117	H10B	C10	C11	C12	119.2(1)
118	C1	C11	C12	C4	7.5(2)

119	C1	C11	C12	C13	177.3(1)
120	C10	C11	C12	C4	-165.2(1)
121	C10	C11	C12	C13	4.6(2)
122	C4	C12	C13	C5	14.8(1)
123	C4	C12	C13	C14	136.2(1)
124	C4	C12	C13	C15	-104.7(1)
125	C11	C12	C13	C5	-156.2(1)
126	C11	C12	C13	C14	-34.7(2)
127	C11	C12	C13	C15	84.3(2)
128	C5	C13	C14	C8	47.5(2)
129	C5	C13	C14	C9	171.5(1)
130	C5	C13	C14	H14	-71.2(2)
131	C12	C13	C14	C8	-63.6(1)
132	C12	C13	C14	C9	60.4(1)
133	C12	C13	C14	H14	177.7(1)
134	C15	C13	C14	C8	175.0(1)
135	C15	C13	C14	C9	-61.0(1)
136	C15	C13	C14	H14	56.3(2)
137	C5	C13	C15	H15A	-54.3(2)
138	C5	C13	C15	H15B	63.5(2)
139	C5	C13	C15	C16	-175.4(1)
140	C12	C13	C15	H15A	58.3(2)
141	C12	C13	C15	H15B	176.1(1)
142	C12	C13	C15	C16	-62.8(2)
143	C14	C13	C15	H15A	176.1(1)
144	C14	C13	C15	H15B	-66.1(2)
145	C14	C13	C15	C16	54.9(2)
146	C13	C15	C16	N1	-51.3(2)
147	C13	C15	C16	H16A	69.5(2)
148	C13	C15	C16	H16B	-172.2(1)
149	H15A	C15	C16	N1	-172.5(1)
150	H15A	C15	C16	H16A	-51.7(2)
151	H15A	C15	C16	H16B	66.6(2)
152	H15B	C15	C16	N1	69.8(2)
153	H15B	C15	C16	H16A	-169.4(1)
154	H15B	C15	C16	H16B	-51.1(2)
155	C1	C19	C20	H20	-4.2(3)
156	C1	C19	C20	C21	175.8(1)
157	H19	C19	C20	H20	175.8(1)
158	H19	C19	C20	C21	-4.3(2)
159	C19	C20	C21	C22	-174.2(2)
160	C19	C20	C21	C24	4.4(2)
161	H20	C20	C21	C22	5.7(2)
162	H20	C20	C21	C24	-175.6(1)
163	C20	C21	C22	H22	-1.5(3)

164	C20	C21	C22	C23	178.5(2)
165	C24	C21	C22	H22	179.7(2)
166	C24	C21	C22	C23	-0.3(3)
167	C20	C21	C24	H24	1.7(3)
168	C20	C21	C24	C25	-178.2(2)
169	C22	C21	C24	H24	-179.5(2)
170	C22	C21	C24	C25	0.5(2)
171	C21	C22	C23	N2	0.4(3)
172	C21	C22	C23	H23	-179.6(2)
173	H22	C22	C23	N2	-179.5(2)
174	H22	C22	C23	H23	0.5(3)
175	C21	C24	C25	N2	-0.9(3)
176	C21	C24	C25	H25	179.1(2)
177	H24	C24	C25	N2	179.1(2)
178	H24	C24	C25	H25	-0.9(3)

Table A.12 Torsion angle data for **162**